2020 AUXDEFENSE

2ND WORLD CONFERENCE ON ADVANCED MATERIALS FOR DEFENSE

6 - 8 July 2020 | **Online Edition**

Book of Abstracts

Edited by Raul Fangueiro

BOOK OF ABSTRACTS

Edited by
RAUL FANGUEIRO

Cover
PIXARTIDEA

Publisher
SCIENCENTRIS, UNIPESSOAL, LDA

Authors
Multiple

Title
Proceedings of the 2nd World Conference on Advanced Materials for Defense

ISBN
978-989-54808-4-5

The editor is not responsible for any author's errors in spelling, grammar or scientific facts. The content of Abstracts is the cole responsibility of the authors.

Organizers


REPÚBLICA
PORTUGUESA
DEFESA NACIONAL


Universidade do Minho


Fibrenamics


SCIENCENTRIS
From Knowledge to Market

FOREWORD

Over the last few decades, materials are facing a continuous revolution due to important scientific and technical achievements obtained in cutting edge areas like physics, chemistry or biology. The possibility to design the materials properties at the molecular level or to enhance their performance using advanced functionalization techniques, are making materials smart, able to respond and adapt to external stimuli, more durable and resistant and, mainly, completely adapted to each specific application.

Research and development on advanced materials for defense is being driven all over the world by the most renowned Universities, Research Centers, Military Institutes and Companies to meet important requirements to enhance safety and survivability of platforms and personnel, along with requirements for enhanced maintainability and operability of platforms.

AUXDEFENSE2020 is focused on advanced materials research in the forward-looking enabling R&D domain where the intersection of key technologies in areas such as nano and microtechnology, biotechnology, meta materials, smart materials and structures, and energy generation and storage are being explored.

It is expected that AUXDEFENSE2020 may continue the work started in the previous edition (2018), contributing for the world important role played by this scientific event on the integration of the whole set of agents involved on this topic, bringing together scientists, researchers, militaries, students, technicians, entrepreneurs, end-users, companies, among others.

Due to the COVID19 pandemic, AUXDEFENSE2020 is taking place in a virtual mode and the scientific program was extended to three full days. Several presentations related to COVID19 are included mainly focusing on advanced solutions to face the pandemic in fields like CBRN protection, smart systems to detect virus and bacteria, smart textiles, nanocomposites, among others.

AUXDEFENSE2020 is the meeting point for all those interested on advanced materials for application in the defense field.

Guimarães/Portugal, 6 July 2020

Raul Fangueiro
Conference Chairman

CONFERENCE CHAIR

Raul Fangueiro, Fibrenamics / Department of Mechanical Engineering, University of Minho

SECRETARIAT

Edite Felgueiras, Fibrenamics, University of Minho

ORGANIZING COMMITTEE

Carlos Mota, Fibrenamics, University of Minho
Cristina Silva, Fibrenamics, University of Minho
Diana Ferreira, University of Minho
Diana Oliveira, Fibrenamics, University of Minho
Fernando Cunha, Fibrenamics, University of Minho
Ivo Cruz, Fibrenamics, University of Minho
Pedro Silva, Fibrenamics, University of Minho
Ricardo Zocca, Fibrenamics, University of Minho
Sara Silva, TecMinho, University of Minho
Tiago Sousa, Fibrenamics, University of Minho

SCIENTIFIC COMMITTEE

TABLE OF CONTENT

KEYNOTE LECTURE
CAN MATERIALS RESEARCH IN EUROPEAN DEFENCE CONTRIBUTE TO FACE THE PANDEMIC?

Giuseppe G. Daquino[1(*)]
[1] European Defence Agency, Brussels, Belgium
[(*)] E-mail: giuseppe.daquino@eda.europa.eu

ABSTRACT
The European Defence Agency Materials Capability Technology Group (Materials CapTech) has developed a Strategic Research Agenda (SRA), including policy areas de facto related to the COVID-19 pandemic to respond to the effects and/or to prevent the contagion. An overview of these policies and related ongoing and proposed projects is here presented.

INTRODUCTION
The European Defence Agency Materials Capability Technology Group (Materials CapTech) has developed a Strategic Research Agenda (SRA) with the objective to identify the technology areas where this working body can provide a valuable response to the European Defence Capability needs (EDA, April 2018).
Some of these policy areas are de facto related to the COVID-19 pandemic to respond to the effects and/or to prevent the contagion. These policies are deployed in 10 Technology Building Blocks (TBBs), namely technology incubators embedding homogeneous lines of technology developments in response to the European Defence Capability Plan and its related Generic Military Task List.
All the TBBs have been deployed in extensive roadmaps, focusing on the line of technology development visualised in the short and medium term, projecting a time window up to 2030. Needless to say, some of these technology development lines are expected to continue further beyond this time window, depending on the actual capability needs and the related geo-political scenarios.
All the projects developed or under development within the EDA Materials CapTech are supposed to be aligned with the SRA and its TBB roadmaps.

RESULTS AND CONCLUSIONS
The main policy areas tackled by the Materials CapTech related to the pandemic are mentioned below. Within these policy areas, specific projects already started or have been proposed in the context of the TBB roadmaps.

European Non-Dependence and Critical Raw Materials
The aim is the achievement of an adequate level of confidence in Security of Supply (SoS) across Europe, including long term assurance of sources of key technologies and willingness of partner governments to facilitate supply.
A central factor of SoS is access to Critical Raw Materials (CRMs) – (EDA, Oct 2018)
In turn, the enhancement of the European non-dependence is visibly beneficial vis-à-vis the response to the pandemic, because in case of heavy disruption of the CRM extraction in Third Countries, the European Union will be sufficiently resilient to the economic and societal shock.

Circular Materials

From the Materials CapTech's perspective, making use of circular materials in different components, structures and systems, as well as the adoption of advanced design/architecture that enhances the recycling of the critical materials used in the devices to respond to the pandemic (e.g. CRMs), are essential in the future vision of a less dependent European defence sector.

Advanced Multifunctional Smart Textiles/Materials for Individual Protection Systems

Smart Textiles are a new generation of materials and related systems with very interesting multifunctional properties (e.g. camouflage, moisture management, electronics integrated in textiles). These properties, together with the possibility of integrating the materials and systems in uniforms/platforms have drawn the attention of civil/defence stakeholders.

Multifunctional smart textile is a remarkable technology advancement enabling a safe and immediate answer to the challenges put forwards by the pandemic. The list below (far from exhaustive) mentions the most relevant technological aspects:

- Early detection and warning of potential CBRN threats
- Monitoring of the healthy status of the personnel/soldier
- Gathering and processing of information/communication
- Personal protection in hostile environments

Emerging Materials

New materials for the improvement of existing platforms and for the development of new platforms are needed for future operations. Some of the characteristics to be improved are lightweight, resistance to degradation and other functionalities.

A relevant example within this policy areas is the use of nanotechnology and graphene-based materials and fluids to create new materials for different civil/military application areas. The technology area is civil driven (e.g. Graphene Flagship), but with dual use possibilities in most areas and military specificities in some of them. In response to the pandemic, effective tools could be the graphene-based sensors or the graphene-based membranes. In fact, membranes can be applied to protect personnel/soldiers against CBRN threats and keeping food fresher for a long time.

ACKNOWLEDGMENTS

The author gratefully acknowledges all the Materials CapTech members from government, industry, academia and RTOs for their excellent contribution to the TBB roadmaps.

REFERENCES

[1] EDA, Materials & Structures CapTech Strategic Research Agenda, April 2018, available to the EDA Materials CapTech members

[2] EDA, Position paper on the impact of the entanglement of REACH regulation, Critical Raw Materials and Circular Economy on European Defence, October 2018, available to the EDA Materials CapTech members

KEYNOTE LECTURE

GRAPHENE AND RELATED 2-D TECHNOLOGIES AND THEIR POTENTIAL DEFENCE APPLICATIONS

Steven Savage
Swedish Defence Research Agency – Sweden

ABSTRACT

Graphene and related two-dimensional materials such as MXenes are attracting much interest due to their unique combinations of for applications development come from the civil sector and include energy storage, aerospace, electro-optic and chemical sensors, corrosion protection and many others. All these are dual-use technologies with similar applications extraordinary physical, optical, electronic, mechanical, and chemical properties. The main drivers in defence systems.

This presentation will explore some of the possibilities, opportunities and limitations on defence applications for these materials, based in part of a recent NATO specialist meeting.

KEYNOTE LECTURE

THE ROLE OF INTERDISCIPLINARITY TO ENABLE RAPID AND NOVEL RESPONSES TO SOCIETAL CHALLENGES - A LEARNING PERSPECTIVE FROM THE ONGOING COVID-19 PANDEMICS

Lars Montelius
INL - The Intergovernmental Nanotechnology Laboratory – Portugal

ABSTRACT

Suddenly the Covid-19 Pandemics hit the world, country by country. And the governments had to take decisions without a large knowledge foundation. And each government handled the challenges rather uniformly. When it comes to the governance actions related to research, the responses were primarily national. The possibilities to learn from each other were initially kind of lost. The world witnessed how each country responded by setting up various commissions to help to fight the pandemics. The world became a bit more isolated. And as a function of various lock-down, so the citizens. Now the recovery phase has started. Primarily because the risk of experiencing a national catastrophic medical acute situation seems to have been lowered. However, the virus will remain for years to come. It will be around us until we have managed to find a vaccine – and managed to deploy a massive worldwide vaccination. So, the risk is still high. Actually, it is just as high as before. And the situation exposes more risk now than a couple of weeks ago. Primarily to the false perception that a face mask protects you. The worldwide learning from the pandemic situation is still to be gathered.

In this presentation, I will discuss the learning perspectives from inside INL gathered as a function of the pandemics. I will cover the time from the beginning of January up to Q2. I will discuss how INL handled the situation and the learning outcomes reflected on the diversity of about 450 people from about 40 different cultures. We were early to understand the seriousness and we initiated remote work as the new norm before the government declared the-state-of-emergency in Portugal. I will describe how we used our diversity, from culture to knowledge, to quickly come together remotely and address the global challenge. The various actions, the immediate ones and the ones that followed – covering all various dimensions from setting up voluntary production of face-shields to setting up new research activities as well as buddy systems to reduce the risk of employee isolation.

In particular, I will discuss actions related to the utilization of our large inherent interdisciplinary capacity to address the pandemic challenge. Through this strong challenge we identified the opportunities and set up mission-oriented activities being able to foster a strong solution-oriented mindset, far outside of our comfort zones, but in a trusted environment, that enabled us to come up with out-of-the-box solutions for addressing the challenge especially related to support the safe re-starting of the economy. Our learning outcomes, well illustrate that it is not enough to have - or create - innovation capacity. It is needed to create “innovations to happen”. A cornerstone for innovation to take place is the ability to address challenges from a new perspective. An important element for such an ability is the mechanism to allow ideas to flourish, by releasing the creative power of the individuals, and the ability to compound and match these ideas to a certain challenge. This holds for organizations, companies, associations, countries and EU as a whole. Advances in Nanotechnology and Advanced Materials have played a profound role for the last few decades

development of the modern society. Further developments in combination with AI, VR, Big data and Quantum Computation, will in the next decade be a major driver for disruptive innovations in various verticals as well as an effective tool for fostering the meaningful utilization of knowledge for a meaningful and sustainable global development. By learning from the present pandemic, we will be in a better position to utilize the vast opportunities.

Nanotechnology is a Key Enabling Technology with promises for making solid interdisciplinary contributions to the grand challenges of today. Solutions to these challenges demands increased transversal interdisciplinary participation. Not only transversal within the Sciences but also transversal in all kind of societal dimensions including an increased empowered participation of people. There is a need for an increased effort to effectively close the gap between societal needs and science & technology offers. The basics for science is curiosity - in the past mostly related to understand how things are related or how things work and nowadays more and more related to missions based on ideas like ”think of we could make X that would do Y, then we could achieve Z”. By involving Arts in the Science & Technology arena, one could foster a new understanding of creating missions by using design-based thinking concepts. It is a process that enables moving into the unknown (with confidence) and discuss abstractions without a solid base. This process could enable a lot of missions to be articulated. Finally, in order to fully tap all possibilities offered within the Key Enabling Technologies there is a continued need to put emphasis on transversal funding support schemes. If not, there is a risk that the enabling character of inventions will either disappear or take very long time to diffuse into other verticals, effectively hampering the innovation capital to be fully exploited.

INVITED LECTURE
ANALYTICAL CHEMISTRY TO SUPPORT COVID19 EMERGENCY

Fabiana Arduini
Tor Vergata University, Department of Chemical Science and Technologies, via della Ricerca Scientifica, 00133, Rome, Italy
E-mail: fabiana.arduini@uniroma2.it

ABSTRACT
On 30 January 2020, the European Commission launched a request for expressions of interest entitled "SC1-PHEC-ORONAVIRUS-2020: Advancing knowledge for the clinical and public health response to the [COVID-19] epidemic" to address the main 4 pillars in life science in COVID-19 emergency with the specific aims for i) improving epidemiology and public health, including our preparedness and response to outbreaks, ii) delivering new treatments, encompassing the development of the ones currently in the pipeline and screening and identifying molecules against virus, iii) development of new vaccines, and iv) rapid point-of-care diagnostic tests. In the last pillar, the main effort is requested by analytical chemistry, which is the science devoted to develop new and affordable analytical tools. Different point of care diagnostic tests are conceived for rapid measurements, including the ones based on immunocromatographic technique which allow for a rapid qualitative analysis by using a paper-based strip and antigen-antibody reaction. The most widespread sensing tool in COVID-19 emergency is the one for IgM and IgG detection for a rapid evaluation of the history of the exposure to SARS-CoV-2, measuring the antibodies against SARS-CoV-2 in the blood of patients. In addition, a similar approach are also recently reported in case of SARS-CoV-2 detection in biological fluids to overcome the drawbacks of the reference method (i.e. PCR), which entails long time analysis, expensive instrumentation, laboratory set-up, and skilled personnel. Useful sensing tools have been also recently fabricated for a customisation of disinfection of the environment, which is another urgent issue to address in COVID-19 emergency. Last issue regards the main issue of medical masks, which are a precious tool to prevent transmission of human coronaviruses from symptomatic individuals. Taking account the need of face masks for a huge number of people, some countries have to face the issue of insufficient amount of personal protective equipment. In Italy, this deficiency has boosted several industries to reset their production chain, moving from their usually target manufacturing towards the production of personal protective equipment in order to match the large quantities requested for the safety of citizens. This urgent request is encountering a barrier, which entails the customization of the production to deliver effective medical and non-medical masks. To face the delivery of safe face masks in a timely fashion, together with ARPA Lazio, Environmental Protection Agency, we developed a smart analytical system able to simulate the inhalation and exhalation and measuring the aerosol able to pass through the face masks tested, for evaluating mask efficiency with a fast screening method.

INVITED LECTURE
SMART TEXTILES AND THEIR POSSIBLE APPLICATIONS IN THE FIELD OF DEFENSE

Baptiste Garnier[1], Philippe Mariage[2], François Rault[1], Cédric Cochrane[1], Vladan Koncar[1(*)]
[1] Ecole Nationale Supérieure des Arts et Industries Textiles, Roubaix, France
[2] Univ. Lille, CNRS, Centrale Lille, Univ. Polytechnique Hauts-de-France, UMR 8520 - IEMN, F- 59000 Lille, France
[(*)] E-mail: vladan.koncar@ensait.fr

ABSTRACT

The main objective of the proposed research project is to bring the small, yet sufficient amount of the electrical energy to all the individuals to supply their electrical devices embedded or not to their clothing, but also other textile-based connected objects. This innovative energy harvesting concept may be realized in several different ways, which are the subjects of the presentation.
The use of textile antennas integrated to the clothing, or other relatively large textile structures resonating at NFC (short-range harvesting - 13,56 MHz, wireless power supply from the smartphone) or higher frequencies using metamaterials (long-range harvesting - 2,4 GHz and more), and even the exploitation of the intelligent relay antennas concept based on the physical principle of the time-reversal of EM (electromagnetic) signals exploited by 5G networks.
The electrical energy, in its different forms, is surrounding us in the form of electromagnetic waves. This existing and free of charge energy will be converted (harvested, recycled) into the electrical energy, and used locally, to power microelectronic circuits, sensors and actuators integrated to underwear, clothing, home, and technical textiles, composites equipped with self-monitoring embedded sensors... It would also be possible to use it to recharge portable electronic devices e.g. Smartphones etc. The conversion of EM (Electro-Magnetic) waves will be done by the use of textile metamaterials for long-range harvesting (2,4 GHz, wi-fi, 3G, 4G, 5G…), and/or resonating textile combiners for short-range harvesting (NFC - 13,56 MHZ). The wireless data transfer will also be realized using the same platforms.
The prototyping of an integral textile NFC combiner for body-centric communication is developed in our laboratory. First, an integral textile NFC combiner is a structure able to transfer power and data thanks to the magnetic induction at 13.56 MHz through textile materials by using the Near Field Communication (NFC) protocol. These structures aim to transfer power and data wireless to all embedded electronics included in the smart textiles by using a single source, for example, a smartphone. Also, the integral textile NFC combiners are realized only in textile materials and do not present any connexion points, which means they are directly usable at the machine outlet and more robust. They are composed of two combined textile NFC antennas realized by an embroidery process with overlapped conductive rotor threads made of copper filaments, polyester, and polyamide. The geometry (coil's radius, length of the transmission line, and the gap between current lines) are determined to make the structure resonating close to 13.56 MHz. The resonant frequency constitutes a fundamental characteristic to enables power to be transmitted through the structure.
Metamaterials (MTMs) having negative permittivity and permeability have also been developed and manufactured by embroidery and weaving textile processes. They are the first promising results in the area of long-range electrical energy harvesting

INVITED LECTURE

THREE-DIMENSIONAL COMPOSITE STRUCTURE WITH NEARLY ISOTROPIC NEGATIVE POISSON'S RATIO BY RANDOM INCLUSIONS

Hong Hu[(*)], **Minglonghai Zhang**
Institute of Textiles and Clothing, The Hong Kong Polytechnic University
[(*)] E-mail: huhong@polyu.edu.hk

ABSTRACT

Composite structures with negative Poisson's ratio are a special type of auxetic materials. They possess a number of enhanced properties including shear modulus, indention resistance and energy absorption due to their unusual deformation behavior and can be exploited for many applications such as automobile, aerospace and defense, civil engineering and sport equipment, etc. Although auxetic composites can be made with laminates using non-auxetic constituent materials through suitable stacking sequences of individual lamina, the negative Poisson's ratio behavior can only be obtained in some direction. Embedding auxetic inclusions or reinforcements into a matrix to achieve negative Poisson's ratio behavior in a composite structure has become an efficient way to make auxetic composite materials. In this presentation, 3D composite structure with nearly isotropic negative Poisson's ratio by randomly embedding inclusions made of 2D textile composite will be presented, and its potential applications will be demonstrated.

INVITED LECTURE

BEHAVIOUR OF FIBRE REINFORCED POLYMER COMPOSITES SUBJECTED TO BLAST LOADING: LESSONS LEARNED

Genevieve S. Langdon[1, 2(*)], Christopher J. von Klemperer[2], Wesley J. Cantwell[3]

[1] Department of Civil and Structural Engineering, University of Sheffield, Sheffield, UK.

[2] Department of Mechanical Engineering, University of Cape Town, Rondebosch, South Africa.

[3] Department of Aerospace Engineering, Khalifa University of Science and Technology (KUST), Abu Dhabi, UAE

[(*)] E-mail: genevieve.langdon@sheffield.ac.uk

ABSTRACT

This work describes the behaviour of fibre-reinforced composites subjected to explosions in air. It elucidates lessons learned from experimental results reported over the last twenty years, showing the influence of fibre type, geometry, loading distribution on the failures observed. Their importance for blast resistant FRP design, future experimental work and numerical modelling are briefly discussed.

INTRODUCTION

Fibre reinforced polymer (FRP) composites are increasingly used in load bearing structures, as they offer advantages including high specific strength and stiffness, excellent thermal resistance and the ability to tailor their properties to a required application. FRPs are deployed in both laminate (for example, aircraft and racing car parts) and sandwich (for example, marine vessels and surfboards) configurations. The performance of FRPs under blast loading conditions is important for both civil and defense applications (Mouritz, 2019).

The behavior of FRPs subjected to blast loading is influenced by a wide range of parameters, including the nature of the blast loading itself (both its temporal and spatial loading distribution), the material properties of the FRP (which are influenced by the choice of fibre, resin, weave, lay-up and manufacturing process) and the structural configuration of the FRP (boundary conditions, geometry). There are a wide range of possibilities for all these influences, and this incredible diversity is reflected in the literature pertaining to the blast response of FRP composites. This paper is an attempt to bring together some of the lessons learnt from research into the behavior of FRPs under blast loading conditions. The work is primarily limited to behaviour arising from loading from explosives detonated in air, and is developed from a review of existing literature (Langdon et al, 2014) and the authors' own experimental work (Langdon et al, 2017, 2018).

LESSONS LEARNED

The complexity of real-life blast loading scenarios means that the simple empirical models of pressure loading often do not apply (Langdon et al, 2018). Moreover, practical FRP composite structures tend to have complex boundary conditions, meaning that the joints cannot be idealised as either simply supported or fully clamped, making closed form predictions of their behaviour difficult, even when failure is not considered. Mouritz (2019) comments that small scale laboratory tests induce deformations, stresses and damage that are markedly different to those experienced at full-scale.

Recent experimental investigations have shown that FRP composites are better able to contain explosion loading that is uniformly distributed (Langdon et al, 2017). Localised loading, even at low charge masses, tended to cause premature rupture. This means that FRP composites are likely to perform poorly in situations where a close-in charge or contact detonation is likely, and where rupture cannot be tolerated. The typical failure modes in FRPs under blast include delamination, matrix cracking, interfacial debonding and fibre fracture. Very low levels of plastic deformation are observed due to the elastic-brittle nature of the composites (Langdon et al, 2014). Thin blast-loaded FRP laminates exhibit large transient displacements,

with peak negative displacements in the opposite direction to the blast (Mouritz, 2019). This complexity makes capturing the transient response of FRP composites under blast loading conditions an important goal for blast experimentalists at present.

Most experiments suggest that sandwich constructions are inferior, on an equivalent mass basis, to FRP panels under blast loading conditions (Langdon et al 2017). This is because the thin face sheet layers tend to rupture, allowing the explosive products to damage the relatively weak core. Improvements could be obtained by considering unequal face sheet thicknesses, if it is certain which side of the sandwich structure faces the explosive loading threat.

Fibre choice is critical. Kevlar, despite having excellent impact properties, behaves poorly in blast conditions. Glass fibre seems superior to carbon fibre under most blast loading conditions, probably due to its extra ductility, although this is controversial as some studies have drawn the opposite conclusion (Langdon et al, 2014). Dyneema, based on ultra high molecular weight polyethylene, offers excellent potential as a blast resistant FRP, and further work on this is recommended. Woven FRPs appear to offer better damage tolerance than unidirectional or cross ply laminates to blast loading, with fewer delamination failures.

Numerical modelling of FRP composite behaviour under blast loading conditions faces significant challenges (Langdon et al, 2018). There have been recent improvements to the simulation of blast loading, which are particularly important as FRPs exhibit great sensitivity to the spatial distribution of the loading. It is vital that the essential failure and response modes can be captured from the chosen material and interface formulations, allowing the delamination and fibre fracture modes to be captured when they are significant. Obtaining accurate material parameters (covering rate dependent plastic hardening, temperature-dependent behaviour and damage) is difficult, especially at high rates of loading.

REFERENCES

[1] Langdon GS, Cantwell WJ, Guan ZW, Nurick GN. The response of polymeric composite structures to air-blast loading: a state-of-the-art, Int Mater Rev, 2014, 59(3), p. 159-177.

[2] Langdon GS, Guan ZW, Cantwell WJ, 8.17 Blast Protection for Polymer Composite Materials in Structures Subjected to Air-Blast Loading, 332-350, Ed(s): P.W.R. Beaumont, C.H. Zweben, In: Comprehensive Composite Materials II, Elsevier, 2018.

[3] Langdon GS, von Klemperer CJ, Sinclair G, Ghoor I, Influence of curvature and load direction on the air-blast response of singly curved glass fiber reinforced epoxy laminate and sandwich panels, Explosion Blast Response of Composites, Elsevier, 2017, p. 133-160.

[4] Mouritz A, Advances in understanding the response of fibre-based polymer composites to shock waves and explosive blasts, Compos Part A: Appl Sci and Manuf, 2019, 125, 105502.

INVITED LECTURE

MECHANICAL PERFORMANCE OF SANDWICH STRUCTURES WITH CONVENTIONAL AND AUXETIC HONEYCOMB SOFT CORES

Paulo J. R. O. Nóvoa[1, 2], Francisco G. M. Rede[1], and António T. Marques[1, 2(*)]

[1] Department of Mechanical Engineering (DEMec), University of Porto, Porto, Portugal

[2] Composite Materials and Structures Research Unit, INEGI, University of Porto, Porto, Portugal

[(*)] E-mail: marques@fe.up.pt

ABSTRACT

The development of both alternative core materials and geometries for sandwich structures has deserved growing interest in both civil and military applications benefiting from lightweight constructions. The present work compares the flexural performance of sandwich structures based on cork agglomerate core materials – continuous commercial agglomerate and cellular alternatives with either circular or hexagonal cells. In the case of hexagonal cells, in addition to testing the traditional honeycomb, the behaviour of the auxetic re-entrant geometry alternative is also discussed.

INTRODUCTION

Sandwich structures are effective in achieving both high specific strength and stiffness, and thereby constitute an important path towards producing lightweight structures (Davies, 2001).

Cork agglomerates and derivatives have been attracting some interest as possible renewable source-based alternatives to traditional core materials, particularly, synthetic polymer foams (Castro, 2010). However, cork agglomerates generally exhibit higher densities compared to commercial polymer foams.

Advances in product development capabilities have enabled the performance evaluation of sandwich structures with core materials having increasingly intricate geometries. This has generated interest for both civil and military applications. The simplifies the possibility of replicating widespread honeycomb-like cores using alternative cell wall materials. Property advantages may result from the use of auxetic materials - in the case of sandwich structures, it has been suggested and demonstrated that an auxetic core material leads to improved quasi-static and impact performances. (Allen, 2015)

Thi work investigates bending and shear properties of composite sandwich structures with cork-based cores. A commercial corkboard product, and lighter honeycomb-type cellular alternatives, with circular or hexagonal cells, are studied. The possibility of broadening the present research to include an auxetic cork-based cellular core with re-entrant hexagonal cells, is discussed.

Three sandwich structures were manufactured using [±45o]s glass fiber reinforced epoxy resin laminate skins (1 mm thick), and 16 mm thick core materials based on a cork agglomerate with reference CoreCork NL10 (Amorim® Cork Composites S.A.) – the sandwich structures were identified based on the core product as reference core (RC), and cellular cores with either circular (CC) or hexagonal (HC) cells. The structures were assembled using a bi-component polyurethane adhesive (SikaForce® 7710 L100).

Sandwich specimens were tested in both three- and third-point four-point bending according to methods described in ASTM C 393 and ASTM D 7250.

RESULTS AND CONCLUSIONS

Load vs. deflection curves for representative specimens loaded in both configurations - three-point and four-point bending - are presented in Fig. 1.

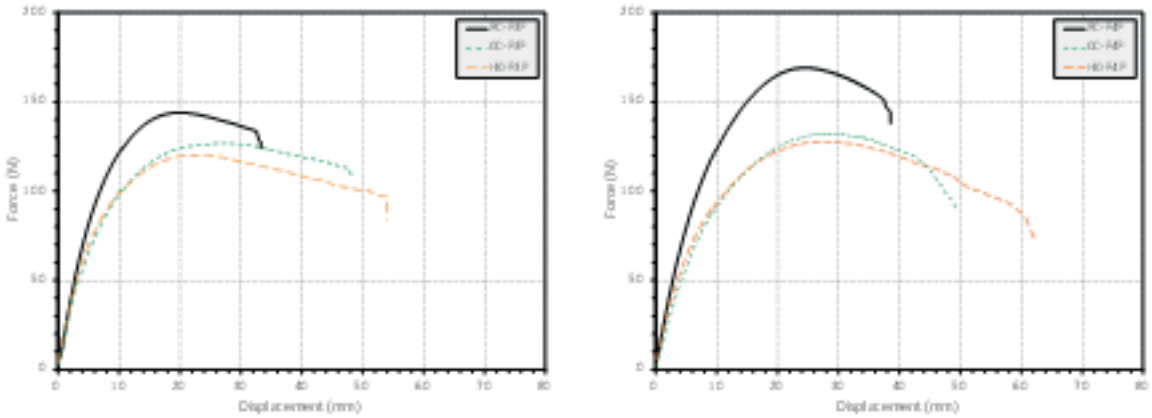

Fig.1 Load vs. displacement curves for three-point (left) and four-point (right) bending tests.

Similar values for maximum core shear, and face-sheet bending stresses resulted for all structures. The values for sandwich flexural stiffness (D) and core shear modulus (G), determined in accordance with ASTM 7250 standard practice are presented in Table 3.

Table 3 Sandwich stiffness and core shear modulus

Sandwich structure	Sandwich flexural stiffness, D [10^{-4} N.mm^2]	Core shear modulus, G [MPa]
RCS	2.90	1.21
CCS	2.06	0.88
HCS	2.20	0.88

The reference structure exhibits the higher flexural stiffness, followed by that of HCS. The fact that HCS has higher stiffness than CCS is an indication of the superior stability of hexagonal compared to circular cells. The results are interesting considering that overall stiffness is dominated by skin properties. The same trend is apparent from the core shear values both cellular cores. Again, the continuous, albeit quite heavier reference core dominates. Considering the reported advantages which may result from auxetic cellular cores, it is planned to study such alternative as well. It remains to be demonstrated to which extent the auxetic behavior of a re-entrant hexagonal honeycomb will be preserved in a structure composed of very low stiffness cork agglomerate walls.

REFERENCES

[1] Allen T, Shepherd J, Hewage TAM, Senior T, Foster L, Alderson A. Low-kinetic energy impact response of auxetic and conventional open-cell polyurethane foams. Phys Status Solidi B, 2015, 252, p. 1631-9

[2] Castro O, Silva JM, Devezas T, Silva A, Gil L. Cork agglomerates as an ideal core material in lightweight structures. Mater Design, 2010, 31, p 425-32.

[3] Davies JM, Lightweight Sandwich Construction. Chicester. Wiley-Blackwell, 2001.

INVITED LECTURE
CARBON MATERIALS FOR SPACE AND OTHER APPLICATIONS

Evaldo José Corat
Brazilian Institute for Space Research – Brazil

ABSTRACT

Carbon materials grown by chemical vapor deposition has advanced in the last three decades and they found a broad applicability including in the satellite technologies and defense, as a consequence. The first part of this talk will present a broad review on CVD diamond and diamond-like carbon (DLC) applications. Second part will focus on recent developments with Vertically Aligned Carbon Nanotubes (VACNT) and their application in space and defense areas. The focus will be on two major subjects. First the direct CNT deposition on carbon fiber (CF) and its implications on CF mechanical properties and matrix adhesion, discussing the implications in structural composites. Second, the novel technology of water condensation on superhydrophobic VACNT and the applications for campaign water collection from air and heat exchange by phase change. New perspective will be presented, including an effort with biological cooperation in virus detection, in which VACNT may become an important matrix for virus capturing and detection.

FLUORESCENCE SENSOR SYSTEM FOR THE GAS-PHASE DETECTION OF TRIACETONE TRIPEROXIDE (TATP)

Benedikt Heller[1](*), Mustafa Biyikal[1], Reinhard Noske[1], Knut Rurack[1]
[1] Federal Institute for Materials Research and Testing (BAM), Berlin, Germany
(*) E-mail: benedikt.heller@bam.de

ABSTRACT
The increase in terrorist activity throughout the world within the last decades has raised the need for rapid and sensitive trace detection of explosives. The most commonly used explosive for terrorist attacks is perhaps triacetone tripeoxide (TATP). In this work we present a fluorescent sensor layer for the detection of TATP in gas-phase.

INTRODUCTION
TATP is a very powerful explosive that can easily be synthesized from acetone and hydrogen peroxide using acidic conditions. It is perhaps the most prominent home-made explosive. TATP has extreme sensitivity to detonation upon impact, friction or heating. At the same time, because of its lack of aromatic and/or nitro groups it does not show significant absorption in the ultraviolet range and exhibits no fluorescence, making straightforward and sensitive detection challenging. Different approaches for the detection of TATP have been developed, including methods like infrared spectroscopy, Raman scattering, ion mobility spectrometry (IMS), liquid chromatography and mass spectrometry (MS). But these are either laboratory-based or stationary analytical systems and often need trained personal. Simpler methods come in reach when using a fluorescent sensor that changes its fluorescence output in the presence of TATP. Fluorescence sensor systems, even in handheld size, are usually highly sensitive and easy to operate.
In this work, we developed a highly sensitive fluorescent sensor layer for the detection of TATP vapor. This detection is based on the in-situ decomposition of TATP to hydrogen peroxide using an acidic reagent. The decomposition follows a cascade of reactions leading to the formation of a strongly light absorbing species. Due to the overlap of its absorption spectra with the emission spectra of an indicator dye, the measured fluorescence intensity is decreased.

RESULTS AND CONCLUSIONS
Typical results of gas-phase experiments are shown in Fig. 1. A swipe sample, wetted with different amounts of TATP was heated to 140 °C. The occurring vapor was then carried over the sensor layer and the change in fluorescence was measured. While the swipe setup allows calibrating the system in a straightforward manner, TATP can also be directly detected in the gas-phase in a sniffing mode of the sensor. The sensor layer is embedded into a home-built handheld sensor device.

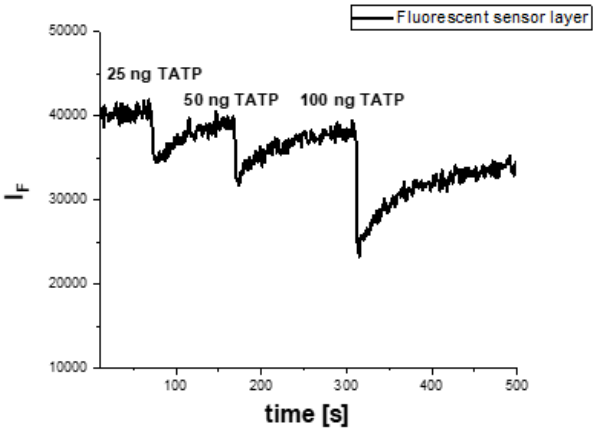

Fig. 1 Fluorescence intensity change of sensor layer after exposure to TATP vapors

This fluorescence sensor system provides a detection technique that is able to measure concentrations down to 25 ng TATP in gas-phase with fast response times of <5 s (full signal amplitude). As devised in a handheld device, the sensor system can be operated in two different measurement modes, in sniffing mode as well as using swipe samples. Such sensory devices provide thus a promising approach toward widely available measurement systems for in-the-field use by public authorities or private enterprises active in the area of security.

ACKNOWLEDGMENTS

The authors gratefully acknowledge funding by the Federal Institute for Materials Research and Testing (BAM), Berlin, Germany.

REFERENCES

[1] Almenar E, Costero AM, Gavina P, Gil S, Parra M. Towards the fluorogenic detection of peroxide explosives through host–guest chemistry. Royal Society Open Science, 2018, 5, 171787.
[2] Taha YM, Saowapono MT, Osthoff HD. Detection of triacetone triperoxide by thermal decomposition peroxy radical chemical amplification coupled to cavity ring-down spectroscopy. Analytical and Bioanalytical Chemistry, 2018, 410, 4203-4212.
[3] Fan S, Lai J, Burn PL, Shaw PE. Solid-State Fluorescence-based Sensing of TATP via Hydrogen Peroxide Detection. ACS Sensors, 2019, 4, 134-142.

CHEMO-RESISTIVE POLYMER NANOCOMPOSITE TRANSDUCERS FOR THE DETECTION OF NEUROTOXIC CHEMICALS

J. F. Feller[1(*)], M. Castro[1], A. Sachan[1], P. Laquintinie[2], C. Lahuec[2], F. Seguin[2], L. Dupont[2]

[1] Smart Plastics Group, IRDL CNRS 6027 – University of South Brittany (UBS), Lorient, France.

[2] Electronics & Optics Dept., Lab-STICC CNRS 3192, IMT Atlantique, Brest, France.

[(*)] E-mail: jean-francois.feller@univ-ubs.fr

ABSTRACT

This work presents the potential of functionalized carbon nanotube (F-CNT) based conductive polymer nanocomposite (CPC) transducers to design sensitive, selective, lightweight, and low consumption (2 W) electronic noses (e-nose) for the detection of neurotoxic chemicals. Such characteristics are required for a portable device to be integrated in soldiers' suit (Fig. 1a). The ability of the e-nose to detect at room temperature the presence of 1.6 ppm of DMMP (dimethyl methyl phosphonate, a simulant of Sarin one major chemical warfare agent), in a complex blend of eight chemicals at concentrations ranging from 4 to 1500 ppm has been evaluated. Using the SVM (support vector machine) algorithm allowed to identify the presence of DMMP in a complex mixture with an accuracy of 98 % getting closer to on field applications.

INTRODUCTION

The early detection of neurotoxic chemicals at low concentration (sub ppm) in complex atmosphere including many pollutants is a major challenge to protect efficiently persons chemical attacks. Nerve agents like Sarin have very low immediately dangerous to life and health (IDLH) values close to 10 ppb. Commercial portable devices such as ion mobility spectrometers weight between 650 g and 4 kg, and cost about 10,000 $. As such, the need for a low-cost, light- weight portable solution for the real time detection of CWA has driven research in the two last decades. Several sensing materials such as semiconducting metal oxides (Tomchenko, Harmer and Marquis, 2005), surface acoustic waves (Singh et al., 2014), quartz micro balance (Shaik et al., 2018) or F-CNT (Wang, Gu and Swager, 2008), were found to be sensitive to DMMP a simulant of Sarin. Among all, F-CNT based are very attractive sensors that can operate at room temperature, have a low power consumption (2 W), a high sensitivity, and a selectivity can be tuned by a chemical or physicochemical functionalization (Du et al., 2008). The extraction of features such as integrals and maximum derivatives from raw responses is done in a pre-treatment step (Yan et al., 2015), then several classification algorithms can be used such as principal component analysis (PCA) (Choi et al., 2005), probabilistic neural networks (PNN) (Chuanzhi et al., 2007), or SVM (Yin et al., 2016).

RESULTS AND CONCLUSIONS

In this study, SVM has been the most successful algorithm for the correct recognition of DMMP in complex vapour blends (cf. Fig. 1b). Six quantum resistive vapour sensors (vQRS) with cross-sensitivities have been assembled into an array (e-nose) and exposed to different chemical atmospheres containing or not DMMP (cf. Tab. 1). The electronic nose system presented in this work allowed to identify the presence of DMMP in a complex mixture with an accuracy of 98 %. The development of a cost-effective, portable e-nose system implementing the proposed feature extraction method and SVM algorithm on a dedicated circuit will thus allow the e-nose system, after downsizing, to be embedded in a military uniform, drastically reducing its power consumption. Tuning the set of transducers in the sensor array will also lower the risk of false alarms, by tailoring the prototype for the specific identification of the DMMP in a broader range of interferants.

	DMMP alone	Hydrocarbons	Background	Background + DMMP
Ethanol	-	-	1500 ppm	1500 ppm
Propanol	-	200 ppm	400 ppm	400 ppm
Water	-	-	1200 ppm	1200 ppm
Toluene	-	200 ppm	300 ppm	300 ppm
Xylene	-	-	80 ppm	80 ppm
Octane	-	200 ppm	40 ppm	40 ppm
Benzaldehyde	-	-	8 ppm	8 ppm
TMB	-	-	4 ppm	4 ppm
DMMP	12 ppm	-	-	1,6 ppm

Table. 1 List of chemical atmospheres tested

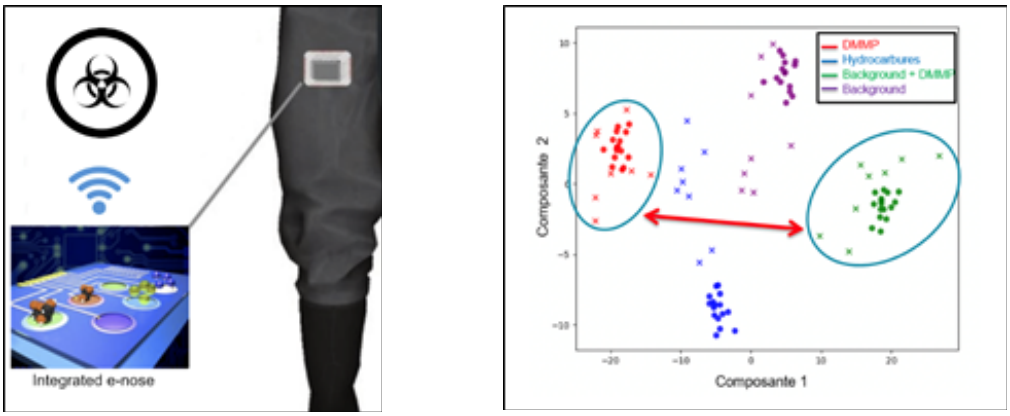

a) b)

Fig.1 a) Principle of an integrated e-nose, b) Discrimination ability of the e-nose

ACKNOWLEDGMENTS

The authors gratefully acknowledge French DGA for funding with grant n°2016337.

REFERENCES

[1] Choi, N. J. et al. (2005) 'Classification of chemical warfare agents using thick film gas sensor array', Sensors & Actuators B: Chemical, 108(1–2), pp. 298–304. doi: 10.1016/j.snb.2004.11.022.

[2] Chuanzhi, C. et al. (2007) 'A novel toxic gases detection system based on SAW resonator array and probabilistic neural network', in 8th International Conference on Electronic Measurement & Instruments. IEEE, pp. 3-499-3–503. doi: 10.1109/ICEMI.2007.4350964.

[3] Du, X. et al. (2008) 'Synthesis and evaluation of a new polysiloxane as SAW sensor coatings for DMMP detection', Sensors & Actuators B: Chemical, 134(2), pp. 409–413. doi: 10.1016/j.snb.2008.05.016.

[4] Shaik, M. et al. (2018) 'P-hexafluoroisopropanol phenyl functionalized graphene for QCM based detection of dimethyl methylphosphonate, a simulant of the nerve agent sarin', RSC Advances, 8(15), pp. 8240–8245. doi: 10.1039/C7RA12272A.

[5] Singh, H. et al. (2014) 'SAW e-nose using single sensor with temperature modulation', in 9th International Conference on Industrial & Information Systems (ICIIS). IEEE, pp. 1–5. doi: 10.1109/ICIINFS.2014.7036550.

[6] Tomchenko, A. A., Harmer, G. P. and Marquis, B. T. (2005) 'Detection of chemical warfare agents using nanostructured metal oxide sensors', Sensors & Actuators B: Chemical, 108(1–2), pp. 41–55. doi: 10.1016/j.snb.2004.11.059.

[7] Wang, F., Gu, H. and Swager, T. M. (2008) 'Carbon nanotube/polythiophene chemiresistive sensors for chemical warfare agents', Journal of the American Chemical Society, 130(16), pp. 5392–5393. doi: 10.1021/ja710795k.

[8] Yan, J. et al. (2015) 'Electronic nose feature extraction methods: A review', Sensors, 15(11), pp. 27804–27831. doi: 10.3390/s151127804.

[9] Yin, X. et al. (2016) 'Temperature modulated gas sensing e-nose system for low-cost and fast detection', IEEE Sensors Journal, 16(2), pp. 464–474. doi: 10.1109/JSEN.2015.2483901.

URANIUM DETECTION IN WATER BY CHEMICAL OPTICAL FIBER SENSORS

Maria Pesavento[1], Letizia De Maria[2], Daniele Merli[1], Antonella Profumo[1], Francesco Arcadio[3], Chiara Milanesi[1], Luigi Zeni[3], and Nunzio Cennamo[3(*)]

[1] Department of Chemistry, University of Pavia, Pavia, Italy

[2] Ricerca sul Sistema Energetico (RSE), Milan, Italy

[3] Department of Engineering, University of Campania Luigi Vanvitelli, Aversa, Italy

[(*)] E-mail: nunzio.cennamo@unicampania.it

ABSTRACT

A specific self-assembled monolayer receptor for uranium detection has been realized on the gold surface of a plasmonic plastic optical fiber sensor. The sensor's gold surface assembled with a ω-phosphonic acid terminated thiol, was investigated for its capability to complex uranyl ions. The novel chemical optical fiber probe, characterized by plasmonic techniques, demonstrated to be effective for the determination of uranyl in water solution in the range 10ppb-30ppm.

INTRODUCTION

The by-product of the uranium enrichment process, the depleted uranium, has been applied as armour-piercing ammunition in several international military conflicts. For instance, ammunitions containing depleted uranium were used in three recent conflicts: up to 321 tons in the Gulf War (1990–1991); approximately 3 tons in Bosnia–Herzegovina, 1995; and approximately 10 tons in Kosovo, 1999 (Danesi, 2003). In particularly, depleted uranium is used because of its high density, hardness, and pyrophoric properties (Danesi, 2003). The testing and use of such ammunitions has led to the release of depleted uranium into the environment at several locations around the world. The issue of the possible presence of depleted uranium in the environment has recently attracted considerable public interest (Saleh, 2016). Utilizing depleted uranium in non-fission nuclear weapons results in the addition of 238U to the natural uranium in the environment, so producing an environmental damage even if depleted uranium weapons are regarded as conventional weapons.

Starting from the consideration that phosphonate is a strong ligand for metal ions (Merli, 2016) and that ω-derivatized phoshonic acid terminated thiols are now commercially available (Sigma-Aldrich), Merli et al. proposed to use 11-mercaptoundecylphosphonic acid (MUPA) to form a self-assembled monolayer (SAM) on the gold electrode for realizing an electrochemical sensor, exploiting its ability to bind uranyl. This is expected since the parent phosphonic acid has a high complexation constant of for this ion and a good selectivity (Merli, 2016). In a similar way, two SAM receptors have been used combined with a surface plasmon resonance (SPR) D-shaped POF sensor for the detection in water of copper(II) (Pesavento, 2019) and iron(III) (Cennamo, 2014).

RESULTS AND CONCLUSIONS

The preparation of the chemical SPR-POF sensor is shown in Fig. 1a, and the SPR spectra obtained at different concentrations of the analyte are shown in Fig. 1b, in the concentration range from 0 ppm to 50 ppm. We have used the same experimental setup already used in (Cennamo, 2014) and (Pesavento, 2019). As shown in Fig. 1b, when the concentration of the analyte increases, the resonance wavelength increases too, shifting right in the range 10ppb-30ppm. This makes it possible the quantification of uranium (as uranyl) in the unknown sample after construction of the standardization curve. The sensing method here proposed is attractive, because in principle it can be applied directly in the field, so giving an analytical response in a fast and not too expensive way. A test has been carried out on the reproducibility of the sensor system.

Moreover, it is a marker-free sensing device, and, as such, it can be applied to different metals, even not electroactive

as in the case of electrochemical transduction, provided that a proper receptor is fixed at the SPR interface.

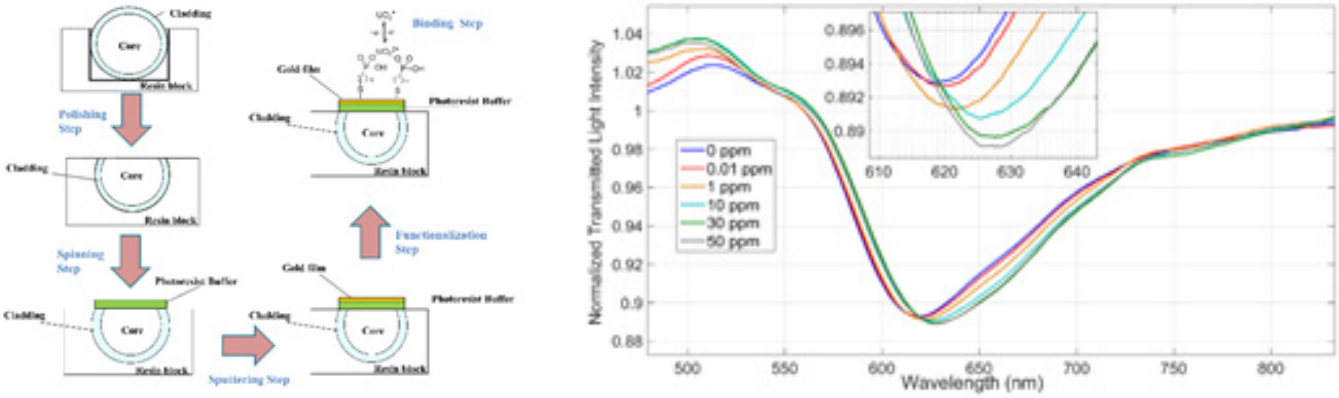

a) b)

Fig.1 (a) Chemical SPR-POF sensor for uranium determination in water. (b) SPR spectra at different concentrations of uranium (uranyl).

REFERENCES

[1] Danesi PR, Bleise A, Burkart W, Cabianca T. Isotopic composition and origin of uranium and plutonium in selected soil samples collected in Kosovo. J. Environ. Radioact., 2003, 64, p. 121–131.

[2] Danesi PR, Markowicz A, Chinea-Cano E, Burkart W. Depleted uranium particles in selected Kosovo samples. J. Environ. Radioact., 2003, 64, p. 143–154.

[3] Saleh IH, Abdel-Halim AA. Determination of depleted uranium using a high-resolution gamma-ray spectrometer and its applications in soil and sediments. J. of Taibah University for Science, 2016, 10, p. 205-211.

[4] Merli D, Protti S, Labò M, Pesavento M, Profumo A. A ω-mercaptoundecylphosphonic acid chemically modied gold electrode for uranium determination in waters in presence of organic matter. Talanta, 2016, 151, p. 119-125.

[5] Pesavento M, Profumo A, Merli D, Cucca L, Zeni L, Cennamo N. An Optical Fiber Chemical Sensor for the Detection of Copper(II) in Drinking Water. Sensors, 2019, 19, p. 5246.

[6] Cennamo N, Alberti G, Pesavento M, D'Agostino G, Quattrini F, Biesuz R, Zeni L. A Simple Small Size and Low Cost Sensor Based on Surface Plasmon Resonance for Selective Detection of Fe(III). Sensors, 2014, 14, p. 4657-4671.

THE DUAL-PROMOTION EFFECT OF PERFLUOROOCTANOATE FERRIC SALT ON THERMAL PROPERTIES OF ACTIVE MATERIALES CONTAINING ALUMINUM AND AMMONIUM PERCHLORATE

Xuyuan Zhou[1(*)], Fei Zhen[2], Fenglei Huang[3], Rongjie Yang[4], Jun Zhou[5], Rui Zhou[6]

[1, 5, 6] China North Industries Corporation, Beijing, the People's Republic of China

[1, 2, 3, 4] State Key Laboratory of Explosion Science and Technology, Beijing Institute of Technology, Beijing, the People's Republic of China

[(*)] E-mail: xuyuan_zhou@bit.edu.cn

ABSTRACT

Aluminum (Al) powder and ammonium perchlorate (AP) are common species to be employed as important components in active materials such as propellants, explosives and pyrotechnics. The dual-promotion effect of a novel-synthesized perfluorooctanoate ferric salt [$Fe(PFO)_3$] on the thermal properties of Al and AP was revealed in this work. The decomposition products of $Fe(PFO)_3$ have the abilities of promoting the thermal pyrolysis of AP and triggering thermite reaction with Al as well. It would be potentially employed in increasing the energy properties of Al/AP-based active materials.

INTRODUCTION

The $Fe(PFO)_3$ is a kind of micro powder which is novel-synthesized based on replacement reaction between perfluorooctanoic-acid and chloride salt. It decomposes at low relative temperature (200~400°C) into several fluorocarbons, fluoride salts and ferric oxides, To verify the dual-promotion effect of $Fe(PFO)_3$, the investigation of AP/$Fe(PFO)_3$ and Al/$Fe(PFO)_3$ powder mixture has been performed as bellow: homo-dispersed AP/$Fe(PFO)_3$ mixtures with different ratio were employed to perform the thermal analysis by differential scanning calorimeter(DSC), at a heating rate of 10°C/min in nitrogen(N_2) over the temperature range of 25–600°C, homo-dispersed Al/$Fe(PFO)_3$ mixture was also used to perform DSC analysis at a heating rate of 10°C/min in argon(Ar) over the temperature range of 25–700°C, thermal reaction residue of Al/$Fe(PFO)_3$ mixture after high-temperature treatment (below 700°C in Ar flow) was studied by X-ray diffraction(XRD). Analysis data of pure AP and pristine Al was used as blank baseline, the particle size distributions of AP and Al range 50-80μm and 4-6μm, separately.

RESULTS AND CONCLUSIONS

Fig. 1 summarized the DSC data of the samples comparing AP/$Fe(PFO)_3$ mixture with pure AP. The addition of $Fe(PFO)_3$ reduces the high-temperature decomposition peak of AP. Heat-release calculation and thermodynamic analysis also show the total heat release of AP/$Fe(PFO)_3$ mixture is higher than that of pure AP under the thermal process, and the addition of $Fe(PFO)_3$ decreases the high-temperature decomposition activation energy by 17.4%. The decomposition products ferric oxides are considered as the catalyst promoting the pyrolysis of AP.

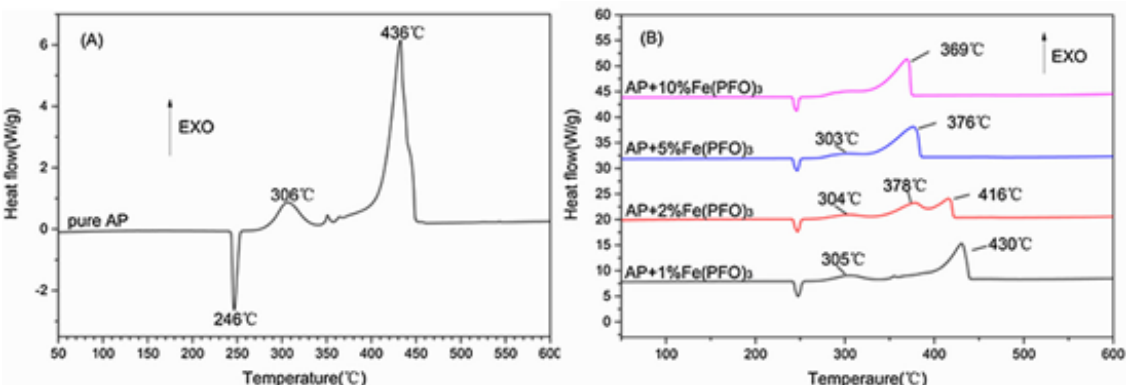

Fig.1 DSC curves of the thermal decomposition of pure AP (A) and AP/$Fe(PFO)_3$ mixture (B)

DSC curves in Fig. 2 reveals the phase transition (melting point) of pristine Al at 660°C, as for Al/$Fe(PFO)_3$ mixture, an obvious exothermic peak at about 635°C was observed, which is a severe heat release with fast chemical reaction. The XRD pattern of high-temperature treated Al/$Fe(PFO)_3$ presents the formation of α-Al_2O_3, it is regarded as a evidence to support the suspicion that the heat release at 635°C derived from the thermite reaction, the thermite reaction was postulated to occur between Al and the solid decomposition products of $Fe(PFO)_3$.

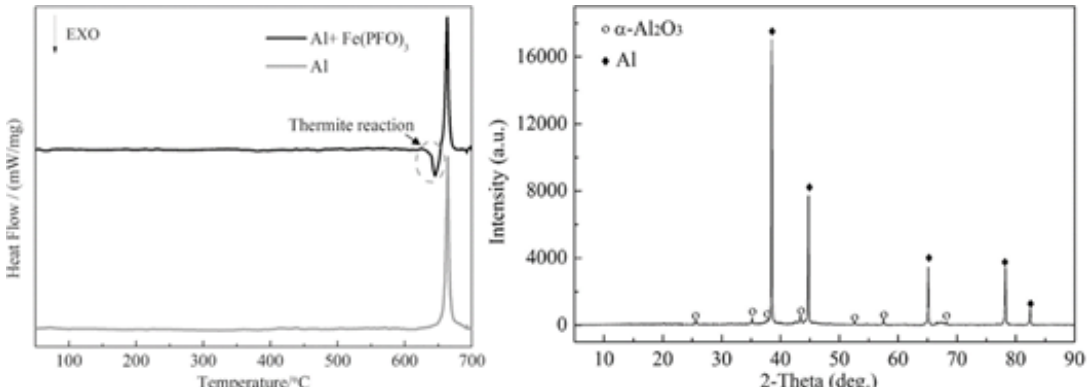

Fig.2 DSC curves of the thermal process of Al/$Fe(PFO)_3$ mixture (left) and the XRD pattern of high-temperature treated Al/$Fe(PFO)_3$ mixture (right)

Based on above results, this work confirmed the dual-promotion effect of $Fe(PFO)_3$ on promoting thermal pyrolysis of AP and triggering thermite reaction with Al under relative low temperature. This dual-promotion effect would be employed to enhance the energy release of active materials containing AP and Al.

ACKNOWLEDGMENTS

We gratefully acknowledge the study assistance supported by China National Engineering Research Center of Flame Retardant Materials.

REFERENCES

[1] Pengkun T, Meishuai Z, Rongjie Y, Xiaoyan G. Synthesis of ferric perfluorooctanoate [$Fe(PFO)_3$] and its catalysis on thermal decomposition of ammonium perchlorate. Thermochimica Acta, 2016, 646, p. 32-38.

[2] Fei Z, Xuyuan Z, Liqiong W, Rongjie Y, Fenglei H. Study on Burning and Thermal Decomposition Properties of HTPB Propellant Containing Synthesized Micro-nano Ferric Perfluorooctanoate. Propellants Explosives Pyrotechnics, 2019, 44, p. 362-368.

CHEMICAL AND RADIOLOGICAL SENSORS INTEGRATION IN UNMANNED AERIAL SYSTEMS WITH ATEX COMPLIANCE

Júlio Gouveia-Carvalho[1], Wilson Antunes[1(*)], Tiago Gonçalves[1], Victor Lobo[2], Filipe Duarte[3], Bernardino Veríssimo[3] and Mário Monteiro Marques[2]

[1] Centro de Investigação da Academia Militar (CINAMIL); Unidade Militar Laboratorial de Defesa Biológica e Química (UMLDBQ);

[2] Centro de Investigação Naval (CINAV);

[3] I-Sky-Ex;

[(*)] E-mail: antunes.wdt@exercito.pt

ABSTRACT

Chemical, biological, radiological and nuclear (CBRN) threats poses many challenges to address in terms of reconnaissance, detection, personnel protection and countermeasures. The scientific and technological developments that led to the use of unmanned aerial systems (UAS) in an ubiquitous manner, enables its integration in CBRN operations, as sensors platforms for detection. GammaEx project targets to validate the concepts of operation using a specifically developed UAS with ATmosphères EXplosives (ATEX) compliance, equipped with chemical and radiological sensors for detection in CBRN scenarios.

INTRODUCTION

Due to the rapid advancement in Unmanned Aerial Vehicles (UAV), CBRN detection in its current form is very likely to experience a fast transition towards a decade of new capabilities, employing UAV technology. In the past, the main focus has been concentrated around mounted and dismounted CBRN reconnaissance. The emergence of new technologies and the focus on force protection in operations, capability requirements are now addressing a new topic of unmanned platforms as part of CBRN defence operations [1]. The use of UAV in CBRN scenarios with its main purpose for detection or sampling tasks, combines the advantages of manned and aerial approaches [2]. UAV use in contaminated environments, have several advantages including: reduction and/or elimination of life loss risk; access to inhospitable and inaccessible environments, increasing the efficiency and speed of missions [3]. A gap was identified in the use of UAV in CBRN scenarios, namely their employment in explosive atmospheres environment (ATEX) [3]. This paper aims to review the main concepts and challenges involving the sensors integration in UAS for specific CBRN environments considering the ATEX compliance, during the course of GammaEx project.

RESULTS AND CONCLUSIONS

Two types of detection equipment's were integrated in the UAV, one for chemical detection and a second for radiological monitoring. A customize chemical detector was developed specially for this ATEX UAV application and the detector was validated in the laboratory, and compared with a similar detection technology. The results for the chemical of the laboratorial validation for the MX6 (commercially off the shelf detector system) and the SGX-4DT sensor (commercially off the shelf sensor used for the development of the on-board customized UAV chemical detector) are shown in Table 1.

The radiological detector used was a commercially off the shelf equipment (RadEye SPRD, from Thermo Scientific), previously tested and calibrated by the brand manufacturer. For the radiological approach, the equipment was integrated in the architecture of the UAV and the communication protocol of this equipment was used to feed the sensor management software, developed to control the ATEX UAV platform as a whole. The ability for radiation detection was tested during a field trial, where the M6 UAV with ATEX compliance was challenge to measure radiation, from a calibrated cesium source previously deployed in the field. The concept of radiological detection through the integra-

tion of a commercial radiological detector (RadEye SPRD, from Thermo Scientific) in a UAV, was possible to demonstrate with this field exercise, where the measurements were taken after landing Figure 1.

The most concerning challenges identified are related to interference between sensors, flight system and

Chemical compound	Standard concentration	Detectors readings	
		MX6	SGX-4DT sensors
H_2S	25 ppm	28 ppm	24 ppm
	50 ppm	55 ppm	49 ppm
CO	101 ppm	80 ppm	105 ppm
	300 ppm	264 ppm	298 ppm

Table 1 Performance characteristics of the SGX-4DT electrochemical sensor

Fig. 1 Field tests: "M6" near radiation source detecting gamma radiation

communication links, system integration and compatibility, validation of the accuracy and sensitivity of the radiological sensors to detect 10 mCi radioactive sources at a 5-meter distance, collision avoidance through sense-and-avoid capability implementation, and compliance with the ATEX directives in order to obtain an ATEX certification of the project. The ATEX compliance has a negative impact on weight and consequently in the autonomy, energy and propulsion requirements, which poses limitations to the operational employment.

The project demonstrated the validity of the concept of the integration of radiological sensors in a UAV specifically designed with ATEX compliance for radiological detection. These results are promising for the consideration of future projects with higher levels of technological readiness for the integration of radiological sensors or proof-of-concept of chemical sensors addressing the specific issues related with chemical detection.

ACKNOWLEDGMENTS

The authors gratefully acknowledge the funding by Ministério da Defesa Nacional, Portugal, under grants MDN/1351520572.

REFERENCES

[1] Using Unmanned Aerial Vehicles (UAVs) for CBRN reconnaissance. Available online: http://www.cbrneportal.com/using-unmanned-aerial-vehicles-uavs-for-chemical-biological-radiological-nuclear-cbrn-reconnaissance/ (accessed on 30.05.2019).

[2] Gouveia-Carvalho, J.; Antunes, W.; Gonçalves, T.; Marques, M.M.; Lobo, V. Unmanned aerial vehicles in chemical, biological, radiological and nuclear environment: Sensors review and concepts of operations. In Book of Papers (International symposium "Mine Action") Proceedings of the International Symposium "Mine Action 2015", Biograd, Croatia 27 to 30 April 2015; Editor-in-Chief Dražen Jakopec, Editor Sanja Vakula; Published by HCR-CTRO d.o.o. Zagreb, Croatia, 2015.

[3] Austin R, (2010) Unmanned Aircraft Systems - UAVs Design, Development and Deployment. Aerospace Series, Wiley.

SENSORS AND ELECTRONIC CIRCUITS DEVELOPMENT PRINTED ON FLEXIBLE SUBSTRATES

Josue Ferri[1(*)], Jorge Moreno[2], Ana Rodes[3], Jose Maria Garcia[4], Elena Mira[5], Eduardo Garcia-Breijo[6], and Raul Llinares[7]

[1, 2, 3, 4, 5] Textile Research Institute (AITEX), Alcoy, Spain

[6] Instituto Interuniversitario de Investigación de Reconocimiento Molecular y Desarrollo Tecnológico (IDM), Universitat Politècnica de València, Valencia, Spain;

[7] Departamento de Comunicaciones, Universitat Politècnica de València, Alcoy, Spain;

[(*)] E-mail: josue.ferri@aitex.es

ABSTRACT

Printed electronics on flexible substrates has raised special interest in the scientific community in recent years thanks to its potential applications. Some of the applications are directly connected with textiles or fabrics substrates as wearables. This work presents capacitive sensors for different purposes that support the flexibility and the stretchability of the substrates without damage.

INTRODUCTION

Electronics that imitate the natural world by bending, flexing and stretching are becoming more and more significant as the technology is integrated into our lives, our environments and even on our bodies. One of the most challenging application is to combine electronics with textiles or fabrics. This idea was defined as smart textiles or smart fabrics where initially products such as conductive fibers and filaments, yarns together with woven, knitted or non-woven structures, which can interact with the environment or users. Smart textiles normally are used as sensors and they are combined with external microprocessors units, so as to analyse the information and create some kind of action as alert or activation. Smart textiles sensors can mainly be classified depending on if they measure resistivity or capacitance variations. On the one hand, resistive sensors measure variations of the resistance of a conductive structure that can be a wire or a conductive stretchable fabric. On the other hand, capacitive sensors use more complex structures that allow to measure a capacitance between two conductive materials that can be also conductive threads or conductive textiles. This idea has been successfully developed in order to measure parameters as strain, pressure, respiration, humidity, gas or temperature among others. Moreover, sensors based on conductive surfaces as electrocardiogram (ECG), electromyography (EMG), electroencephalogram (EEG) have also been implemented.

RESULTS AND CONCLUSIONS

The conductive particles or materials can be printed also on the top of surface of the textile. Printed electronics on flexible substrates has attracted special interest in the scientific community during the last years thanks to its great potential in terms of flexibility and possible end applications. Furthermore, these electronics has lower costs than the current standard techniques, which is an added value, due to the fact that can be implemented with reel to reel industrial machines.

Most common types of conductive inks are based on conductive nanoparticles or microparticles dispersed into a polymer matrix. These particles are based on carbon particles, metallic, such as carbon, silver and gold as well as conductive oxides such as ITO or ZnO. These inks are usually dried or cured by heating, however, laser or UV curing is also possible. When the ink is cured by heat, the binder and solvent are removed, forming a conductive layer on the surface of the substrate. The required curing temperature depends on the type of the ink, but their typically range comes from 100ºC to 250ºC for 5 to 30 minutes. According to the type of the substrate the curing procedure should be adjusted.

Different ink characterization tests were carried out on different substrates, evaluating temperature and optimum

curing time. In these tests results have been obtained about the orientation of the tissues should have respect to printing as well as parameters to be taken into account such as fabric roughness, fabric materials and possible surface finishes. These tests have been performed using different printing technologies depending on the substrate.
It can be observed that for the case of the fabrics with higher thickness and higher diameter of thread, the samples did not show electrical conductivity and the values of resistance obtained were very high. The rougher a substrate is, the more quantity of inks should be printed to reduce the negative effect of the substrate surface. In this type of substrates screen-printing technology offers best performance.
On the other side technologies as flexography or inkjet allow control with more precision the quantity of ink and the line thickness. But these technologies need substates smooth substates to have good conductivities and high reproducibility.

ACKNOWLEDGMENTS

The authors gratefully acknowledge the funding by the Conselleria d'Economia Sostenible, Sectors Productius i Treball, through IVACE (Instituto Valenciano de Competitividad Empresarial). Hybrid project. Application No.: IMAMCI/2020/1.

REFERENCES

[1] Lymberis, A.; Paradiso, R. Smart fabrics and interactive textile enabling wearable personal applications: R&D state of the art and future challenges. Proc. 30th Annu. Int. Conf. IEEE Eng. Med. Biol. Soc. EMBS'08 - "Personalized Healthc. through Technol. 2008, 5270–5273.
[2] Molinaro, N.; Massaroni, C.; Lo Presti, D.; Saccomandi, P.; Di Tomaso, G.; Zollo, L.; Perego, P.; Andreoni, G.; Schena, E. Wearable textile based on silver plated knitted sensor for respiratory rate monitoring. Proc. Annu. Int. Conf. IEEE Eng. Med. Biol. Soc. EMBS 2018, 2018-July, 2865–2868.
[3] Gonçalves, C.; Ferreira da Silva, A.; Gomes, J.; Simoes, R. Wearable E-Textile Technologies: A Review on Sensors, Actuators and Control Elements. Inventions 2018, 3, 14.
[4] Ferri, J.; Lidón-Roger, J.; Moreno, J.; Martinez, G.; Garcia-Breijo, E. A wearable textile 2D touchpad sensor based on screen-printing technology. Materials 2017, 10(12), 1450.
[5] Khan, S.; Lorenzelli, L.; Dahiya, R.S. Technologies for printing sensors and electronics over large flexible substrates: A review. IEEE Sens. J. 2015, 15, 3164–3185.

CBRNE PERSONAL PROTECTIVE EQUIPMENT: THE POTENTIAL OF MULTIFUNCTIONAL FIBROUS STRUCTURES

Diana P. Ferreira[1(*)], Sofia Costa[1], Joana Araújo[1] and Raul Fangueiro[1,2]

[1] Centre for Textile Science and Technology (2C2T), University of Minho, 4800 Guimarães, Portugal

[2] Department of Mechanical Engineering, University of Minho, Guimarães, Portugal

[(*)] E-mail: diana.ferreira@det.uminho.pt

ABSTRACT

The main goal of this work was the functionalization of natural fibers with nanoparticles (NPs) for the development of multifunctional fibrous systems. Thus, natural fibres were functionalized with metal and metal oxide NPs by in-situ synthesis (using water as solvent and a minimal concentration of reducing agent) and the precursor was chosen depending on the kind of NPs under use. Besides in situ synthesis, the dip-pad-dry method was also used for the fibers' impregnation with the NPs formulations. The developed systems were characterized using Field Emission Scanning Electron Microscopy (FESEM), Attenuated Total Reflectance-Fourier-Transform Infrared Spectroscopy (ATR-FTIR) and Ground-State Diffuse Reflectance (GSDR). Several properties were analysed including degradation of chemical agents, antibacterial activity, self-cleaning capability, UV protection, electrical conductivity and piezoresistive response.

INTRODUCTION

One of the long-standing goals of military research area is to achieve protection against chemical, biological, radiological, nuclear or explosive warfare without adding extra weight to the soldier's protective system. The fibers' functionalization with nanoparticles, due to their lightweight properties and high surface area, can be used for this purpose (Petkov, 2018). Synthetic ones such as polyamide HT, UHMWPE and aramid are valuable options, however natural fibers, like flax, jute, sisal or cotton, are very promising materials for replacing the synthetic, due to their low cost, lightness, durability, abundance, biocompatibility and biodegradability (Ferreira, 2019).

Metal oxide nanoparticles (such for example: Ag, MgO, NiO, CaO, TiO2, ZnO, Al2O3, Fe2O3) and also graphene nanoplatelets are known as effective decomposing agents against organophosphates (DMMP mimicking nerve gases). The degradation of organophosphates is not the only advantage since several nanoparticles can also present antibacterial activity which is very important for their use in the degradation of biological harmful toxins. In this way, the development of new materials with multifunctional properties, such as degradation of DMMP, antibacterial activity, UV-protection, self-decontaminating properties and sensing, could be achieved by the incorporation of nanoparticles onto fibrous structures (Costa,2018)(Ferreira, 2018). In this work, several natural fabrics were functionalized with Ag, ZnO, CaO, SiO2, MgO and graphene NPs. All the samples were characterized by GSDR, FESEM, ATR-FTIR and XRD. Degradation tests were performed using DMMP and methylene blue, the antibacterial activity was evaluated and several other properties including electrical conductivity and piezoresistive response for their possible use in military sensing applications.

RESULTS AND CONCLUSIONS

Ag NPs were successfully incorporated onto the natural fibres (in this case flax fabrics) by using polyethylene glycol (PEG) as reducing agent and stabilizer of the Ag NPs. UV radiation was also applied for the Ag NPs reduction. For the ZnO NPs synthesis, sodium hydroxide was used as reducing agent and the in-situ synthesis onto jute fabrics was performed in aqueous medium. CaO and MgO NPs were also synthesized and the methodologies under used were optimized to increase the sustainability of the processes. Besides metal and metal oxide NPs, graphene nanoplatelets

(GNPs) were also tested. Therefore, flax fabrics were subjected to an alkali treatment, followed by the incorporation of the GNPs using biopolymeric formulations of chitosan and PEG. Figure 1 exhibits as example, the FESEM images of the fibers coated with the Ag/ZnO NPs, CaO and GNPs. The presence of NPs onto the natural fabrics is visible in all the percentages of materials under study and the dispersion seems to be uniform.

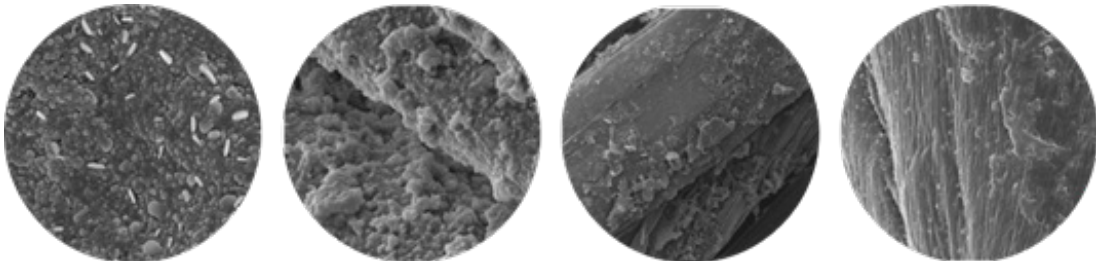

Fig.1 From left to right: FESEM images of natural fabrics functionalized with Ag/ZnO NPs, CaO NPs, Graphene nanoplatelets and Ag NPs.

The optimized fibrous systems exhibited electrical conductivity values ranging from ~ 3×10-4 S/m (0.1%GnPs) to 0.8 S/m (2% GnPs). The pressure sensing properties of the fabrics was quantified by the gauge factor, values from 1.6 to 1.8 were obtained. The antibacterial tests revealed that Ag/jute, ZnO/flax and CaO/jute systems are effective against gram-positive and gram-negative bacteria. The degradation preliminary tests indicated promising results in the methylene blue degradation as well as DMMP adsorption and degradation ability. Several materials presented excellent UV protection values and superhydrophobic character.

ACKNOWLEDGMENTS

The authors are thankful to project UID/CTM/00264/2019 of 2C2T – Centro de Ciência e Tecnologia Têxtil, funded by National Founds through FCT/MCTES and Diana Ferreira is also thankful to CEECIND/02803/2017.

REFERENCES

[1] Costa, Sofia M et al. 2018. “Multifunctional Flax Fibres Based on the Combined Effect of Silver and Zinc Oxide (Ag/ZnO) Nanostructures.” Nanomaterials 8(12): 1069.

[2] Ferreira, Diana P, Juliana Cruz, and Raul Fangueiro. 2019. Green Composites for Automotive Applications Surface Modification of Natural Fibers in Polymer Composites. Elsevier Ltd.

[3] Ferreira, Diana P, Armando Ferreira, and Raul Fangueiro. 2018. “Searching for Natural Conductive Fibrous Structures via a Green Sustainable Approach Based on Jute Fibers and Silver NPs.” Polymers 10(63).

[4] Petkov, Plamen, Dumitru Tsiulyanu, Cyril Popov, and Wilhelm Kulisc, eds. 2018. Advanced Nanotechnologies for Detection and Defence against CBRN Agents. 1st ed. Springer Netherlands.

EVALUATION OF RESPONDERS PROTECTIVE SUITS IN THE FIELD BY USING SIMULANTS OF CHEMICAL WARFARE AGENTS

Denis Josse[1(*)], Jean-Bernard Feral[2], Jean Ulrich Mullot[3]

[1,] Alpes-Maritimes Fire and rescue services, France

[2,] Aveyron Fire and rescue services, France

[3,] French Navy analysis and environmental monitoring laboratory, Toulon, France

[(*)] E-mail: denis.josse@sdis06.fr

ABSTRACT

In this work, our goal is to evaluate whether the choice of chemical protective suits (CPS) for rescuers during mass casualty incidents can be validated by a risks assessment approach and by using the results of efficacy standard tests, or whether additional tests, e.g. field tests that better fit the rescuers working conditions and operational constraints, are required.

Preliminary field tests were conducted to evaluate the protective efficacy of CPS by using methylsalicylate (MeS) as sulfur mustard simulant. Our results showed that air-permeable CPS could be better adapted than air-impermeable for responders, at least in the warm zone.

INTRODUCTION

During the initial response to mass casualty chemical incidents, rescuers from both the Fire & Rescue Services and Health Services contribute to the prehospital care at the incident site. Their main mission is to extract victims from the hot zone (HZ) into the warm zone (WZ) where they will perform victims triage, emergency treatment and decontamination before their evacuation to the cold zone (CZ).

According to the current French interagency plan, only squads of firemen wearing type 1 or 2 suits, i.e. impermeable to gas, can enter the HZ once it is secured and cleared of any explosive and radioactive risks. However, especially if the CBRN nature of the event has not been recognized yet, it is expected that 1st responders wearing fire suits and equipped with self-contained breathing apparatus might be involved in the emergency extraction of victims.

In the WZ, the choice of chemical protective suits (CPS) for rescuers is recommended to be based on a risks assessment approach and on the anticipated psycho-physiological constraints. Currently, air impermeable - non breathable or air permeable - breathable CPS are most often worn by default by rescuers present in this hazardous area.

RESULTS AND CONCLUSIONS

HZ, WZ, CZ were designed in a firefighter (FF) station. Three dummies contaminated with MeS were placed in the HZ and 3 pairs of FF, wearing either FF suits, or air permeable (type-4) or air-impermeable (type-3) CPS, were exposed in the HZ and the WZ for 20 min. Permeatec pads were used to evaluate the penetration of MeS vapours through the CPS.

Our results showed that in the HZ (n=6/CPS), air-permeable CPS were at least as protective as air-impermeable CPS to MeS vapours. When extrapolated to SM, our results (< 5 mg on the pads after 20 min) suggested that the 3 CPS might be used for 20 min without leading to significant adverse effects for the responders. In the WZ (n=4/CPS), our results (< 5 mg on the pads after 20 min) indicated that the 3 CPS gave satisfactory skin protection to MeS.

In agreement with other field studies (eg workers spraying pesticides), air-impermeable (type-3) CPS do not necessarily confer a better protection than air permeable (type-4) CPS.

The combination of results from standard tests performed in a lab with man in simulant tests and field tests that both mimic real interventions could help the responders to make more relevant choices of personal protective equipments.

REFERENCES

[1] Van Wely E, Current global standards for chemical protective clothing: how to choose the right protection for the right job? 2017, 55, 485-499.
[2] Shimasaki N, Shinohara K, Morikawa H, performance of materials use for biological PPE against blood splash penetration, 2017, Industrial health, 55, 521-528.
[3] Bodurtha P, Gudgin Dickson EF, Decontamination science and Personal Protective Equipment (PPE) selection for Chemical-Biological-Radiological-Nuclear (CBRN) events, scientific report, DRDC – RDDC – 2016-R236, Nov 2016.
[4] Circulaire n° 700/SGDSN/PSE/PSN du 2 octobre 2018, relative à la doctrine nationale d'emploi des moyens de secours et de soins face à une action terroriste mettant en œuvre des matières chimiques.
[5] Espanhol-Soares M, Nociti LA, Machado-Neto JG, Procedures to evaluate the efficiency of protective clothing worn by operators applying pesticide, 2013, 57(8), 1041-53.

ANTIBACTERIAL ACTIVITY OF ORGANO-PHOSPHORUS FLAME RETARDANT INCORPORATED IN PA6 TEXTILE FIBRES

Jelena Vasiljević[1(*)], Marija Čolović[2], Danaja Štular[3], Andrej Demšar[4], Matic Šobak[5], Brigita Tomšič[6], Barbara Simončič[7], Ivan Jerman[8]

[1, 3, 4, 6, 7] University of Ljubljana, Faculty of Natural Sciences and Engineering, Ljubljana, Slovenia

[2, 5, 8] National Institute of Chemistry, Ljubljana, Slovenia

[(*)] E-mail: jelena.vasiljevic@ntf.uni-lj.si

ABSTRACT

This study evaluates the antibacterial properties of flame retardant polyamide 6/organophosphorus nanocomposite textile fibres developed by our research group. The organophosphorus flame retardant (OP-FR) was incorporated in the polyamide 6 (PA6) matrix during the in situ water-catalysed ring-opening polymerization of ε-caprolactam. Thus prepared PA6 with nanodispersed OP-FR was further used for the melt-spinning of textile filaments. Whilst the uniformly distributed nanodispersed OP-FR enabled achievement of the highly efficient flame retardancy, the specific chemical structure of OP-FR also provided an excellent antibacterial protection against bacteria Escherichia coli and Staphylococcus aureus. This novel flame retardant and antibacterial PA6 textile material represents the promising fundamental structure that can be upgraded to highly valuable multifunctional material.

INTRODUCTION

The development of high-performance multifunctional textiles is of high importance for their advanced protective applications. The excellent processing properties of PA6 and chemical recyclability resulted in the broad use of the PA6 fiber in the construction industry, transport vehicles, home textiles, upholstering furniture and carpets. However, the biggest drawback of PA6 is its inherent flammability and burning with intensive flammable melt-dripping. In spite of the successful production of the FR polyamide melt-compounded materials, the commercially available FR PA6 textile fibers still do not exist (Horrocks et al. 2019, Simonetti et al. 2019, Mourgas et al. 2019, Vasiljević et al. 2019). By using the in situ polymerization of ε-caprolactam in the presence of non-reactive bridged DOPO derivative, our research group developed one-step production of a fiber-forming PA6 with well-dispersed physically incorporated FR in the PA6 matrix, which has proven to be highly beneficial for the effective flame retardancy at lowered FR concentrations. Despite the broad use of the organophosphorus compounds as pesticides, the antimicrobial activity of the organophosphorus flame retardants is rarely investigated.

The antibacterial properties of the reference PA6 fibres, and PA6 fibres with incorporated OP-FR at concentrations equal to 10 and 15 wt. % (samples codes: PA6, PA6/10 OP-FR and PA6/15 OP-FR, respectively) were evaluated for the Gram-negative bacterium Escherichia coli ATCC 11229 and the Gram-positive bacterium Staphylococcus aureus ATCC 25923 according to the ASTM E 2149–01 standard method.

RESULTS AND CONCLUSIONS

The results for the antibacterial activity against bacteria E. coli and S. aureus are shown in Fig. 1. The tested PA6, PA6/10 OP-FR and PA6/15 OP-FR samples showed different ability towards the reduction of bacterial growth in inoculum. Different ability of E. coli and S. aureus to adhere to the fibres surface cased the reduction of S. aureus growth up to 84 %, whilst the reduction of E. coli was equal to 7.5 %. The reason for this was higher adherence tendency of S. aureus compared to E. coli, because S. aureus possess intercellular adhesins, which uses as adhesion-promoting materials, whilst E. coli adhesion is mainly driven by interplay of van der Waals, electrostatic, and hydrophobic interactions. In the case of PA6/10 OP-FR and PA6/15 OP-FR, the reduction of E. coli growth increased up to 100 % for the

higher OP-FR concentration, indicating OP-FR's biocidal activity. The OP-FR also promoted the reduction of S. aureus growth up to 100 % even for the PA6/10PHED sample.

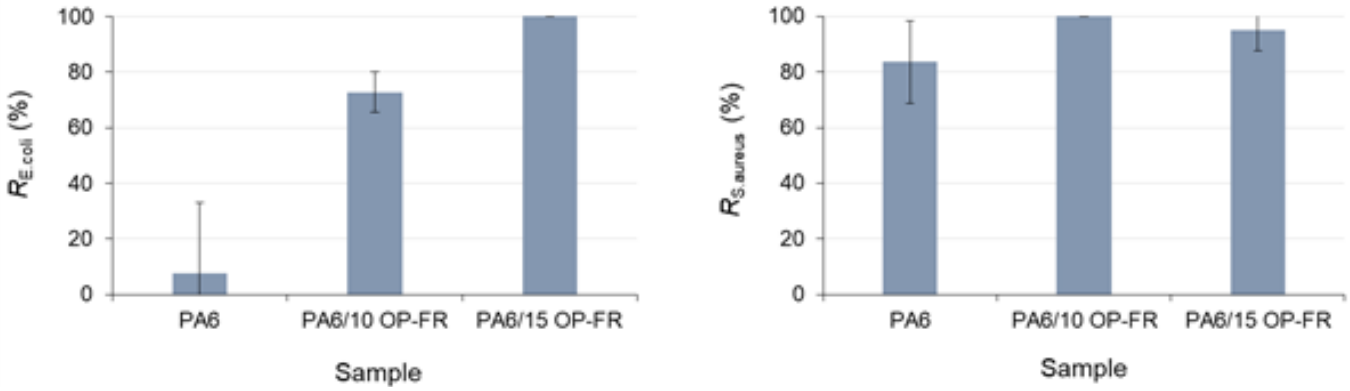

Fig.1 Bacterial reduction, R, of E. coli (left) and S. aureus (right) obtained on PA6, PA6/10 OP-FR and PA6/15 OP-FR samples

ACKNOWLEDGMENTS

The authors gratefully acknowledge the funding by Slovenian Research Agency—Slovenia, under grants Z2-9250, P2-0213 and P2-0393.

REFERENCES

[1] Horrocks AR, Sitpalan A, Kandola BK. Design and characterisation of bicomponent polyamide 6 fibres with specific locations of each flame retardant component for enhanced flame retardancy. Polym Test, 2019, 79, p. 106041.
[2] Simonetti P, Nazir R, Gooneie A, Lehner S, Jovic M, Salmeia KA, Hufenus R, Rippl A, Kaiser J-P, Hirsch C. Michael addition in reactive extrusion: A facile sustainable route to developing phosphorus based flame retardant materials.
[3] Compos Part B Eng, 2019, 178, p. 107470.
[4] Mourgas G, Giebel E, Schneck T, Unold J, Buchmeiser MR. Syntheses of intrinsically flame-retardant polyamide 6 fibers and fabrics. J Appl Polym Sci, 2019, 136, p. 47829.
[5] Liu K, Li Y, Tao L, Liu C, Xiao R. Synthesis and characterization of inherently flame retardant polyamide 6 based on a phosphine oxide derivative. Polym Degrad Stab, 2019, 163, p. 151-160.
[6] Vasiljević J, Čolović M, Jerman I, Simončič B, Demšar A, Samaki Y, Šobak M, Šest E, Golja B, Leskovšek M, Bukošek V, Medved J, Barbalini M, Malucelli G, Bolka S. In situ prepared polyamide 6/DOPO-derivative nanocomposite for melt-spinning of flame retardant textile filaments. Polym Degrad Stab, 2019, 166, p. 50-59.

HYBRID MATERIALS FOR RADIATION SHIELDING

José Carlos Almeida[1(*)], Luís M. Ferreira[2,3], M. Helena Casimiro[3], Fernanda M.A. Margaça[2,3], Isabel M.M. Salvado[1]
[1] CICECO, Department of Materials and Ceramic Engineering, University of Aveiro, 3810-193 Aveiro, Portugal
[2] DECN, Departamento de Engenharia e Ciências Nucleares, Instituto Superior Técnico, Universidade de Lisboa, 2695-066 Bobadela, Portugal
[3] C2TN, Centro de Ciências e Tecnologias Nucleares, Instituto Superior Técnico, Universidade de Lisboa, 2695-066 Bobadela, Portugal
[(*)] Email:jcalmeida@ua.pt

ABSTRACT
In the present work a new organic-inorganic hybrid material based in the system polydimethylsiloxane (PDMS)–SiO2–BO3 is being developed for neutron shielding applications. Some compositions containing ZrO2 and Bi2O3 were prepared for X-ray and gamma radiation shielding. Research work involved the structural characterization of these new materials by FT-IR, solid state nuclear magnetic resonance, and X-ray diffraction, before and after radiation exposure to determine if any structural change occurs.

INTRODUCTION
High-energy ionizing radiation can be a problem in industrial and medical systems, aerospace industries (cosmic radiation), particle accelerator work, nuclear power facilities and in any scenario with a risk of radioactive contamination etc. It is important to contain the radiation, preventing it from causing physical harm to operational agents and equipment [1].
The process of controlling the effects and degree of penetration of radiation varies according to the type involved: electrons, protons, neutrons, gamma rays, or X-rays. The materials shielding capacity for the different types of radiation dependent on their composition and structural organization interaction [1].
During the last two decades the study of nanocomposites demonstrated that due to their high surface area/volume ratio, nanoparticles can have an enhanced ability to absorb and/or scatter ionizing radiation [2,3]. Hybrid materials based on polydimethylsiloxane (PDMS) has been considered a good material for coatings of metals [4], stones [5] and textiles [6]. Different hybrid PDMS-oxide systems have been studied in the last years for applications like biomaterials [7,8], stone coating protection and photonics [9,10]. Some nanocomposites based in the PDMS-TiO2 [3] and PDMS-Bi2O3 [11,12] systems were evaluated regarding their radiation shielding capability and demonstrated good potential for such application, besides that with Bi2O3 can be an efficient friendly substitute to harmful lead based compounds, still in use nowadays for general shielding purposes.
Further its radiation shielding capability, these PDMS-based materials presents a high hydrophobic surface and can withstand working temperatures [13] exceeding the limits (150 to 200 °C) presented by materials with polyethylene-containing compositions (commonly used for neutron radiation shielding applications) [1,14].
With the knowledge obtained in recent works [7,15,16], it is possible to prepare, using sol-gel technology, true PDMS based hybrid structures, with very small inorganic nanodomains (bellow 10 nm size) of oxides known by their ability to absorbed (ZrO2, HfO2, Bi2O3) or scatter (boron oxide) radiation produced by different sources [1–3,11,14,17,18].
The proposed challenge is to develop new hybrid materials by sol-gel chemical process, and achieve a unique solution that can serve simultaneously to protect from ionizing radiation and neutrons. For this, PDMS-based systems should include in their composition oxides of bismuth or tungsten (for ionizing radiation shielding) and boron (for neutrons shielding). Materials preparation is underway at CICECO (Univ. Aveiro) and the radiation assays are under the responsibility of C2TN, area of Radiation Technologies (Instituto Superior Técnico).

ACKNOWLEDGMENTS

This work was developed within the scope of the project CICECO-Aveiro Institute of Materials, UIDB/50011/2020 & UIDP/50011/2020, financed by national funds through the FCT/MCTES and when appropriate co-financed by FEDER under the PT2020 Partnership Agreement.

Authors also thank to C2TN Strategic Program, C2TN UIDB/04349/2020, financed by national funds through the FCT/MCTES.

REFERENCES

[1] A.I. Wozniak, V.S. Ivanov, O.A. Zhdanovich, V.I. Nazarov, A.S. Yegorov, Orient. J. Chem. 33 (2017) 2148–2163.

[2] A. Mesbahi, H. Ghiasi, Appl. Radiat. Isot. 136 (2018) 27–31.

[3] S. Nambiar, J.T.W. Yeow, ACS Appl. Mater. Interfaces 4 (2012) 5717–5726.

[4] N. Hijon, M. Manzano, A.J. Salinas, M. Vallet-Regi, Chem. Mater. 17 (2005) 1591–1596.

[5] M.R. Elvira, M.A. Mazo, A. Tamayo, F. Rubio, J. Rubio, J. Chem. Chem. Eng. 7 (2013) 120–131.

[6] Z.-Y. Deng, W. Wang, L.-H. Mao, C.-F. Wang, S. Chen, J. Mater. Chem. A 2 (2014) 4178.

[7] J.C. Almeida, A. Wacha, P.S. Gomes, M.H.R. Fernandes, M.H.V. Fernandes, I.M.M. Salvado, Mater. Sci. Eng. C. Mater. Biol. Appl. 64 (2016) 74–86.

[8] J.C. Almeida, A. Wacha, P.S. Gomes, L.C. Alves, M.H.V. Fernandes, I.M.M. Salvado, M.H.R. Fernandes, Mater. Sci. Eng. C 62 (2016) 429–438.

[9] X.-X. Zhang, B.-B. Xia, H.-P. Ye, Y.-L. Zhang, B. Xiao, L.-H. Yan, H.-B. Lv, B. Jiang, J. Mater. Chem. 22 (2012) 13132.

[10] X. Zhang, H. Ye, B. Xiao, L. Yan, H. Lv, B. Jiang, J. Phys. Chem. C 114 (2010) 19979–19983.

[11] H.A. Maghrabi, A. Vijayan, P. Deb, L. Wang, Text. Res. J. 86 (2016) 649–658.

[12] P. Jarka, T. Tanski, W. Matysiak, L. Krzeminski, B. Hajduk, M. Bilewicz, Appl. Surf. Sci. 424 (2017) 206–212.

[13] J.C. Almeida, A.G.B. Castro, J.J.H. Lancastre, I.M. Miranda Salvado, F.M.A. Margaça, M.H.V. Fernandes, L.M. Ferreira, M.H. Casimiro, Mater. Chem. Phys. 143 (2014) 557–563.

[14] M.I. Sayyed, Chinese J. Phys. 54 (2016) 408–415.

[15] J. Carlos Almeida, A.G.B. Castro, I.M. Miranda Salvado, F.M.A. Margaça, M.H. Vaz Fernandes, Mater. Lett. 128 (2014) 105–109.

[16] J.C. Almeida, A. Wacha, A. Bóta, L. Almásy, M.H. Vaz Fernandes, F.M.A. Margaça, I.M. Miranda Salvado, Polymer (Guildf). 72 (2015) 40–51.

[17] A. Labouriau, T. Robison, C. Shonrock, S. Simmonds, B. Cox, A. Pacheco, C. Cady, Radiat. Phys. Chem. 144 (2018) 288–294.

[18] S. Nambiar, E.K. Osei, J.T.W. Yeow, J. Appl. Polym. Sci. 127 (2013) 4939–4946.

LIQUID DETECTION BASED ON C-OTDR AND OPTICALLY HEATED CO^2+-DOPED FIBERS

Agnese Coscetta[1], Ester Catalano[1], Enis Cerri[1], Nunzio Cennamo[1], Aldo Minardo[1], and Luigi Zeni[1]
[1] Department of Engineering, Università della Campania Luigi Vanvitelli, Via Roma 29 Aversa - Italy
(*)E-mail: aldo.minardo@unicampania.it

ABSTRACT
In this work, we propose a scheme for quasi-distributed detection of liquids based on optically absorbing (Co^2+--doped) optical fibers. The proposed sensor exploits periodical heating of short sections of Co^2+-doped fibers, and phase modulation detection using Coherent-Optical Time Domain Reflectometry (C-OTDR). We show that the sensor is able to discriminate the medium surrounding the doped fibers.

INTRODUCTION
Fluid leaks or liquid intrusions often indicate serious failure conditions in systems like pipelines, industrial plants, water supply systems, etc. These systems necessitate distributed or multiple point liquid detection sensors. In sensors based on actively heated optical fibers, the temperature transient may be employed to gain information about the medium surrounding the fiber, such as its phase (Chen, 2005), or thermal conductivity (Agliata, 2019). Optical active heating may be obtained in specialty fibers, whose core is doped with transition metal ions (namely Co^2+ or Vn+). In this work, we propose the use of C-OTDR in order to discriminate the medium surrounding one or more Co^2+-doped fiber sections. The proposed approach can be used to perform vibration measurements along the whole fiber, by C-OTDR measurements at 850 nm, as well as liquid detection in selected positions by active heating at 1550 nm. Co^2+-doped fibers are characterized by high optical absorption at 1550 nm. By pumping the fiber with a modulated optical pump, the induced modulation of the fiber temperature can be monitored through C-OTDR, as the latter is sensitive to optical phase changes occurring along the sensing fiber. For a given optical pumping modulation frequency, the induced phase modulation (i.e. the C-OTDR signal) is affected by the thermal conductivity of the surrounding medium: in case of fluids with low thermal conductivity, like air, the time constant will be higher, compared to the case in which the fiber is surrounded by water or other conductive fluids. The pump modulation frequency must be carefully chosen. In fact, if the modulation frequency is too low, the laser noise will be dominant. Conversely, for too high modulation frequencies, the heat generated into the core does not reach the surrounding medium, thus the fiber response will be independent of the external medium. In our tests, a 5 Hz modulation frequency was found to be a good choice, in order to discriminate between air, water and acetone.

EXPERIMENTAL RESULTS
The C-OTDR sensor used for the tests is shown in Fig.1. The setup implements an intensity-based heterodyne C-OTDR scheme, with the addition of an 850nm/1550nm wavelength division multiplexing (WDM) splitter. Heating is performed by a 1550-nm DFB diode laser, with a nominal output power of 40 mW. The laser optical power was directly modulated at 5-Hz frequency and 13% modulation depth, by acting on its driving current. The sensing fiber was composed by a 160m-long standard single mode fiber (SMF), followed by a 10-cm section of Co^2+ doped fiber, a 10-m section of SMF, and a final 10-cm segment of Co2+-doped fiber. The Co^2+-doped fibers had an optical absorption equal to 50 dB/m at 1550 nm.

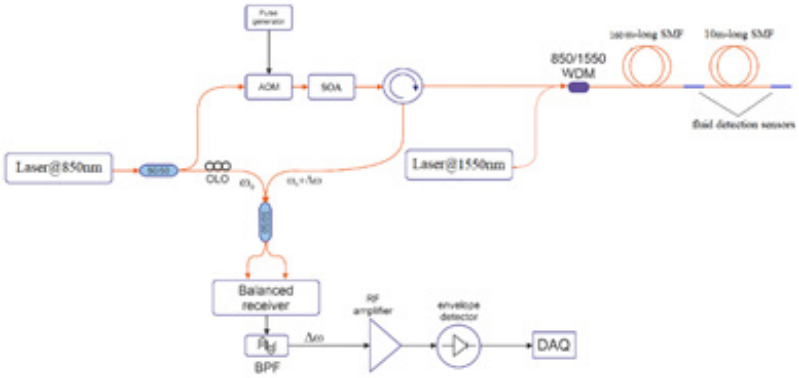

Fig.1 Experimental setup. AOM: acousto-optic modulator; SOA: semiconductor optical amplifier; WDM: wavelength division multiplexing; BPF: bandpass filter; DAQ: data acquisition card.

Figure 2 reports the average and standard deviation of the detected signal at 5-Hz, over a set of 100 consecutive measurements. The reported amplitude has been calculated as the ratio between the 5-Hz spectral component of the C-OTDR signal at the monitored section, divided by the mean signal over the same section. The obtained results are in qualitative agreement with what expected: in fact, the signal increases with the thermal conductivity of the external medium, being the largest when the fiber is immersed into water, compared to acetone (intermediate thermal conductivity) and air (lowest thermal conductivity).

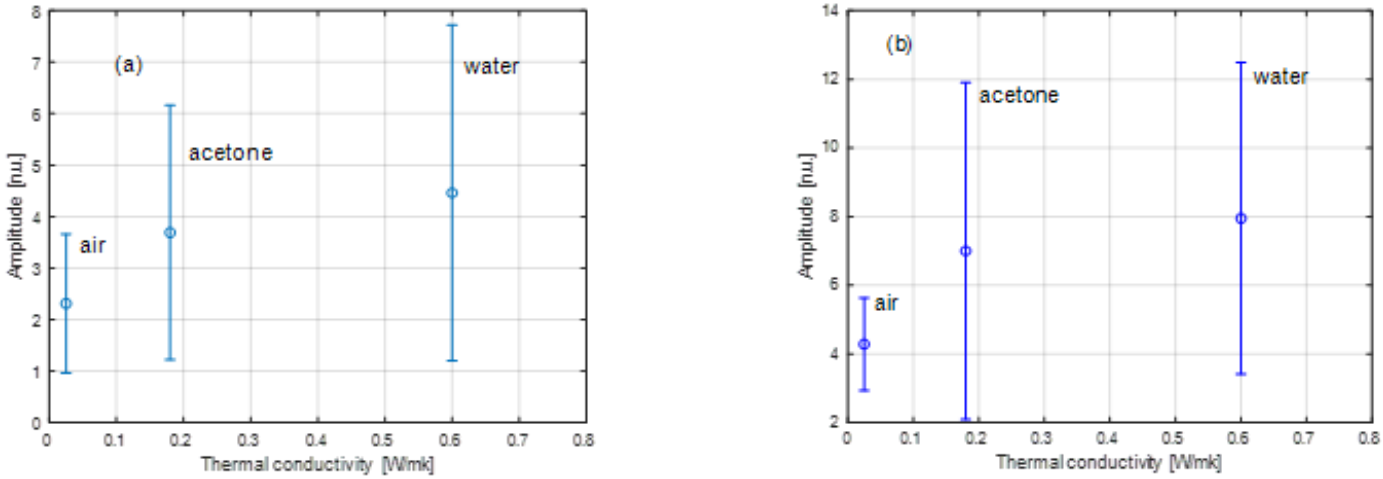

a) b)

Fig. 2 Normalized amplitude of the 5-Hz spectral component at the (a) first section or the (b) second section.

REFERENCES

[1] Agliata R, Bogaard TA, Greco R, Minardo A, Mollo L, Steele-Dunne S.C. Non-invasive water content estimation in a tuff wall by DTS. Constr Build Mater, 2019, 197, p. 821-829.

[2] Chen KP, McMillen B, Buric M, Jewart C, Xu, W. Self-heated fiber Bragg grating sensors. Appl Phys Lett, 2005, 86, p. 143502.

FROM COLORIMETRIC SENSORS TO DETOXIFYING SENSORS FOR ENHANCED PERSONAL PROTECTIONS AGAINST VAPOROUS TOXICANTS

Peixin Tang, Gang Sun(*)
Department of Biological and Agricultural Engineering, University of California, Davis, USA.
(*) E-mail: gysun@ucdavis.edu

ABSTRACT
Highly sensitive, easy use, and paper like colorimetric sensors were developed for rapid and onsite detection of several fumigants that are widely employed in agricultural production in California. The sensors were developed based on a combination of novel nanofibrous materials, colorimetric reactions, surface and theoretical chemistry, and Hansen Solubility parameter theory. Based on the success, advanced sensors that can detoxify fumigants and then reveal a color change when the exposure level of the toxicant has accumulatively reached a critical level. Both sensors can be employed by farm workers and residents living near agricultural fields. This presentation will present the design, selection of materials and colorimetric reactions, and outstanding performance of the sensors.

INTRODUCTION
Highly sensitive and portable sensors are tools to improve personal protection from exposures to unwanted toxic chemicals. Fumigants, a group of odorless, colorless, and highly toxic compounds, are widely used in agricultural productions, post-harvest and household pest controls, including methyl bromide, methyl iodide, 1,3-dichlorrpropyne, chloropicrin, methyl isothiocyanate, and sulfuryl fluoride. Based on the properties of high vapor pressure, colorless, acute and chronical toxicity, the developments of highly sensitive and personal use sensors and protective materials has been challenging to researchers. In recent years, we adopted chemical and biological detoxification and toxicological reactions in the human body as colorimetric detection methods to design the colorimetric sensors for these fumigants and achieved significant progresses [1-6]. Several key design features of the ultrasensitive and easy to use sensors will be discussed in detail in the presentation. Here are several key features of the sensors.

The first important feature is the use of nanofibrous membranes. In order to achieve the ultrahigh sensitivity in detection of trace amount of the chemicals by the designed sensors, nanofibrous membranes possessing ultrahigh specific surface areas are selected as sensor matrices to achieve the requirements of ultrahigh detection sensitivity, low limit of detection, and personal use. The membranes are paper-like materials which can be made into a filter device for easy use.

Additionally, selected solvent systems play another important role in increasing sensitivity and selectivity of designed sensors, which were determined based on Hansen solubility parameter theory. The solvents are none evaporative under ambient environment and highly interactive with specific fumigant molecules.

Furthermore, the reagents were selected based on computational analysis and experimental tests, possessing the highest colorimetric reaction efficiency. The entire sensor system presents a compromise of innovation and practicality.

With the successful development of colorimetric sensors for several fumigants, novel colorimetric sensors with de-

toxifying functions were designed and prepared. The materials can effectively remove and detoxify the target toxic chemical and show a color change when the sensor has been accumulative exposed to a critical level of the toxicant. This sensor can further enhance personal protection to users if it is used on protective clothing.

CONCLUSIONS

Three simple paper based colorimetric sensors were prepared and demonstrated ultrahigh sensitivity in ambient environment. Advanced detoxifying colorimetric sensor for alkylating fumigants was prepared as well, which can serve as a good example for development of future smart sensors.

ACKNOWLEDGMENTS

California Department of Pesticide Regulation financially supported the work.

REFERENCES

[1] Tang P, Sun G. Highly sensitive colorimetric paper sensor for methyl isothiocyanate (MITC): Using its toxicological reaction, Sensors & Actuators: B. Chemical, V261, 2018, 178-187.

[2] Tang P, Leung HT, Gomez, MT, Sun G. Sensitivity-tunable Colorimetric Detection of Chloropicrin Vapor on Nylon-6 Nanofibrous Membrane Based on a Detoxification Reaction with Biological Thiols. ACS sensors 2018, 3 (4), pp 858–866. DOI: 10.1021/acssensors.8b00135

[3] Tang P, Leung HT, Sun G. Colorimetric Detection of Carcinogenic Alkylating Fumigants on Nylon-6 Nanofibrous Membrane. Part I: Investigation of 4-(p-Nitrobenzyl)pyridine as a “New” Sensing Agent with Ultrahigh Sensitivity, Anal. Chem., 2018, 90 (24), pp 14593–14601

[4] Tang P, Gomez, MT. Leung HT, Sun G. Bio- inspired ultrasensitive colorimetric detection of methyl isothiocyanate on nylon-6 nanofibrous membrane: A comparison of biological thiol reactivities. Journal of Hazardous Materials, 2019, 362, pp.375-382.

[6] Tang P, Nguyen NT, Lo J G, Sun G. "Colorimetric Detection of Carcinogenic Alkylating Fumigants on Nylon 6 Nanofibrous Membrane. Part II: Self-Catalysis of 2-Diethylaminoethyl Modified Sensor Matrix for Improvement of Sensitivity." ACS applied materials & interfaces, 2019. 1 (14), pp 13632–136415.

[7] Tang P, Zhang M, Ji B. Yong T, Sun G. Hierarchical Nucleophilic Nanofibrous Membranes for Fast, Durable, and Bare-Eye Visible Detoxification of Carcinogenic Alkylating Toxicants, Advanced Functional Materials, 2019, 29. 1905990 (10 pages).

MECHANICAL METAMATERIALS FOR SENSOR PROTECTION UNDER BLAST CONDITIONS

Luuk Lubbers[1(*)], Mat Philippens[1] and Jaap Weerheijm[1,2]
[1] TNO, Defence Security and Safety, P.O. Box 480, 2496 ZA Den Haag, The Netherlands
[2] Faculty of Civil Engineering and Geosciences, Delft University of Technology, Delft, The Netherlands
[(*)] E-mail: luuk.lubbers@tno.nl

ABSTRACT
Mechanical metamaterials – man-made materials which derive their unusual properties from their structure rather than their composition (Bertoldi, 2017) – are able to prohibit the propagation of mechanical waves in a pre-defined frequency band, the so-called band gap (Hussein, 2014, Krushynska, 2017). Here we show how metamaterials that exhibit a bandgap can be used to design a mechanical low-pass filter with a given frequency-characteristic, with the goal to protect acceleration sensors under blast and ballistic conditions. These metamaterials should replace improvised methods for sensor protection, which commonly consist of clamped rubbers with a non-reproducible transfer function (Drysdale, 2014). Based on simulations and experiments we demonstrate how our metamaterial performs as an efficient low pass filter according to the designed transfer function.

INTRODUCTION
Accelerometers are widely applied for shock measurements on military vehicle systems that are subjected to ballistic and blast threats. Resulting structural shocks typically lead to accelerations that consist of a wide frequency spectrum ranging from 0 to 100 kHz. From an experimental point of view only frequencies up to approximately 5 kHz are of interest for the occupants and mechanical equipment, and up to 10 kHz for electronics, as these low frequency ranges carry the largest energy density. To measure accelerations it therefore seems evident to utilize an accelerometer that is designed to accurately capture frequencies within the 0-10 kHz range, while simultaneously neglecting the higher frequency components. However, accelerometers suitable for the low frequency components (< 10 kHz) are unable to cope with and get damaged by the high frequency components (> 10 kHz). On the other hand, broad-banded accelerometers could be used, but these in turn lead to unsatisfying signal resolutions for the frequency regime we are interested in.
Current workarounds that enable the application of sensitive accelerometers (0 -10 kHz) consist for instance of a protective layer formed by rubber layers clamped between plates (Drysdale, 2014). This solution is badly controlled however, since the transfer function is sensitive to small differences in e.g. the amount of clamping, such that the initial signal cannot unambiguously be reconstructed.
Here we show how a mechanical low-pass filter can be developed that does not suffer from the above mentioned issues. To do so, we will develop a metamaterial inspired filter – based on the phononic bandgap – which exhibits a well-defined transfer function, thus opening up new avenues for sensor protection. Our filter design is guided by numerical simulations and we show experimentally that our filter outperforms a conventional plain rubber filter.

RESULTS AND CONCLUSIONS
The results from our simulations and experiments are shown in Fig. 1. First, we have simulated circular steel inclusions on the square grid that are embedded in a rubber matrix. As can be seen, plane wave perturbations that approach from the left (blue indicates low displacements, yellow/red high displacements) cannot propagate through the metamaterial: the plane wave's frequency lies inside the bandgap. Second, we have manufactured an experimental sample based on the numerical simulations, and in addition we also fabricated a plain rubber reference sample. We

then tested these samples on a shaker and measured the input versus output amplitude as function of frequency; the result is shown in Fig.1 This clearly demonstrates that the metamaterial (blue) displays a bandgap around 2-7 kHz and damps much more effectively than the plain rubber (red).

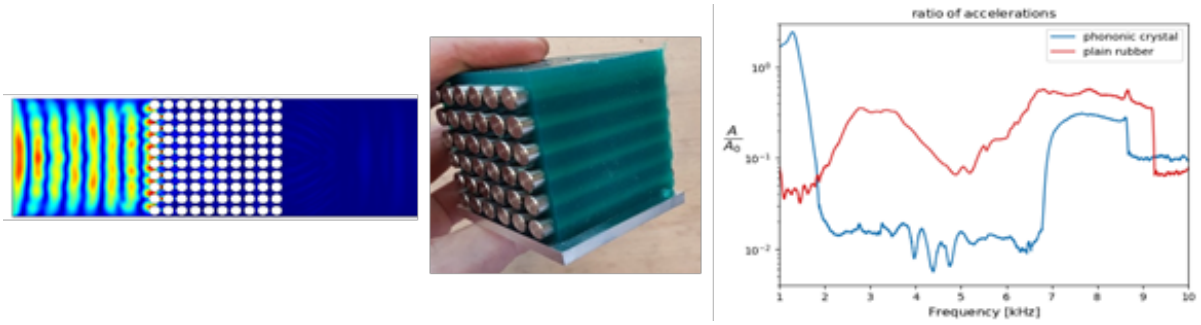

Fig.1 From left to right: simulations, experimental sample and experimental results.

This study demonstrates the potential of bandgap mechanical metamaterials for sensor protection. Further research should be performed in order to shift the bandgap towards higher frequencies and to widen the bandgap in order to finalize the design for the mechanical low-pass filter. Preliminary simulations have already shown that this can possibly be achieved by using a stiffer matrix material and by using gradients in the inclusion geometry. Finally, we note that the bandgap method applied here does not constrain the maximum allowable size of the metamaterial to that of the sensor, thus enabling broad practical applicability.

ACKNOWLEDGMENTS

The authors gratefully acknowledge the funding by the Dutch Ministry of Defence in the RVO program.

REFERENCES

[1] Bertoldi, K., Vitelli, V., Christensen, J., & van Hecke, M. (2017). Flexible mechanical metamaterials. Nature Reviews Materials, 2(11), 1-11.

[2] Hussein, M. I., Leamy, M. J., & Ruzzene, M. (2014). Dynamics of phononic materials and structures: Historical origins, recent progress, and future outlook. Applied Mechanics Reviews, 66(4).

[3] Krushynska, A. O., Miniaci, M., Bosia, F., & Pugno, N. M. (2017). Coupling local resonance with Bragg band gaps in single-phase mechanical metamaterials. Extreme Mechanics Letters, 12, 30-36.

[4] Drysdale, A., Sorensen, R., Prichett, J., Low-Frequency Foam Insulator (LOFFI) accelerometer mount characterization, Results and analysis for phase I (FY2013), ARL-TR-6977, June 2014. Army Research Laboratory, Aberdeen Proving Ground, MD 21005-5068

OPTIMIZATION OF GRADIENT LATTICE CORE SANDWICH STRUCTURES UNDER DYNAMIC LOADING WITH ARTIFICIAL NEURAL NETWORK AND GENETIC ALGORITHM

Konstantin Kappe[1(*)], Marius Bierdel[1], Aron Pfaff[1], Klaus Hoschke[1]
[1] Fraunhofer-Institut für Kurzzeitdynamik, Ernst-Mach-Institut, EMI, Freiburg, Germany
[(*)] E-mail: konstantin.kappe@emi.fraunhofer.de

ABSTRACT
In this paper we present an optimizied procedure to effectively design gradient lattice core sandwich structures (GLS) under dynamic loading like crash, impact or blast in order to improve the energy absorbing characteristics and decrease the mass. The modelling and simulation of GLS is time consuming and computable expensive. To model and simulate the structures efficiently a simplified simulation FE-model is introduced. The simulation data is verified with experimental tests. Furthermore, an automatic system to generate the FE-models under varying input parameters is created. To find the optimal configuration of the GLS an artificial neural network (ANN) is used to predict the energy absorbing characteristics for the given design parameters. The ANN is trained by a set of FE-simulations. Subsequently, a genetic algorithm (GA) is used to find the optimal combination of the design parameters.

INTRODUCTION
For the last years lightweight cellular structures like honeycombs, foams or lattices have gained notable attention. Their remarkable mechanical properties such as increased specific strength and stiffness or their energy absorbing capabilities make them attractive for many applications (Altenbach, 2010). They are used for applications under dynamic loads, such as crash, impact or blast mitigation. However, numerous configurations of geometries, arrangements or dimensions of unit cells are imaginable. Therefore, it is difficult to find an optimal design for different requirements without great effort.
The importance of geometrical parameters like lattice diameter or the topology of the unit cells for sandwich structures on the dynamic response and energy absorbing characteristics is proven in various studies (Imbalzano, 2016),(Tancogne-Dejean, 2016). It is shown, that the variation of certain parameters could improve resistance and energy absorbing capabilities. Furthermore, studies have shown that advanced configurations with functionally grated properties like beam diameter show improved characteristics when compared with uniform structures and materials. They show a controlled collapse and higher energy absorbing efficiency (Xu, 2018).
Therefore, the application of numerical optimization methods in the design of sandwich structures to further improve the energy absorbing characteristics has attracted increasing attraction. However, the characteristics of energy absorbing materials imply nonlinearities like large displacements, contact and material nonlinearities. Furthermore, multi-objectives are common in energy absorbing structures. For crashworthiness, for example, maximizing the absorbed energy and minimizing the reaction forces are fundamental.
In (Qi, 2013) aluminum foam-cored sandwich panels under blast loading are optimized using ANN approximation models, minimizing the maximum back face deflection and maximizing the specific energy absorption. The influence of material and geometry in the performance of auxetic lattice core sandwich structures are investigated in previous studies (Imbalzano,2016). In order to find an optimal configuration for blast loads, various parameters are investigated and the preferred combination is determined with design of experiment and a general linear model.

In this study GLS are optimized under dynamic loading. An example of a GLS is shown in Figure 1. The objective is to improve the specific energy absorbing characteristics of the GLS by varying the geometric design variables like average beam diameter, lattices gradient, and back and front plate thickness as well as the cell topology. Thereby, different auxetic and nonauxetic cell topologies are investigated. The optimization is performed by ANN and GA. The optimization procedure is shown in figure 2. While ANN is used to reduce computational effort and effective prediction of the structural response under dynamic loading, GA is applied to find the global optimum. The ANN is trained by a set of near random samples of variation of the design variables. The set is created using uniform latin hypercube sampling. Automated FEmodeling and simulations of the variations are performed to calculate the structural behavior. Therefore, a simplified beam- and shell-based simulation model for GLS is developed.

Fig 1 Graded lattice core sandwich structure

RESULTS AND CONCLUSIONS

In this paper a method for optimizing GLS is presented. To train the ANN a simplified simulation FE-model is developed and verified with drop weight and impact experiments. Genetic algorithm enables a global optimization for the given design variables. This procedure enables the optimization of GLS for dynamic loading conditions. Optimization is performed for blast loading. However, optimization for local impact and crashworthiness as well as optimization of multilayer sandwich structures are also imaginable and potential for further research.

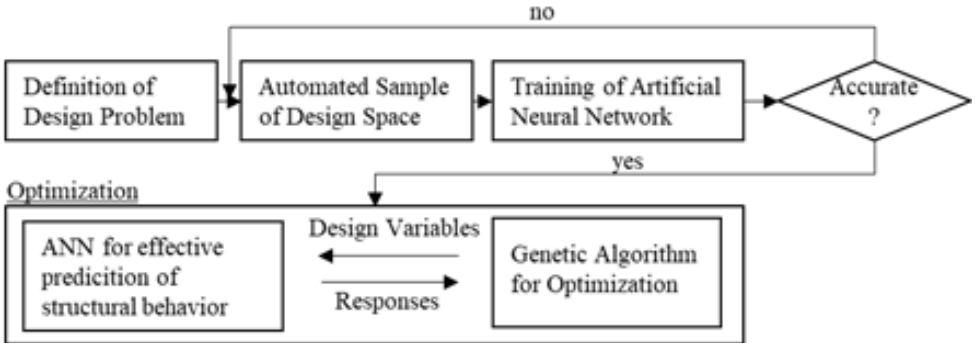

Fig 2 Optimizing procedure for graded lattice core sandwich structures

REFERENCES

[1] Altenbach H., Oechsner A., Cellular and porous materials in structures and processes, SpringerVerlag Wien, 2010
Qi C., et al., Blast resistance and multi-objective optimization of aluminum foam-cored sandwich panels, 2013, Composite Structures, 105, pp. 45-57
[2] Imbalzano G., et al., Influences of Material and Geometry in the Performance of Auxetic Composite Structure under Blast Loading, Appl Mech Mater, 2016. 846: pp. 476-481
[3] Tancogne-Dejean T., Additively-manufactured metallic micro-lattice materials for high specific energy absorption under static and dynamic loading, Acta Mater,116(2016), pp.14-28
[4] Xu F., et al., A review on functionally graded structures and materials for energy absorption, Eng Struct, 171 (2018), pp. 309-32

USING MACHINE LEARNING TO PREDICT THE BALLISTIC RESPONSE OF MATERIALS AND SUPPLEMENT DATASETS

Samuel Thompson[1(*)], Filipe Teixeira-Dias[2], Mariana Paulino[3]
[1,2] Institute for Infrastructure and Environment, the University of Edinburgh, Edinburgh, Scotland
[3] Faculty of Science, Engineering and Built Environment, Deakin University, Australia
[(*)] E-mail: samuel.thompson@ed.ac.uk

ABSTRACT
The primary goal of this research is to make better predictions regarding the perforation of projectiles through armour systems. This paper demonstrates the ability of Generative Adversarial Networks (GAN) to learn directly from ballistic data and generate new ballistic samples representative of the dataset that it was trained on. A GAN is a more recent framework of machine learning system that can generate entirely new data and make predictions through unsupervised learning. It aims to reduce the costs associated with ballistic experiments by minimising the number of experiments performed and supplementing the dataset by using the GAN model instead. In this paper three training sets of varying quality are used to train three separate GAN models, the predictions of which are then compared with an analytical model.

INTRODUCTION
The Generative Adversarial Network (GAN) is a framework that was first proposed by Goodfellow et al. (Goodfellow, 2014) for estimating generative models via an adversarial process, in which two neural networks compete against one another and are trained together. It is a machine learning technique that learns to generate fake samples indistinguishable from real ones via a competitive game. The base architecture of a GAN is composed of two neural networks: a discriminator and a generator. The discriminator D is set up to maximise the probability of assigning the correct labels to real and fake samples. Meanwhile, the generator is trained to fool the discriminator with synthesised data (Chen, 2020). Multi-Layer Perceptron (MLP) networks were used to create both D and G networks as they are well equipped to deal with regression tasks. The adversarial modelling process is straight forward to apply when both models are MLPs. To test the capabilities of the method, the GAN is challenged with generating data representative of that produced by the Lambert formula (Dor, 2002).

$$v_{res} = a\left(v_{imp}^{p} - v_{bl}^{p}\right)^{\frac{1}{p}}, \quad v_{imp} > v_{bl}$$

(1) where v_{res}, v_{imp} and v_{bl} are the impact, the residual and the ballistic limit velocities in normal impact respectively and a and p govern the shape of the ballistic curve. This was selected for two reasons; the first is that the formula can be used to generate training sets of various quality for each test case and secondly, the parameters are useful metrics to quantitively compare the results of the GAN predictions. The samples generated by the GAN models are fit to the Lambert curve and parameters specific to each model are computed and compared with the original Lambert parameters of $a = 1$, $p = 3$ and $v_{bl} = 100$. The authors considered three different training sets to test the performance of the model where each training set exists as a [N×2] array where the first column corresponds to v_{imp} and the second column to v_{res}. The first training set represents an optimal test case for the machine learning algorithm consisting of 100 logarithmically spaced data points to maximise the number of points around v_{bl}. The second training set consists of 50 data points that are randomly distributed along the Lambert curve. The third training set is most representative of experimental data consisting of only 10 randomly generated samples. However, this time up to ±10 % artificial

noise was added to v_{res} to mimic measurement error to add variance to the training set.

RESULTS AND CONCLUSIONS

Figure 1 (a) shows results from the training process for the GAN trained on the second training set. It shows the percentage error of fitted parameters *a, p* and v_{bl} of samples generated by the GAN at that point in training with the Lambert parameters along with the RMSE. The model was trained for 1 million iterations and a sample output from the trained model is shown in Figure 2 (b). Due to the stochastic nature of the GAN predictions, the GAN was used to generate 100 samples 1000 times and the average RMSE was calculated at 11.99%. Similarly, the Lambert parameters specific to the GAN network were calculated as *a* = 1.00 (±0.00 %), *p* = 3.11 (+ 3.60%) and v_{bl} as 99.27 (- 0.73 %). The samples generated by the GAN model show good agreeability with the Lambert model and is evidence to suggest that the GAN model successfully learned to generate new points representative of the training set.

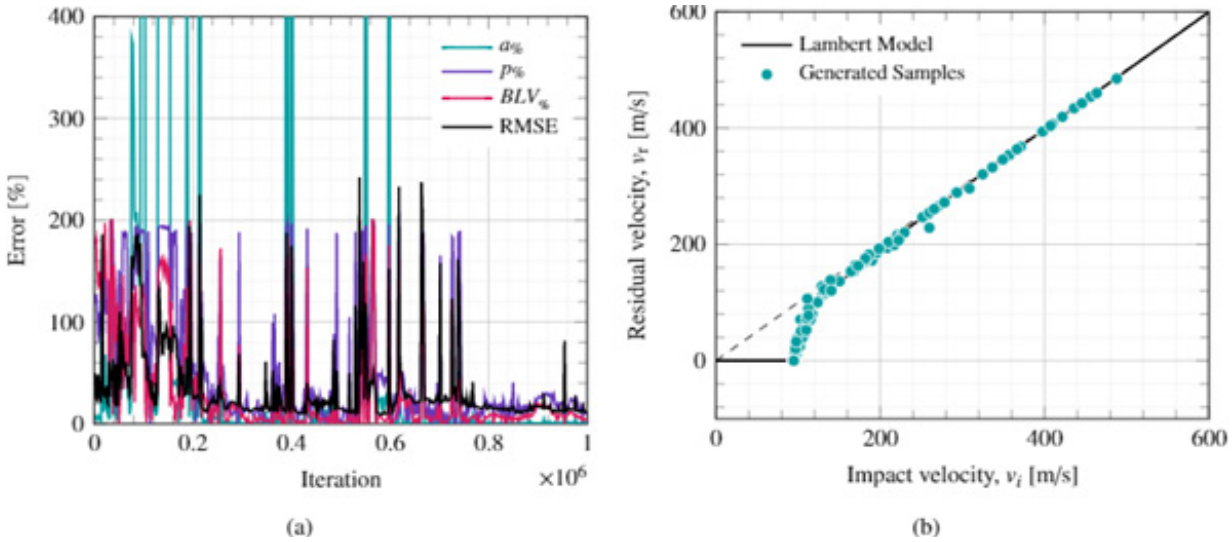

Fig.1 Training process and 100 samples generated by trained GAN2 network

ACKNOWLEDGMENTS

This work was supported by the Engineering and Physical Sciences Research Council [grant number EP/N509644/1].

REFERENCES

[1] I. Goodfellow, J. Pouget-Abadie, M. Mirza, B. Xu, D. Warde-Farley, S. Ozair,A. Courville, Y. Bengio, 2014. Generative adversarial nets, Advances in Neural Information Processing Systems, pp. 2672–2680.

[2] Chen, Z., Wang, C., Wu, H., Shang, K. and Wang, J., 2020. DMGAN: Discriminative Metric-based Generative Adversarial Networks. Knowledge-Based Systems, 192, p.105370.

[3] Ben Dor, G., Dubinsky, A. and Elperin, T., 2002, On the Lambert-Jonas approximation for ballistic impact. Mechanics Research Communications, 29(2-3), pp. 137-139.

FABRICATION OF AUXETIC AND GRADIENT CLOSED CELL FOAM FOR PROTECTIVE EQUIPMENT

Olly Duncan[1(*)], Tom Allen[1], Andrew Alderson[2]
[1] Department of Engineering, Manchester Metropolitan University, Manchester, UK
[2] Materials and Engineering Research Institute, Sheffield Hallam University, Sheffield, UK
[(*)] E-mail: o.duncan@mmu.ac.uk

ABSTRACT
Open cell auxetic foam can have higher indentation resistance and energy absorption during than conventional open cell foam, but is less stiff than closed cell foam often used in protective padding. Following recent work using steam processing to fabricate auxetic closed cell foam, we used constraints during processing to modify cell structure, Young's modulus and Poisson's ratio. From a candidate closed cell foam used in protective equipment, we obtain Poisson's ratios between -1 and 1, and Young's moduli between 1 and 13 MPa.

INTRODUCTION
Auxetic (negative Poisson's ratio) and gradient open cell foams have shown promise for their conformability, indentation resistance and impact energy absorption – useful in protective equipment.1 Open cell auxetic foams are fabricated using compression to modify cell structure, and heating then cooling to fix the imposed cell structure.2 Gradient foams, with different Young's moduli and Poisson's ratios in different regions, have been fabricated by passing pins through foam to vary compression during fabrication.3 Closed cell foam used in protective padding, and foam used in helmets, have Young's moduli of ~1 MPa and ~5 to 20 MPa, respectively;4 ~2 orders of magnitude greater than of open cell auxetic foam (~50 kPa).1 Closed cell auxetic foam can be produced by steaming conventional closed cell foam to drawing cell walls inward to leave a re-entrant cell structure and negative Poisson's ratio upon condensation of steam trapped in the cells.5 Methods to control closed-cell structures in different regions of a sample, or to impact anisotropic characteristics, have not been tested.

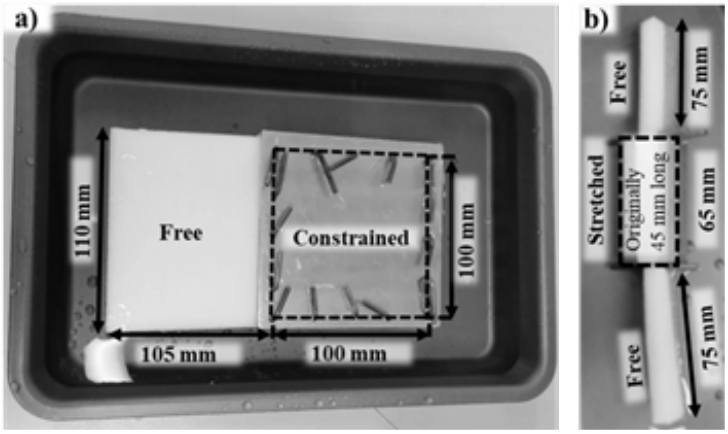

Fig.1. a) Foam sheet with constraints, in container with water, and b) cuboid with central stretched region

Methods developed herein produce auxetic and gradient closed cell foams from commercially available low-density polyethylene foam (Plastazote LD60, Algeos.com). Pins passed through the foam constrained a 10 x 10 x 1 cm region of a 20 x 10 x 1 cm sheet in both 10 cm directions (Figure 1a), and stretched 5 cm long region of a 15 x 2 x 1 cm

cuboid by 1.5 times during conversion (Figure 1b). Samples and constraints were sealed in containers filled to 80% with water (Figure 1a), then placed in conventional ovens at 105 ˚C for 4.5 hours. Samples were removed from containers and left to cool to room temperature within 1 minute of removal from the oven, without removing constraints, then dried (~1 week). Imparted cell structures were compared using micro-computed tomography. Tensile and compression tests up to 10% applied strain, with full-field strain measurement by 2D digital image correlation (LaVision), were used to obtain tangent moduli and Poisson's ratios over 0.5% strain increments.

RESULTS AND CONCLUSIONS

Micro-CT showed that constraining a region of foam focused the volumetric compression imparted by steam in one direction; creating long, thin, re-entrant cells. The constrained region of the gradient sheet had anisotropic Poisson's ratios between 0.2 and -1 (Figure 2, z through thickness), and Young's moduli between 1 and 10 MPa. The gradient cuboid had Poisson's ratios between 1 and -1, and Young's moduli between 1 and 13 MPa; varying across this entire range within gradient foam samples. The produced range of Young's moduli cover a broad spectrum of the range of foams used in protective equipment (~1 MPa) and helmets (~1 to 20 MPa). The wide range of imparted characteristics make an extensive range of application based development and testing possible.

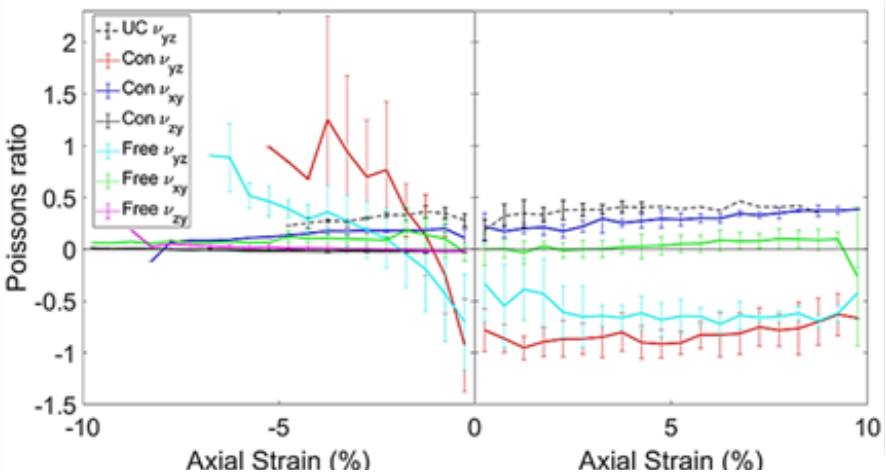

Fig.2 Poisson's ratio vs. axial strain for the gradient sheet, combined with the unconverted (UC) foam, at 0.5% strain increments, error bars show 1 S.D.

REFERENCES

[1] Duncan, O.; Shepherd, T.; Moroney, C.; Foster, L.; Venkatraman, P. D.; Winwood, K.; Allen, T.; Alderson, A. Review of Auxetic Materials for Sports Applications: Expanding Options in Comfort and Protection. Appl. Sci. 2018, 8 (6), 941. https://doi.org/10.3390/app8060941.

[2] Lakes, R. S. Foam Structures with a Negative Poisson's Ratio. Science (80-.). 1987, 235 (4792), 1038–1040. https://doi.org/10.1126/science.235.4792.1038.

[3] Sanami, M.; Alderson, A.; Alderson, K. L.; McDonald, S. a.; Mottershead, B.; Withers, P. J. The Production and Characterization of Topologically and Mechanically Gradient Open-Cell Thermoplastic Foams. Smart Mater. Struct. 2014, 23 (5), 055016. https://doi.org/10.1088/0964-1726/23/5/055016.

[4] Mills, N. J.; Fitzgerald, C.; Gilchrist, A.; Verdejo, R. Polymer Foams for Personal Protection: Cushions, Shoes and Helmets. Compos. Sci. Technol. 2003, 63 (16), 2389–2400. https://doi.org/10.1016/S0266-3538(03)00272-0.

[5] Fan, D.; Li, M.; Qiu, J.; Xing, H.; Jiang, Z.; Tang, T. A Novel Method for Preparing Auxetic Foam from Closed-Cell Polymer Foam Based on Steam Penetration and Condensation (SPC) Process. ACS Appl. Mater. Interfaces 2018. https://doi.org/10.1021/acsami.8b02332.

COMPARISON OF 3D PRINTED CONVENTIONAL AND AUXETIC COMPOSITE STRUCTURES UNDER QUASI-STATIC COMPRESSION FOR SEVERE LOADING APPLICATIONS

Clare A. Burnett[1(*)], Zafer Kazancı[1], and Brian G. Falzon[1]

[1] Advanced Composites Research Group, School of Mechanical and Aerospace Engineering, Queen's University Belfast, Belfast, BT9 5AH, United Kingdom

[(*)] E-mail: cburnett04@qub.ac.uk

ABSTRACT

This study investigates the energy absorption behaviour of various non-auxetic and auxetic unit cells under quasi-static compression. Four cellular structures with identical relative volume were designed and additively manufactured using a composite 3D printing technique.

Compressive results conclude that the auxetic anti-tetra-chiral structure provides superior energy absorption compared with the other structures tested. This therefore promotes the use of auxetic structures as sandwich panel cores under severe loading scenarios.

INTRODUCTION

Sandwich panels are commonly used under a variety of severe loading scenarios given their ability to combine high energy absorbing capabilities with relatively low density. More recently, auxetic structures have been identified as an alternative for the core layer of sandwich panels for defensive applications given the advantageous material enhancements provided (Renet al., 2018). Auxetic structures have been found to behave counterintuitively because of their negative Poisson's Ratio. Within defensive applications, auxetic sandwich structures are commonly composed of metallic face sheets with an embedded metallic core (Imbalzano et al., 2016). Therefore, research is required to investigate auxetic cellular structures composed of lighter alternatives, for example composite materials.

METHODOLOGY

Several common auxetic unit cells are reported within literature (Lim, 2015), and when stacked and repeated form a cellular structure. However, with so many variables dictating the structure's geometry and therefore mass, comparisons between different auxetic cellular topologies can prove difficult. This study investigates the energy absorbing capability of four structures under quasi-static compression. The cellular structures were designed to occupy an overall volume of 60 x 60 x 30 mm3 and have an equal relative volume and hence, mass. Samples were 3D printed using the Markforged Mark Two 3D printers using a composite printing material commercially referred to as Onyx.

The investigated structures are presented in Fig. 1 and include a non-auxetic (a) hexagonal structure and three auxetic alternatives, namely: (b) re-entrant, (c) anti-tetra-chiral, and (d) double arrowhead. Three samples of each structure were compressed using the Zwick Z100 Universal Test Machine with a 100 kN load cell. Compression was conducted at a quasi-static speed of 3 mm/min up to 80% deformation.

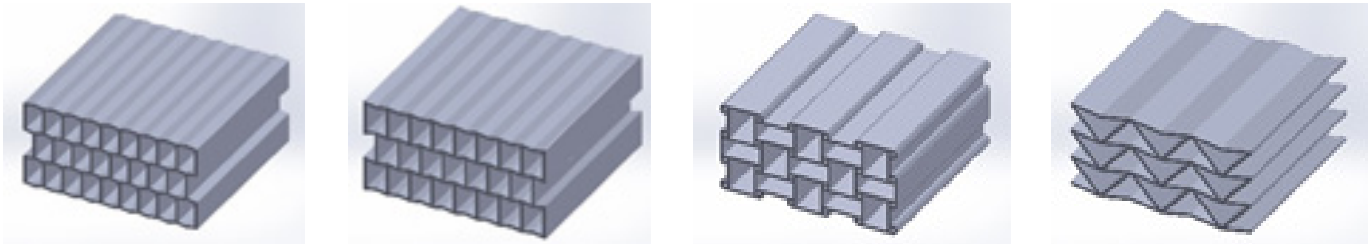

a) Hexagonal (HEX) **b)** Re-entrant (REE) **c)** Anti-tetrachiral (ATC) **d)** Double arrowhead (DAH)

Fig.1 CAD models of the selected structures with equal relative volume of 29%

RESULTS AND CONCLUSIONS

The total energy absorbed by each structure up to 20 mm deformation is presented in Fig. 2. Between 60% - 80% deformation the structures entered final densification. As presented, the anti-tetra-chiral structure provided the greatest energy absorption. This was primarily due to the cylindrical structures which act as hinges and provide internal densification under an applied compressive force. The re-entrant structure provides the lowest energy absorption despite its geometric similarity with the hexagonal structure. However, the re-entrant has fewer unit cells than the hexagonal and therefore provides lower energy absorption despite their similar compressive deformation behaviour.

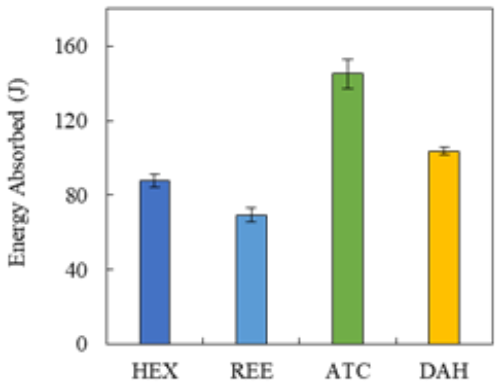

Fig.2 Compressive energy absorption results

As high energy absorption is desirable in severe loading applications, the anti-tetra-chiral cellular structure outperforms the other auxetic and non-auxetic unit cells tested. Future work will involve investigating the compressive capability of auxetic samples under dynamic scenarios.

ACKNOWLEDGMENTS

This research is kindly funded by the Royal Academy of Engineering Industrial Fellowship Programme, the Department for the Economy (NI) and the Dunville Scholarship from Queen's University Belfast.

REFERENCES

[1] Imbalzano G, Tran P, Ngo TD, Lee PVS. A numerical study of auxetic composite panels under blast loading. Composite Structures, 2016, 135, p. 339-352.

[2] Ren X, Das R, Tran P, Ngo TD, Lee PVS. Auxetic metamaterials and structures: A review. Smart Materials and Structures, 2018, 27(2), p. 1-38.

[3] Teik-Cheng Lim. Micromechanical Models for Auxetic Materials. In: Auxetic Materials andStructures. Springer Science + Business Media, Singapore, 2015, p. 45-103.

MANUFACTURING AND STAB RESISTANCE TEST OF 3D WARP INTERLOCK FABRICS WOVEN WITH HMWPE YARNS FOR SOFT BODY AMOUR

Mengru Li[1], Peng Wang[2], Francois Boussu[1(*)], Damien Soulat[1]

[1] Génie des Matériaux Textiles (Gemtex), Ensait, University of Lille, Roubaix, France

[2] Laboratoire de Physique et Mécanique Textiles (Lpmt), Ensisa, University of Upper Alsace, Mulhouse, France

[(*)] E-mail: francois.boussu@ensait.fr

ABSTRACT

In an attempt to overcome many of the problems with the manufacturing and properties of laminates, considerable attention has been given over the past 30 years to the development of advanced composites reinforced with 3D fibre architectures. Meanwhile, stab resistance is a crucial material property in the case of fabrics used in personal protection equipment due to the extensive occurrence of this threat. In this paper, recent advancements in the manufacturing technique of 3D warp interlock fabrics (3DWIFs) with high molecular weight polyethylene (HMWPE) for body armour are presented. Four of the main different types of 3D warp interlock structures fabrics have been designed and produced. Both problems encountered during the weaving process and solutions are discussed and described. This paper also investigates the effect of the fabric architecture on the stab resistance after stab behaviour of different architectures of 3D warp interlock HMWPE laminates. It has been found that the 3D warp interlock fabric with the Orthogonal and Layer to layer (O-L) architecture for the binding warp yarns reveals the best stab resistance compared with other structures.

INTRODUCTION

In addition to the use of dedicated means of violence (firearms and explosives), “lowtechnology” objects, such as utility knives, have been more commonly used for malicious purposes (Rozenfeld, 2018). Knife attack on police officers and civilians are not a new problem and stabbings are still a persistent and worrying concern and growing life-threatening assaults to police officers and the public due to the restrictions imposed by firearms control legislation, especially in Europe and Asia (Decker, 2007). Recent trends have led to an increase in the number of applications for body armour with stab protection. Thus, stabresistant personal protective equipment (PPE) has been gradually issued (Rodríguez-Millán, 2019) because it is a valid and necessary problem to be addressed in a modern, developed society. Generally, conventional body armour is designed for ballistic protection, which is not necessarily resistant to penetration of blades and offers little resistance to puncture and stab. Therefore, an increase demand of materials used for stab protection should be more protective, flexible and lightweight. In this study, we have investigated the stab resistance of 3DWIFs.

RESULTS

Five different structures were fabricated according to the four main categories of structure: Angle /Through-the-thickness (A/T), Angle /Layer-to-layer (A/L), Orthogonal /Through-thethickness (O/T), Orthogonal /Layer-to-layer (O/L). A series of stab experiments with the energy of 2.5 J, the drop height 0.121 m and 2.11 kg in mass were carried out, with HOSDB/P1/B sharpness blades which have the total length of 100 mm, the cutting edge length of 33 mm, and the blade thickness of 2 mm.

Besides, it was observed that F4 structure fabric can have the best stab resistance compared with other structures and the stab resistance in weft direction is higher than weft direction. In addition, the through-thickness binding yarns

also have an effect on the stab resistance of F4 O-T structure.

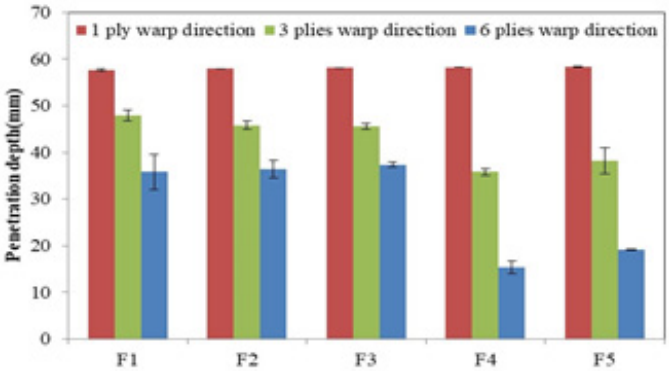

Fig.2. DOP of different fabrics and different plies in warp direction (0°) stab tests.

CONCLUSIONS

This study has compared five 3DWIFs for resisting against dynamic stab attacks It is expected that the evaluation of stab resistant performance and behaviour of 3DWIFs can provide a useful measure for the design and optimization of stab resistant with flexible fabrics.

Future research on armour will focus on the selection of more advanced high performance materials, structures, finishes, and designs to improve the stab resistance of soft body armour.

ACKNOWLEDGMENTS

Authors would like to acknowledge the China Scholarship Council (Project no. 201708420167) for supporting this research.

REFERENCES

[1] Rozenfeld, M.; Givon, A.; Peleg, K. Violence-related Versus Terror-related Stabbings. Ann. Surg. 2018, 267, 965–970.

[2] Decker, M.J.; Halbach, C.J.; Nam, C.H.; Wagner, N.J.; Wetzel, E.D. Stab resistance of shear thickening fluid (STF)-treated fabrics. Compos. Sci. Technol. 2007, 67, 565–578.

[3] Rodríguez-Millán, M.; Álvarez-Díaz, A.; Aranda-Ruiz, J.; Álvarez-Díaz, J.; Loya, J.A. Experimental analysis for stabbing resistance of different aramid composite architectures. Compos. Struct. 2019, 208, 525–534.

SCALABLE SPIDER-SILK-LIKE SUPERTOUGH FIBERS WITH POTENTIAL IN DEFENCE

Jinlian Hu[1(*)], Yuanzhang Jiang[2]

[1] Department of Biomedical Engineering, City University of Hong Kong, P. R. China

[1,2] Institute of Textiles and Clothing, The Hong Kong Polytechnic University, Hong Kong, P. R. China

[(*)] E-mail: jinliahu@cityu.edu.hk

ABSTRACT

Spiders silks have extraordinary strength and toughness simultaneously, thus has become dreamed materials by scientists and industries. Although there have been tremendous attempts to prepare fibers from genetically manufacture spider silk proteins, however, it has been still a huge challenge to artificially make a material with such high performance, do not mentioning the scaling-up because of extremely low productivity and high cost. Here, a facile spider-silk-mimicking strategy is firstly reported for preparing a scalable supertough fiber from chemical synthesis route. Supertoughness (~387 MJ m-3) is achieved by introducing β-sheet crystals and α-helical peptides simultaneously in a pseudoprotein polymer. The toughness of this fiber is more than twice the reported value of a normal spider dragline silk, and comparable with the toughest spider silk, aciniform silk of Argiope trifasciata.

INTRODUCTION

High-performance fibers, such as glass fiber, Kevlar fiber, carbon fiber as well as spectra fiber, have been used in defense area. For example, Kevlar fiber were chosen to make ballistic armor (Kevlar vest) because of its excellent stress, toughness and relatively light weight. As the most resilient protein fiber in nature, the tensile-strength of spider dragline-silk can be in the GPa range, and its toughness can reach 180 MJ m^{-3}, which is two to three times that of man-made fibers like Kevlar or Nylon (Ebrahimi 2015, Du 2006). Consequently, spider silk is the most desirable materials for high-performance applications like space-suits, bullet proof, balloon-parachutes, medical-devices and specialty-ropes. Tremendous worldwide efforts have been made particularly in genetic-engineering spider-silk-proteins (Heim 2009, Fink 2018), but it is still a huge challenge to scale-up due to its low-efficiency, high-cost and uncontrollable-quality. Furthermore, the mechanical properties of reconstituted spidroin fibers were not comparable to those of natural spider silks because of molecular-weight limitation and self-assembling difficulties. Here, a simple strategy that replicates spider silk is reported for preparing scalable supertough fibers through chemical synthesis.

RESULTS AND CONCLUSIONS

High-performance pseudoprotein polymers for fibers which contained α-helix and nanosized-β-sheet formed from an amine-terminated peptide poly(γ-benzyl-L-glutamate (PBLG) are connected by a small diamine and further linked to a random-coil-like-chain of spider-silk-proteins using urea linkage.The tensile test results of the chemically synthetic fibers showed that the pseudoprotein fibers have excellent mechanical properties. Particularly, Fiber P2 has a tensile strength of ~100 MPa, an elongation at break of ~750% and thus a toughness of 387 MJ m^{-3}, which is more than twice the toughness of spider dragline silk (~160 MJ m^{-3}) and comparable to that of the toughest spider silk—the aciniform silk of Argiope trifasciata (~320 MJ m^{-3}).

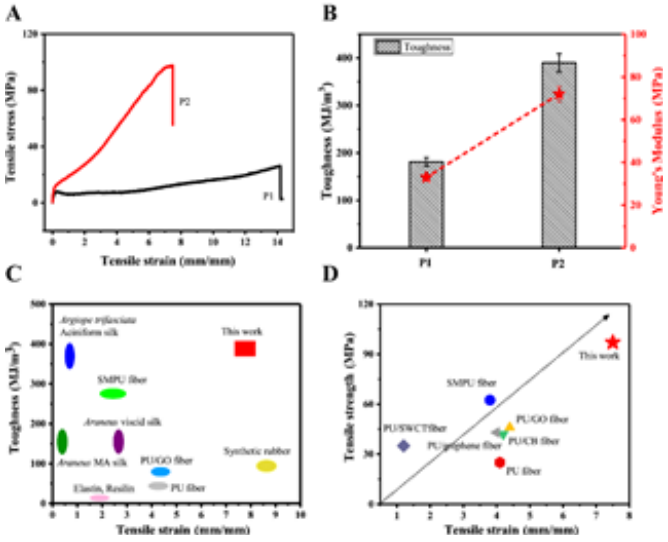

Fig.1 Mechanical properties of the pseudoprotein polymer fibers.

The toughness of the fibers reported in this study is not only comparable to that of the most robust spider silk, but also much greater than that of many other natural fibers or synthetic fibers. The chemical structure of this fiber is similar to that of polyurethane, but its strength is much higher than that of ordinary polyurethane and polyurethane composite fibers (Fig 1D). In addition, the pre-stretching experiments results showed that the β-sheet content and crystallinity of the fibers after pre-stretching are increased, but meanwhile, the crystallite size is reduced. The tensile strength of the fibers after pre-stretching reached 200 MPa, but their toughness was reduced to 190 MJ/m3 due to the decrease in tensile strain, but they are still tougher than the dragline silk of common spiders (Fig 1B). Moreover, the cost-effective, widely available feedstocks and facile preparation of pseudoprotein fibers make it possible for large-scale production for high-performance applications.

ACKNOWLEDGMENTS

The authors gratefully acknowledge the funding by the National Natural Science Foundation of China (51673162), the Hong Kong General Research Fund (15201719 and 152098/15E).

REFERENCES

[1] Ebrahimi D, Tokareva O., Rim NG, Wong JY, Kaplan DL, Buehler MJ. Silk–its mysteries, how it is made, and how it is used. ACS biomaterials science & engineering, 2015, 1, p. 864-876.

[2] Du N., Liu XY, Narayanan J, Li L, Lim MLM, Li D. Design of superior spider silk: from nanostructure to mechanical properties. Biophysical journal, 2006, 91, p. 4528-4535.

[3] Heim M, Keerl D, Scheibel T. Spider silk: from soluble protein to extraordinary fiber. Angewandte Chemie International Edition, 2009, 48, p. 3584-3596.

[4] Fink TD, Zha RH. Silk and Silk-Like Supramolecular Materials. Macromolecular rapid communications, 2018, 39, p. 1700834.

PROTECTION OF INFRASTRUCTURES AND SYSTEMS AGAINST EXPLOSIVES – ADVANCED PROTECTIVE COATINGS – BLAST TESTING CAMPAIGN

G.J. Gomes [(*),1,4,5], J.L. Mingote[1], J.R. Tortosa (PhD)[2], L.C. González-Atance[2],L. Martínez[2], S. Martínez[3], J. Marques[5], V. Lúcio (PhD)[6]

[1] NATO Counter IED Centre of Excellence (Hoyo de Manzanares-Madrid).C-IED COE.

[2] Instituto Nacional de Técnica Aeroespacial "INTA", Campus La Marañosa (Madrid).

[3] Escuela Politécnica Superior del Ejército (Madrid). ESPOL.

[4] Centro de Investigação e Desenvolvimento do Instituto Universitário Militar. Lisboa (Portugal)

[5] PhD Student at Faculdade de Ciências e Tecnologia da Universidade Nova de Lisboa, Portugal.

[6] Faculdade de Ciências e Tecnologia da Universidade Nova de Lisboa - CERIS, Portugal.

[(*)] E-mail: ggomes@ciedcoe.org; gomes.gj@mail.exercito.pt

ABSTRACT

This project intends to study, characterize the properties of existing commercial available protective coatings and perform a benchmark between several brands of polyuria as retrofitting system against explosions. The first results obtained have shown that the system is very effective in terms of performance even though some best practises should be followed in the application process.

INTRODUCTION

The terrorist activity worldwide and more than that, an increase lethality has demonstrated the vulnerability of existing structures to blast loading, especially when large amounts of explosives are used (e.g. Vehicle Borne Improvised Explosive Devices – VBIED). From several real cases and studies it has been observed that hollow, unreinforced, concrete masonry unit (CMU) infill walls, commonly used in reinforced concrete or steel framed structures, are particularly vulnerable to blast loads and tend to disintegrate into a large number of fragments ranging in size from full CMU blocks to pebble-size debris, that penetrate into a structure at very high velocities depending on the severity of the blast loads presenting a severe to lethal hazard for the building's occupants and equipment. These results led to the conclusion that, in many cases, a significant reduction in secondary debris can be achieved by focusing on retrofitting the wall elements [1].

The use of elastomers glued to the surface of the walls in order to absorb part of the energy induced by the explosion can present a very interesting alternative [2]

The use of polymers seems to offer good benefits for the retrofitting of masonry, providing an increase in ductility, allowing significant deflections outside the plane of the Wall [3].

The testing setup consisted in three walls, two of them retrofitted with polyuria and one control wall. The explosive charge was positioned to guarantee the same distance for all the walls. The amount of explosives and standoff was designed to break apart the control CMU wall and the success of the retrofitted system.

RESULTS AND CONCLUSIONS

The image below intends to illustrate the first conclusions drawn from the testing:

- No fragments perforated the polyuria layer to the protected side.
- The good bond of polyuria made it work as a strenghtening system (skin layer)
- Reference wall collapsed by flexure but shear cracks are visible

• Shear fracture – Overpressure overcame shear resistance of the CMU.
• Polyuria thickness could be reduced significantly – Estimate 4-5mm.
• Anchor is essential. The system could fail by peeling of the anchor region

Fig.1 preliminary results of the testing

ACKNOWLEDGMENTS

The authors gratefully acknowledge the funding under the NATO Defense Against Terrorism Program of Work and NATO Counter IED COE.

REFERENCES

[1] L. Muszynski and M. Purcell, "Use of composite reinforcement to strenghten concrete and air-entrained concrete masonry walls against air blast," Journal of composite structures, Vol 7 (2), pp. 98-108, 2003.
[2] Carol F. Johnson, "Concrete Masonry Wall Retrofit Systems for Blast protection," Texas, 2013.
[3] AFRL, "Engineering Technical Letter (ETL) 02-4: Airblast Protection Polymer Retrofit of Unreinforced Concrete Masonry Walls," Tyndal, 2002.

DEVELOPMENT OF LIGHTWEIGHT PROTECTIVE BARRIER MADE OF ULTRA-HIGH-PERFORMANCE FIBRE-REINFORCED CEMENTITIOUS COMPOSITE

Radoslav Sovják[1(*)], Michal Mára[2], Jindřich Fornůsek[3], Jan Zatloukal[4], Petr Konvalinka[5]

[1, 2, 3, 4, 5] Experimental Centre, Faculty of Civil Engineering, Czech Technical University in Prague, Czech Republic

[(*)] E-mail: sovjak@fsv.cvut.cz

ABSTRACT

A protective barrier is a system based on high mobility and versatility which is achieved by linking the basic plate elements together to several possible shapes according to the needs of the situation. The material solution consists of the application of ultra-high-performance fibre-reinforced cement-based composites, which meets the requirements for enhanced resistance against extreme loads such as blast or impact. The proposed barrier was subjected to various load evens and demonstrated enhanced resistance to projectile impact and blast.

INTRODUCTION

The proposed protective barrier represents a new protective measure to mitigate the consequences of various extreme load evens by proving a lightweight flexible structure that can be built very quick on-site without the need for heavy machinery. Barriers are based on the utilization of ultra-high-performance fibre-reinforced cement-based composites (UHPFRC), which is well known as a material with increased energy absorption and dissipation capacity and it is, therefore, well suited as a material for protective structures.

The resulting structure was designed as a flexible precast system that is based on high mobility and versatility which is achieved by linking the basic elements. The shape of the basic element - protective plate - is 1.4 m in length, 0.4 m in width (Fig. 1). The plates are 40 mm tall and the weight of the UHPFRC plate is 55 kg, assuring easy manual operation. There is no rebar reinforcement in the slab and only steel fibres were uniformly distributed into the mixture. The fibre volume content was set on 1.5%, which was derived from previous studies as an optimal trade-off between the price, workability and resulting performance.

RESULTS AND CONCLUSIONS

Lightweight protective barrier benefits from using an ultra-high performance fibre-reinforced concrete (UHPFRC) that is well-pronounced for its increased strength, ductility and energy dissipation capacity (Wille et al. 2014; Yoo et al. 2015; Pyo et al. 2015; Yoo and Banthia 2016). Protective barriers were designed and tested against various extreme load events such as vehicle impact, projectile impact and blast. By linking individual plates together, several possible structures can be built such as the wall or closed structures with tetragonal or hexagonal base. By using locks that are provided at the ends of each plate from both sides there is no need for any additional fastening material as UHPFRC plates easily fit together. Moreover, there is no need for a foundation as the system itself is self-bearing.

Fig.1 Example of a lightweight protective barrier made of UHPFRC plates.

This study presented the lightweight protective barrier that may serve primarily for the protection of objects, buildings and strategic infrastructure, special checkpoints or fortified posts, mobile city barriers and lightweight barricades for crowd control, protection and support of music and sports events and safety corridors at shooting ranges and training centres. The advantages of the lightweight protective barrier are significantly lower costs compared to conventional materials such as high strength steel or ceramics, very quick assembly on-site without the need for heavy machinery, ballistic resistance class ranging from FB 4 to FB 7 according to EN 1522 and increased resistance to fragments and explosion.

ACKNOWLEDGEMENTS

The authors gratefully acknowledge the funding by Ministry of Industry and Trade, Czech Republic, under grants FV10547.

REFERENCES

[1] Pyo S, Wille K, El-Tawil S, Naaman AE (2015) Strain rate dependent properties of ultra high performance fiber reinforced concrete (UHP-FRC) under tension. Cem Concr Compos 56:15–24. https://doi.org/10.1016/J.CEMCONCOMP.2014.10.002

[2] Wille K, El-Tawil S, Naaman AE (2014) Properties of Strain Hardening Ultra High Performance Fiber Reinforced Concrete (UHP-FRC) under Direct Tensile Loading. Cem Concr Compos 48:53–66. https://doi.org/10.1016/j.cemconcomp.2013.12.015

[3] Yoo DY, Banthia N (2016) Mechanical properties of ultra-high-performance fiber-reinforced concrete: A review. Cem Concr Compos 73:267–280. https://doi.org/10.1016/j.cemconcomp.2016.08.001

[4] Yoo DY, Yoon YS, Banthia N (2015) Flexural response of steel-fiber-reinforced concrete beams: Effects of strength, fiber content, and strain-rate. Cem Concr Compos 64:84–92. https://doi.org/10.1016/j.cemconcomp.2015.10.001

ANALYSIS OF MULTILAYERED COMBINATIONS OF UHMWPE

Jairo Peinado[1,2], Liu Wang[1], Álvaro Olmedo[2], Carlos Santiuste[1]
[1] Fábrica Española de Confecciones, SA, SS. De los Reyes, Madrid, España
[2] Department of Continuum Mechanics, University Carlos III of Madrid, Leganés, Madrid, España
[(*)] E-mail:jpeinado@fecsa.net

ABSTRACT

This work compares the efficiency of 3 types of UHMWPE composites used in ballistic bulletproofs. The study analyses several combinations (stacking sequences) of these kinds of composites. Mechanical test, both dynamic and quasi-static, joined with an extensive numerical parametrical research allowed to characterize completely their dynamic response.

INTRODUCTION

The rising of military risks has maximized the necessity of developing materials, as para-aramids and UHMWPE, capable of absorb huge energy when high velocity impact situations occur.

The industry needs models that analyse and compare different UHMWPE to face each threat easily. Nevertheless, there is a gap between the academic research and industry requirements. This work introduces a versatile numerical model that may be effortlessly calibrated to reproduce the ballistic performance of UHMWPE protections aligning both science and industry.

The model was validated comparing Lambert-Jonas regressions among experimental tests carried out on three different qualities for UHMWPE and numerical results. These high-velocity impacts were conducted on single and multi-layered configurations. Finally, the optimal solution was reached using the numerical model by mixing the three validated materials.

The 17 stacking sequences shown in Table 1 were selected to have an areal density of around 1870 Kg/m2. The experience of FECSA indicated that the best results should be obtained with stacking sequence [9·Type3] because Type3 is the best material, but it is also the most expensive one. The main objective of this analysis was to reduce the cost of the panel combining Type3 with Type2 and Type1, but with a slight reduction of ballistic performance.

RESULTS AND CONCLUSIONS

The results from analysis are shown in Table 1. There is an important growing in efficiency when compare monolithic packages with those made mixed. The results show that the better location of the best qualities of UHMWPE must be located on the rear face.

Applicability of the model has been validated through 6 different stacking sequences when compared with their analogs experimentally as in Fig. 1. There is an excellent agreement between numerical predictions and experimental data for high impact velocity. However, the accuracy of the model is reduced near the ballistic limit due to the non-linearity of the experimental results. The change in the slope of the numerical curve is softer than the experimental one.

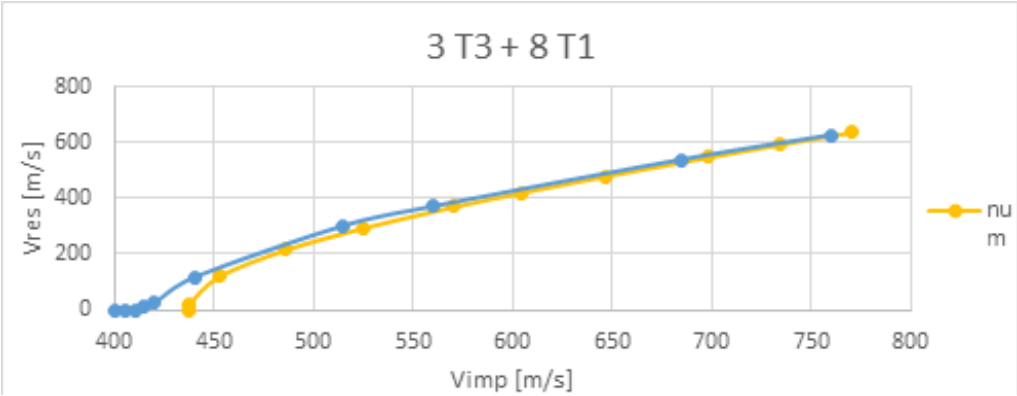

Fig.1 Comparison between numerical model and experimental test

Stacking sequence	FEM (m/s)	exp. (m/s)	Areal dens (g/m²)	Type 1	Type 2	Type 3
Type3/8-SB21	419	437	1808	64%	0%	35,8%
8-SB21/3-SB117	425		1808	64%	0%	35,8%
6-SB117/4-SB21	445		1876	31%	0%	69,1%
4-SB21/6-SB117	465		1876	31%	0%	69,1%
6-SB117/1-SB51/2-SB21	475		1839	16%	14%	70,5%
7-SB117/3-SB21	478	478,8	1947	22%	0%	77,7%
3-SB21/7-SB117	495	467,1	1947	22%	0%	77,7%
6-SB117/2-SB51	495		1802	0%	28%	71,9%
6-SB117/2-SB21/1-SB51	495	489,6	1839	16%	14%	70,5%
2-SB51/6-SB117	495		1802	0%	28%	71,9%
2-SB21/6-SB117/1-SB51	495		1839	16%	14%	70,5%
1-SB51/6-SB117/2-SB21	497		1839	16%	14%	70,5%
1-SB51/2-SB21/6-SB117	500		1839	16%	14%	70,5%
2-SB21/1-SB51/6-SB117	507	518,5	1839	16%	14%	70,5%
9-SB117	520		1944	0%	0%	100,0%
8-SB117/1-SB51	545		1981	0%	13%	87,2%
1-SB51/8-SB117	550	531,3	1981	0%	13%	87,2%

Table 1 Stacking sequence of combinations

ACKNOWLEDGMENTS

The authors acknowledge the Regional Government of Madrid under the project IND2017/IND-7762, and the Ministry of Economy and Competitiveness of Spain and FEDER program under the Project RTC-2015-3887-8 and the Project DPI2017-88166-R for the financial support for this work.

REFERENCES

[1] M.R.O'Masta, D.H.Crayton, V.S.Deshpande, H.N.G.Wadley. Mechanisms of penetration in polyethylene reinforced cross-ply laminates. International Journal of Impact Engineering Volume 86, Pages 249-264, December 2015.

[2] A.R.Othman, M.H.Hassan. Effect of different construction designs of aramid fabric on the ballistic performances. Materials & Design, Volume 44, Pages 407-413, February 2013.

[3] Nguyen, L. H., Lässig, T. R., Ryan, S., Riedel, W., Mouritz, A. P., & Orifici, A. C. (2015). Numerical Modelling of Ultra-High Molecular Weight Polyethylene Composite under Impact Loading. Procedia Engineering, 103, 436–443.

[4] Chen, X., Zhou, Y., & Wells, G. (2014). Numerical and experimental investigations into ballistic performance of hybrid fabric panels. Composites Part B: Engineering, 58, 35–42. https://doi.org/10.1016/J.COMPOSITESB.2013.10.019

VESTLIFE – A NEW ULTRALIGHT BALLISTIC MODULAR SOLUTION

Gilda Santos[1(*)], José Gomis Gisbert[2], Paul Brasser[3], Asko Kylkilahti[4], Iñigo Agote[5], Mirco Chiodi[6]

[1] CITEVE - Centro Tecnológico das Indústrias Têxtil e do Vestuário de Portugal, V. N. Famalicão, Portugal

[2] AITEX - Asociación de investigación de la Industria Textil, Alicante, Spain

[3] BRAPA CONSULTANCY, MN De Lier, Netherlands

[4] FY-COMPOSITES, Pirkkala, Finnland

[5] TECNALIA, Derio, Spain

[6] PETROCERAMICS S.p.A, Stezzano BG, Italy

[(*)] E-mail: gsantos@citeve.pt

ABSTRACT

The demands of protective clothing are strict and mostly contradictory, since they require the combination of optimal protection and comfort. For instance, dense, non-permeable textiles increase the protection, but are uncomfortable, making the design and development of effective protective clothing a complex issue. Optimization between physiological burden and protection is needed to create the ideal suit for a specific mission. Current commercial ballistic systems present several disadvantages, such as the overall weight, reduced flexibility and design shortcomings due to differences in anatomy. Additionally, protection approaches are mainly based against kinetic energy threats and CBRN protection is limited. VESTLIFE project aims to develop a new lightweight and modular bulletproof integral solution, which integrates a CBRN detection system.

INTRODUCTION

The VESTLIFE project is under the Preparatory Action on Defence Research (PADR), the grant for the Research Action call on the topic of 'Force protection and advanced soldier systems beyond current programmes', in the subtopic 'Tailor-made blast, ballistic and CBRN protection of military personnel'. It was signed on April 27th, 2018, and has a duration of 36 months. This project is led by AITEX (Spain), encompassing 5 other participants in the consortium from 5 countries: CITEVE (Portugal), Brapa Consultancy (Netherlands), TECNALIA (Spain), Petroceramics (Italy) and FY-Composites (Finland).

This project aims to develop different types of ballistic protection armour with advanced features. The protection system will consist of different levels, mainly soft and hard armour. The optimum architecture of materials on the body will encompass an equilibrium established, based on both the comfort experience and the protective performance. A software model will provide insights and the ability to define clothing architectures to be created in the integration step and to validate the performance of the clothing.

The technical work (depicted in Figure 1) of the current project lies in the development of lighter and modular ballistic protections, and therefore, the possibility of increasing the covered surface without handicapping comfort, and customize the protection requirement of the different body areas (adapting it to the mission's risk level and to the vital body organs). In parallel, CBRN sensors will be integrated for the detection of possible risks, in addition to developing a mathematical model predictive of the possible expected risks in the different scenarios that may arise.

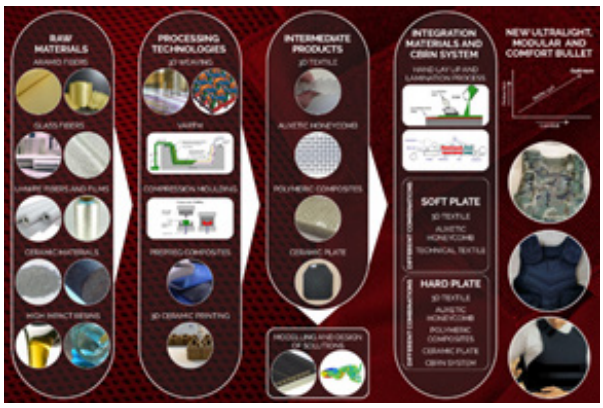

Fig.1 Work flow schematic representation for achieving a new ultralight, modular and comfortable ballistic protection armour.

RESULTS AND DISCUSSION

The scenarios and the requirements have been defined, both ballistic and comfort, taking into account international testing standards and first-hand information collected through the conduct of surveys to soldiers. Ballistic protections are being formulated through the development of composite materials of an auxetic nature and three-dimensional textiles that complement the materials of more traditional use (Figure 2).

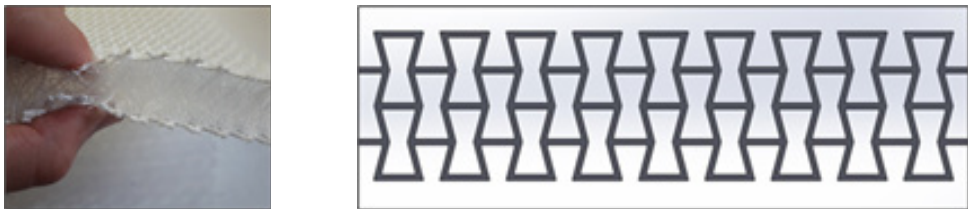

Fig.2 Example of a 3D fabric (left) and scheme of the auxetic structure used in the project (right).

Simultaneously, polymeric panels based on ultra-high molecular weight polyethylene (UHMWPE) are being developed and modified to serve as a basis under which the auxhetic materials that complement and improve their behavior are included. These panels have proven to be suitable for ballistic room testing under NATO Standard STANAG 2920, establishing a NIJ III requirement level with a V50 x 847 m/s using a 7.62 mm FMJ (Full Metal Jacket) ammunition or metal-coated bullet tip. Synthesis of modified ceramics for ballistic panels that reach NIJ IV level, maximum in protection, is also underway. Figure 3 depicts a ballistic test that was carried out.

Fig.3 Ballistic test: a) Measurement Software, b) Front View, and c) and d) Back view.

These developments and, consequently testings, are currently ongoing in their respective work packages.

ACKNOWLEDGMENTS

The authors gratefully acknowledge the funding by the European Union's Preparatory Action on Defence Research under Grant Agreement No 800876.

ASSESSMENT OF STRUCTURAL DAMAGE TO CARBON FIBRES UNDER A RANGE OF HEAT/FIRE CONDITIONS

Francesca McKenzie[1(*)], Baljinder Kandola[2], Emmajane Erskine[3]
[1,2] Institute for Materials Research and Innovation, University of Bolton, Deane Road, Bolton, BL3 5AB, UK
[3] DSTL, Porton Down, Salisbury, SP4 0JQ, UK
[(*)] E-mail: flm1res@bolton.ac.uk

ABSTRACT
This study examines the damage caused by high temperatures to carbon fibres and the effects on their physical properties, including fibre diameter reduction and electrical conductivity, with the aim to provide further insight into potential hazards posed by exposed fibres after high heat situations. PAN TR30S carbon fibres were tested in a controlled environment over a range of temperatures, from 350°C to 650°C, for varying periods of time in air and nitrogen atmospheres. No reductions in carbon fibre diameter or surface defects were observed when testing in a nitrogen environment. A linear relationship between temperature and fibre diameter reduction was found in air and this correlated to the change in carbon fibre conductivity. Carbon fibre-reinforced epoxy composites are also currently being subjected to different heat fluxes under a cone calorimeter using both piloted and non-piloted ignition modes, and to a propane burner test for different periods of time. The hazard will be tested in terms of electrical conductivity of the damaged composite laminate as well as single carbon fibres taken from different parts of the composites. The physical and mechanical properties of the latter will also be tested to assess the overall hazard.

INTRODUCTION
Carbon fibre is commonly used to make carbon fibre-reinforce composites, which are increasing in popularity due to their high strength-to-weight ratio and resistance to corrosion. However, at temperatures above 300°C the polymer matrix begins to decompose and start burning. The residual carbon fibres being electrically conductive, may pose a hazard to the surrounding electronics. Moreover, at over 550°C the carbon fibres begin to oxidize [1]. This can lead to fibre de-fibrillation, which poses significant harm to their surroundings. Including, interference with electronics, and fibres under 7μm can be inhaled and damage the human respiratory tract [2].
Using a tube furnace, carbon fibres were held at a range of temperatures in both air and nitrogen environments. Using SEM, decrease in fibre diameter and any surface damage were recorded. Single fibre conductivity tests were used to measure change in the fibre's electrical conductivity. Carbon fibres and their epoxy composites were then irradiated on the top surface using cone calorimetry at heat fluxes of 50 kWm-2 and 75 kWm-2. In order to achieve a higher heat flux of 116 kWm-2 a propane burner set up was used. Assessing and understanding the damage to carbon fibres in different high heat situations and atmospheres, can help inform new ways to improve the structural retention of carbon-fibre reinforced in composites.

RESULTS AND CONCLUSIONS
TGA results (Figure 1) show that carbon fibre begins to oxidize in air at 520°C, while in nitrogen there is only a weight loss of 1.2% at 450°C due to the removal of the fibre's polymer sizing.

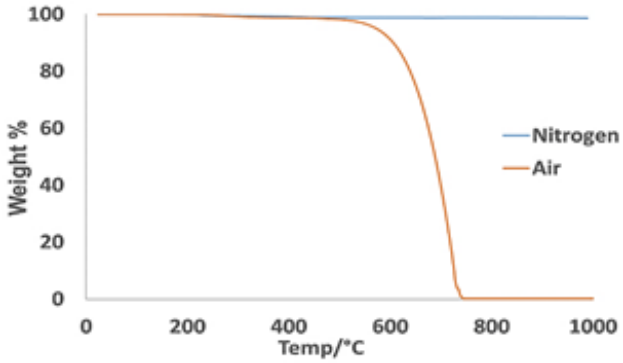

Fig.1 TGA of carbon fibres in air and nitrogen at 20°C/min

Tube furnace results in air for 30 minutes (Table 1), show that as the temperature begins to reach that for carbon fibre oxidation, there is a linear relationship between reduction in fibre diameter and temperature. At higher temperatures, 650°C the carbon fibre is partially oxidized into fragments, while at 700°C there is complete oxidation. While held at the same temperature and time in nitrogen, no reduction in fibre diameter or surface damage is found.

Temperature/°C	Average carbon fibre diameter/µm	Electrical conductivity x10^4 S/m
23	7.68 ± 0.23	5.38
500	7.13 ± 0.15	5.46
550	6.57 ± 0.28	1.85
600	5.26 ± 0.32	0.61

Table 1 Tube furnace, Time 30min, Atmosphere Air

Cone Calorimeter results show that at a heat flux of 50 kWm-2 there is no reduction in carbon fibre diameter or electrical conductivity. However, at 75 kWm-2 major reduction in diameter is observed (Table 2).

	Before heat exposure	After heat exposure
Weight/g	0.79	0.34
Avg. fibre diameter/µm	7.68 ± 0.23	5.88 ± 0.16

Table 2 Cone calorimeter, Heat flux 75 kWm-2, Time 600s

This study shows that carbon fibres sustain significant damage when exposed to temperatures above 500°C, and at high heat fluxes, due to surface oxidation. Future work is focused on reducing the risk of both damage to the carbon fibres, and of carbon fibre release during exposure of composites to fire. This includes modification of the resin by adding cross-linkers to improve mechanical integrity of the char and adherence to the fibre, and chemically coating the fibre surfaces.

ACKNOWLEDGMENTS

The authors gratefully acknowledge the funding by DSTL

REFERENCES

[1] Mouritz, A.P., Gibson, A.G. (2006) Fire properties of polymer composite materials. Dordrecht: Springer-Verlag New York.

[2] Inthavong, K., Mouritz, A. P., Dong, J., & Tu, J. Y. (2013). Inhalation and deposition of carbon and glass composite fibre in the respiratory airway. Journal of Aerosol Science, 65, pp. 58–68

ELECTRONIC TATTOOS FOR ELECTROPHYSIOLOGICAL MONITORING AND HMIS AND IMPACT RESISTANT SYSTEMS

Mahmoud Tavakoli

[1,] Institute of Systems and Robotics, Department of Electrical Engineering, University of Coimbra

[(*)] E-mail: mahmoud@isr.uc.pt

ABSTRACT

This works reports fabrication and application of ultrathin stretchable printed circuits for acquisition of electrophysiological signals, such as muscular signals (Electromyography), Cardiac Signals (Electrocardiography), and Brain signals (Electroencephalography), as a novel method for continuous, comfortable, and imperceptible monitoring of the human health. At the same time, such thin-film stretchable electronics, may be used to integrate low cost sensors and electronics system, over any surface, including complex non developable surfaces of 3D printed objects. This can be used for the next generation of Human Machine Interfaces (HMIs). Moreover, soft and stretchable electronics, can be used for cases where a large number of medical systems should be delivered from air. These systems can withstand he impact they suffer after falls (e.g. from an airplane).

INTRODUCTION

During the last couple of years, some reports on fabrication and applications of ultrathin stretchable electronic films, also called epidermal electronics1 or electronic tattoos, or have been presented2345. The interest on E-tatoos is mainly because these films are comfortable and nearly imperceptible. They can follow the dynamics morphology of the human skin, without losing their function. Applications of these films has been shown in monitoring muscular activity through Electromyography (EMG) to control UAVs 6 or prosthetic hands7, to monitor heart rate through Electrocardiography (ECG)8-9, for acquisition of brain signals through Electroencephalography (EEG) for monitoring of sleep10, for electrochemical analysis of sweat 11. To move toward utilization of these sensors in real-world scenarios, a combination of high conductivity, stretchability, a facile and low cost fabrication is yet remained as a challenge. This article discusses a novel electronic tattoo based on printed stretchable circuits,

Here, we present a method for fabrication of ultrathin electronic films, that provides simultaneously these characteristics, and demonstrate applications in monitoring of human´s electrophysiological data, as well as to Human machine interfaces.

RESULTS

Figure 1 summarizes the method for fabrication of printed stretchable thin film electronics. The fabrication starts with printing circuit pattern using a laser printer, followed by coating the printed circuit using condutcive silver epoxy paste, and consequently Eutectic Gallium Inidum Alloy (EGaIn). Such circuit can be then transferred to the human epidermis for acquisition of biopotentials, such as EMG or ECG signals (Figure 2), or can be transferred to complex 3D surfaces, using the hydrotransfer process. Figrue 3, demonstrates the elechteromechanical coupling of the printed circuits against uniaxial strain.

Fig.1 Step-By-Step production of stretchable circuits over the tattoo or transfer paper. Laser Printing(i), followed by coating wit Ag based epoxy, and Eutectic alloy of Gallium and Indium

Fig.2 Applications of the electronic tattoo in EMG/ECG monitoring, and novel forms of Human Machine Interfaces

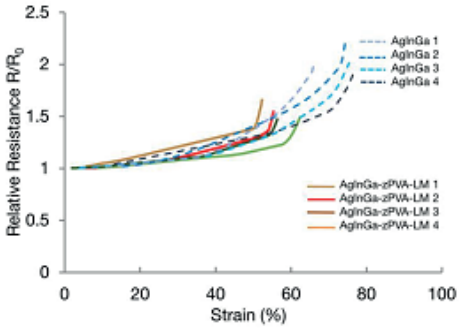

Resistance vs. Strain applied to printes stretchable circuits

REFERENCES

[1] Kim, D.-H. et al. Epidermal Electronics. Science (80-.). 333, 838–843 (2011).

[2] Gong, S. et al. Tattoolike Polyaniline Microparticle-Doped Gold Nanowire Patches as Highly Durable Wearable Sensors. ACS Appl. Mater. Interfaces 7, 19700–19708 (2015).

[3] Zucca, A. et al. Tattoo Conductive Polymer Nanosheets for Skin-Contact Applications. Adv. Healthc. Mater. 4, 983–990 (2015).

[4] Bareket, L. et al. Temporary-tattoo for long-term high fidelity biopotential recordings. Sci. Rep. 6, (2016).

[5] Ferrari, L. M. et al. Ultraconformable Temporary Tattoo Electrodes for Electrophysiology. Adv. Sci. (2018) doi:10.1002/advs.201700771.

[6] Jeong, J. W. et al. Materials and optimized designs for human-machine interfaces via epidermal electronics. Adv. Mater. (2013) doi:10.1002/adma.201301921.

[7] Greco, F., Zucca, A., Taccola, S., Mazzolai, B. & Mattoli, V. Patterned free-standing conductive nanofilms for ultraconformable circuits and smart interfaces. ACS Appl. Mater. Interfaces 5, 9461–9469 (2013).

[8] Kabiri Ameri, S. et al. Graphene Electronic Tattoo Sensors. ACS Nano (2017) doi:10.1021/acsnano.7b02182.

[9] Ha, T. et al. A Chest-Laminated Ultrathin and Stretchable E-Tattoo for the Measurement of Electrocardiogram, Seismocardiogram, and Cardiac Time Intervals. Adv. Sci. (2019) doi:10.1002/advs.201900290.

[10] Shustak, S. et al. Home monitoring of sleep with a temporary-tattoo EEG, EOG and EMG electrode array: A feasibility study. J. Neural Eng. (2019) doi:10.1088/1741-2552/aafa05.

[11] Jia, W. et al. Electrochemical Tattoo Biosensors for Real-Time Noninvasive Lactate Monitoring in Human Perspiration. (2013).

INFLUENCE OF THE STABILIZATION PROCESS ON THE MECHANICAL PROPERTIES OF A HONEYCOMB

L. Blanc[1(*)], F. Brun[2], A. Bracq[1], J. Sampaio[1], M. Stanczak[1], T. Fras[1]
[1] ISL, French German Research Institute of Saint Louis, Saint-Louis, France
[2] Engineering Composite 3D, Démouville, France
[(*)] E-mail: ludovic.blanc@isl.eu

ABSTRACT

ISL has been working on blast effects mitigation for more than 15 years. Targets with different characteristic dimensions, from the unprotected soldier to the steel-reinforced concrete bunker, can be exposed to blast waves generated by high explosive detonation. Blast mitigation can be split into two different aspects: mitigation of the detonation and mitigation of the blast load.

EC3D imagine, conceptualize, test and patent advanced technological solutions, to make them available to industrial customers who benefit from them in production, to differentiate themselves in their markets. The company focused on research and development of new generation three-dimensional structures, aimed to be used as core material.

In this extended abstract, the focus will be brought on honeycomb, a structure allowing to dissipate energy through plastic deformation. This structure can be used inside a sacrificial cladding to mitigate a blast or impact load [1, 2]. Nevertheless, there exists a difference between most of the theoretical characterization of the honeycomb, based on the ASTM C365M and ASTM D7336M norms, and how it really behaves once integrated to an armour plate. In fine, a variation in its energy absorption capacity can be seen, simply due to the height of the final sample and its necessary stabilization during its integration in a panel.

INTRODUCTION

The honeycomb stabilization is the process upon which a honeycomb is glued to the plates of the cladding. Through this process, the boundary condition evolves and the behaviour of the sample differs from the one measured following the norms. This modification alone makes all numerical simulation based on the homogenisation method inaccurate at some point, especially if the honeycomb data derives from non-stabilized honeycomb compressive tests. To confirm this, quasi-static compressive tests were performed at the French-German research institute of Saint-Louis using an universal machine. Non-stabilized and stabilized samples (75 x 75 mm2) of different height were tested and compared at two different strain rates. The standard head displacement rate is fixed to 0.5 mm/min to study the elastic phase and switched to 25 mm/min at the start of the plastic phases (once the stress decreased to 80 % of the ultimate force prior to failure).

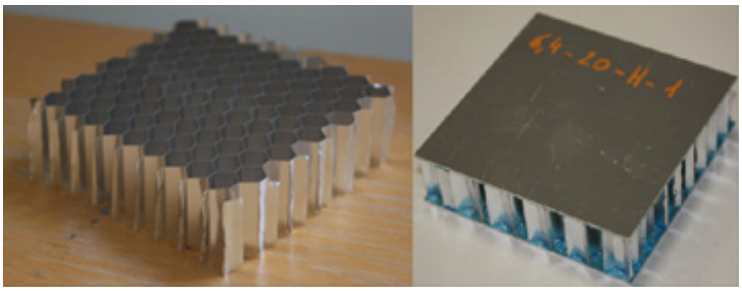

Fig.1 Non stabilized (left) and stabilized (right) 20 mm height hexagonal honeycomb

RESULTS AND CONCLUSIONS

The stress-strain curves of a hexagonal honeycomb is well known in the literature, and can be split into three phases: the pseudo-elastic phase, characterised by the bulk modulus E, the plastic collapse stress Pc and the elastic strain εy; the plastic phase, characterized by the plateau stress σ0; and the densification phase, characterized by the onset of densification εd. The methodology to compute these parameters, presented in table 1, is based on the work from Li [3].

	Density ρ_0 (kg/m^3)	Densification Strain ε_d	Plateau Stress σ_0 (kPa)	Mean Toughness T (kJ.m^{-3})	Young Modulus (MPa)	Plastic Collapse Stress (kPa)
20 mm	43.09	0,544	613	333	250.6	1579
20 mm NS	43.09	0.754	544	412	258.6	1613
60 mm	45.90	0.662	597	413	470.5	1544
60 mm NS	45.90	0.803	537	429	418.6	1300
100 mm	46.60	0.747	611	457	554,2	1502
100 mm NS	46.60	0.809	578	466	611.8	1357

Tab.1 Material parameters of Stabilized and Non Stabilized Honeycomb

After analysis, a clear influence of the stabilization process has been seen (Fig. 2). This influence varies depending on the height of the sample.

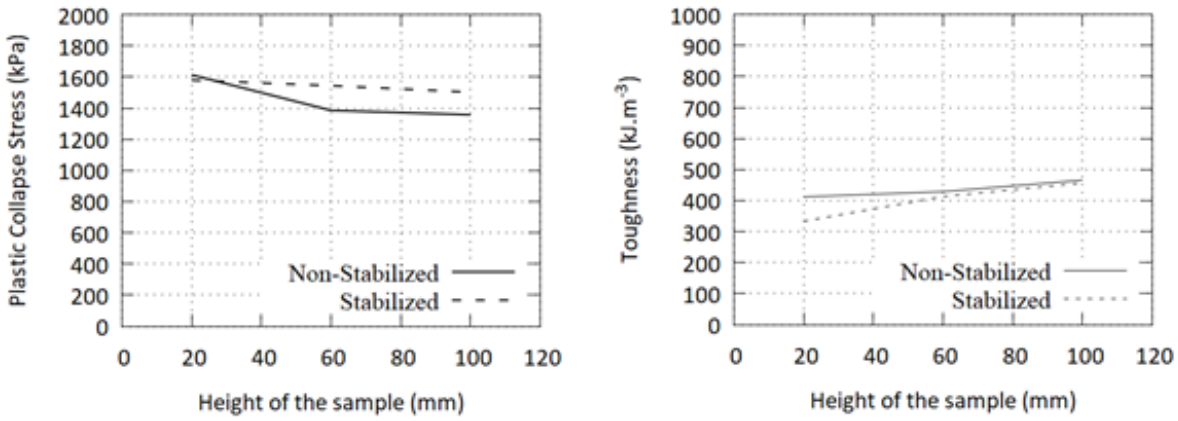

Fig.2 Influence of the stabilization process on the sample plastic collapse stress and toughness

The influence of the glue used in the stabilization process has already been established in the literature, and is the main reason why the plastic collapse stress is higher, and the densification strain lower. It is however hard to quantify its influence, and numerical simulations usually simplify the model by considering the cells imbued in glue rigid.

REFERENCES

[1] Li X , Zhang P , Wang Z , Wu G , Zhao L., 2014, Dynamic behavior of aluminum honeycomb sandwich panels under air blast: experiment and numerical analysis, Composite Structures 108, pp. 1001–1008

[2] Theobald M., Langdon G., Nurick G., Pillay S., Heyns A., Merrett R., 2010, Large inelastic response of unbonded metallic foam and honeycomb core sandwich panels to blast loading, Composite Structures 92, pp. 2465-2475

[3] Li Q.M., Magkiriadis I., Harrigan J.J., 2006, Compressive strain at the onset of densification of cellular solids, Journal of Cellular Solid 42 (5): 371-392

TITANIUM DIOXIDE NANOPARTICLES IN CARBON FIBRE-REINFORCED POLYMER MATERIAL FOR PROTECTION AGAINST DAMAGE BY THERMAL RADIATION AND LASER

Thomas J. Schuster*, Till K. Tetzlaff
Bundeswehr Research Institute for Materials, Fuels and Lubricants (WIWeB), Erding, Germany
(*) E-mail: thomasschuster@bundeswehr.org

ABSTRACT

Titanium dioxide (TiO2) nanoparticles are known to be effective in scattering of light. Therefore, the potential of these particles as fillers for protection of carbon fibre-reinforced polymers (CFRP) against infrared radiation, which may occur during a fire or attack by laser weapons, was analysed.
CFRP material was produced at a high quality with a homogeneous distribution of TiO2-nanoparticles using a three-roll-mill and an adapted wet lay-up process. Nanoparticle concentrations up to 10 wt.% (of the polymer matrix) were used. To identify the optimal nano-filler type, different crystalline phases of TiO2 as well as different diameters of nanoparticles were examined.
By adding TiO2 nanoparticles to CFRP, an increase in time to ignition of up to 20 % can be observed when samples were irradiated with an electrical heater at 35 kW/m2, producing infrared radiation that simulates fire or a low power laser with a wide focus. The mechanical properties, interlaminar shear strength and compression strength, are not degraded by the introduction of these nanoparticles.
In addition, first experiments on samples of neat polymer (without carbon fibres) filled with TiO2 nanoparticles show a decrease in material damage when exposed to an UV-laser.

INTRODUCTION

Due to their good mechanical properties and their low overall density, carbon fibre-reinforced polymers (CFRPs) are used for many lightweight applications. One disadvantage is their high flammability (i.e. Zhang, 2014) due to the polymeric matrix. Another potential threat for CFRP material are laser weapons (i.e. Allheily, 2016). Both, fire as well as laser, act in a comparable way: there is some sort of radiation that causes damage to the material.
In this work, the goal is to extend the lifetime by increasing the time to ignition of the material when it is exposed to heat sources like (kerosene) fires or affection by laser weapons by protecting the material against such radiation. To achieve this goal, particles that may scatter the infrared radiation from the fire/laser may be distributed within the CFRP-material. One possible type of particle may be TiO2. It has a high refractive index (Winkler, 2003) and is therefore often used as a white pigment. The scattering effect is depending on the wavelength, the modification and the particle diameter. Because of this, different diameters and crystalline phases of TiO2 nanoparticles were used for the experiments.

RESULTS AND CONCLUSIONS

Due to their high specific surface area, nanoparticles typically tend to agglomerate. To get the TiO2 nanoparticles separated inside the resin, a multi-level process using a three-roll-mill was designed. After this, a modified wet lay-up process was developed to get the resin with the nanoparticles between the layers of carbon fibres without any filtration effects. By this it was possible to produce high quality CFRP with different amounts of homogeneously

dispersed, unagglomerated TiO2 nanoparticles, as shown in Fig. 1.
The nanoparticles do not degrade the mechanical performance of the CFRP material within the examined concentration limits.
When irradiating the CFRP material inside a cone calorimeter with a heat flux of 35 kW/m², samples with TiO2 nanoparticles show a retarded time to ignition, with its maximum at 3 wt.% particles of the rutile phase with a diameter of 200 nm, as shown in Fig. 2. Analysis of the residue after combustion shows particle-enriched scales formed during the experiments. These scales show their maximum size at 3 wt.% particles and may be the reason for retarded ignition and inhibited combustion.

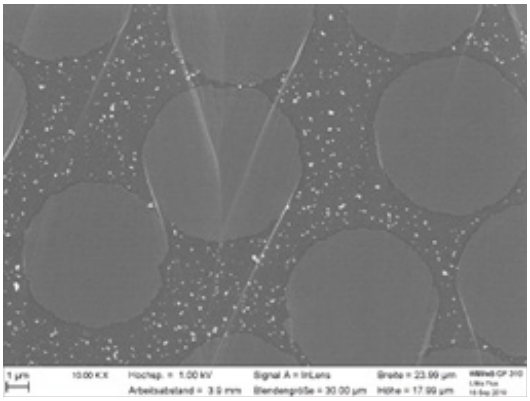

Fig.1 SEM-image of a cross section of CFRP with 3 wt.% TiO2 nanoparticles

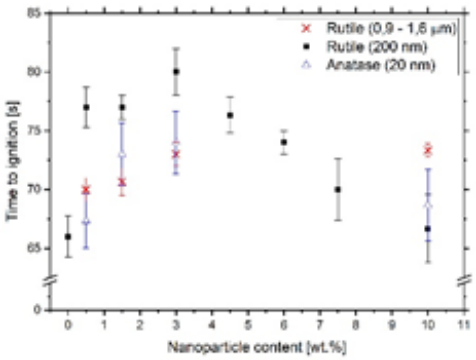

Fig.2 Time to ignition of CFRP with different TiO2 nanoparticles when irradiated at 35 kW/m²

This study shows that TiO2 nanoparticles are a promising candidate as filler for CFRP material to enhance its lifetime when exposed to a fire or laser threat. To analyse the potential of this new material against threats by real laser weapon systems, further tests with high energy laser should be performed.

REFERENCES

[1] Zhang W, He X, Song T, Jiao Q, Yang R. The influence of phosphorous-based flame retardant on the flame retardancy of epoxy resins. Polymer Degradation and Stability, 2014, 109, p. 209-217
[2] Allheily V, Lacroix F, Eichhorn A., Merlat L, L'Hostis G, Durand B. An experimental method to assess the thermo-mechanical damage of CFRP subjected to a highly energetic 1.07 µm-wavelength laser irradiation. Composites Part B: Engineering, 2016, 92, p. 326-331.
[3] Winkler J. Titanium Dioxide: Production, Properties and Effective Usage. Vincentz. Hannover, (2003), 9783866308121.

EPIDERMAL SYSTEMS AND VIRTUAL REALITY: EMERGING DISRUPTIVE TECHNOLOGY FOR MILITARY APPLICATIONS

Marco Marsili
Centro de Investigação, Inovação e Desenvolvimento da Academia Militar (CINAMIL); Centro de Investigação e Desenvolvimento do Instituto Universitário Militar (CIDIUM); Centro de Estudos Internacionais (CEI-IUL), Instituto Universitário de Lisboa (ISCTE-IUL); Centro de investigação do Instituto de Estudos Políticos da Universidade Católica Portuguesa (CIEP-UCP), Lisboa, Portugal.
E-mail: info@marcomarsili.it

ABSTRACT
This work analyzes at what extent invisibility is possible by emulating nature, and if military applications can benefit from technology that combines epidermal systems and virtual reality.

INTRODUCTION
Camouflage and mimicry and have a long-standing tradition in military applications from the 19th century (Forbes, 2009), but eventually have proved to have a limited effectiveness (Scott-Samuel, 2011). In more recent times, has been introduced a multi-scale camouflage that combines patterns at two or more scales, often with a digital camouflage pattern created with computer assistance (Billock, 2010). This function, that is called “scale-invariant camouflage” or called fractal camouflage, does not of itself guarantee improved performance.

ADAPTIVE CAMOUFLAGE
The skin is a relatively underexplored sensory interface that could significantly enhance experiences. The research focuses on the fundamental and applied aspects of silicon nanomembranes, ranging from synthesis and manipulation to manufacturing, device integration and system level applications, including uses in bio-integrated electronics, three-dimensional integrated photonics, solar cells, and transient electronics (Rogers, 2016).
Material scientists have developed a color-changing sheet inspired by squid and octopus, whose skin can transform to blend with its surroundings (Yu, 2014). The basic idea is that the creatures use light-sensitive molecules in the skin to register the light coming from the background against which they sit, and then use this information to alter the appearance of colour-changing cells.
To make the adaptive displays, the researchers began by imprinting a 16x16 grid of cells on a soft plastic. The cells, each about a millimetre across, contain a colour-changing dye embedded in a polymer. The dye is black at room temperature, but when warmed to around 47°C (117°F) its chemical structure changes and it becomes transparent. Cool it, and it becomes black again. At the corners of each cell the researchers added tiny light sensors that record how much light falls on the cell, and this signal is used to control an electric current that helps warm up the dye. Shine a light on the material, and the black dye will turn transparent and expose a reflective silvery material beneath. A fabric coated with miniaturised Light Emitting Diodes (LEDs) and cameras that, by projecting the appropriate background image in all directions, could confer genuine invisibility.

EPIDERMAL VIRTUAL REALITY
A thin, wireless and battery-free system adds a sense of touch to any virtual reality (VR) experience (Yu, 2019). It is a platform of electronic systems and haptic interfaces capable of softly laminating onto the curved surfaces of the

skin to communicate information via spatio-temporally programmable patterns of localized mechanical vibrations. Referred to as an "epidermal VR" system, this equipment communicates touch through a fast, programmable array of individually programmable, millimeter-scale actuators, fused in skin-interfaced wearable scalable device, with almost no encumbrances on the user.

Each actuator — currently they have diameters of 18 millimeters and thicknesses of 2.5 millimeters — resonates most strongly at 200 cycles per second, where the skin exhibits maximum sensitivity. The frequency and amplitude of each actuator can be adjusted quickly and on-the-fly through a graphical user interface, to maximize the sensory perception of the vibratory force delivered to the skin. The patch wirelessly connects to a touchscreen interface. When a user touches the touchscreen, the devices produce a sensory pattern, simultaneously and in real-time, through the vibratory interface to the skin.

This emerging disruptive technology could be combined with a VR headset. Eventually, the devices could be thin and flexible enough to be woven into clothes. And along with VR headsets, people could wear suits to become fully immersed into VR. The result is a thin, lightweight system that can be worn and used without constraint, indefinitely.

RESULTS AND CONCLUSIONS

This study shows that, to be effective, camouflage needs to match the environment and to be disruptive. Military applications can benefit greatly from adaptive and epidermal VR.

ACKNOWLEDGMENTS

The author gratefully acknowledges the funding by Ministério da Ciência, Tecnologia e Ensino Superior, FCT, Portugal, under grant SFRH/BD/136170/2018.

REFERENCES

[1] Billock VA, Cunningham DW, Tsou BH. In: Andrews DH, Herz RP, Wolf MB (eds.) Human Factors Issues in Combat Identification. What Visual Discrimination of Fractal Textures Can Tell Us about Discrimination of Camouflaged Targets. 2010, Ashgate, Farnham, p. 99-101.

[2] Forbes P. Dazzled and Deceived: Mimicry and Camouflage. 2009, Yale University Press, New Haven, CT.
Rogers JA, Ahn JH (eds.). Silicon Nanomembranes: Fundamental Science and Applications. John Wiley & Sons, Hoboken, NJ, 2016.

[3] Scott-Samuel NE, Baddeley R, Palmer CE, Cuthill IC. Dazzle camouflage affects speed perception. PLoS One, 2011, 6(6), e20233. DOI: 10.1371/journal.pone.0020233.

[4] Yu C, Li Y, Zhang X, Huang X, et al. Artificial adaptive camouflage skins. PNAS, 2014, 201410494. DOI: 10.1073/pnas.1410494111.

[5] Yu X, Xie Z, Yu Y, et al. Skin-integrated wireless haptic interfaces for virtual and augmented reality. Nature, 2019, 575, p. 473–479. DOI: 10.1038/s41586-019-1687-0.

NANOSTRUCTURED POLYLACTIC ACID COMPOSITE FILAMENTS FOR SENSING APPLICATIONS

Maria C. Paiva[1(*)], Yilong Li[2], Petra Pötschke[2], Fernando N. Ferreira[3], Paulo E. Lopes[1], Mariana M. Silva[1]

[1]Institute for Polymers and Composites, University of Minho, Portugal

[2] Leibniz Institute of Polymer Research, Dresden, Germany

[3] Centre for Textile Science and Technology, University of Minho, Portugal

[(*)] E-mail: mcpaiva@dep.uminho.pt

ABSTRACT

Electrically conductive filaments were produced based on polylactic acid (PLA)/carbon nanoparticle composites. Polypropylene glycol was incorporated in the nanocomposites aiming at improving the carbon nanoparticle dispersion and increasing the flexibility of the filaments. Filaments with a range of compositions were produced and characterized in terms of their mechanical, thermal and electrical properties. The conductive filaments were tested for sensing activity using saturated acetone vapour, demonstrating a suitable response.

INTRODUCTION

PLA is a biodegradable polymer that presents high potential for medical and sensing applications. Ongoing works reported in the literature concern mainly applications based on 3D printing processing [1], while textile applications are hindered by the limited flexibility of the composite filaments obtained with these materials. In the present work PLA nanocomposite filaments were produced with enhanced flexibility and electrical conductivity, which may be applied on a textile structure for sensing applications

RESULTS AND CONCLUSIONS

Semiconducting fibers based on PLA and carbon nanoparticles were melt-processed using a twin-screw extruder. Multi-walled carbon nanotubes (MWCNT) and exfoliated graphite (GnP) were suspended in poly(propylene glycol) (PPG) to form an electrically conductive paste which was then mixed with PLA in a twin screw extruder. The suspension of the carbon nanoparticles in PPG aided the dispersion and uniform distribution of the nanoparticles in the PLA matrix, as demonstrated by optical microscopy (Fig. 1 a and b) and scanning electron microscopy of the nanocomposite filaments. The electrical conductivity of the PLA nanocomposite filaments with different MWCNT, GnP and PPG compositions was measurement from the I/V curves. The DC conductivity was in the range of 10-7 to 10-2 S.cm-1 (Fig. 1 c). The effect of the addition of PPG upon the thermal characteristics of the composite was evaluated by Differential Scanning Calorimetry (DSC). The plasticizing effect of PPG considerably decreased the glass transition temperature and influenced the crystallization of PLA in the nanocomposites. Thermogravimetric analysis (TGA) showed that the nanocomposite filaments are stable up to 200ºC and that the addition of GnP delays the degradation of composite fibers containing PPG, possibly acting as a 2D barrier to the degradation gases formed. The sensing performance of the composite filaments towards saturated acetone vapor was investigated by measuring the relative change in electrical resistance in cyclic tests on filaments produced with a draw ratio of approximately 3.1 (with~540 µm diameter). The filaments with 3 wt.% MWCNT and PPG demonstrated high sensor response and reversibility (Fig. 1 d).

The plasticizing effect of PPG increases the deformation and flexibility of the PLA composite filaments which is an advantage for textile applications as wearable devices with cost-effective production.

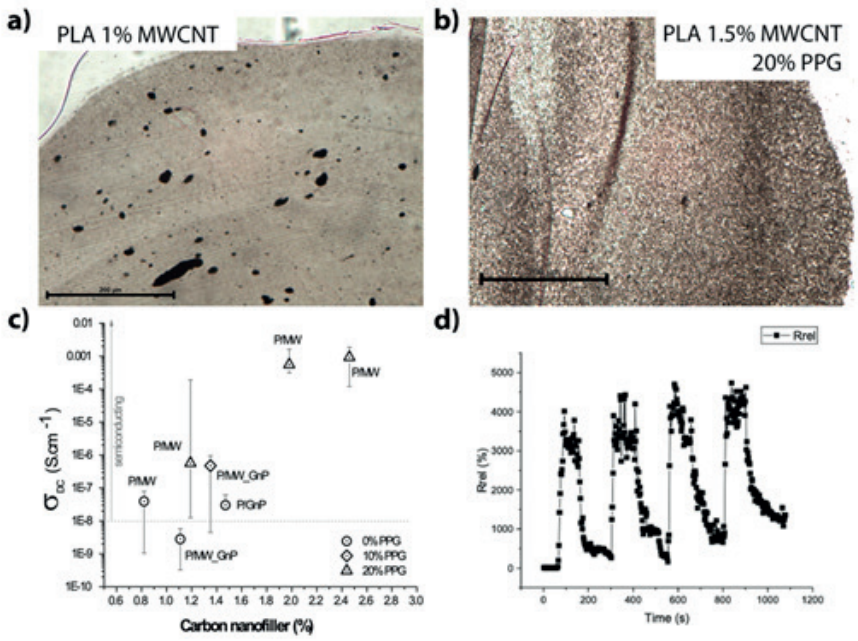

Fig.1 Optical microscopy of the filament cross sections processed without PPG (a) and with the aid of PPG (b); σDC conductivity of the filaments produced as a function of the carbon nanofiller and PPG content (c); relative resistance change vs. the time of exposure to saturated acetone vapor for filaments with 3% MWCNT and PPG (d).

In conclusion, lightweight, flexible and electrically conductive nanostructured PLA composites were produced. The plasticizing effect of PPG was observed, decreasing the composite Tg. At 3 wt.% MWCNT all the processed composites display electrical conductivity in the range 10-2 S.cm-1. The produced electrically conductive filaments were tested for sensing activity towards saturated acetone vapor and were observed to be sensitive, demonstrating potential for the application in fabrics with sensing capacity.

ACKNOWLEDGMENTS

The authors acknowledge the Portuguese Foundation for Science and Technology (FCT) for project PEst-C/CTM/LA0025/2013 (LA 25 – 2015–2018) and for project TSSiPro – NORTE-01-0145-FEDER-000015.

REFERENCES

[1] E. Ivanov, R. Kotsilkova, H. Xia, et al., PLA/Graphene/MWCNT Composites with Improved Electrical and Thermal Properties Suitable for FDM 3D Printing Applications, Appl. Sci. 2019, 9, 1209; doi:10.3390/app9061209.

MULTIFUNCTIONAL COATING BASED ON MWCNTS FOR THERMAL CONFORT AND SENSORIC APPLICATIONS

M. de Dios[1(*)], C. Bandrés[1]
[1]Automotive Technology Center of Galicia (CTAG), Materials Innovation Area, Porriño, Spain
[(*)] E-mail: miguel.dedios@ctag.com

ABSTRACT
This work presents a novel formulation based on MWCNT and a method for the fabrication of electrical contacts that allows the development of multiple applications related with thermal comfort (heating surfaces) and sensing properties (capacitive, resistive, near field and temperature sensors). Although this developments are focused in the range of the automotive industry, there is no limitations to extend their applicability to other sectors like aeronautics, construction industry, and plastic moulding industry, among others, in which their added value has also been proved.

INTRODUCTION
The use of MWCNT for thermal and sensoric applications is a well-known approach present in many sectors in the last decade (Cheng, 2019, Jingjing, 2018). However, most of the attempts to develop “in market” products based on nanomaterials never reach the industrialization stage. In this sense, it is necessary to find an equilibrium between properties, manufacturing cost and simplicity of implementation. CTAG has developed a multipurpose electrically conductive dispersion based on MWCNTs that is fully applicable for the development of heating surfaces, capacitive and resistive actuators, and temperature sensors. The dispersion can be applied by different standard painting methods over a variety of substrates: plastic, textiles, paper, wood, ceramics, glass, etc. Depending on the application, the electrical conductivity can be tuned. Also, the patented electrical contacts allow the fabrication of flexible heating and sensing devices. Some of the real applications for the automotive, construction and plastic moulding sectors will be presented, focused on the simplicity of the fabrication process and its implementation.

RESULTS AND CONCLUSIONS
The applicability of the MWCNT dispersion developed by CTAG has been demonstrated in the fabrication of different prototypes: heating surfaces prototypes and sensoric prototypes.
As an example of heating surfaces, a flexible heating textile has been fabricated. The method patented by CTAG for the fabrication of the electrical contacts based on an electrochemical process avoids the appearance of hot spots and delamination issues. The distribution of temperatures along the surface is highly homogeneous in contrast with the existent heating wire technology.

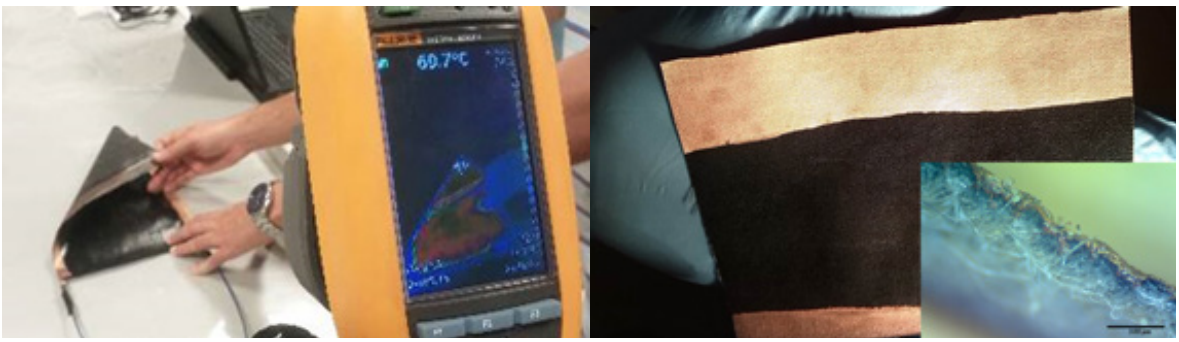

Fig.1 Left image: Flexible heating device with homogeneous temperature distribution based on an electrically con-

ductive textile. Right image: Detail of the electrically conductive textile based on MWCNTs and electrical contacts, developed by CTAG.

As an example of sensing applications, CTAG has developed different devices based on the same formulation: capacitive sensors, near field sensors, resistive actuators and temperature sensors. Real applications of that devices for different sectors will be shown.

ACKNOWLEDGMENTS

The authors gratefully acknowledge the funding by Ministerio de Ciencia, Innovación y Universidades, Spain, under grants RTC-2017-6680-5 Rotoheat. Fábrica 4.0 para procesos de rotomoldeo eficientes. (Convocatoria Retos-Colaboración)

REFERENCES

[1] Cheng Zhang, Lingyu Sun, Bincheng Huang, Xudong Yang, Yantao Chu, Bowen Zhan Electrical and mechanical properties of CNT/CB dual filler conductive adhesives (DFCAs) for automotive multi-material joints, Composite Structures, 2019, Volume 225.

[2] Jingjing Wang, Xiubing Huang, Hongyi Gao, Ang Li, Chen Wang Construction of CNT@Cr-MIL-101-NH2 hybrid composite for shape-stabilized phase change materials with enhanced thermal conductivity, Chemical Engineering Journal, 2018, 350, p. 164-172.

EMERGING APPLICATIONS FOR 3D GRAPHENE AND BN FOAMS FOR HARSH ENVIRONMENTS

Edwin Theo
School of Materials Science and Engineering, Nanyang Technological University, Singapore

ABSTRACT

Ultralight three-dimensional Graphene (3D-C) and boron nitride (3D-BN) foams are renowned for many of their exceptional properties such as high thermal conductivity, mechanical robustness, chemical and thermal stability, structural compatibility and complementary electronic performances. Capable of withstanding high temperatures of up to 550 °C and 900 °C under ambient air for graphene and BN, respectively, and resistant to chemical corrosion and atomic oxygen erosion, we discuss their emerging applications for harsh environments including space applications. The interconnected and highly compressible structures of 3D-C and 3D-BN render excellent surface conformity and high cross-plane thermal conductivity (62–86 W m−1 K−1) which are characteristics essential for thermal management needs. Comparative studies to state-of-the-art thermal interface materials (TIMs) and other materials currently under research for heat dissipation revealed that the 3D-foam improved cooling performance by 20–30%. With matching structural configurations, 3D-C and 3D-BN can be integrated to form hybridized 3D-BNC with tunable electronic performances and electromagnetic interference (EMI) shielding capabilities. The extremely high porosity (~99% porosity) and interconnected networks of 3D-C made them an ideal filler material for efficient phonon and electron transport. We further discuss their roles for enhancing the thermal, electrical and mechanical performances of various composites of polyimides (PIs), shape memory polymers (SMPs) and phase-change materials (PCMs). To cater for space applications, the reliability of the PI composites were tested out undergoing various bending and thermal cycles, as well as in oxidative and aggressive simulated space environments. On the other spectrum, being an insulating dielectric, the potential of using 3D-BN as a dielectric layer for capacitive sensor application was demonstrated. Because of its unique highly porous nature and low elastic modulus, the foam-based sensor device can perform multiple sensing functions such as environmental monitoring and high sensitivity pressure sensor.

CAPILLARY BREAKUP EXTENSIONAL ELECTRORHEOLOGY OF FERROFLUIDS FOR ELECTROHYDRODYNAMICS APPLICATIONS

J. Hermenegildo García-Ortíz[1], F. J. Galindo-Rosales[2(*)]

[1] Departamento de Ingeniería Mecánica y Diseño Industrial, Escuela Superior de Ingeniería, Universidad de Cádiz, Av. Universidad de Cádiz, 10, 11519 Puerto Real, Cádiz España

[2] Department of Mechanical Engineering (CEFT), Faculdade de Engenharia da Universidade do Porto, Portugal

[(*)] E-mail: galindo@fe.up.pt , curro@galindorosales.com

ABSTRACT

This work analyses the rheological properties of a commercial oil-based ferrofluid under uniaxial extensional flow and the simultaneous application of an external electric field. Different intensities of electric field have been imposed and also the influence of the polarity has been analyzed. The results showed that the ferrofluid changed from Newtonian to viscoelastic behaviour as the intensity of the electric increases. Moreover, the polarity has an important effect on counterbalancing the gravitational force in the filament thinning process.

INTRODUCTION

Ferrofluids consist of suspensions of magnetic nanoparticles (MNPs) dispersed in a carrier fluid, which can be water, hydrocarbons, silicones, glycerol, etc. The magnetorheological properties of the ferrofluid can be tuned by means of the composition, size and concentration of the MNPs. These unique rheological behaviors have resulted in many different applications, such as viscous dampers, accelerometers, gyroscopes, sealant for rotary shafts, loudspeakers, magnetic inks, medical applications, etc. (Kaiser, 1970; Popplewell, 1984). Recently, Zahn et al. (2015) proposed a method for cleaning oil-spills consisting of the following steps: 1) Collecting and transferring the water-oil mixture to an oil recovery system onboard a confined space 2) magnetizing one of two liquid phases by adding MNPs 3) separation of the magnetic phase from the nonmagnetic phase using a Halbach array 4) separation of magnetic particles from the magnetic phase using a high gradient magnetic separator system allowing for the particles to be recycled and reused in step 2 5) storing of processed oil, while the clean water is released back into the ocean. Within the military applications, it is worth to highlight that United States Air Force (USAF) introduced radar-absorbent paints made from ferrofluidic to some of their stealth aircraft in order to weaken or eliminate the energy of the reflected radar waves over a specific frequency band (Mouritz, 2012).

The rheological characterization of ferrofluids has been traditionally carried under simple shear flow in a rotational rheometer, equipped with a magnetorheological cell that allows for the application of an external magnetic field perpendicularly oriented to the flow field. Galindo-Rosales and co-workers (2015, 2020) designed a magnetorheological cell to be used in the Capillary Breakup Extensional Rheometer, so that it is currently possible to characterize the magnetorheological properties of ferrofluids under uniaxial extensional flow and the simultaneous application of magnetic field, both perpendicular and parallel to the extensional flow field. Results confirmed that the ferrofluids are more sensitive to the application of an external field aligned with the extensional flow than a shear flow under the influence of a perpendicular magnetic field. However, to the best of the authors' knowledge, ferrofluids have never been characterized under the presence of an external electric field. Very recently, Sadek et al. (2020) have developed an add-on, also for the CaBer, which allows for the characterization of complex fluids under extensional flow and the application of an external electric field. This device has opened a new door for the rheological properties of complex fluids under extensional flow and the application of an electric field aligned with the flow direction, which is the same configuration used in electrospinning, electrospraying and Electrohydrodynamic jet (e-jet) printing processes (Pikul et al. 2011).

This preliminary study has been conveyed with a commercial oil-based ferrofluid (EMG905 Ferrotec Co.). The experiments were developed at room temperature (22 ºC) in the Capillary Breakup Extensional Rheometer (CaBER, Thermo-Haake) equipped with the electrorheological cell, which allowed the application of a potential difference of 3 kV. The 4mm plates and an initial gap of 2 mm were used in all the experiments. As low viscosity samples are prone to suffer from inertial effects, which will result in unreliable results, the Slow Retraction Method was followed, by imposing a linear stretch profile with a velocity of separation of the plates 0f 0.11 mm/s (Campo-Deaño, 2010).

RESULTS AND CONCLUSIONS

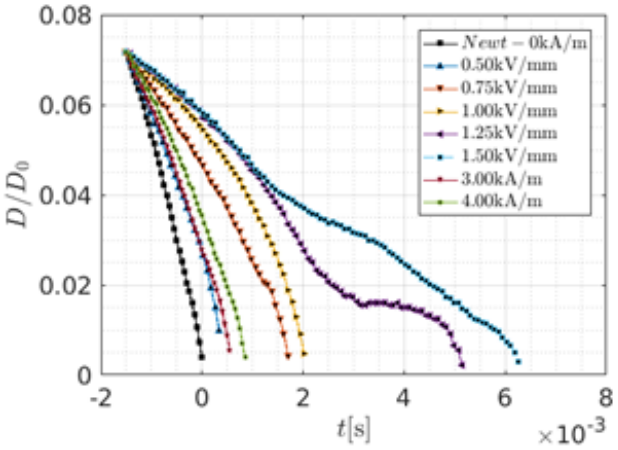

The preliminary results from the CaBEER device are shown in the figure. As the magnetic field is applied aligned with the flow, the filament thinning process slows down and the filament lives around 0.9 ms longer. However, if an electric field is applied between the plates, it can be observed that the filament lives much longer than with the magnetic field. Moreover, results confirm that the rheology of the ferrofluid EMG 905 is very sensitive to the external and its rheological behaviour changes from Newtonian to viscoelastic, which may have a big influence on the electrohydrodynamic processes. Further tests are currently being developed in order to analyze other mechanical properties, such as flexural properties.

ACKNOWLEDGMENTS

The authors gratefully acknowledge the funding by Ministério da Ciência, Tecnologia e Ensino Superior, FCT, Portugal, under grants MIT-EXPL/IRA/0077/2017 and POCI-01-0145-FEDER-030765.

REFERENCES

[1] Campo-Deaño, L. and Clasen, C. (2010) Journal of Non-Newtonian Fluid Mechanics, 165, 1688-1699.
[2] Galindo-Rosales F.J., Segovia-Guitérrez J.P. Pinho F.T., Alves M.A., de Vicente J.. Journal of Rheology, 59, 2015, p.193
[3] Mouritz A.P. Introduction to Aerospace Materials, 2012, p.268-302.
[4] Sadek S.H., Najafabadi H.H., Galindo-Rosales F.J. Journal of Rheology 64(1), 2020, p. 43-54
[5] Sadek S.H., Najafabadi H.H., Galindo-Rosales F.J. Journal of Rheology 64(1), 2020, p. 55-65
[6] Zahn M., Hatton A., Krushrushahi S.R.. US Patent 8,945,393B2 (2015).

NUCLEAR POWER SUPPLY FOR DIRECTED ENERGY DEVICES

Liviu Popa-Simil[1(*)]
[1] Los Alamos Academy of Sciences, Los Alamos, NM 87544, USA
(*) E-mail: laaos@laaos.org

ABSTRACT

Photon and beam based directed energy weapons require compact, solid-state power supply, in order to assure battle-space portability and flexibility. The development of the new space force will require the use in outer space on LTE or exo-planetary orbits of directed energy devices to be used as conflict deterrence and aggression denial systems as well for planetary protection against space threats, as meteorites. The use of these devices in outer space requires high efficiency on all systems from the power supplies to directed energy devices that may be lasers, accelerators or plasma jet devices, each having own features and application range. Novel families of meta-materials for direct nuclear energy conversion to electricity, presently in TRL=3 stage may drive to the construction of ultra high efficiency, solid-state, compact fission, transmutation or fusion batteries, as a prime condition of obtaining a compact portable tool for seamless operation on airborne, or space crafts equipped with a high efficiency directed energy device, in order to minimize the heat sink size, and increase manoeuvrability in tactical field.

INTRODUCTION

The actual range of directed energy devices are operating mainly in pulsed power regime, due to limited continuous power capabilities and scarce cooling resources, using most of the time to accumulate energy and to remove the low grade heat via heat sink.

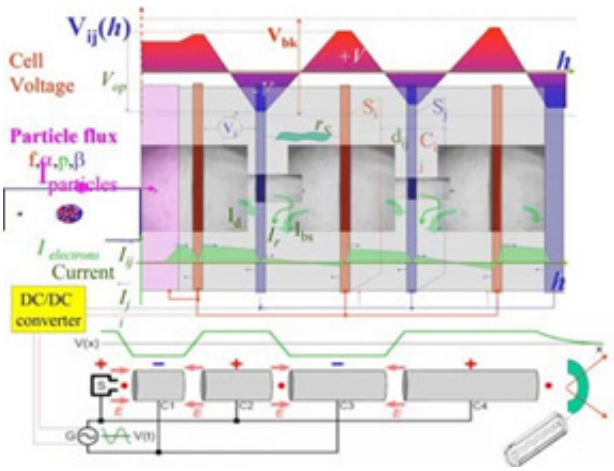

Fig.1 Direct Nuclear Energy converter in electricity powering a pair of linear accelerators for positive ions and for complementary electrons, to stay neutral.

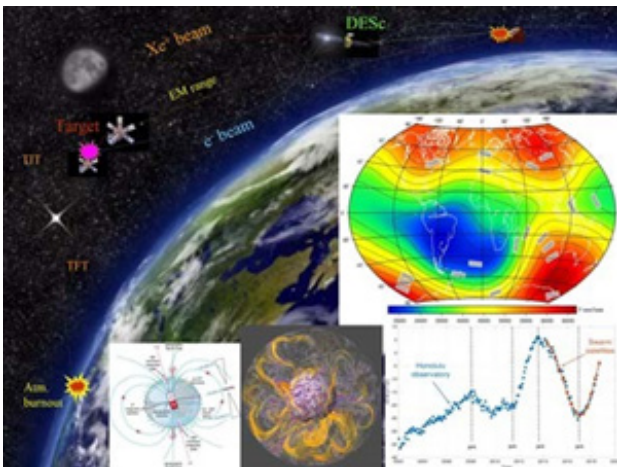

Fig.2 Directed energy application in space for BMD and other space objects using laser and quasi-neutral beam (dual beam).

The new trend in hypersonic ballistic missiles and gliders that shortens the intercontinental time from launch to target less than 6 min. and make classical anti-missile shields based on kinematic-impactor or local blasts impractical require development of new defense systems.
The only reasonable option is to place directed energy weapons in space, able to annihilate a targets after few seconds from its launch pad, and may have plenty of time to chose right moment for annihilation based on enhanced

OODA protocol able to prevent any unintended consequence. In order to have such MW equipment in space very high conversion efficiency is required both for the power supply and for accelerators provided by compact, light devices. Novel super-capacitor like direct nuclear energy converter into electricity, made using engineered nano-hetero structures is susceptible of delivering MW power at efficiencies higher than 90% and so does the RFQ accelerators used to produce the charged particle beam and the complementary electron beam, remaining less then 20% of the total power to be eliminated using heat sinks, that will reduce the dimensions of space shuttle under 50m, being able to reach targets in 4000 miles range, interlacing the beans and using customized aiming as shown in Fig. 2 that consider magnetic and plasma fields distribution along the trajectories.

RESULTS AND CONCLUSIONS

The system shown in Fig. 1 is using a nano hetero structure generically called “CIci”, that converts the kinetic energy of fission products, emerging from high electron availability conductive layer “C”, by producing a n electron shower, that travels ballistic through insulator layer “I”, being collected in the conductive layer “c” that becomes negatively polarized as it emits no electron shower, and it is insulated by the layer “i” from the next conversion cell. The typical range of the fission products in this structure is of about 20 μm, there are about 200-400 CIci repetitive cells connected in series or parallel to harvest the entire energy of the fission product that is about 35 pJ/fission act, and customize the power delivery [1]. The system is embedded in a solid-state fission reactor structure that adjusts the reactivity to comply with the power demand[2]. The accelerator system consists in a positive ion beam accelerator, operating simultaneous with an electron accelerator that delivers the same current, in order to maintain neutral the polarization of the entire system. It may also have an LED laser based system to increase the impact on target and an aiming calculator unit, and other functional electronics for flight control and collateral applications.

The conversion system efficiency is higher than the usual power sources, because it uses directed energy inside the capacitor in about 1 eV range (equivalent of 11,000 K) where even Carnot efficiency over 95%. The nuclear structure has about 2 ft radius being able to deliver up to few GW in pulsed or continuous power regime depending on heat removal capabilities onboard. It is known that a 100 mA, 100 MeV ion beam applied on a surface of ¼ m2 may evaporate 2 Kg/s of Al alloy, inducing in a 5 ton target a 2 m/s2 acceleration due to target’s mass evaporation, while all electronics on board is instantly upset. These performances may be reached at maturation, of such system that presently is in R&D phase.

ACKNOWLEDGMENTS

The authors gratefully acknowledge the support of LAAS and LAVM LLC.

REFERENCES

[1] Popa-Simil L., Advanced Space Nuclear Reactors from Fiction to Reality. Proceedings of Space, Propulsion & Energy Sciences International Forum (Space, Propulsion & Energy Sciences International Forum), AIP, 2011.

[2] Popa-Simil L., Accelerator Enabled Nano-Nuclear Materials Development. Advanced NanoMaterials and Technologies for Energy Sector, 2017. 1(1): p. 12.

MECHANICAL DESIGN AND MANUFACTURING OF SIGNAL INTERCEPTION ANTENNA IN COMPOSITE MATERIALS FOR NAVAL APPLICATION

Daniele Santoro[1(*)], Umberto Lecci[1], Pera Fabio Massimo[1], Giovanni Di Santo[1], Domenico Gaetano[1], Pietro Bia[1], Antonio Manna[1]

[1] Elettronica Group, Elettronica S.p.A., Rome

[(*)] E-mail: daniele.santoro@elt.it

ABSTRACT

This work shows the mechanical design and the FE analyses performed for an innovative naval Antenna Unit for signal interception application: more than 20 Electromagnetic sensors operating from HF up to Ka band and microwave modules are integrated in a unique structure designed for a top mast installation (i.e. for naval platform). The number of constraints in terms of weight and electromagnetic transparency calls for the employment of composite materials such as glass, aramidic and carbon epoxy prepregs. Primary structures have been modelled by using FE codes: both orthotropic and isotropic models have been implemented as well as non-linear contacts and bolted joints. The mast-mounted installation requires high mechanical stiffness and strength but the exposure to saline environment needs many manufacturing issues to be respected. In particular, the selection process of suitable materials and the sealing manufacturing procedures to protect them from the external agents has been reported. Another key feature of the presented design concern the electromagnetic compatibility requirement: to avoid electromagnetic emissions (EMC) generated by antenna's internal units and to protect antenna sensors by external platform's emitters, an appropriate stacking sequence has been chosen for composite laminates with a prepreg copper mesh.

INTRODUCTION

Typical signal interception sensors for naval application have to overcome big problems in terms of available space and position on platform. In fact, in order to guarantee the expected performances, the need the higher position, such as top mast, where no obstacles can reduce the antenna's field of view [1]. In order to allow this, the primary structures have to be designed as much lighter as possible with excellent structural and thermal response under high loads. Composite materials offer a solution for this purpose, giving higher specific stiffness and strength superior than conventional metallic materials, such as aluminum or steel [2]. In some instances, the difference is as high as 16 times the specific strength. Furthermore, composite materials such as fiberglass or aramidic fibers (plus epoxy resin), are able to guarantee good electromagnetic transparency without causing reduction in sensor's performance. Numerical models have been developed with a batch-type parametric approach to rapidly evaluate the combined effect of geometric and material parameters. Static and dynamic simulations have been performed in order to predict the structure's response under operative mechanical loads [3]. The antenna is composed of multiple stages, each composed essentially by primary structures in composite material and metallic interconnection flanges. The overall stack is depicted in Figure 1(a), while multiple friction ties joint each stage with the next one. Each stage has a particular function in terms of capabilities except the so-called "Base Section" which contains processing and microwave electronics. As consequence, this last section, will be more thermal stressed stage and requires high cooling performance by using only natural convection. Furthermore, a proper EMC design has been carried out inserting a proper copper mesh in the antenna composite laminates.

RESULTS AND CONCLUSIONS

The most severe load condition shall be the half-sine shock profile with maximum amplitude of 30g (~300 m/s2) applied in 6 ms. The results from FE structural simulation are reported in Figure 1(b), where a stress contour plot of failure index is indicated following the Tsa-Wu criterion for composite based structures. The maximum value reached is 0.5 at the connection between composite structure and flanges. However, this value gives a good margin below plies failure under operative conditions.

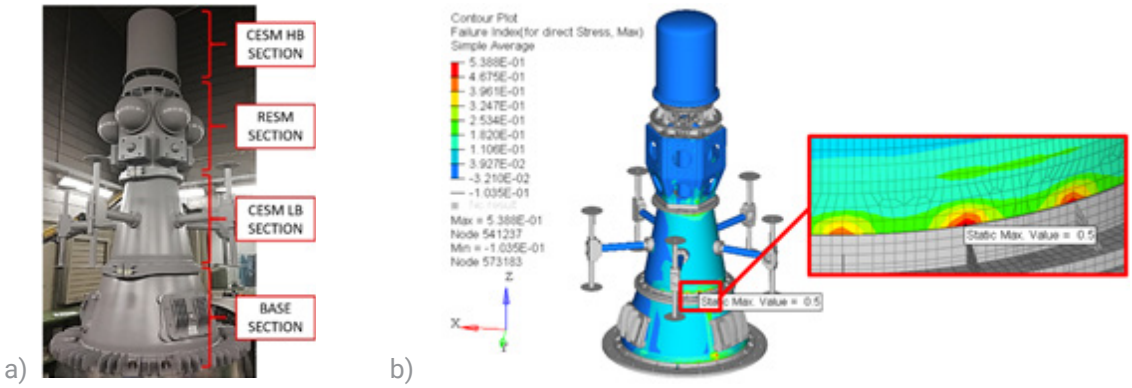

Fig.1 a) Schematic description of antenna divided in stages of the actual antenna and b) Tsai-Wu contour plot criterion for the composite material antenna.

As discussed previously, the antenna has been designed in order to isolate the internal electronics from the external environment in terms of electromagnetic emissions (the so-called EMC design). In order to do that, a proper prepreg copper mesh has been included as last layer of stacking sequence of composite laminates. Several electrical conductivity measurements have been performed in order to establish the material and stacking sequence fit for the required performance for mast-mounted naval installation (see Figure 2(a)).

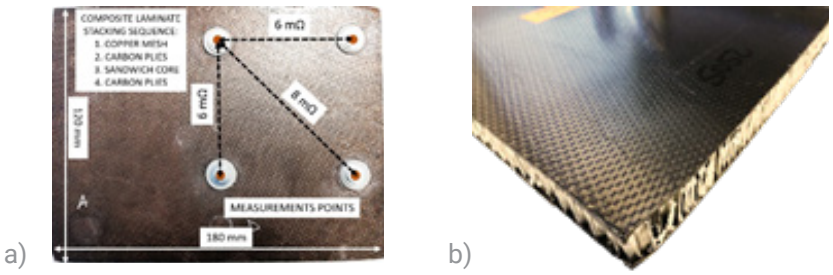

Fig.2 Composite panel with copper mesh used for electrical conductivity measurements.

REFERENCES

[1] G. Barrows e B. Krantz, “Integrated RF sensors for electronic warfare applications,” in IEEE International Symposium on Circuits and Systems. Emerging Technologies for the 21st Century, 2000.

[2] Santoro D, Lecci U, Quadrini F, Santo L, “Structural design of hybrid processing unit chassis for airborne electronic systems”, Proceedings of the ASME 13th International manufacturing science and engineering conference, 2018-6422, College Station, Texas, USA.

[3] Clay S., and P. M. Knoth. “Experimental results of fatigue testing for calibration and validation of composite progressive damage analysis methods”, Journal of Composite Materials, 51, (2016) pp. 2083-2100.

[4] Baskey, H.B., and M.J. Akhtar. “Electromagnetic design and testing of carbon black and carbon fiber-epoxy composites for defence stealth applications”. 2013 IEEE Applied Electromagnetics Conference, AEMC 2013, (2014) art. no. 7045065.

DURABLE AND HIGHLY DISSIPATIVE FIBROUS COMPOSITES FOR STRENGTHENING COASTAL MILITARY CONSTRUCTIONS

Cesare Signorini[1(*)], Andrea Nobili[1,2]

[1] Research Centre "En&Tech", University of Modena and Reggio Emilia, Reggio Emilia (RE), Italy

[2] Department of Engineering "Enzo Ferrari", University of Modena and Reggio Emilia, Modena (MO), Italy

[(*)] E-mail : cesare.signorini@unimore.it

ABSTRACT

Reinforced concrete military structures are often established in coastal or offshore areas, subjected to severe saline and acid environments. The peculiar porosity of cementitious conglomerates favours the penetration of chlorides, which corrode the internal metallic rebar. The reinforcement of structures with fibrous composite materials is a viable solution to restore the initial requirements of the building. Among synthetic fibres, polyphenylenebenzobisoxazole (PBO) is an organic fibre with high elastic modulus and tensile strength and highly dissipative attitudes. In this work, the assessment of durability of continuous fibre-reinforced cementitious mortar (FRCM) composites is carried out, comparing the mechanical performance of laminates subjected to uni-axial tensile tests. PBO-FRCM presents high resistance against aggressive environments and preserve its mechanical strength in the presence of salt-water, where other reinforcing materials undertake a dramatic degradation.

INTRODUCTION

Weakening of bearing capacity of reinforced concrete is common when coastal and offshore military buildings or bunkers are considered, due to penetration of chlorides through the porosity of the conglomerate. Fibrous materials have been employed for military use since the Sixties, exploiting the remarkable dissipative and durability properties of the fibres and their composites. Besides, continuous fibres gathered in woven textiles embedded in polymeric resins have found interest as reinforcing techniques for ballistic applications (Carr, 1999). The mechanical behaviour of such kind of composites, also in hybrid forms, has been widely investigated (see the ample review by (Safri et al., 2018) and references therein). Similarly to aramid, PBO macromolecules are kept together by weak bond forces, fibrillating (fibrils diameter ranging from 10 to 50 nm) upon abrasion. Besides, PBO fibres present high tenacity, outstanding stiffness and high alkali resistance (Wilusz, 2008) that allow the embedment of PBO fabrics in cementitious matrices. From the structural standpoint, inorganic matrix continuous reinforcement presents several attractive features for building refurbishment. In particular, the addition of a tough strengthening fabric (i.e. PBO) may enhance the response to impact of military buildings. We focus on the durability assessment of PBO-FRCM composite materials, subjected to the exposure to salt-water, simulating severe weathering due to chloride attacks typical of coastal areas (Signorini et al., 2018), and acid conditions. Uni-axial tensile tests are carried out. PBO-FRCM has proved to offer very reliable performance even after a severe accelerate aging treatment.

RESULTS AND CONCLUSIONS

Tensile tests are carried out on 1-ply laminates manufactured according to a well-established protocol detailed in the literature. Test set-up complies with what prescribed by (RILEM 232-TDT, 2016) with wedge friction clamps. Accelerated aging of composite materials is performed into saline and acid environments, at controlled temperature for 1000 hours (ICC AC434, 2013).

The mean values of strength, strain and energy dissipated at failure are displayed in Figure 1.

Fig.1 Mean ultimate strength, strain and mechanical energy dissipated at failure for PBO-FRCM composite laminates in traction (CC = control, DW = distilled water, HA = hydrochloric acid, AK = alkaline, SW = salt water).

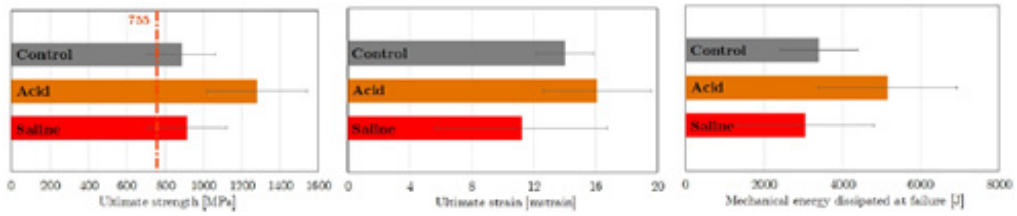

PBO fibres exhibit high resistance to the chemical attacks typical of coastal environments. Indeed, mean strength values never breach the acceptance threshold of 85% of the strength measured in inert environment (namely "control"). However, detrimental effects brought by accelerated aging exposure are spotted in the decrease of deformability of the laminate as well as in the increased data scattering, when salt-water attack is considered. Anyway, PBO can be safely employed in refurbishing military building owing to its dissipative capacity and negligible strength losses under severe and prolonged saline and acid attacks, contrarily to what found for other fabrics like glass or carbon (Nobili & Signorini, 2017).

REFERENCES

[1] Carr, D. J. (1999). Failure mechanisms of yarns subjected to ballistic impact. Journal of Materials Science Letters, 7(18), 585–588.

[2] ICC AC434. (2013). Acceptance criteria for masonry and concrete strengthening using fiber-reinforced cementitious matrix (FRCM) composite systems. In Whittier, CA.

[3] Nobili, A., & Signorini, C. (2017). On the effect of curing time and environmental exposure on impregnated Carbon Fabric Reinforced Cementitious Matrix (CFRCM) composite with design considerations. Composites Part B: Engineering, 112, 300–313. https://doi.org/10.1016/j.compositesb.2016.12.022

[4] RILEM 232-TDT. (2016). Test methods and design of textile reinforced concrete. In Materials and Structures (Vol. 49, Issue 12). https://doi.org/10.1617/s11527-016-0839-z

[5] Safri, S. N. A., Sultan, M. T. H., Jawaid, M., & Jayakrishna, K. (2018). Impact behaviour of hybrid composites for structural applications: A review. In Composites Part B: Engineering (Vol. 133, pp. 112–121). Elsevier Ltd. https://doi.org/10.1016/j.compositesb.2017.09.008

[6] Signorini, C., Nobili, A., & Falope, F. O. (2018). Mechanical performance and crack pattern analysis of aged Carbon Fabric Cementitious Matrix (CFRCM) composites. Composite Structures, 202, 1114–1120.

[7] Wilusz, E. (2008). Military Textiles. Woodhead Publishing.

STRUCTURAL DNA BIOPHOTONICS: UNDERSTANDING AND OPTIMIZING LIGHT HARVESTING AND TRANSFER ON THE NANOSCALE

Sebastián A. Díaz[1(*)], Paul D. Cunningham[2], Divita Mathur[1], Mario G. Ancona[2], William P. Klein[1], Brian S. Rolzynski[2], Sean M. Oliver[3,4], Patrick M. Vora[3,4], Joseph S. Melinger[2], and Igor L. Medintz[1]

[1] Center for Bio/Molecular Science and Engineering, Code 6900, U.S. Naval Research Laboratory, Washington, D.C. 20375, USA

[2] Electronic Science and Technology Division, Code 6800, U.S. Naval Research Laboratory, Washington, DC 20375, USA

[3] Department of Physics and Astronomy, George Mason University, Fairfax, VA 22030, USA

[4] Quantum Materials Center, George Mason University, Fairfax, VA 22030, USA

[(*)] E-mail: sebastian.diaz@nrl.navy.mil

ABSTRACT

DNA is a biocompatible scaffold that allows for the design of a variety of nanostructures, from double stranded DNA to more complex DNA origami and 3-D structures. By modifying the structures, with dyes, nanoparticles, or enzymes, we create complex light harvesting and energy transfer systems with features on the nanometer level. We study these systems with the intent to recreate the incredible efficiency observed in natural systems (e.g. photosynthetic systems) by parsing basic design rules. One focus area is looking at optimizing parameters, including geometries and densities of organic dyes in the weakly coupled regime by what is commonly referred to as the Förster resonance energy transfer (FRET) mechanism. A recent example include a DNA origami molecular photonic wire (MPW) whose dye density was optimized so that 59 ± 6 % energy transport efficiency over a length of 29 nm was obtained, this was an approximate 10-fold increase in efficiency over previously reported DNA-MPWs of similar length.[1] Other applications include utilizing a DNA dendrimer as an unconventional encryption keys based on physically unclonable functions with the capability to generate ~10^{37} unique challenge key combinations through geometric variation that could be read-out with a simple cell-phone based spectrometer.[2] We investigate how other parameters including geometries, cryogenic conditions, and fluency conditions can optimize light harvesting and controlled transfer. Additionally the use of inorganic nanoparticles allows us to exploit other mechanisms such as plasmonics, while enzymes can provide bioluminescent properties.

ACKNOWLEDGMENTS

The authors gratefully acknowledge the funding by U.S. Naval Research Laboratory (NRL) and the NRL Nanosciences Institute.

REFERENCES

[1] Klein W, Rolczynski B, Oliver S, Zadegan R, Buckhout-White S, Ancona G, Cunningham P, Melinger J, Vora P, Kuang W, Medintz I, Díaz, S. DNA Origami Chromophore Scaffold Exploiting HomoFRET Energy Transport to Create Molecular Photonic Wires. ACS Appl. Nano Mat., 2020, Just accepted.

[2] Klein W, Díaz, S, Chiriboga M, Walper S, Medintz I. Dendrimeric DNA-Based Nanoscaffolded BRET-FRET Optical. ACS Appl. Nano Mat., 2019, 2, p. 7459-7465.

ADVANCED HIERARCHICAL COMPOSITES – ARE POTENTIAL MATERIALS FOR DEFENSE APPLICATIONS?

Sohel Rana[1(*)], Shama Parveen[2], Subramani Pichandi[3]
1, 2, Department of Fashion & Textiles, University of Huddersfield, Huddersfield, UK
[3] IComp, University of Limerick, Limerick, V94 T9PX, Ireland
[(*)] E-mail: s.rana@hud.ac.uk

ABSTRACT
This paper gives an overview of hierarchical composites and discusses their application potential in advanced technical sectors including defence. The concept of hierarchical composites, their production methods and properties have been discussed and compared with conventional composites. Production and properties of hierarchical composites fabricated with bio-based and sustainable reinforcing materials such as cellulose microcrystals have also been discussed.

INTRODUCTION
Hierarchical composites are found abundantly in nature and composed of different components which are hierarchically organised to provide specific set of properties. One example of such composites is wood, which is made of micro ad nano-scale cellulosic materials hierarchically organised in a polymeric matrix (i.e. lignin). As these composites are fabricated using materials from different scales, they are also known as multi-scale composites. Inspired by nature, researchers have also developed different types of hierarchical composites using natural as well as synthetic fibres (Pichandi, 2018). Mainly two approaches have been used for developing these composites such as: (a) dispersing a micro/nano-scale filler such as carbon nanotubes, graphene, nano cellulose, microcrystalline cellulose, etc. within a polymeric resin and then, fabricating composites by impregnating natural or synthetic fibres with the nano/micro filler dispersed resin, and (b) incorporating the nano or micro materials on the surface of the reinforcing fibres through coating, grafting, spraying or growing (in some cases) and then, fabricating the composites by impregnating these nano/micro filler integrated fibres with a polymeric resin (Pichandi, 2018; Rana, 2011).

EXPERIMENTAL RESULTS
Hierarchical composites exhibited a number of advantages over conventional composites such as improved strength and stiffness, fracture toughness, interlaminar shear strength, impact resistance, dynamic mechanical properties and thermal stability, electrical and thermal conductivities (in case of conductive nano/micro fillers), and so on (Pichandi, 2018; Rana, 2011). Table 1 shows the improvement of flexural strength (σf) and fracture energy (FE) of cellulose microcrystal (CMC) based glass/epoxy hierarchical composites over conventional glass/epoxy composites. The improvement of interlaminar shear strength of hierarchical composites over neat glass/epoxy composites is shown in Fig. 1.

Sample	σf (MPa)	% Increase	FE (N.m)	Increase (%)
Glass/epoxy	290	-	429	-
Glass/epoxy + 1% CMC	510	76.0	940	119
Glass/epoxy + 1.5% CMC	480	66.0	759	77
Glass/epoxy + 3% CMC	435	50.0	713	66

Table 1 Flexural properties of neat glass/epoxy and hierarchical composites (Parveen, 2020)

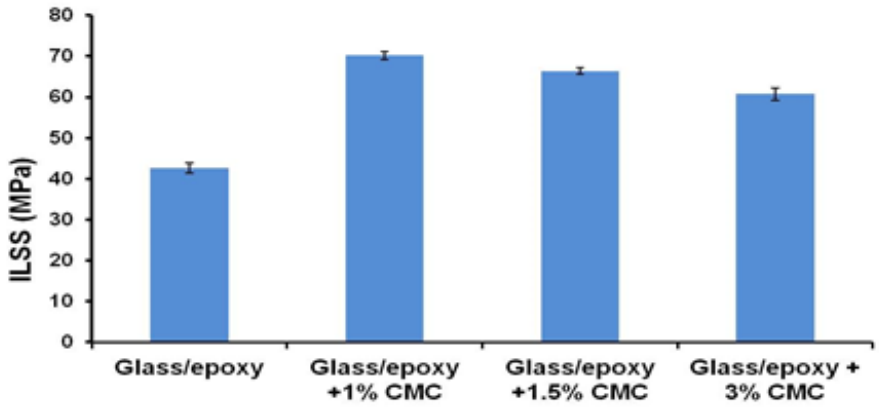

Fig.1 Interlaminar shear strength of neat glass/epoxy and hierarchical composites (Parveen, 2020)

It can be observed from the above results that the addition of a small amount of CMC can strongly improved the mechanical properties, fracture energy and interlaminar shear strength of glass/epoxy composites, presenting significant benefits of hierarchical composites over conventional composites.

CONCLUSIONS

Hierarchical composites exhibit strong improvement in fracture energy, delamination and damage resistance as well as impact performance of composites, making them an ideal candidate for a number of defence applications such as bullet proof vests, helmet, etc.

REFERENCES

[1] Parveen S, Pichandi S, Goswami P, Rana S. Novel glass fibre reinforced hierarchical composites with improved interfacial, mechanical and dynamic mechanical properties developed using cellulose microcrystals. Materials & Design, 2020, 188, p. 108448.

[2] Pichandi S, Rana S, Parveen S, Fangueiro R. A green approach of improving interface and performance of plant fibre composites using microcrystalline cellulose. Carbohydrate polymers, 2018, 197, p. 137-146.

[3] Rana S., Alagirusamy R, Joshi, M. Development of carbon nanofibre incorporated three phase carbon/epoxy composites with enhanced mechanical, electrical and thermal properties. Composites Part A, 2011, 42, p. 439-445.

BALISTIC IMPACT RESISTENCE OF AL-2024 ALLOY AND COMPOSITE MATERIALS

Manuel Gomes[1(*)], José Sousa[1], Ricardo Rocha[2], and Luis Pina[2]
[1]ISQ, Research Development and Innovation Division, Oeiras, Portugal
[2] INEGI, Composite Materials and Structures Unit, Oporto, Portugal
[(*)] E-mail: magomes@isq.pt

ABSTRACT

The present work compares the ballistic impact resistance of an aeronautical grade 2024 aluminium alloy and several composite materials, as part of the work developed within the PASSARO project. Impact tests using steel spheres at velocities roughly in the range of 50-200 m/s were performed in a new test facility developed by ISQ. Al-alloy plates of different thicknesses and composite materials, which are being considered to benchmark further composites under development, were tested. At similar areal densities the composite materials could approximately match the ballistic resistance of the conventional aluminium alloy.

INTRODUCTION

CFRP and other composite materials are being increasingly used in aeronautical industry both as structural and fuselage skin materials. The pinnacle of this trend are probably the Boeing 787 and Airbus 350 with their almost all-composite fuselage. The driving force for this trend is the reduction of weight with consequent increase of payload and fuel efficiency of the aircraft. However, composites can pose different challenges to designers, particularly because their behavior under impact conditions, can cause internal damage not always obvious from surface observations [1]. On the other hand, some of the most threatening events to aircraft flight safety are impacts with birds or hail, often with severe consequences for skin and structural members alike [2].

The PASSARO project is concerned with the development of new composite materials for fuselage usage which can fulfill different requirements, among them improved impact protection [3]. Impact tests were performed on a compressed air cannon specifically developed for this project [4], Figure 1a), at speeds between roughly 50 and 200 m/s using hardened steel spheres with diameters of 12 and 19 mm. The target materials were Al -2024 alloy plates 1.2 mm thick, typical of aeronautical fuselages and taken as reference material, and three different composites Figure 1b).

a)

b)

Material	Composition	Areal Density (%)
BSL1	Al 2014 T3 - 1.2 mm thick	100
BSL1A	Al 2014 T3	67
BSL1B	Al 2014 T3	133
BSL2	Al+Rohacell 71WF+Al	238
BSL3	T700 CFRP	100
BSL3A	IM7/8552	77
BSL3B	IM7/8552	166

Fig.1 a) Compressed air cannon and b) materials tested.

RESULTS AND CONCLUSIONS

The results of the impact tests are summarised in Figure 2. The somewhat small number of tests performed so far impaired an analysis based on commonly accepted models such as the one proposed by Lambert and Jonas [5] except for the Al-alloy. Therefore, that model was used to obtain the ballistic limit of the Al-alloy 1.2 mm thick and this value

was then used as reference to normalize the data in Figure 2. Then, for comparative purposes, a simple log fit was performed on the data of the different materials to allow some approximate conclusions to be drawn up. In general, the ballistic limit was around 100-110 % for all materials impacted with 12 mm spheres, decreasing to about 90% or lower with the 19 mm sphere. The composite materials exhibited a very similar behaviour to the Al alloy at similar areal densities. However, the use of a sandwich composite with more than twice the areal density of Al or laminate composites only lead to a 50% increase in the ballistic limit. Likewise, doubling the areal density of laminates only produced a marginal increase of the ballistic limit.

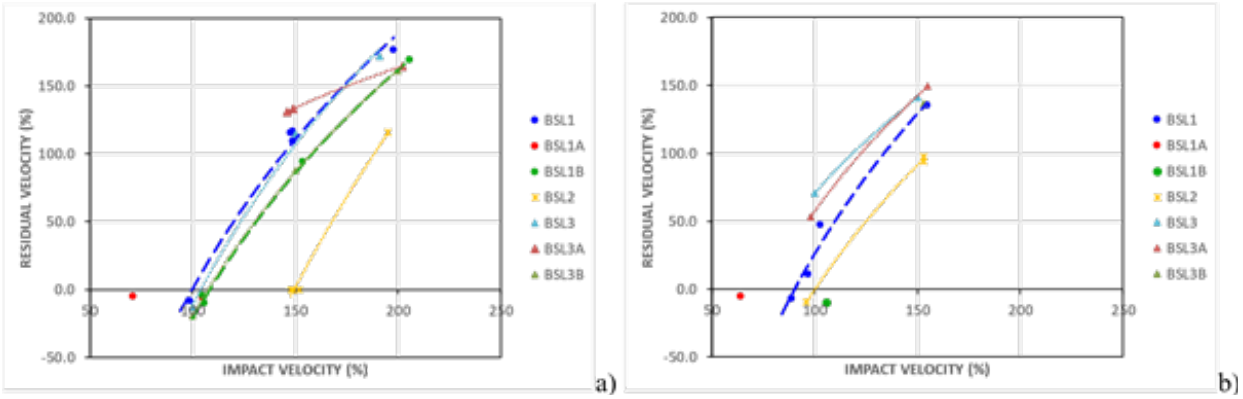

Fig.2 Residual velocity on impacts with spheres of diameter, a)12 mm, and b) 19 mm

ACKNOWLEDGMENTS

The present work was funded by the Clean Sky 2 Joint Undertaking under the European Union's Horizon 2020 research programme under Grant agreement No 807083, to which the authors would like to express their acknowledgement.

REFERENCES

[1] S Abrate, "Impact on Laminated Composite Materials", Appl. Mech. Rev., Vol 44, April 1991.

[2] J. Thorpe, "Fatalities and Destroyed Civil Aircraft due to Bird Strikes, 1912-2002", International Bird Strike Committee, IBSC26/WP-09, Warsaw, 5-9 May 2003

[3] R. Rocha, S. Sadek, M. Gomes, and J. Sousa, "AIR O-B-3.3.9.2-3 (OT3.3) Preliminary Design: WP3 – Medium and High Energy Impact Protection Materials," Porto, 2019

[4] M. Gomes, "High Energy Impact Test Procedure", PASSARO Auxiliary Document, Oeiras, April 2019.

[5] S. Abrate, "Ballistic Impact on Composites", 16th International Conference on Composite Materials, Kyoto, Japan, 2007.

THERMAL AND ELECTRIC PROTECTION BEHAVIOUR OF GNP'S FUNCTIONALIZED WOOL FABRICS

Francisca Guedes[1], Gabriela Queirós[2], Cristina Silva[2(*)], Diana Ferreira[2], José Fiadeiro[3], Frederico Nogueira[3] and Raul Fangueiro[1,2]

[1] Department of Mechanical Engineering, University of Minho, Portugal

[2] Centre for Textile Science and Technology (2C2T), University of Minho, Portugal

[3] A Penteadora, S.A, Unhais da Serra, Portugal

[(*)] E-mail: cristinasilva@fibrenamics.com

ABSTRACT

Technical textiles and functional garment assemblies can be engineered to optimize the protection against heat, flame, molten metal, static electricity, electromagnetic radiation, chemical agents, among others. The present work aims to study the use of wool-based fabrics as a fibrous substrate for thermal and electric protection by surface functionalization with Graphene Nanoplatelets (GNP's) in polymeric-based dispersions. Wool fabrics were functionalized with 1% GNPs dispersed in chitosan and polyurethane, using impregnation and coating techniques. The results show that wool fabrics coated with polyurethane (PU) functionalized with 1% GNPs present an interesting approach regarding multiscale protection.

INTRODUCTION

Flame retardancy (FR) properties in fabrics can be influenced by the manipulation of the yarn characteristics, yarns density and construction, and finish treatments [1]. Nowadays, the most common solution, for protective equipment, are fluorocarbon-based coatings, due to their strong adhesion, chemical attack resistance and high-temperature resistance. However, these chemical agents contribute to environmental contamination, and therefore, several international regulations are being implemented worldwide restricting their application [2]. Wool is a natural flame retardant fibre, presenting low ignitability, burning with a selfextinguishing flame, and forming a soft dissipating ash residue, whereas most synthetic fibres form a hard, molten bead residue with melt-drip behaviour. Its inherent fire resistance is due to the high nitrogen and water content, requiring higher levels of oxygen and heat to actually burn. However, these exceptional characteristics are not sufficient to guarantee protection against some external agents, and for that reason, many studies have been carried out in order to promote the performance of technical textiles through multiscale functionalization [1]. Regarding electric protection, and to improve the anti-static ability of wool fabrics, graphene nanoplatelets (GNP's) have been widely studied due to the excellent thermal, mechanical, and electrical properties [3]. Additive treatments with polymeric solutions, such as PU, with GNP's, may offer alternatives to obtain a shielding effect on wool. As an alternative to the conventional processes in textiles, chitosan (CS) biopolymer was also implicated in the present work, due to its biodegradable and bioabsorbable characteristics, that are increasingly relevant on the market, given the current environmental regulations [4].

RESULTS AND CONCLUSIONS

A 100% woven wool fabric (Sample A) provided by A Penteadora, S,A was: (1) impregnated with 1% GNP's in polymeric formulation of chitosan (CS) (Sample B), (2) coated with PU (Sample C) and (3) coated with 1% GNPs functionalized polyurethane (Sample D).

Mechanical stirring and ultrasonication techniques were used for homogeneous dispersion of GNP´s before the fabrics coating and impregnation processes. Electrical and thermal properties of wool samples were evaluated using ISO 11925-2 and EN 1149-2 standards. The ignitability tests were carried according to ISO11925-2 and the results ob-

tained are shown in Figure 1. Taking into account the intensity and the extension of the burnt area, it can be observed that the substrates with GNP's (Samples B and D) present better performance showing the positive effect of GNP's on the flame retardancy performance.

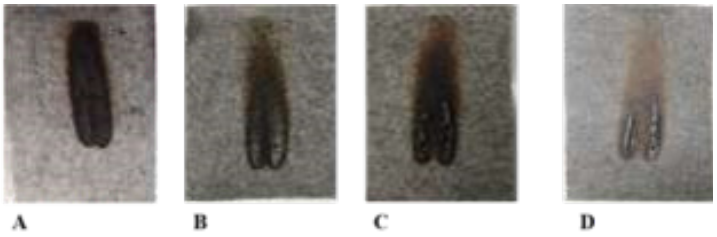

Fig 1 Results of the Ignitability Test for Wool – sample A; Wool with 1% GNP's in polymeric formulation of chitosan (CS) - sample B; Coated Wool with PU – sample C; Coated Wool with PU and 1% GNP's – sample D.

The results for electrical resistance and radiant heat, are presented in Table 1. Analyzing the electrical properties, it can be observed that, when compared to wool without GNP's, sample B shows a lower electrical longitudinal resistance. In fact, GNP's act as promoters of electrical conductivity, decreasing the electrical resistance. On the other hand, when comparing sample B and sample D, it's possible to conclude that PU acts as a blocker of the electric current, increasing electrical resistance. For the radiant heat tests, the temperature of the outer surface of the fabrics (in direct contact with heat source) was measured when the inner surface reached 200 ºC, in order to understand the performance of the fabrics as a heat barrier. The best results are obtained for sample B, that exhibits a temperature gradient of 161ºC in between the inner and outer fabric surface, showing great potential in ensuring the thermal comfort during use when in contact with strong heat force.

Sample	Composition	Electrical Resistance (Ω)	Radiant heat test		
			Inner surface (ºC)	Outer Surface (ºC)	ΔT (ºC)
A	Wool	$9{,}6x10^{9}$	200±0,5	**55,7**	145
B	Wool with CS and 1% GNP's	$1{,}6x10^{6}$		**39,4**	161
C	Coated Wool with PU	$4{,}00x10^{9}$		**47,7**	152
D	Coated Wool with PU and 1% GNP's	$4{,}3x10^{9}$		**45,0**	155

Table 2 Results of the electrical longitudinal resistance and the radiant heat tests

In conclusion, wool fabrics coated with 1% GNPs functionalized PU present better results for electrical and inflammable properties, followed by wool with CS functionalized with GNPs, that also presented great performance in insolation of radiant heat. The overall results show the high potential of wool fabrics functionalized with GNP for protective solutions.

ACKNOWLEDGMENTS

The authors would like to express appreciation for the support of Portugal2020 for funding the project nº 038328," MultiscaleProtech", granted by Fundo Europeu do Desenvolvimento Regional (FEDER). Are also thankful to CEECIND/02803/2017 and UID/CTM/00264/2019 funded by National Founds through FCT/MCTES.

REFERENCES

[1] J. M. Cardamone, Flame resistant wool and wool blends. Woodhead Publishing Limited, 2013.
[2] "Fluorocarbon - an overview." [Online]. Available: https://www.sciencedirect.com/topics/engineering/fluorocarbon.
[3] J. Molina, "Graphene-based fabrics and their applications: A review," RSC Advances, vol. 6, no. 72. Royal Society of Chemistry, pp. 68261–68291, 15-Jul-2016. W
E. Pascual and M. R. Julià, "The role of chitosan in wool finishing," J. Biotechnol., vol. 89, pp. 289–296, Aug. 2001.

NUMERICAL STUDY ON THE THERMO-MECHANICAL RESPONSE OF HYBRID CARBON-ALUMINIUM BOLTED JOINTS

Aravind Sasikumar[1](*), José Manuel Guerrero[1], Josep Costa[1], Joaquim Vila[1], Narcis Gascons[1]
[1] AMADE, Polytechnic School, University of Girona, Campus Montilivi s/n 17073, Girona, Spain
(*) E-mail: aravind.sasikumar@udg.edu

ABSTRACT
Bolted joints have been extensively used in aeronautical structures due to its high stiffness and the easiness of the joint for inspection purposes. This work aims to understand the thermo-mechanical response of a single lap carbon composite-aluminium hybrid bolted joint using a detailed numerical finite element model. Mimicking the flight operational cycle, the hybrid bolted joint is subjected to positive or negative thermal jumps before subjecting to a shear load. Further an extensive parametric study is performed to understand the influence of the key parameters (bolt clearance, friction coefficient, bolt clamping force, thermal load, etc.) on the response of the bolted joint. The study identifies the different stages of the joint behaviour during thermal-mechanical loading and discusses the evolution of the stress states and the bolt-plates contact interaction with respect to the different parameters studied.

INTRODUCTION
Bolted joints are widely used in aeronautical structures due to their relatively reliable way to transfer loads and the easiness of assembly and disassembly [1, 2]. With innovation in the material field, hybrid material joints are used in the primary aircraft structures namely carbon fibre reinforced polymers (CFRP)-aluminium or CFRP-titanium joints etc. The mechanical response of bolted joints is complex due to the interaction of several parts during the load transfer between the bolt and the plates. In this framework, this work is associated with a European Cleansky2 project partnered between Dassault Aviation, AMADE research group and Eurecat, where the objective is to study the thermal behaviour of a primary aircraft structure consisting of hybrid assemblies.
Thermal cycles in an aircraft induce differential deformation in the carbon-aluminium joints leading to shear loads in the bolted joints [3]. This study investigates the thermal and mechanical response of a single lap carbon-aluminium bolted joint using a detailed numerical finite element model in ABAQUS Implicit software [4]. The model consists of three steps namely Preload (where a pre-determined clamping force is applied to the bolt), thermal (positive or negative thermal jump) and shear (longitudinal displacement to simulate the shearing of the joint). Using this model, we aim to understand (a) how different is the thermal response of aluminium plate compared to the carbon one; (b) different stages of the joint response during thermal and mechanical loading and (iii) the effect of various parameters such as the friction coefficient, bolt clamping force, bolt clearance, thermal load (zero, positive or negative), thickness of the aluminium plate on the joint response through detailed 3D simulations.

RESULTS AND CONCLUSIONS
Force-displacement curve from the baseline configuration (a preload followed by shear loading without a thermal step in between) is presented in Figure 1. The different stages of the joint response are identified in the same figure as: Sticking between the plates (initial stiffness in the curve) due to the preload of the bolt, to sliding between the plates (second stiffness) to contact between the plates and the bolt (high stiffness in the later part of the curve). The evolution of contact force and the sliding between the parts are also demonstrated in the figure.

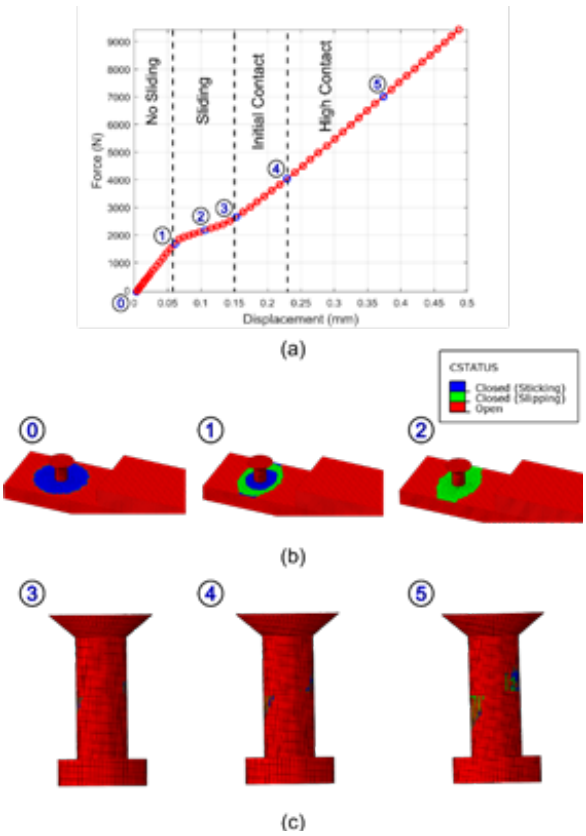

Fig.1 Force displacement response and the different stages of a single lap carbon-aluminium bolted joint under shear loading shown in (a) and the evolution of the contact status in the aluminium part (b) and the steel bolt (c). (Only aluminium plate and the bolt is shown here for better understanding. Contour indicates the contact status between the plates, where blue refers to sticking, green refers to sliding)

The results revealed a significant differential expansion or contraction of the hybrid plates during thermal step that modified the bolt clamping force. A negative thermal difference of 80˚C led to around 50% reduction in the bolt clamping force. The parametric studies demonstrated the importance of each parameter in affecting the force-displacement response and the subsequent stages of stiffness. An increase in the friction coefficient led to an extended stage I (as noted in Figure 1), similarly with the bolt clamping force parameter. An increased bolt-hole clearance led to extended sliding (stage II as shown in Figure 1). Hence, the study demonstrates the thermal effects on a hybrid bolted joint, followed by the effect of various parameters on the force-displacement response of the joint.

ACKNOWLEDGMENTS

This work has been accomplished in the framework of the H2020 Clean Sky 2 Project INNOHYBOX - Innovative solutions for metallic ribs or fittings introduced in a composite box to optimally deal with thermo-mechanical effects - (Call H2020-CS2-CFP06-2017-01, reference 785433) which provided the financial support.

REFERENCES

[1] Stocchi C, Robinson P, Pinho S T, A detailed finite element investigation of composite bolted joints with countersunk fasteners. Composites Part A: Applied Science and Manufacturing, 2013, 52, p. 143-150.
[2] P. E. Irving, C. Soutis, Polymer composites in the aerospace industry, Woodhead Publishing, 2019
[3] Coman C, Constantinescu D, Temperature effects on joint strength and failure modes of hybrid aluminium-composite countersunk bolted joints, Journal of materials: design and application, 2019, p. 1-15
[4] ABAQUS User Manual, 6.14, Providence RI, USA: DS SIMULIA Corp (2014)

EXPERIMENTAL VALIDATION OF AN ALGORITHM FOR IED DETECTION AND LOCALIZATION AT MICROWAVES

Adriana Brancaccio[1(*)], Giovanni Leone[1], Raffaele Solimene[1]
[1] Dipartimento di Ingegneria (DI), University of Campania Luigi Vanvitelli, Aversa, Italy
[(*)] E-mail: adriana.brancaccio@unicampania.it

ABSTRACT
In this work we present experimental results for the detection and localization of objects buried in the terrain at a small depth. The measurements of the scattered field under a single-view single-frequency non-cooperative illuminating source represent the input data of the problem. A linear inversion algorithm is applied to the data and provides as output a 2D map of the terrain, where the presence of a buried object emerges as a spot. The algorithm implements a scattering model based on the equivalence theorem, where the scattering object presence is seen as an equivalent electric current density. Spatially undersampled data can be managed by performing measurements at more than one (few) properly chosen frequencies. Results show the robustness of the proposed algorithm against undersampling and on field conditions.

INTRODUCTION
Improvised Explosive Devices (IED) can be encountered both in combat scenarios and in civil humanitarian missions. They have various forms and can be hidden in different ways. (www.difesa.it/Content/Pagine/IED.aspx,www.nato.int/cps/en/natohq/topics_72809.htm). When placed along roads, they are often buried at few centimeters below the terrain surface or concealed under vegetation. Detection and localization of such shallow buried objects is of crucial importance. In this kind of application a map of the investigated zone along the horizontal plane is required, while the exact depth and shape of the objects are not of interest. Also, because range resolution (i.e. the resolution in depth, along the propagation direction) is inversely proportional to the frequency bandwidth, an actual 3D reconstruction for shallow buried objects would require an adequate bandwidth of the equipment, arising sometimes in an expensive measurement set-up. These considerations suggested (Brancaccio et al. 2016) to cast the problem of detection and localization of buried objects as a 2D one, where the investigated domain is a virtual plane, parallel to the air/ground interface, whose depth has to be properly chosen. The proposed model has the great advantage of being lighter than a 3D one in terms of computational burden. Furthermore, it does not require a wideband measurement system. In addition, the analysis of the involved mathematical model allows to adopt a strategy to deal with undersampled data (Brancaccio et al. 2019).
In this work the proposed model has been applied and validated with data collected on a test site. The site consists of a tank full of sand of about 3.5 m (length) 2.5 m (width) and 1.5 m (depth). A transmitting antenna is positioned 1.5 m height from the sand ground, at the end side of the tank. The receiving antenna is mounted on a wooden slide (so that it can move on a horizontal plane) placed at about 130 cm of height. Data have been acquired in the frequency band 2-9 GHz (201 equispaced frequencies) at different positions of the receiving antenna (see figure below).

RESULTS AND CONCLUSIONS
Different metallic objects, placed at different positions in the soil, have been used as targets. The terrain has been turned over in order to work in the worst case of rough surface. In the following we show one of the results obtained in the case of rectangular plate 17.5 cm × 48 cm buried at a depth of about 10 cm. The soil relative permittivity is not known, but it likely stands between 4 and 9 pertinent to a wet ground. So, an “apparent” target depth ranging from 20cm to 30 cm is expected. Here, we show the result obtained by setting the investigation plane depth at 30 cm. Only

3×3 spatial measurements, thus having severe undersampling, and 7 frequencies chosen in the band[2.0-3.0]GHz spaced according to the criterio reported in (Brancaccio et al. 2019) have been used.

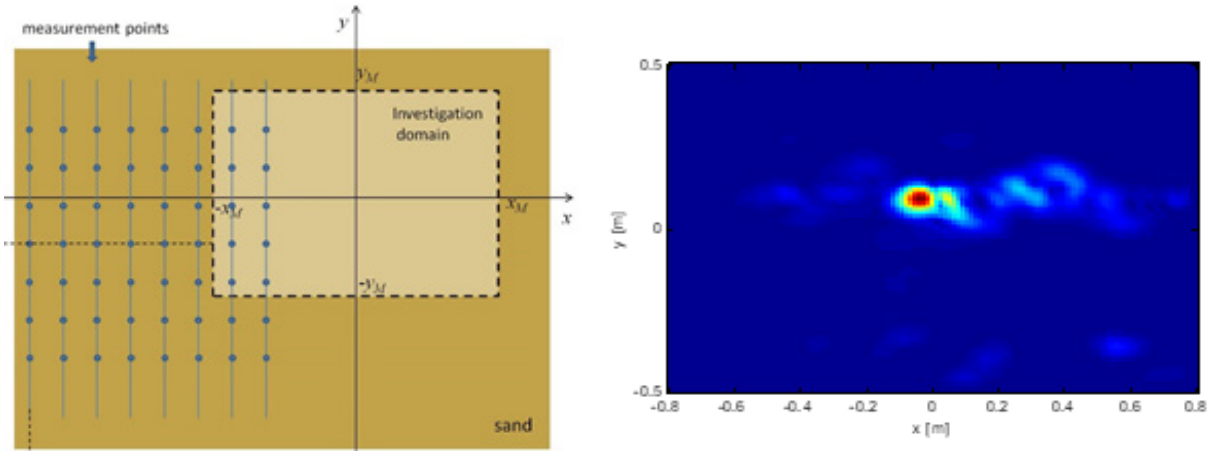

Fig.2 Sketch of the measurement points and investigation domain relative positions (left) and reconstruction of the target from undersampled data (right).

The experimental results show that successfully detection and localization can be obtained by undersampled data at few single frequencies, in the realistic case of unknown terrain permittivity and rough air-soil interface.

ACKNOWLEDGMENTS

The authors gratefully acknowledge the funding by Ministero dello Sviluppo Economico, within the program UE-FESR, PON “Imprese e competitivitá” 2014–2020, under the project “IDROS” (Impiego di Droni per la Ricerca nel sottOSuolo) grant number F/050187/02/X32.

REFERENCES

[1] Brancaccio, A. Leone, G. and R. Solimene (2016): Single frequency subsurface remote sensing via a non-co-operative source, Journal of Electromagnetic Waves and Applications, Volume 30, Issue 9, Page 1147-1161, DOI: 10.1080/09205071.2016.1182086

[2] Brancaccio, A. Dell'Aversano, A. Leone, G. and R. Solimene (2019): Subsurface Detection of Shallow Targets by Undersampled Multifrequency Data and a Non-Cooperative Source, Applied Sciences 9 (24), 5383.

[3] Brancaccio, A. Del Vecchio, A. and G. Maiello (2015): An algorithm for mine detection and localization by single frequency near field measurements, International conference on Electromagnetics in Advanced Applications ICEAA 2015 (Torino, September 2015).

A THROUGH-THE-WALL IMAGING PROCEDURE BASED ON A LEBESGUE-SPACE INVERSION METHOD

Andrea Randazzo[1(*)], Alessandro Fedeli[1], and Matteo Pastorino[1]

[1] Department of Electrical, Electronic, Telecommunications Engineering, and Naval Architecture, University of Genoa, Genoa, Italy

[(*)] E-mail: andrea.randazzo@unige.it

ABSTRACT

A novel through-the-wall imaging method is presented in this paper. The approach is based on a linearized scattering model, which is inverted by means of an efficient algorithm performing a regularization in the framework of Lebesgue spaces. Some preliminary numerical results are reported for assessing the capabilities of the approach.

INTRODUCTION AND OVERVIEW OF THE DEVELOPED APPROACH

In the last years, microwave imaging has acquired an ever growing importance in several fields, such as nondestructive testing and biomedical diagnostics (Pastorino and Randazzo 2018). In this framework, an important applicative scenario is represented by through-the-wall imaging (TWI), in which the aim is to retrieve information (e.g., position, size, dielectric properties) about targets hidden behind dielectric structures such as walls (Amin 2011). Indeed, microwaves represent a good candidate for such an application, since they are able to penetrate inside building materials (e.g., concrete, cinderblocks, and so on). However, the relationship between the wanted information and the quantities that can be measured (i.e., the electric field) is in general severely ill-posed, requiring the use of properly designed inversion algorithms.

In particular, assuming a monostatic setup, the scattered electric field can be expressed by using a linear approximation of the full scattering equations as (Solimene et al. 2009)

$$E_{scatt}(\mathbf{r}_{ant}) \cong \int_D I(\mathbf{r}')g_{ml}(\mathbf{r}', \mathbf{r}_{ant})g_{ml}(\mathbf{r}_{ant}, \mathbf{r}')d\mathbf{r}', \ \mathbf{r}_{ant} \in M \qquad (1)$$

where is the inspected region, is the position of the antenna in the probing line, and is the Green's function for the considered scenario. Starting from measurements of the scattered electric field, an image showing the support of the target can be obtained by inverting (1) in order to retrieve the function, which assumes high values on the target. In this work, in order to address the ill-posedness of the problem, the inversion is performed by means of a novel procedure developed in the framework of the spaces (Estatico et al. 2012), which has been found to provide very good regularization capabilities in microwave imaging problems. The main difference with respect to standard inversion procedures commonly adopted in microwave imaging is related to the use of the more general norm to weight the residuals and errors instead of the common least square norm. Such a choice allows the introduction of an additional parameter (the norm of the adopted space), which can be tuned for increasing the reconstruction quality. For instance, low values of enhance the sparsity of the solution, thus allowing cleaner reconstructions of localized targets (Bisio et al. 2018).

RESULTS AND CONCLUSIONS

The developed procedure has been preliminarily tested by means of numerical simulations. A single circular metallic cylinder of radius 10 cm located at a distance of 1 m from a lossless wall of thickness 0.2 m and relative dielectric permittivity, 4 has been considered. Monostatic measurements, with the antenna scanning a probing line of length 1 m located 1 m away from the wall, have been simulated by using a finite-difference time-domain solver. A ricker

pulse with center frequency of 2 GHz has been used to feed the antenna. In order to apply the inversion procedure, 41 frequency samples between 1 and 3 GHz has been extracted from the simulated signal by means of the fast Fourier transform. The inversion procedure has been executed with the following parameters: Maximum number of iterations, 100; threshold on the relative variation of the residual, 0.01. The result obtained assuming 1.3 is shown in Figure 1. As can be seen, the reconstructed image allows to correctly identify the location and position of the target, although the size of the target is slightly underestimated. Moreover, the image is characterized by a very clean background and no artefacts are present. Further numerical and experimental results will be shown in the presentation for assessing the capabilities of the approach with different targets and in more realistic operating conditions.

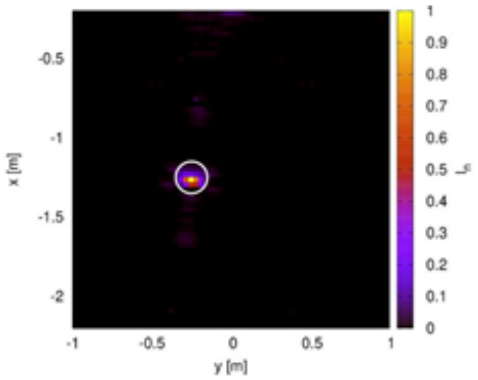

Fig.1 Reconstructed scenario with 1.3. Single PEC cylinder behind a dielectric wall.

ACKNOWLEDGMENTS

This work has been supported by the Italian Ministry of Education (MIUR) under the PRIN project “Ultra-wideband Virtual Imaging Extra Wall (U-View) for high-penetration high quality imagery of enclosed structures” (grant no. 20152HWRSL).

REFERENCES

[1] Amin MG. Through-the-wall radar imaging. CRC Press, Boca Raton, FL, 2011.

[2] Bisio I, Estatico C, Fedeli A, Lavagetto F, Pastorino M, Randazzo A, et al. Brain stroke microwave imaging by means of a Newton-conjugate-gradient method in Lp Banach spaces. IEEE Trans Microw Theory Tech, 2018, 66(8), p. 3668–82.

[3] Estatico C, Pastorino M, Randazzo A. A novel microwave imaging approach based on regularization in Lp Banach spaces. IEEE Trans Antennas Propag, 2012, 60(7), p. 3373–81.

[4] Pastorino M, Randazzo A. Microwave Imaging Methods and Applications. Artech House, Boston, MA, 2018.

[5] Solimene R, Soldovieri F, Prisco G, Pierri R. Three-Dimensional Through-Wall Imaging Under Ambiguous Wall Parameters. IEEE Trans Geosci Remote Sens, 2009, 47(5), p. 1310–7.

ANALYSIS OF LONGITUDINAL AND TRANSVERSAL DYNAMIC BEHAVIOR OF MULTIFILAMENT BI-HELICAL AUXETIC YARNS

Gabriel Vinha[1(*)], Carla Pinheiro[1], Raul Fangueiro[2]

[1] Brazilian Marine Corps, Brazilian Navy, Rio de Janeiro, Brazil

[2] Department of Mechanical Engineering, University of Minho, Guimarães, Portugal

[(*)] E-mail: davinha2@hotmail.com

ABSTRACT

Bi-helical yarns when made by single yarns with different diameters, helix angles and tensile strengths, present a dynamic behaviour that results in a significant difference in the relationship between the transversal and longitudinal variation, that is, in the Poisson´s ratio.

The longitudinal and transversal measurement of a bi-helical yarn in a dynamic test is a complex process, especially when dealing with multifilament yarns. For this reason, a methodology was specially developed using image analysis. To demonstrate the dynamic behaviour of the bi-helical yarns under tensile loads, the results obtained for four different samples using polyamide and polyester multifilament yarns are presented and analysed.

INTRODUCTION

A textile yarn presents a variable longitudinal behavior as a function of longitudinal tensile load. When tensioned, three distinct behavior ranges can be identified, especially in polymeric yarns, that is, in the 1st zone or elastic zone, the yarn immediately returns to its initial length when relaxed, in the 2nd zone or viscoelastic zone, the yarn returns to its initial length after a long time or under the effect of applied external energy (for example, heat) and the 3rd zone or plastic zone there is a permanent deformation of the yarn.

In the transversal behavior, the yarns differ significantly as they are tensioned. In the case of multifilament yarns specifically, when relaxed, the component filaments are not completely aligned to the longitudinal direction of the yarn, resulting in the yarn presents a large volume. With a minimal tension applied these yarns significantly reduce in volume (Vinha, 2018).

In the case of bi-helical yarns, this observation is more complex, since it consists of two yarns of different materials and diameters, which when tensioned they compress each other, and also present different longitudinal and transversal behaviors at different moments. Because of this, a more detailed dynamic monitoring in necessary, so that it is possible to accurately monitor the relationship between longitudinal and transversal variation depending on the applied force.

The study of the relationship between the transverse and longitudinal behavior of a bi-helical yarns subjected to longitudinal tension is of relevant importance in order to obtain the variation of the Poisson´s ratio during the test. Bearing in mind that with the combinations between yarns of different materials and diameters or helix angle of the secondary yarn, the bi-helical yarn can even present a negative Poisson´s ratio during the dynamic test. This study therefore, can result in an important step toward obtaining multifilament yarns build by conventional materials or with auxetic behavior that results in a yarn that exhibits an auxetic behavior.

There are different methods of cross-sectional yarn measurement in the literature. Among the optical methods, TEM (Transmission Electron Microscopy), (Miao, 2010) and SEM (Scanning Electron Microscope). (Miao, 2010), (Feng, 2014) and (Miao, 2015). However, these methods perform the static measurement of the yarn, which means that during the test the yarn is tensioned to a certain length, the test is interrupted to perform the measurement and restarted

successively, this process being repeated for each measurement performed. These test interruptions are limited in quantity due to the complexity of the measurements. Furthermore, the interruptions affect the arrangement of the component fibers of the sample, since they are not tensioned continuously.
Due to the complexity of the static measurement and the possibility that they are not reliable to the dynamic behavior of the tensioned yarn, an alternative method can be used to take continuous measurements during a dynamic test. (Behtaj, 2015) used a method employing image analysis to obtain transverse and longitudinal measurements of textured yarn samples with an accuracy of the order of 0.06 mm. Using a similar concept, but with a different computational model and methodology, as presented in (Vinha, 2019), it is possible to measure the longitudinal and transversal dynamic behavior of yarns with a precision of the order of 7 µm, obtaining above 1,500 measurements in an uninterrupted dynamic test.

RESULTS AND CONCLUSIONS

Results of the tests performed for the four bi-helical yarns demonstrate that although there is some similarity in the dynamic profiles obtained for the relationship between the applied force and elongation variation, it differs significantly in the transversal behavior of the samples and consequently in the Poisson´s ratio. Fig. 1 shows the results obtained for a tested sample.

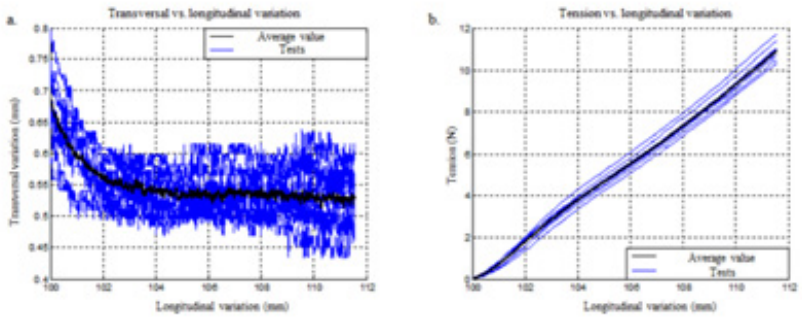

Fig.1 Longitudinal and transversal variation of the bi-helical yarn composed of multifilament yarns of polyamide and polyester. a. Transversal vs. longitudinal variation and b. Longitudinal variation vs. tension.

These tests allow analyzing the behavior of bi-helical yarns composed of different materials, diameters and helix angle of the secondary yarn. In addition, of the relevance of their use to develop technical fabrics, it is possible to demonstrate through the tests performed the relevance of the use of image analysis as a tool for measuring the behavior of textile yarns with irregular surfaces and behavior.

REFERENCES

[1] Behtaj S, Tavanai H, Sadri S. Characterization of air-jet textured yarn structure through image analysis. The Imaging Science Journal, 2015, 63, p. 1-6.
[2] Feng J, Xu B, Tao X. Structural analysis of finer cotton yarns produced by conventional and modified ring spinning system. Fiber and Polymers, 2014, 15(2), p. 396-404.
[3] Miao M. Characteristics of carbon nanotube yarn structure unveiled by acoustic wave propagation. Carbon, 2015, 91, p. 163-170.
[4] Miao M, McDonell J, Vuckovic L, Hawkins SC. Poisson´s ratio and porosity of carbon nanotube dry-spur yarns. Carbon, 2010, 48, p. 2802-2811.
[5] Vinha G, Fangueiro R. Longitudinal and transversal behavior of multifilament yarn subjected to longitudinal load using image analysis. Key Engineering Materials, 2019, 812, p. 134-140.

MICROPOROUS MOLECULAR SIEVE BASED DAYTIME PASSIVE RADIATIVE COOLING COATING

Chenglong Lv[1], Mei Zu[1(*)], Haifeng Cheng[1]
[1] Science and Technology on Advanced Ceramic Fibers and Composites Laboratory, College of Aerospace Science and Engineering, National University of Defense Technology, Changsha, China
[(*)] E-mail: Mei Zu: zumei2003@163.com

ABSTRACT
In this paper, the microporous molecular sieve was investigated as the passive radiative cooling material. The solar spectral reflectivity and infrared emissivity of different types of microporous molecular sieve such as 4A, 5A and 13X were measured. In addition, the cooling effect of 4A zeolite-based coating was compared with the aluminium plate, TiO2 coating and CaCO3 coating. The results demonstrate that the 4A zeolite is a promising energy-saving material for daytime passive radiative cooling.

INTRODUCTION
To reduce the increasing energy consumption and slow down the global warming, passive radiative cooling (PRC) materials have attracted considerable attention in the recent years. PRC materials exhibit high reflectivity in the solar spectrum region (0.3–2.5 μm in wavelength) and high emissivity in the atmospheric window (8–14 μm in wavelength) (Raman, 2014). For buildings and equipment that are exposed to the direct sunlight, the employment of PRC materials can effectively decrease the internal temperature by several degrees.
Considering the fabrication techniques and costs, easily processable cooling materials with simple structures are desirable for further exploration. In recent years, Mg11(HPO3)8(OH)6 (Xu, 2018), NaZnPO4 (Ao, 2019) and AlPO4 (Li, 2019) have been studied as the PRC materials. In this paper, we select several types of microporous molecular sieves (4A, 5A, 13X zeolite) as the research materials, and test the spectral changes of these molecular sieves before and after annealing at 800°C. What's more, the cooling effect of 4A-800°C zeolite coating was also evaluated by a homemade thermal testing platform.

RESULTS AND CONCLUSIONS

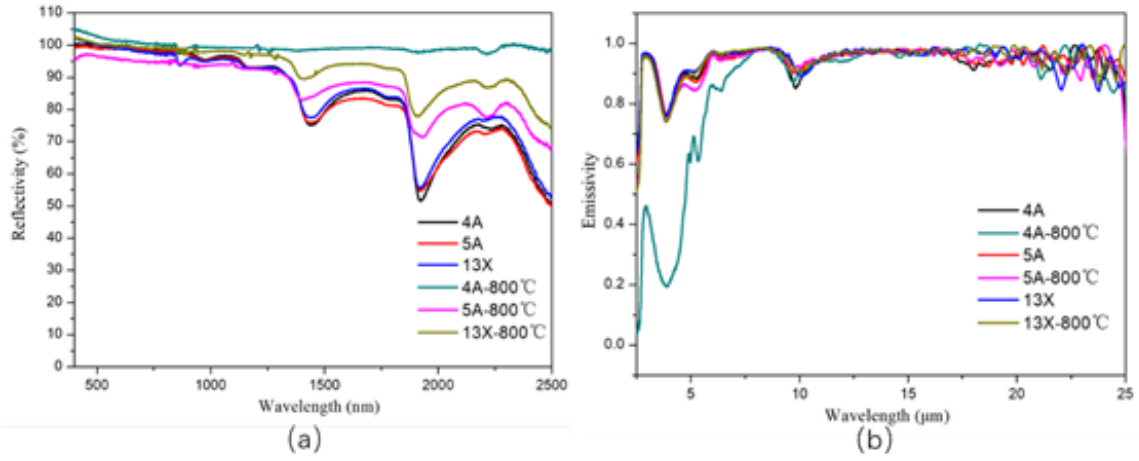

Fig.1 The spectral curves of several microporous molecular sieves before and after annealing at 800°C.

Fig.1 shows that the spectrum of microporous molecular sieve can be affected by the heat treatment. It can be seen that the spectrum change of the zeolite mainly occurs in the solar spectral band (Fig. 1(a)), and the reflectivity of the 4a zeolite after annealing at 800°C (named as 4A-800°C) is higher than that of other zeolites. As for the infrared region (Fig. 1(b)), all the types of zeolites have a high emissivity in the atmospheric window.

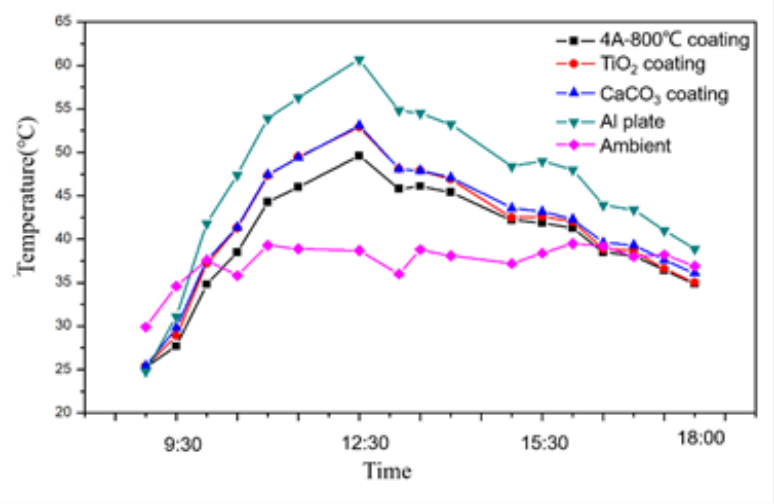

Fig.2 Comparison of measured cooling effect of coatings, specifically: 4A-800°C, TiO_2, $CaCO_3$, aluminum plate and ambient temperature.

Fig. 2 shows the cooling ability of 4A-800°C zeolite based coating and other coatings (Polyvinylidene Fluoride resin as the binder and N-methylpyrrolidone as the solvent) by a homemade thermal testing platform in a sunny day. The results showed that the temperatures in space below 4A-800°C zeolite coating were ~4 °C lower than those below the coatings based on commercial solar heat reflection materials such as TiO_2 and $CaCO_3$, and ~10 °C lower than that below the Al plate.

This study shows that among the common microporous molecular sieves, 4A zeolite is a promising energy-saving material for daytime passive radiative cooling.

ACKNOWLEDGMENTS

This work was supported by the Scientific Research Plan Program of National University of Defense Technology (ZK17-03-47).

REFERENCES

[1] A.P. Raman, M.A. Anoma, L. Zhu, E. Rephaeli, S. Fan. Passive radiative cooling below ambient air temperature under direct sunlight. Nature, 2014,515, p. 540–544.

[2] Z. Xu, N. Li, D. Liu, X. Huang, J. Wang, W. Wu, H. Zhang, H. Liu, Z. Zhang, M. Zhong. A new crystal Mg11(HPO3)8(OH)6 for daytime radiative cooling. Sol. Energy Mater. Sol. Cells, 2018, 185, p. 536–541.

[3] X. Ao, M. Hu, B. Zhao, N. Chen, G. Pei, C. Zou. Preliminary experimental study of a specular and a diffuse surface for daytime radiative cooling. Sol. Energy Mater. Sol. Cells, 2019, 191, p. 290–296.

[4] N. Li, J. Wang, D. Liu, X. Huang, Z. Xu, C. Zhang, Z. Zhang, M. Zhong. Selective spectral optical properties and structure of aluminum phosphate for daytime passive radiative cooling application. Sol. Energy Mater. Sol. Cells, 2019,194, p. 103–110.

NUMERICAL MODELLING OF HIGH IMPACTS ENERGY ON CFRP PANELS

Seif H. Sadek[1(*)], Ricardo Jorge Rocha[2], Luís Pina[3]
[1, 2,] INEGI – Pólo FEUP, Rua Dr. Roberto Frias, 400, 4200-465 Porto, Portugal
[(*)] E-mail: ssadek@inegi.up.pt

ABSTRACT

Work objective, presenting a validated numerical model of previous experimental work done by the group [1]. The model is simulating adhered carbon fibers coupons (T700-MTC801). The coupons is impacted with metal sphere that has different weights and velocities. The work provided is representing first stage in progress to simulate bird and hail strike on aircraft nose panels. The present work uses standard Abaqus library to and focus on the reliability of continuum shell models technic to simulate carbon fibers laminate combined with cohesive surface behaviour.

INTRODUCTION

Polymer composite materials are increasingly used for primary aircraft structures, strengthen the aircraft frames. Besides, the fuselage coupons that carry pressurization loads. Which overall lowering the fuel consumption, emission and increases the flight range. Nonetheless, it has to maintain structural integrity with respect to damage threats regardless to the cause. Collision is a part of the everyday concerns for the aircraft industry, during not only the flight but also while loading, unloading passengers and cargo or, when it is being repaired. On other hand, impact velocity is one of the fundamental aspect in the strike dynamics. That distinguish the various impact damage scenarios and effects. After the impact occurs, a series of events can happen such as elastic, plastic and shock wave propagation, fracture and fragmentation, delamination, perforation and spallation [2].

While projectiles can be categorized as soft, semi-hard or hard depending on the impactor material and its degree of deformation during impact. Soft projectiles undergo significant deformation during impact, such as a bird impact on an aircraft, where the bird behaves in a fluid manner after the impact suffering extreme distortion and the body breaks up into particles. On the other hand, hailstones can be considered semi-hard projectiles since the deformation strongly depends on the impact energy. Lastly, hard projectiles, as metallic objects, that experience negligible deformations [3].

In the work below, experimental data is obtained in previous work [1], [4], [5] Figure 1. The numerical work presented use continuum shell element in order to validate the models compatibilities.

a) 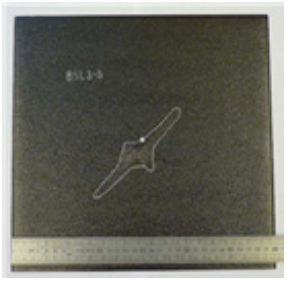 b) 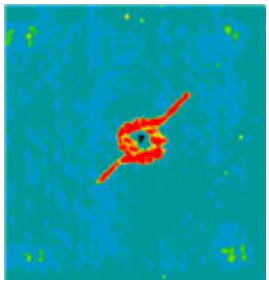

Fig.1 Experimental damaged area on T700 coupons, a) Experimental test, b) NDI test [1].

The coupons 14 layer 300x300mm subjected to metal sphere impact, weighted (7.05, 28.2 g) that has different velocities (97-191 m/s). Numerical model adopt cohesive surface in order to represent the epoxy adherent.

RESULTS

As presented below Figure 2 and Table 1 the results obtained numerically are close to the experiment Figure 1. Damage shape has follow the fibers direction as observed experimentally. As concluded, continuum shell model combined with cohesive interaction is reliable to represent composite layup in acceptable computational cost.
Continuum shell model, time step 0.6ms, 162318 SC8R element, converged in 2:05 hour.

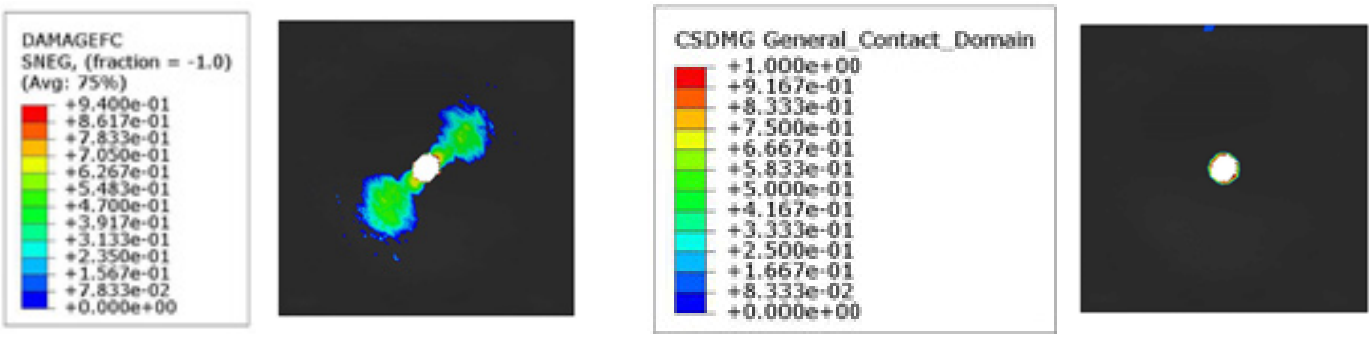

a) b)

Fig.2 Numerical results, a) Ply damaged area and b) Inter-ply damage on T700 coupons.

Table 1 Comparison between the experimental and numerical impact results for the T700.

Shot Ref.	Ref	Sphere Weight [g]	Impact Velocity [m/s]	Residual Velocity [m/s]		ERROR [%]	Energy [J]		Numerical Absorbed Energy [J]	ERROR [%]
				Exp.	Num.		Impactor	Absorbed		
A87	BSL3-4	7.05	150	114.7	126	-9.85	79.313	32.937	23.350	29.1
A95	BSL3-5	7.05	191	171.6	169.8	1.05	128.596	24.796	26.963	-8.7
A77	BSL3-3	28.2	97	70.5	81.0	-14.89	132.667	62.586	40.157	35.838
A99	BSL3-6	28.19	153	140.6	143.0	-1.71	329.950	51.315	41.721	18.696

ACKNOWLEDGMENTS

The authors gratefully acknowledge the collaboration with Juan Tomás Viana Lozoya in the scope PASSARO, a CleanSky 2 Core Partnership led by Airbus Defence and Space. This project has received funding from the Clean Sky 2 Joint Undertaking under the European Union's Horizon 2020 research and innovation program under grant agreement No 807083.

REFERENCES

[1] R. Rocha, M. Gomes, and J. Sousa, "PASSARO-WP3-R002 WP3 – Impact Tests Results," Porto, 2019.
[2] M. A. Meyers, Dynamic behavior of materials. Wiley, 1994.
[3] J. A. Zukas, T. Nicholas, H. F. Swift, L. B. Greszczuk, and D. R. Curran, "Impact dynamics," John Wiley Sons, Ltd, vol. 50, pp. 702–703, 1982.
[4] R. Rocha and M. Gomes, "WP3 - Material Characterization Tests Report," 2018.
R. Rocha, S. Sadek, M. Gomes, and J. Sousa, "AIR O-B-3.3.9.2-3 (OT3.3) Preliminary Design: WP3 – Medium and High Energy Impact Protection Materials," Porto, 2019.

THERMAL BLANKET WITH LOW RF REFLECTIVITY

Miguel Santos[1(*)], Mário Pereira[2], Marília Pirralho[3], Pedro Teixeira[4], Carlos Fernandes[5], Mário Silveirinha[6], Luís Rolo[7]

[1, 2, 3, 4] Frezite High Performance Lda., (FHP), Porto, Portugal

[5, 6] Instituto de Telecomunicações (IT), Lisboa, Portugal

[7] ESA/ESTEC, Noordwijk, The Netherlands

[(*)] E-mail: miguel.santos@frezitehp.com

ABSTRACT

In this paper the design of a generic RF absorber is proposed that shall be an integrant part of an overall MLI blanket to be used on the antenna as a substitute of a typical MLI. It is the main objective of this RF absorber blanket to mitigate these RF issues shown in Fig. 2, whilst still maintaining the same properties of the standard MLI, i.e., thermal and optical properties as well as electrical grounding properties.

INTRODUCTION

It is a known fact that MLI causes unwanted interference and even PIM problems due to its high RF reflectivity in the specular direction. Usually, this is accounted for in the RF design of antenna payloads by representing the MLI as perfectly flat conducting ground plane. In fact, this is the standard practice in the industry. However, this is merely an approximation. In reality, the MLI is not a perfectly flat surface, i.e., due to its flexible nature wrinkles inherently are formed as shown in Fig. 1.

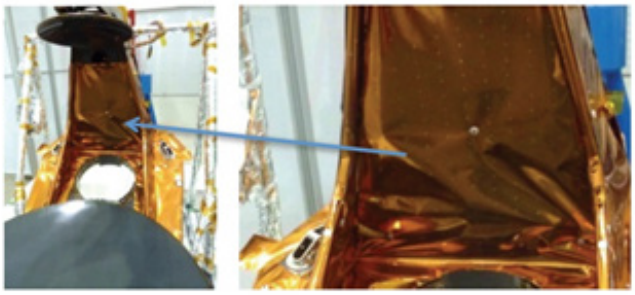

Fig.1 MLI assembled on antenna

As it can be seen in Fig. 1, this type of wrinkles is usual and sometimes even necessary in order to fit the MLI blankets on the structure. This wavy pattern however, causes diffuse reflection patterns that are difficult, if not impossible, to predict. The case study used in this paper is a Ka-band top-deck antenna for a high throughput satcom. During the RF tests of this top-deck antenna it was possible to see, very clearly, the harmful impact of the MLI in the antenna far-field performance. The results are shown in Fig. 2.

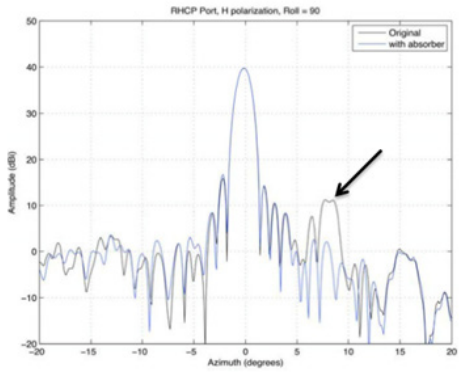

Fig.2 Antenna radiation pattern within the Ka-band

RESULTS AND CONCLUSIONS

Fig. 3 shows the new blanket performance for different angles of incidence, namely 30º, 45º and 60º. Fig. 3 (left) depicts the absorber performance for TE polarized waves, whereas Fig. 3 (right) depicts the absorber performance for TM polarized waves. As we can see from both figures, the absorber reflection response excellent for incidence angles up to 30º as the reflection coefficient is below -25 dB. On the other hand, and as expected, due to high incidence angle, the reflection response is not within specification for 60º, nevertheless a significant absorption level is still verified for the entire Ka-band.

As a final note, we refer that the new blanket is designed with space flight in mind, hence, all the materials taken into consideration for the design as space qualified materials.

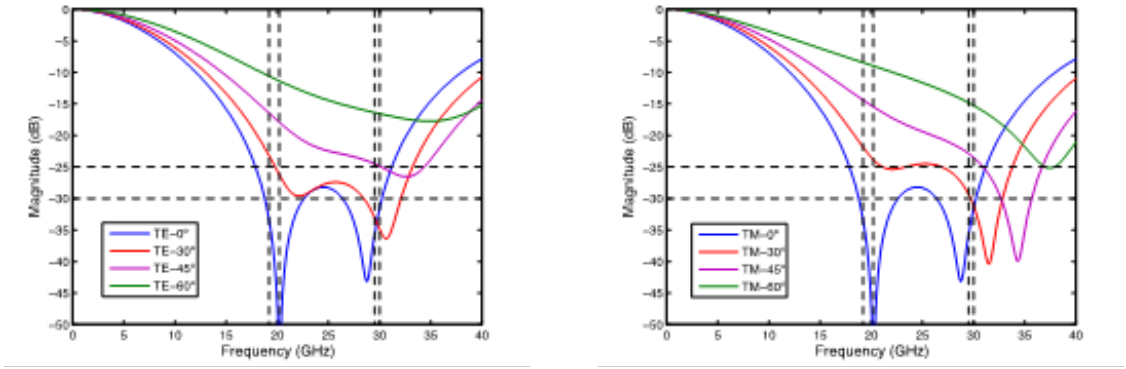

Fig.3 Frequency reflection response (3D electromagnetic simulation)

ACKNOWLEDGMENTS

The authors gratefully acknowledge the funding by European Space Agency (ESA) under contract Nº 4000106436/12/NL/NR.

STUDY ON THE STABILITY OF FLUORINATED POROUS ORGANIC MATERIALS IN HUMID ENVIRONMENT

Shuyuan Zhou[1(*)], Hao Han[1], Kai Kang[1], Hong Zhou[1], Jian Kang[1], Shupei Bai[1], Ye Yuan[2(*)], Lili Wang[2]

[1] State Key Laboratory of NBC Protection for Civilian, Changping District, Beijing, China

[2] Key Laboratory of Polyoxometalate Science of Ministry of Education, Northeast Normal University, Changchun, China

[(*)] E-mail: zhoushuyuan1987@126.com

ABSTRACT

Water vapor in the air can affect the stability of porous materials in practical applications. As such, it is important to study the effect of water vapor on the stability of the porous materials. In this work, porous organic materials C-1 and fluorinated C-1 (denoted as C-1-F) are prepared. When these materials are subjected to a saturated salt solution atmosphere under different relative humidity, C-1-F shows good stability, while gradual collapse of the framework can be observed for C-1. The hydrophobicity of the material is characterized using a water contact angle test and water vapor adsorption-desorption isotherms test. Based on these results, it is shown that C-1-F is hydrophobic. Thus, the introduction of fluorine atom can convert C-1 from hydrophilic to hydrophobic, which results in the strengthened stability of C-1-F in humid environment.

INTRODUCTION

In recent years, porous organic framework materials are widely used in the adsorption and catalysis of chemical toxic agents and volatile organic compounds (VOCs). However, in these practical applications, the stability of the material is of vital importance. Air is one of the most common operating environments for porous materials. The water vapor in the air is a crucial factor which can affect the stability and the performance of these porous materials. Thus, it is of practical significance to explore the stability of organic porous materials in humid environment. In this study, 1, 3, 5-tris (4-aminophenyl) benzene and 1, 4-Phthalaldehyde are used to synthesis a hydrophilic porous organic material, denoted as C-1. In order to prepare a hydrophobic porous organic material, denoted as C-1-F, 1, 4-Phthalaldehyde used in the earlier preparation of C-1 is replaced with 2, 3, 5, 6-tetrafluoroterephthaldehyde. Based on the results, the introduction of fluorine atom can convert C-1 from hydrophilic to hydrophobic. This in turn leads to an enhanced stability of the hydrophobic C-1-F in humid environment.

RESULTS AND CONCLUSIONS

To investigate the stability of the materials, these as-prepared materials are kept in saturated standard salt solution environment with controllable humidity, i.e., relative humidity of 33%, 65%, 75%, and 97%, for 24 hours. With the increase in relative humidity, infrared spectroscopy shows gradual increase in the characteristic peaks of aldehyde group and amino group for C-1, which indicates the decomposition of the C-1 skeleton. However, the characteristic peaks for C-1-F remains relatively unchanged. Thus, this result indicates that the stability of C-1-F is improved by doping with fluorine atoms.

As shown in Fig. 1, the contact angles of C-1 and C-1-F are 74 and 98 degrees, respectively. With 90 degrees as the boundary between hydrophilicity and hydrophobicity, it is observed that the material changes from a hydrophilic to hydrophobic wetting behavior after doping with fluorine atom.

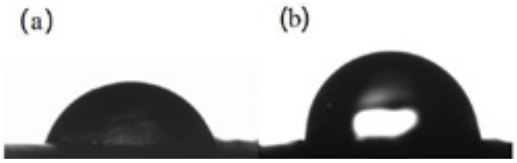

Fig.1 Contact angle of C-1 (a) and C-1-F (b)

The results from the water vapor adsorption-desorption isotherms are shown in Fig. 2. The area of the hysteresis loop for C-1-F is smaller than that for C-1. The narrowing hysteresis loop presented in this result suggest that the adsorbed water vapor can be easily desorbed from the material. Furthermore, this also implies a weaker interaction between C-1-F and water vapor.

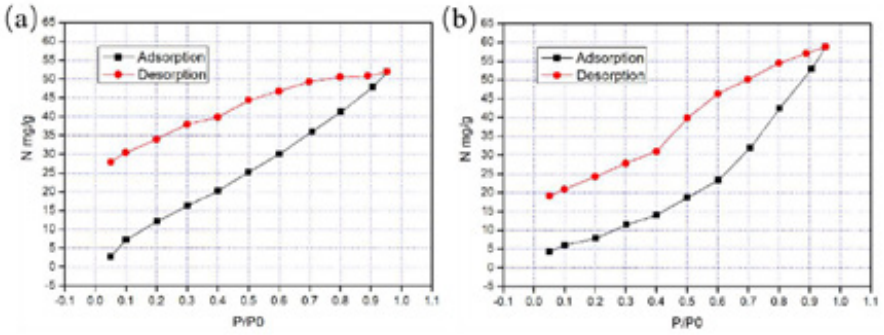

Fig.2 Water vapor physisorption isotherms (298 K) for C-1 (a) and C-1-F (b)

This study shows that the damage of water vapor to the material framework is reduced by changing the wetting behavior of the material from hydrophilic to hydrophobic. Hence, according to this study, the stability of the hydrophobic C-1-F is enhanced in humid environment.

ACKNOWLEDGMENTS

The authors gratefully acknowledge the funding by National Natural Science Fund of China (21701186).

REFERENCES

[1] Padial NM, Procopio EQ, Montoro C, Lopez E, Oltra JE, Colombo V, Maspero A,

[2] Masciocchi N, Galli S, Senkovska I, Kaskel S, Barea E, Navarro JAR. Highly hydrophobic isoreticular porous metal–organic frameworks for the capture of harmful volatile organic compounds. Angewandte Chemie International Edition, 2013, 52, p. 8290-8294.

ATOMISTIC MODELING OF STRUCTURAL AND MECHANICAL PROPERTIES OF SEMICRYSTALLINE POLYETHYLENE

In-Chul Yeh(*) and Jan W. Andzelm(*)
U.S. Army Research Laboratory, Aberdeen Proving Ground, Maryland 21005, USA
(*) Email: in-chul.yeh.civ@mail.mil and jan.w.andzelm.civ@mail.mil

ABSTRACT

We investigated structural and mechanical properties of semicrystalline polyethylene (PE) with atomistic molecular dynamics simulations. As a first step toward modeling inter-fibril interactions in PE fibers, we estimated profiles of free energy during debonding and shearing processes between the surfaces of crystalline PE. We also studied interactions of binders and semicrystalline PE in composite materials using atomistic simulations. Using PE fiber models containing long but finite chains, we studied changes in structural and mechanical properties of PE fiber during tensile deformation. After the yield point, the pattern of changes in effective lattice parameters estimated with the PE fiber model with finite chains was significantly different from that estimated with the crystalline PE without chain ends but was in an excellent agreement with those observed in recent experiments on PE fibers.

INTRODUCTION

Ultra-high-molecular-weight polyethylene (UHMWPE) fibers are widely used in a variety of industrial materials for ballistic protection, personal armor, and outdoor and marine applications due to their superior mechanical properties, low densities, and chemical resistances. The morphology and mechanical properties of UHMWPE fibers depend on various processing conditions such as drawing temperature, draw ratio, and strain rates. A significant gap still exists between the experimental tensile strength and its theoretical maximum value, whereas the experimental modulus of fibers is rather getting closer to the theoretical limit. It is important to understand the relationship between structural and mechanical properties to improve the ultimate properties of UHMWPE fibers. Raman spectroscopic data of strained PE fibers displayed carbon-carbon (C-C) stretching bands that can be fitted with two Gaussian curves, indicating the existence of bimodal distributions of stress or strain due to strain-insensitive domains near chain ends. Recently, Balzano et al. investigated structure and microscopic deformation mechanisms of gel-spun UHMWPE fibers with X-ray diffraction in static and dynamic condition during tensile testing and observed an unusual deformation mode of the unit cell of the orthorhombic PE crystal, contraction of the lattice parameter a with simultaneous expansion of the lattice parameter b during the plastic deformation stage after the yield. Atomistic details of the lattice distortion and the chain rotation during deformations that can be gained from molecular dynamics simulations could provide valuable insights into the relationship between structural and mechanical properties of UHMWPE fibers to complement the experimental efforts. In this study, we investigated structural and mechanical properties of PE fibers during tensile deformations and inter-fibril surface interactions with atomistic molecular dynamics simulations.

RESULTS AND CONCLUSIONS

To study inter-fibril interactions in PE fibers, we performed debonding simulations of crystalline PE surfaces (Yeh et al., 2018). The estimated surface free energies of two different crystallographic surfaces of the crystalline PE were in an excellent agreement with that obtained from an experiment on PE single crystal aggregates. We also characterized interactions of binders and semicrystalline PE with different simulation conditions and force fields to aid efforts to develop novel composite materials. To characterize mechanical propeties of PE fibers, we performed simulations of tensile deformations of the PE fiber model with very long but finite chains in the orthorhombic crystalline configuration (Yeh et al., 2020). Figure 1 summarizes our results. We confirmed the yield behavior associated with chain

slippage near the chain-end region observed in the previous simulation (O'Connor et al., 2016). Diverging distributions of local strains were observed near the chain-end region and in the middle of the chain, which is consistent with bi-modal distributions of C-C stretching bands observed in Raman spectra of stressed PE fiber. The trend of the change of lattice parameters of the orthorhombic PE crystal in PE fiber models with finite chains observed in our simulations was in an excellent agreement with the observations in recent experiments on UHMWPE fiber. The conformational mismatch between chains developed during tensile deformation triggered the rotation of the chain in specific directions, resulting in the changes of the effective lattice parameters of the orthorhombic PE crystal.

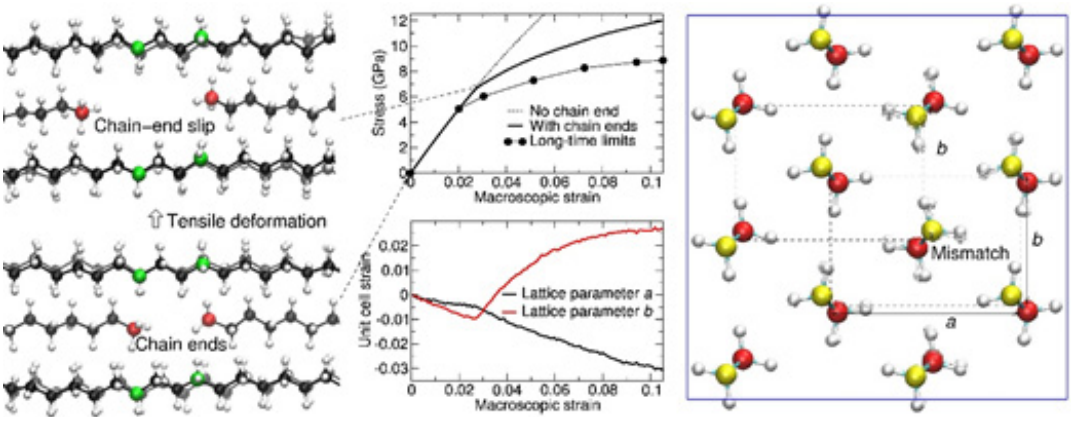

Fig. 1. Structural and mechanical properties of polyethylene fibers during tensile deformation (Yeh et al., 2020)

ACKNOWLEDGMENTS

We thank Drs. Harm van der Werff, Luigi Balzano, Randy A. Mrozek, and Joseph L. Lenhart for helpful discussions and comments.

REFERENCES

[1] Balzano, L.; Coussens, B.; Engels, T.; Oosterlinck, F.; Vlasblom, M.; van der Werff, H.; Lellinger, D., Multiscale Structure and Microscopic Deformation Mechanisms of Gel-Spun Ultrahigh-Molecular-Weight Polyethylene Fibers. Macromolecules 2019, 52, 5207-5216.

[2] Yeh, I.-C.; Balzano, L.; van der Werff, H.; Mrozek, R. A.; Lenhart, J. L.; Andzelm, J. W., Effects of Finite Lengths of Chains on the Structural and Mechanical Properties of Polyethylene Fibers. Macromolecules 2020, 53, 18-28.

[3] O'Connor, T. C.; Robbins, M. O., Chain Ends and the Ultimate Strength of Polyethylene Fibers. ACS Macro Lett. 2016, 5, 263-267.

[4] Yeh, I.-C.; Andzelm, J. W., Calculations of Free Energy of Surface Interactions in Crystalline Polyethylene. The Journal of Chemical Physics 2018, 149, 014701.

EVALUATION OF THE COOLING CAPACITY OF COMMERCIALLY AVAILABLE COOLING VESTS

Urša Ciuha[1](*), Tamara Valenčič[1], Igor B. Mekjavic[1]
[1]Jozef Stefan Institute, Department for Automation, Biocybernetics and Robotics, Jamova 39, 1000 Ljubljana, Slovenia
(*) E-mail: ursa.ciuha@ijs.si

ABSTRACT
The study evaluated twenty commercially available cooling vests with different cooling concepts, including evaporative, conductive, hybrid and active cooling vests. All vests were evaluated in controlled hot conditions inside an environmental chamber on a whole-body thermal manikin. Thermal insulation, evaporative resistance and conductive cooling capacity were assessed. The vests and cooling concepts indicated a substantial range in both cooling power and operating time.

INTRODUCTION
Work and other everyday scenarios may include longer periods of heat exposure, in some cases concomitant with insufficient heat loss, thus leading to heat strain. Such conditions can be experienced due to increased physical activity, when wearing protective clothing, exposure to sun radiation or other sources of heat, and combinations thereof. Heat loss can be encouraged by exposing skin to the ambient, but can also be further improved by using different cooling strategies, such as cooling vests (Barwood et al. 2009; Caldwell et al. 2012; Ciuha et al. 2016). Cooling vests incorporate different cooling concepts, and consequently have different cooling efficiencies.
The present study evaluated twenty commercially available cooling vests with different heat exchange concepts, including evaporative (wet), conductive, hybrid and active vests. Conductive vests have integrated inserts filled with either water, gels or phase change material of different melting temperatures, whereas hybrid vests combine both evaporative and conductive cooling concepts. The vests were tested in a controlled environment inside an environmental chamber on a thermal manikin. Three aspects of the cooling vests were assessed: thermal insulation, evaporative resistance and conductive cooling capacity. To observe the cooling capacity of each vest, eight-hour tests were performed on a manikin and two parameters were monitored: cooling power and operating time of each vest. For the purpose of these tests the manikin and the chamber temperature were maintained at 35°C. The cooling power of the vests was determined based on the power, supplied to the manikin torso, required to maintain the manikin skin/shell temperature at 35°C. Electrical power (W.m-2), required by the heaters in the torso region, represented the cooling power of a specific vest. Once the cooling source of a vest was exhausted, electrical power would return to 0 W.m-2, and the vest would represent an additional thermal and evaporative barrier.

RESULTS AND CONCLUSIONS
All vests had some level of cooling capacity, which, however, varied widely for the vests investigated. The greatest cooling capacity was observed in the hybrid vest, combining evaporation and PCM of the lowest melting point tested (6.5°C). Similar efficiency was also provided by vests with ice and frozen gel inserts, as well as active vest with circulating ice-cold water (60 – 80 W.m-2). Evaporative vests provided lower cooling capacity (40 W.m-2), however their operating time was often longer (up to 8-hr) compared to the cooling concepts with greater cooling power (up to 4-hr).
The choice of the most suitable cooling vest for a specific purpose will depend on the ambient conditions (temperature, relative humidity), activity level (from sedentary to very active) and whether the vest can be worn over or underneath other clothing. An important characteristic is also the duration of the cooling capacity time of the vests.

Global warming will increase the need for cooling vests, particularly during the summers months in industry. The results of the present study reveal an urgent need to establish a standardized test protocol for evaluating cooling efficiency of cooling vests. Results of such tests would allow potential users to choose the optimal vest for their particular requirement.

ACKNOWLEDGMENTS

The study was supported by the Slovene Research Agency (project no. Z7-9412).

REFERENCES

[1] Barwood MJ, Newton PS, Tipton MJ (2009) Ventilated vest and tolerance for intermittent exercise in hot, dry conditions with military clothing. Aviat Space Environ Med 80: 353-359

[2] Caldwell JN, Patterson MJ, Taylor NAS (2012) Exertional thermal strain, protective clothing and auxiliary cooling in dry heat: evidence for physiological but not cognitive impairment. European journal of applied physiology 112: 3597-3606

[3] Ciuha U, Grönkvist M, Mekjavic IB, Eiken O (2016) Strategies for increasing evaporative cooling during simulated desert patrol mission. Ergonomics 59: 298-309

CHARACTERIZATION OF REINFORCED CONCRETE WITH STEEL FIBERS AND CARBON NANOTUBES – CNT

João Pedro Lopes[1(*)], Vladimir Ferrari[2], Aloysio Gomes de Souza Filho[3], Aires Camões[4], Raul Fangueiro[5]
[1, 2]Department of Civil Engineering, (PCV/UEM), State University of Maringá, Paraná, Maringá, Brazil
[3]Department of Civil Engineering, Federal University of Technology – Paraná, Apucarana, Brazil
[4]Department of Civil Engineering (DEC), University of Minho, Guimarães, Portugal
[5]Department of Mechanical Engineering (DEM), University of Minho, Guimarães, Portugal
[(*)] E-mail: engjoaopedrolopes@gmail.com

ABSTRACT
This work has as main objective the evaluation of the effect of the content of hybrid fibers on the flexural strength, toughness and residual resistances of reinforced concrete with hybrid fibers (RFC) of steel and carbon nanotubes (CNT). Three different quantity of CNT were previously dispersed by ultrasonication using a Pluronic F-127 surfactant concentration. A fixed quantity of steel fibers was used in concrete. The results obtained shows improvement in mechanical properties of RFC as compressive strength, flexural strength, flexural modulus, good interaction between steel fibres and CNTs, in the microstructure of concrete matrix and in the Pull Out steel fibre strength. The concrete showed a ductile behaviour improved with the hybridization when compared just with steel fibres. This high performance material can be applied in specific buildings like defense engineering with sensing properties.

INTRODUCTION
Fibres are added to concrete to improve the material's tensile strength and ductility, which is called fibre reinforced concrete (CRF) (Ghadban, Wehbe And Underberg, 2018). The addition of nano particles in cementitious matrices have been studied due to their high rigidity and resistance. (Al Rub et al, 2012). The CNTs were previously dispersed by ultrassonication using 1%, 3% and 5% of Pluronic F-127 surfactant concentration (Praveen et al, 2015). The raw materials were characterized by standards to produce the concrete.
In total, eight different mixture were prepared, one without any fibres, three with the quantity of CNTs (0,05%, 0,10% and 0,15%), one with 1% of steel fibres and three combined 1% of steel fibres and the quantity of CNTs. The specimens were submmited to flexural tests adapted from EN 14651:2007. The samples dimensions is 50 mm x 50 mm x 200 mm with a notch in the middle span to force the occurrence of the first crack in middle span, according to the standard EN 14651. In addition, tests for characterization of materials, characterization of steel fibers and carbon nanotubes, axial compression tests, pullout of steel fibers from the cementitious matrix were also carried out.

RESULTS AND CONCLUSIONS
As results, the concrete that had one both fibres showed a slight improvement in the compression behavior of up to 5%. In terms of flexural behavior, hybridization with the lowest addition of CNT (0,05%) resulted in an improvement in maximum flexural strength of approximately 14% when compared to steel fiber and more than 66% compared to concrete without fibers, as shown in Fig. 1. Residual resistances also showed a significant improvement. According to the EN 14651 the residual resistances were those that correspond to the size of CMOD (Crack Month Opening Displacement).

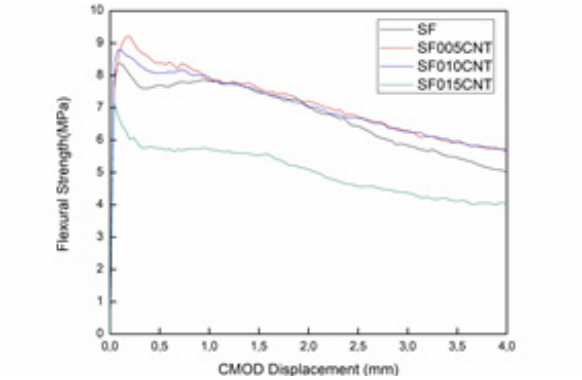

Fig.1 Flexural test results

The pullout tests of the steel fibre in the cementitious composite with CNT also showed improvements of 15% in comparison of without CNT. Fig. 2 shows the CNT acting in cracks as tensions bridges absorbing the energy, while the concrete cracks.

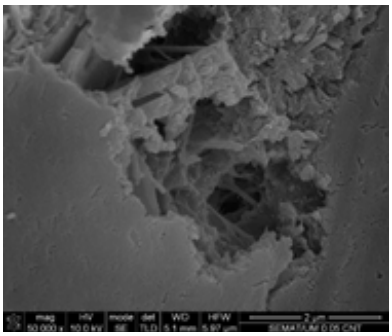

Fig.2 CNT acting in cracks

This study shows the iteration between fibres in concrete matrix. As results has shown, the fibres present benefits in the mechanical behavior to flexion of the CRF when hybridizing the steel fibers with the CNTs, ensuring greater rigidity, maximum resistance to flexion, residual strengths and better fiber-matrix interaction. Further, according to Alshaghel (2018), due to the presence of CNTs, the concrete can be designed to be capable of detecting some strains and deformations, and can be applied to structural health monitoring. Since this properties, this high performance material can be applied in specific buildings like defense engineering.

REFERENCES

[1] GHADBAN, AA, WEHBE, NI, UNDERBERG, M. Effect of Fiber Type and Dosage on Flexural Performance of Fiber-Reinforced Concrete for Highway Bridges. ACI Materials Journal, v. 115, n. 3, 2018.

[2] ALSHAGHEL, A, PARVEEN, S, RANA, S, FANGUEIRO, R. Effect of multiscale reinforcement on the mechanical properties and microstructure of microcrystalline cellulosecarbon nanotube reinforced cementitious composites. Composites Part B, v. 149, 122-134, 2018.

[3] PARVEEN, S. RANA, S. FANGUEIRO, R. PAIVA, MC. Microstructure and mechanical properties of carbon nanotube reinforced cementitious composites developed using a novel dispersion technique. Cement and Concrete Research, v. 73, 215-227.

ULTRA-STRONG KNITS FOR PERSONAL PROTECTIVE EQUIPMENT

Liudmyla Halavska[1], Svitlana Bobrova[2], Tetiana Ielina[3], Daiva Mikucioniene[4], and Rimvydas Milasius[5(*)]

[1, 2, 3]Department of Textile Technology and Design, Kyiv National University of Technologies and Design, Kyiv, Ukraine

[4, 5] Department of Production Engineering, Kaunas University of Technology, Kaunas, Lithuania

[(*)] E-mail: rimvydas.milasius@ktu.lt

ABSTRACT

This work was focused on the development of ultra-strong knitted fabrics intended to protect against mechanical damage in personal protective equipment. Six variants of weft knitted structures were developed and knitted from ultra-high molecular weight polyethylene. The mechanical tests performed allowed to identify dependence of mechanical properties on structural parameters of the knits.

INTRODUCTION

The production of ultra-strong knits is a promising and important direction for personal protective equipment. This group of products includes gloves and sleeves protecting various parts of the hands, vests, helmets, long hose, etc. One of the main characteristics of such products is the enhanced resistance against mechanical damage such as cutting, tearing, puncture, abrasion. Several problems can be faced in development and production of such knitted products. Knits from ultra-high strength yarns, used for this type of products, can be knitted on knitting machines with sinkers which ensure concentrated execution of individual loop forming, safely fix the yarn during its entry under the needle hook and form loops with constant yarn tension. The knits have to have enhanced mechanical strength properties, which strongly depend on a knitting pattern, on the other hand, they have to ensure good comfort.

Two variants of weft knitted structures with 3 different loop lengths of each, i.e. 6 variants in total, were developed and used for experimental tests. Knits of the first structural variant were knitted from ultra-high molecular weight polyethylene yarn with 132 tex linear density in plain weft pattern. Knits of the second variant were knitted from the same ultra-high molecular weight polyethylene yarn with additional elastomeric Spandex yarn with 100 tex linear density, laid in every fourth course in tuck-miss pattern with 1×3 repeat. Such a structure gives significantly higher density, tightness, not forgetting a higher transversal elasticity of the knit, which ensures better wearing comfort. To assess the level of protection provided by the developed knits, the following mechanical properties were investigated: breaking force and elongation at break, resistance to abrasion, tearing and cutting.

RESULTS AND CONCLUSIONS

The results from the breaking tests are presented in Fig. 1. The obtained results demonstrate that increasing the loop length of the knits with elastomeric tuck-miss yarn (WPE) has higher influence on decrease of the breaking force and increase of the elongation at break than of the knits without the elastomeric yarn (WP). It means that even small changes in the loop length can affect tensile strength.

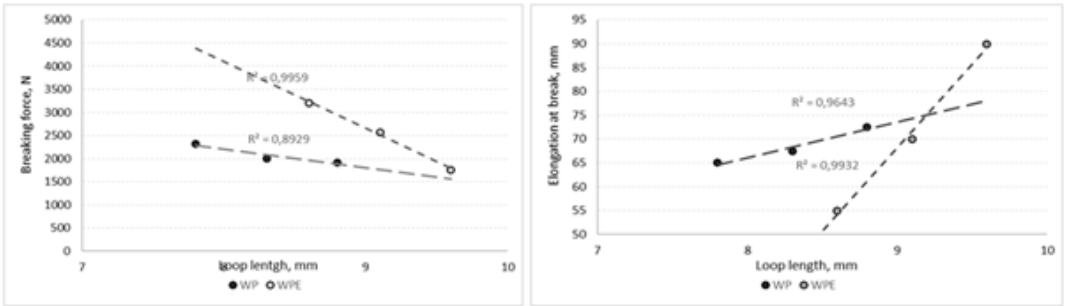

Fig.1 Tensile test results

This study shows that there are substantial differences on the mechanical properties of different urogynecology meshes. Further tests should be performed in order to analyze other mechanical properties, such as flexural properties.

Results of the abrasion test (a 300 g/m2 glass paper was used as an abrasive material) showed an interesting tendency. The increase of the loop length of the plain weft structure (WP) was associated with decreased abrasion resistance. However, the increase of the loop length of the structure with elastomeric tuck-miss yarn (WP) was associated with higher abrasion resistance. This can be explained by the fact that elastomeric yarn in such fleece structure results formation of the relief surface of the knit.

The essence of the cutting resistance tests was to determine the load required for cutting through textile material with the edge of the blade length of 20 mm. The obtained results showed that the looser knitted structure gives higher cut resistance. A 12-13% increase in the loop length gives 50% increase of the cutting load of the WP knits and 4.2 times reduction in cutting load in the WPE knits. However, presence of the elastomeric yarn in the structure caused 1.5 times higher tearing resistance.

ACKNOWLEDGMENTS

This work was supported by the Lithuanian-Ukraine cooperation project “Knitted Materials for Personal Protective Equipment Against Mechanical and Flame Damages (PERPROKNIT)” by Research Council of Lithuania and Ministry of Education and Science of Ukraine.

REFERENCES

[1] Mikucioniene D., Ciukas R., Mickeviciene A. The influence of knitting structure on mechanical properties of weft knitted fabrics. Materials Science, 2010, 16(3), p. 221-225.

[2] Kyzymchuk O., Mel'nyk L., Yermolenko I. The analysis of assortment of protective textiles. Bulletin of Kiev National University of Technology and Design: A series of "Engineering", 2016, 6(104), p. 115-125 (in Ukrainian).

INFLUENCE OF KNITTED STRUCTURE ON FLAMMABILITY AND COMFORTABILITY OF PROTECTIVE CLOTHING

Daiva Mikucioniene[1(*)], Rimvydas Milasius[2]

[1,2] Department of Production Engineering, Faculty of Mechanical Engineering and Design, Kaunas University of Technology, Kaunas, Lithuania

[(*)] E-mail: daiva.mikucioniene@ktu.lt

ABSTRACT

This research was focused on the development of knitted structures for protective clothing with enhanced flame resistance and good comfort characteristics. The main goal was to find the optimal relation between the low flammability and high comfortability by changing structural parameters of the knitted fabric. Eight variants of knitted specimens were prepared for this work. Specimens were arranged in multiple layer packets and burning time, i.e. the time until the upper layer of the packet starts to break-up, was measured. It was established, that the number of yarns in the loop influences the flammability more than the number of layers. The burning time has a medium correlation with air permeability, however, areas with similar burning time and very different values of air permeability were found.

INTRODUCTION

The safety and comfort of human being is an important issue, especially in designing of fire-fighter's clothing or personal equipment of special forces personnel. Such clothing must be flame resistant, form a heat barrier and be comfortable. The level of clothing protection depends on the raw material, structure of the textile fabric, finishing, and construction of a garment. While permeability to air, which is one of the most important comfort properties, depends on the shape and value of pores and inter-thread channels, which are dependent on the structural parameters of the fabric, such as yarn diameter, knitting structure, course and wale density. Meeting the seemingly contradictory requirements of creating a barrier against heat and flame as well as maintaining breathability in functional clothing is challenging.

Four groups of knits, that differ in the yarn linear density and, additionally, in the loop length in the group, were made in a single jersey pattern on a flat (14E gauge) weft knitting machine from Nomex Delta TA yarns. Burning behaviour and air permeability of the fabrics was evaluated in packets of two or four layers. Flammability of the knits was investigated by using the horizontal test method according to standard DIN 50050-1:1989. The air permeability of the knits was investigated according to the standard EN ISO 9237:1997 using a head area of 10 cm2 and a pressure difference of 100 Pa.

RESULTS AND CONCLUSIONS

The results obtained showed that the higher density of loops in a knit, higher number of yarns in the loop as well as higher number of layers in the packet result the increase in the burning time and decrease in air permeability. It was found that one layer of the knit with two yarns in the loop has significant better protective properties against fire than two layers of the knit with one yarn in the loop.

Also, it was found that the burning time and air permeability of a knit can be predicted depending on tightness factor of the knit. By increase of tightness factor, the burning time increases and permeability to air decreases. Very important is the fact that different zones of the correlation between the tightness factor and burning time or air permeability were obtained in this investigation. The highest influence of the tightness factor alteration on the burning time was found in the zone of 12÷13 tex1/2cm-1, the recommended tightness factor for single jersey knits.

A high correlation between air permeability and the burning time was not obtained. Three different zones of correla-

tion were obtained in this research. In the case of multilayer packet of tightly knitted fabrics, burning time increases approx. twice and air permeability decreases only slightly. In the case of one layer of loose knitted fabrics, the alteration of air permeability by approx. 2 times influences the burning time of knit only in few percent. And the most important is the third zone, where can be found areas with very similar permeability to air but significant different burning time, and vice versa. It means, it is very simple to increase comfortability of a knit without decreasing of its flammability by only changing the knit structure.

Thus, it can be concluded that the influence of structural parameters on protective and comfort properties of knitted garments is very high.

ACKNOWLEDGMENTS

The authors gratefully acknowledge the contribution of the COST Action CA17107 CONTEXT.

REFERENCES

[1] Buzaite V, Repon Md R, Milasiene D, Mikucioniene D. Development of multi-layered weft-knitted fabrics for thermal insulation. Journal of Industrial Textile, 2019, Early access Sept.2019.

[2] Mikucioniene D, Milasiute L, Milasius R. Influence of Knits Structure on Flammability and Comfortability. Autex Research Journal, 2014, 14(4), p. 226-232.

[3] Mikucioniene D, Baltusnikaite J, Milasius R. Influence of the Number of Yarns in a Loop on the Flammability of Knits. Fibres&Textiles in Eastern Europe, 2011, 19 (6), p. 71-74.

[4] Mikučionienė D. Milasiute L, Baltusnikaite J, Milasius R. Influence of Plain Knits Structure on Flammability and Air Permeability. Fibres&Textiles in Eastern Europe, 2012, 20 (5), p. 66-69.

TOWARDS THE DEVELOPMENT OF STRONG YET LIGHT CARBON FIBRE REINFORCED PLASTICS (CFRP) USING NANOWELD®: STRUCTURAL DESIGN INSPIRED BY NATURE

Katerina Loizou[1], Angelos Evangelou[1], Demetris Photiou[1], Katerina Sofocleous[1], Orestes Marangos[2], Stylianos Yiatros[2], Vassilis M. Drakonakis[1(*)]

[1]AmaDema- Advance Materias Design & Manufacturing Ltd, Nicosia, Cyprus

[2]Cyprus University of Technology (CUT), Limassol, Cyprus

[(*)] E-mail: vassilis@amdmcomposites.com

ABSTRACT

The focus of this work is to investigate a novel approach to reinforce fibre reinforced polymer composites in order to enhance their mechanical properties whilst keeping the desired volume fraction constant. NanoWeld®, a proprietary process developed by AmaDema utilises a bio-inspired fractal design, aiming at boosting the strength of composite at lower weight. This process involves an interlayer made from polymer nanofibers (nanofabric) that is consolidated on the fibre bed. In this extended abstract the characterisation of four different nanofabrics will be outlined, including both visual inspection via Scanning Electron Microscopy (SEM) and through tensile strength tests. The effect of nano-reinforcement on the strength of the nanofabrics will also be explored, in an attempt to investigate the strength augmentation they offer on Carbon fibre reinforced plastics.

INTRODUCTION

The current momentum in the field fiber reinforced polymers entails the use of strong yet light structures. Since fiber reinforced polymers are increasingly used in several industries such as defense, aerospace or automotive industries over aluminum or metal structures, a lot of effort has been focused in improving the strength of such structures. A bio-inspired approach has been selected in this case due to the multi-functionally and efficiency potential it offers (Drakonakis, 2016). More specifically a fractal structure mimicking the feathers has been employed to enhance the strength of conventional CFRPs, shaping the NanoWeld® process. This process is unraveled in three steps. The first step is the creation of a nanofabric via an electrospinning process (Christophorou, 2010). Then the nanofabrics are placed on the top and bottom of the fiber bed and they are pressed together. Finally, the sandwich configuration is consolidated using ultrasonic welding. The resulting structure is still a dry fabric, which can be used through any resin processing technology.

Four types of nanofabrics have been employed; PAN, PVDF, PA6 and PA6 with 0.35% Carbon Nanotubes (CNTs). All four nanofabrics are of 2gsm grammage and their thickness is 8μm. These nanofabrics have been tested to assess their tensile strength along with the effect of the addition of CNTs on the resulting tensile strength. Additionally, Scanning Electron microscopy has been utilised to visualise the nanofiber structure. Tensile strength tests have been carried out in an in-house assembled rig designed to test low strength specimens. Each nanofabric specimen was 210mm long, 32 mm wide and two layers of each were tested per run in order to obtain a higher measurement range. The nominal gauge length was 12.5mm and the displacement applied had an average rate of 2mm/min. The average strength was calculated taking into account five runs per type of nanofabric tested.

RESULTS AND CONCLUSIONS

The tensile strength of the four tested nanofabrics is presented in Fig.1. As observed the nanofabric that exhibits the maximum tensile strength is the one that is reinforced with CNTs. Comparing the three nanofabrics without rein-

forcement, PVDF is the nanofabric with the highest tensile strength and the highest elongation under tension (40%). The effect of the nano-reinforcement on the strength is apparent as it results in a 69% increase compared to the PA6 without the added nanoparticles. Finally, SEM imaging of the nanofabrics unravels the effect of the addition of CNTs on the average fibre diameter. Upon addition of CNTs, a50% increase in the average diameter of the electrospun fibres has been observed through scanning electron microscopy (SEM).

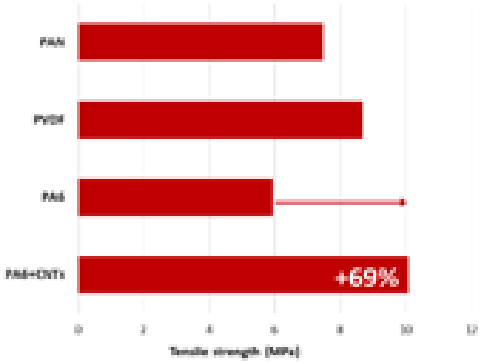

Fig.1: Tensile test results

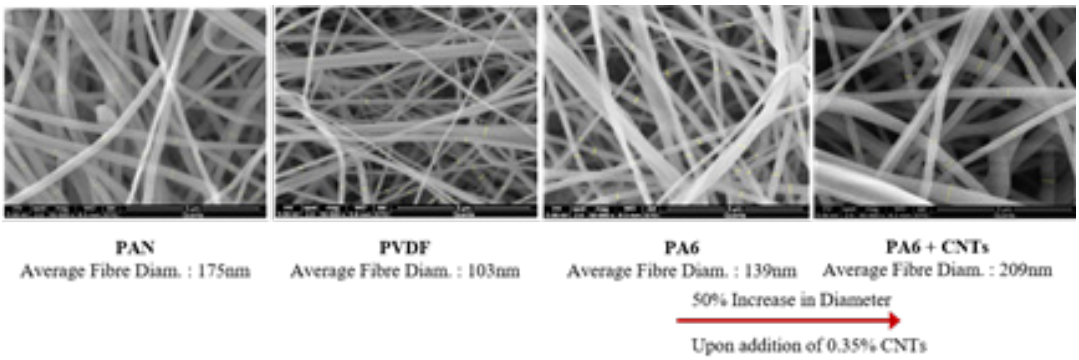

Fig.2 Scanning Electron Microscopy images for the four nanofabrics employed

This study demonstrates that the incorporation of nanoparticles results in a sharp increase of the measured tensile strength of the resulting nanofabrics. Further ongoing work investigates the effect of nano-reinforcement with CNTs in PVDF and PAN. Outcomes of the above experimental campaign will be presented.

ACKNOWLEDGMENTS

This work was co-funded by the European Regional Development Fund and the Republic of Cyprus through the Research and Innovation Foundation (Project: ENTERPRISES/0618/0051)

REFERENCES

[1] Drakonakis, V.M.; Velisaris, C.N.; Seferis, J.C.; Doumanidis, C.C. Feather-inspired carbon fiber reinforced polymers with nanofibrous fractal interlayer. Polym. Compos. 2016, 37, 168–181.
[2] Christoforou, T.; Doumanidis, C. Biodegradable Cellulose Acetate Nanofiber Fabrication via Electrospinning. J. Nanosci. Nanotechnol. 2010, 10, 6226–6233.

DEVELOPING TUNGSTEN FILLED METAL MATRIX COMPOSITE MATERIALS USING LASER BEAM MELTING

Martin Jäcklein(*), Aron Pfaff, and Klaus Hoschke
Fraunhofer Institute for High-Speed Dynamics, Ernst-Mach-Institut, EMI, Freiburg, Germany
(*) E-mail: martin.jaecklein@emi.fraunhofer.de

ABSTRACT
In this work, we present a study on metal matrix composite (MMC) material development using Laser Beam Melting (LBM). The composite material generated is composed of an X3NiCoMoTi 18 9-5 steel as matrix and filling spherical tungsten particles. The presented results focus on aspects regarding the manufacturing process like achieved material density in dependence of the tungsten content in the composite. The failure analysis of a tensile test specimen allows first conclusions on the quality of the composite material.

INTRODUCTION
Additive Manufacturing (AM) offers possibilities of generating new materials, which are challenging or unfeasible to produce by conventional means. Such new materials enable the adaption of their mechanical properties for specific applications (Kang, 2018). The manufacturing of composite materials, especially metal matrix composites, is of strong interest as MMCs combine the mechanical properties of their components (Chen, 2020). Thus, a heavy material like tungsten, which is very brittle itself, can be combinated with a ductile matrix material. Thinking of penetrator materials, this grants a higher acceleration resistance in trade-off for lower density. The resulting mechanical properties of MMCs can even be superior than expected from each component itself. Generally, multiple combinations of materials are possible. Thus, metallic particles as well as ceramic components can be applied as filling material of a metallic matrix.
In this study, an X3NiCoMoTi 18 9-5 steel was chosen as matrix material, which should enclose spherical tungsten particles. For this purpose, the steel and tungsten raw material powders were mechanically blended. The mixed powder was then processed via LBM, a powder bed based AM technique. During the process, the steel particles were molten and solidified around the tungsten particles. A series of powder mixtures with tungsten contents of 40-70 vol% was processed in order to adapt the process parameters such as laser power, scanning velocity or hatch distance. The archimedic densities of the resulting test cubes were measured and considered as a first quality criterion. Subsequently, the cubes were prepared by metallographic means and analyzed using light microscopy regarding aspects like the distribution and shape of the tungsten particles as well as the porosity of the composite material. Moreover, for a selected composition, a tensile test was carried out. The failure surface was then investigated in a scanning electron microscope (SEM).

RESULTS AND CONCLUSIONS
Within the parameter variation studies, a decreasing trend of the relative archimedic density could be observed with increasing tungsten content. A parameter adaption performed for tungsten contents of 60-70 vol% lead to an overall rise of the density level. However, the negative trend regarding the relative density for higher tungsten content remained. Another optimization of the process parameter sets for samples with 60 vol% tungsten resulted in densities near the theoretical density. Metallographic investigations revealed a fairly uniform distribution of the tungsten particles in the steel matrix. SEM images of a failure surface of a tensile test specimen are presented in Fig. 1.

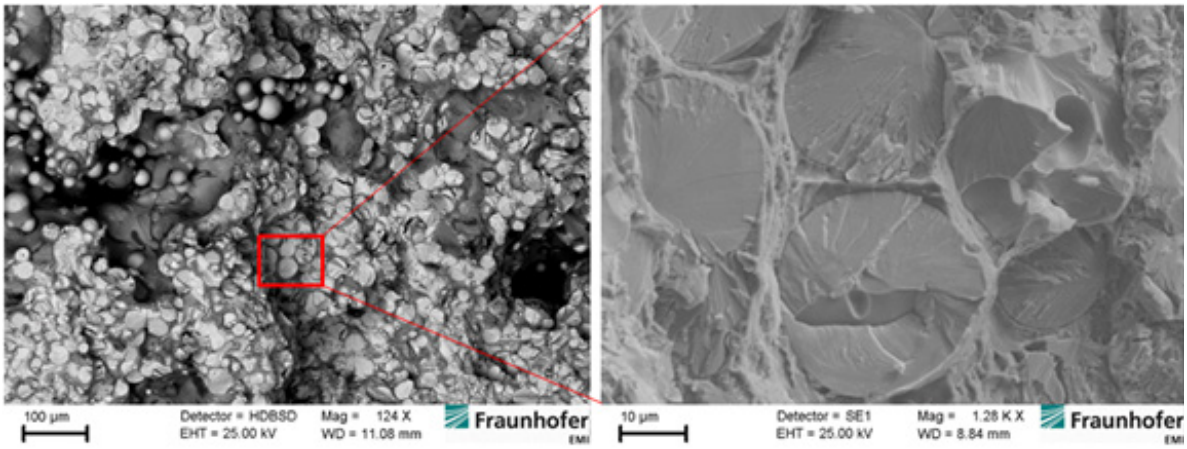

Fig.1 SEM images of a failure surface of a tensile test specimen. Left: Backscatter image showing tungsten particles (bright) and matrix phase (dark). Right: Zoom-in of the left image. Cleavage of the tungsten particles well embedded in the steel matrix can be observed.

In the backscatter image (left), it can be seen that the heavy tungsten particles (bright) are distributed over the whole specimen. The dark areas represent the lighter steel matrix phase. However, porosity is clearly visible, e.g. the dark hole at the right side of the image. Having a closer look on the failure surface (right image), it can be observed that the tungsten particles exhibit cleavage planes. Moreover, the reinforcement particles are not ripped off the matrix. This indicates that the contact between matrix and reinforcing particles is strong enough to withstand the applied tensile forces.

In this study, we presented the feasibility of processing two powders in the LBM process by melting the matrix material, which encloses the filling particles. Further investigations taking into account different material combinations should be carried out in order to identify promising composites for civil as well as for defense applications.

ACKNOWLEDGMENTS

The authors gratefully acknowledge the help of Jun Young Hong regarding sample preparations.

REFERENCES

[1] Kang N., et al., Selective laser melting of tungsten carbide reinforced maraging steel composite. Additive Manufacturing, 2018, 22, p. 104-110.

[2] Chen H., et al., Microstructure and mechanical properties of additive manufactured W Ni Fe Co composite produced by selective laser melting. Int. Journal of Refractory Metals & Hard Materials, 2020, 86, 105111.

DESIGN OF THE HYBRID BALLISTIC PLATES FOR PERSONAL PROTECTIONS

Marcin H. Struszczyk, Paulina Dmowska-Jasek, Marcin Łandwijt
Institute of Security Technologies "MORATEX", Sklodowska-Curie 3, 90-505 Lodz, Poland
(*) E-mail: itb@moratex.eu

ABSTRACT
The presented research is focused on the idea of the advanced ballistic personal protections design taking into account the requirements of the safety as well as performance. The application of the multi-criterial analysis (MCA) allows to compare the whole property of the material and to select the optimal variants of the ballistic protections considering mechanical, ballistic, physical behaviour, as well as comfort and the economic aspects.

INTRODUCTION
The selection of the raw material for the design of the ballistic personal protections (BPP) is most crucial for the fulfillment of the required properties of the final product. Several parameters describe the behavior of BBP, such as: ballistic resistance, mass, area of the protections, additional functionalities (e.g. spike, knife resistance). Moreover, the several other features define the properties of the BPP being difficult to compare with above-mentioned and among each other (such as: the main ballistic components cost, comfort aspects, etc.). The most critical properties for the selection of the optimal group of BPP features are as follow: ballistic resistance (including bullet velocity, V50), safety (including the depression depth, area of the depression, depression volume, protection area), mechanical properties (mechanical strength, tearing resistance, hardness), physical properties (areal density, thickness), stability (thermal stability, time stability), ergonomic behavior and economical aspects.
The useful tool for the proper selection of optimal solution for the BPP design is multi-criterial analysis (MCA) proposed by Zurek (Zurek W., et al., 1983) and Karolinski (Karolinski W., et al, 1974). The adaption of the MCA was performed by Struszczyk (Struszczyk M.H., et al., 2009 and Struszczyk M.H. et al., 2011) for selection of the most optimal variant of the hernia implants made by knitting.
The aim of the presented research was to adopt the MCA accounted hybrid ballistic plates (HBP) specify as well as to perform the selection of the optimal variant of the ballistic inserts for the bullet- and fragment-proof vest. The process of the MCA was helpful for the selection the proper raw-materials and design of the HBP originated from the originally designed one-stage process of the fabrication.

RESULTS AND CONCLUSIONS
The selection of the optimal ballistic raw material for design of the HBP was performed based on the results of a multi-criterial analysis (MCA) with an economic factor by determining General Coefficient of the Quality (GCQ) using parameterized relative criteria for each group of parameters determining a characteristic or functional property being critical in order to optimize the choice of the best option. Following parameters (aggregated in three groups) have been applied for the MCA: 1) physical properties (areal density, thickness); 2) usable properties (average velocity of bullet, maximal deep of the depression; area of the deformation; volume of the deformation); 3) other properties (whole cost of the fabrication; operational cost; number of the layers in HBP). The grouped parameters describing the functionalities and safety of the developed HBP variants was transformed to criterial markers. The applied parameters are described by various units and therefore it is convenient to used relative coefficient to describe the particular features. MCA allowed to choose the best quality variants of HBP due to the parametrically grouped characteristics of HBP variants and the comparison, among themselves, of various functional characteristics with different names, providing a validated tool to choose the best variant with the required qualities. Additionally, the obtained GCQ was compared with the monolith ballistic plate (one type ballistic material used for the fabrication of the ballistic plate)

(MBP).

The examples of the results of MCA for HBP and MBP are presented in Figures 1 ÷ 2 (optimal and the worst rated).

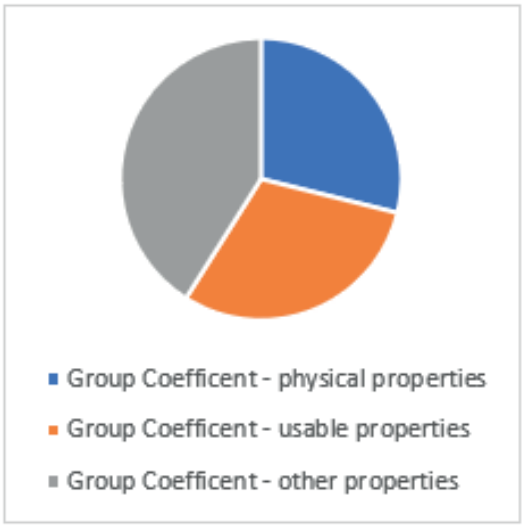

Fig.1. The relation of the grup coefficient for the HBP variant (GCQ = 4)

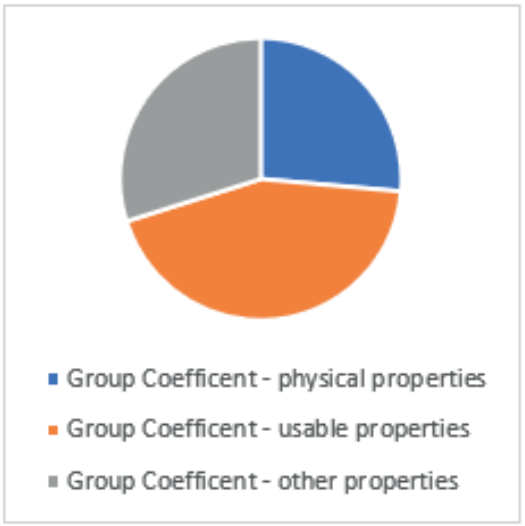

Fig.2 The relation of the grup coefficient for the MBP variant (GCQ = 6)

ACKNOWLEDGMENTS

Research was supported by European Regional Development Found in frame of the project No. POIR.04.01.02-00-0028/17 “Development of one-stage process of the hybrid ballistic plate technology characterized by the improvement of the safety use”

REFERENCES

[1] Zurek W., et al., Struktura płaskich wyrobów włókienniczych, Wydawnictwa Naukowo-Techniczne, Warszawa, Poland, 1983.

[2] Karolinski W., et al., Analiza metod oceny maszyn dziewiarskich i ich aplikacja do szydełkarek cylindrycznych, Przegląd Włókienniczy, 1974, 278 – 284.

[3] Struszczyk M.H., et al., Elaboration of the Optimal Structure of Flat Implants for Hernia Treatments, Fibres & Textiles in Eastern Europe, January/March 2009, 1 (72), 103-110

[4] Struszczyk M.H., et al., Ultra-Light Knitted Structures for Application in Urologinecology and General Surgery – Optimization of Structure, Medicaland Health Care, ISBN 978-952-15-2607-7, FiberMed11 28-30 June 2011, Tampere, Finland.

POLYURETHANE NANOCOMPOSITE COATED FABRICS AND LAMINATES FOR DEFENCE APPLICATIONS

Mangala Joshi
Department of Textile and Fibre Engineering
Indian Institute of Technology, Hauz Khas,New Delhi 110016, India
E-mail: mangalajoshi9@gmail.com, mangala@textile.iitd.ac.in

ABSTRACT

Thermoplastic polyurethane (TPU) is a versatile polymer having excellent flexibility and elastic recovery, excellent adhesion property, good abrasion resistance, good chemical resistance and heat sealability and therefore finds extensive applications in coatings. However, with the growing demand of different functionality in coated textiles for technical applications, polymer nanocomposite coatings is being looked as an attractive option. Incorporation of nano materials in the polymer coating formulations can enhance several properties such as gas barrier, antimicrobial, self-cleaning, microwave absorbency, wear and tear resistance or weather resistance. This paper discusses the potential of polymer nanocomposites as an emerging new advanced material for coatings on different substrate media such as textile fabrics to metal surfaces. The highlights of some of the work we have undertaken at IIT Delhi over past few years in this area would be highlighted.

In this direction an initiative has been taken by our group to improve the weather resistance and gas barrier property of TPU coatings by incorporating nanoclays and functionalized graphene in polyurethane matrix.of pristine TPU. One of the applications for TPU coated textile fabric is inflatables such as parachute, hot air balloon filled with helium gas and aerostats are extensively used at present in defence as a platform for air surveillance etc. Other uses include lifesaving jackets, emergency rafts, dinghies, balloon, parachute etc. Needless to say, these inflatables require very good mechanical properties such as tensile strength, modulus, bursting strength, abrasion resistance as well as good thermal stability. Conventionally polyurethane coated nylon or polyester fabrics are used for these inflatable structures. The retention of helium /hydrogen and weather resistance properties are most crucial for this product as far as durability and service life is concerned. Apart from significantly enhancing various attributes of the nylon base fabric, the most interesting observation is that, the presence of nanoclay markedly reduces the permeability to gases such as nitrogen and helium for both solution and melt coated sample. Also, as gas permeability and weather resistance goes hand-in–hand, it was encouraging to observe that PU/nanoclay nanocomposite coated fabrics had much better gas retention property as compared to the neat PU coated samples on addition of clay. This is evident from reduced loss in strength and helium permeability on exposure of coated samples to outdoor weathering conditions.

ACKNOWLEDGMENTS

The authors gratefully acknowledge the funding by Aerial Delivery Research and Development Establishment, Defence Research and Development association (DRDO), Govt of India for funding the project under which this work was done. The author also acknowledges the contributions of coworkers BS Butola, Bapan Adak, Gaurav Singh and Upashana Chatterjee

REFERENCES

[1] Joshi, M., Adak, B., & Butola, B. S. (2018). Polyurethane nanocomposite based gas barrier films, membranes and coatings: A review on synthesis,characterization and potential applications. Progress in Materials Science. 97, 230-282.
[2] Adak, B., Joshi, M., & Butola, B. S. (2019) Polyurethane/functionalized-graphene nanocomposite films with enhanced weather resistance and gas barrier properties, Composite Part B: Engineering, 176, 107303.

[3] Adak, B., Butola, B. S., & Joshi, M. (2019) Calcination of UV shielding nanopowder and its effect on weather resistance property of polyurethane nanocomposite films. Journal of Materials Science, 54 (19), 12698-12712,
[4] Adak, B., Butola, B. S., & Joshi, M. (2018). Effect of
organoclay-type and clay-polyurethane interaction chemistry for tuning the morphology, gas barrier and mechanical properties of clay/polyurethane nanocomposites., Applied Clay Science, 161, 343-353.
[5] Adak, B., Joshi, M., & Butola, B. S. (2018). Polyurethane/clay nanocomposites with improved helium gas barrier and mechanical properties: Direct versus maste batch melt mixing route. Journal of Applied
Polymer Science, 135(27), 46422.

ACTIVE THERMAL REGULATION SYSTEMS FOR FOOTWEAR: DEVELOPMENT OF NEW INNOVATIVE TECHNOLOGIES

Sónia Silva[1(*)], João Ferraz[2], Helena Fernandes[3], Joana Pimenta[4], José Gonçalves[5], Carla Matos[6], Fernando Merino[7], Rita Pedrosa[8] and Teófilo Leite[9]

[1, 2, 3, 4, 5] Centre of Nanotechnology and Smart Materials, Vila Nova de Famalicão, Portugal

[6, 7, 8, 9] ICC Lavoro - Indústrias e Comércio de Calçado S.A., Guimarães, Portugal

[(*)] E-mail: smsilva@centi.pt

ABSTRACT

This work developed active heating systems for thermoregulate footwear, printed directly on polyurethane foams. Different commercial conductive inks, with different properties, were tested for circuits with different geometries. Cooling systems have also been developed, using commercial Peltier modules, and the development of efficient thermal transfer mechanisms, adaptable to footwear, without causing user discomfort.

INTRODUCTION

The use of footwear for long periods, in hot or cold environments, can lead to an increase or decrease in temperature inside, resulting in discomfort for the user [1]. Mainly in terms of work activity, the thermal conditions to which the foot is exposed, can be extreme, when considered work in confined environments and using hard physical work. As an example, in jobs that require constant mobility of workers in hot environments, it is necessary to deal with excessive sweating of the feet, which causes a discomfort sensation and increases the diseases appearance, like athlete's foot. On the other hand, in activities in which workers are exposed to cold environments and without much physical activity, there is a difficulty in maintaining a comfortable temperature inside the shoes. In this context, the development of footwear with active thermal management is of great relevance, especially for working environments with extreme temperatures.

The main goal of this work is the development of active heating and cooling systems, based on innovative materials and technologies, and the development of advanced integration methodologies.

RESULTS AND CONCLUSIONS

The active heating systems were printed directly on polyurethane substrates (typical insole material) using screen-printing technology. Given the direct integration of printed systems on flexible and stretchable substrates, several specific conductive inks were studied. In addition, for the maximization of the system's performance, two types of electronic circuits were developed: in series and in parallel. Regarding parallel circuits, these are ideally suited for inks with moderate resistivity values, such as carbon inks. On the other hand, series circuits prove to be functional for inks with very low resistivities, such as silver inks. Table 1 shows some electrical characterization results for printed circuits.

Conductive ink	Sheet Resistivity (Ω/sq)	Circuit type	Electrical resistance (Ω)
Carbon 1	20-30	parallel	23,3
Carbon 2	<40	parallel	32,1
Silver 1	<0,010	series	24,6
Silver 2	0,012 – 0,015	series	9,9

Table 1. Results of electrical characterization for the printed heating circuits.

The cooling systems developed presuppose the integration of Peltier modules in shoes. For this, efficient dissipation methods have been studied that can be integrated into shoes, without causing discomfort to the user. To achieve this, different forced air mechanisms have been studied. To characterize the systems, some tests were carried out in a conditioned environment, using a climatic test chamber.
Figure 1 shows that when the cooling system was turned on, there was an increase in the loss of heat flows to ≈190 W/m2 and to ≈95 W/m2, respectively. These variations show that the cooling system had an influence on the referred areas to increase heat losses and therefore, the cooling capacity.

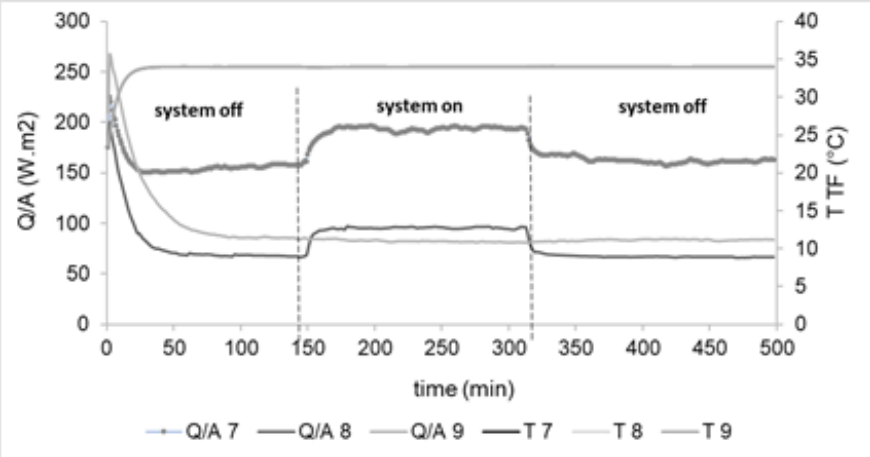

Fig.1. Results of the evaluation of thermal flow losses, obtained through the use of a thermal monitoring foot. Q/A7, Q/A8 and Q/A9 correspond to the loss of thermal flow in the different foot areas: 7 (front), 8 (middle) and 9 (heel). T7, T8 and T9 correspond to the temperatures in zones 7, 8 and 9, respectively.

Regarding the electronic system, hardware and firmware have been developed to manage and control the systems, as well as wireless charging systems. For the control of the systems by the user, a mobile application has been developed.

ACKNOWLEDGMENTS

This work was developed in the framework of Individual R&D project TERMICC – Thermal Management Feet, number 38438, a project co-financed by COMPETE 2020 – the Operational Programme for Competitiveness and Internationalization, under Portugal 2020 through the European Regional Development Fund (ERDF).

REFERENCES

[1] Nardin, R. A., Fogerson, P. M., Nie, R., Rutkove, S. B., Foot Temperature in Healthy Individuals, Journal of the American Podiatric Medical Association, 2010, 100, p. 258-264.

THERMAL CAMOUFLAGE CLOTHING IN DIURNAL AND NOCTURNAL ENVIRONMENTS

Catarina Pimenta[1(*)], Carla Morais[2], Raul Fangueiro[3]

[1, 3,] Center for Textile Science and Technology (2C2T), University of Minho, Guimarães, Portugal

[3,] Department of Mechanical Engineering, University of Minho, Guimarães, Portugal

[2,] Faculty of Architecture, University of Lisbon, Lisbon, Portugal

[(*)] E-mail: catarina.rpimenta@hotmail.com

ABSTRACT

This paper shows the possibility to thermally camouflage a human body in a beach environment, during the day and at night, through the use of two knitted fabric clothing prototypes. The conceptual design process applied was initially developed based on the need to firstly understand the behaviour of an individual dressed under the focus of a thermal imaging camera in the light of the infrared spectrum. The thermal tests undertaken to observe the model's thermal camouflage in certain positions/perspectives in both environments, enable simultaneously running of different solutions while introducing changes to the clothing. Printing with copper pigments and the patchwork using stitched structures in polyester knitted fabric played a decisive role to capture the thermal colours of the thermal image intended for the camouflage effect.

INTRODUCTION

In a modern war scenario, where the capture of spectral infrared images becomes a reality, clothing camouflage plays a decisive role in the soldier protection (Owens, 2011). In thermal camouflage, the thermal difference between the target and the environment is associated with the atmospheric effect (Vu & krejčí, 2017). Clothing is thus involved in energy transfers, triggered between environment-clothing-body, where the emissivity and the temperature of the surface are interconnected with radiation (Fourt & Hollies, 1970). The air and the subsequent movement (from the interactions between textile-skin-environment) can also interfere with the clothing's dynamics depending on the composition of the textile material, the design applied to the clothing, as well as the movement triggered by the user (Havenith, 2003). The quest to reduce the thermal signature, is equivalent to the reduction of emissivity and to the implementation of a single colour in thermal image to be applied in thermal camouflage clothing. An example of this is observed by a thermal imaging camera, in an outfit with the use of metallic materials, on the human body (Rubežienė, Padleckienė, Žuravliova & Baltušnikaitė, 2013) such as a small sample with use of materials with physical properties which exceed those observed in nature, the metamaterials, on the hand of a human body (Kumar, Agarwal & Ramakrishna, 2018).

RESULTS AND CONCLUSIONS

The results of the selected materials are shown in Table 1. These stem from the study previously performed in a laboratory environment by simulating the diurnal and nocturnal outdoor environments for future camouflage and that of the skin temperature (Pimenta, Morais & Fangueiro, 2019; Pimenta, in press). The thermal tests' results of the two thermal camouflage outfits, one for the diurnal environment and another for the nocturnal environment, are shown in Fig. 2. Through the use of the thermal imaging camera (in the “Ferro” range) and the human figure, it is possible to observe, in some of the model's positions/perspectives, the harmony of the colours idealized in the outfits' design in thermal image: the yellow (A4*), orange (A4*1/A4*3) and magenta (A4*2/A4*3) colours in the diurnal outfit; and the magenta (A4*2/A4*3) and orange (A4*1/A4*3) colours in the nocturnal outfit. The movement of the model boosts instability in the design and behaviour of the materials' colours in thermal image. In parallel, the appearance of other

colours in the materials and selected techniques is also noticeable, namely: orange and magenta (A4*); yellow, magenta and blue (A4*1); and blue (A4*2/A4*3). The embossed structures' techniques did not show great differences among themselves in terms of colour behaviour in thermal image. In some moments, it is still possible to observe the yellow colour outlining areas of the model's silhouette in motion, especially at night.

Sample	Photography	Thermal Image		Emissivity (ε)
		24 ºC	18 ºC	
A4*				0,76
A4*1				0,50
A4*2				
A4*3				

Table 1 . Textile materials and selected techniques adapted from the paper (Pimenta, in press).

* Knitted fabric: Jersey 100% Polyester; 153,39 g/m2; 0,42 mm; 26,9 Tex; 15 wales/cm; 20 courses/cm
*1 with printed copper pigment (80 g Hydra Clear for Metallic with 20 g Cooper Powder)
*2 with application of sewing technique and interlining in the totality of the quadrangular form)
*3 with application of sewing technique and interlining only on its side fitting)

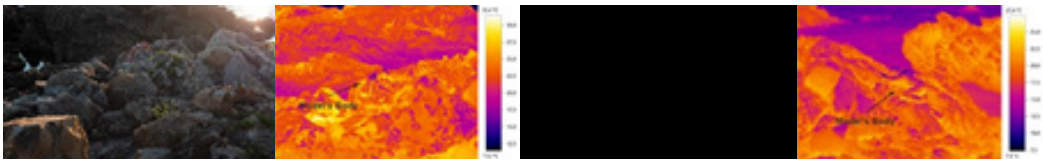

Fig.1 . The conceptualized thermal camouflage outfits: a) diurnal environment; b) nocturnal environment.

This study shows that there is a possibility of controlling the yellow, orange and magenta colours in thermal image (in the "Ferro" range) in certain positions/perspectives in the outdoor environment (diurnal and nocturnal) through the use of knitted fabric clothing with the application of printing and sewing techniques. Although the movement is driving instability in the behaviour of the clothing's colours, the use of materials with different emissivity and air manipulation techniques can disguise the military's thermal signature.

REFERENCES

[1] Owens J. Key elements of protection for military textiles. In: Pan N, Sun G (eds.) Functional textiles for improved performance, protection and health. Woodhead Publishing Limited, Cambridge, 2011, p. 249-268.
[2] Fourt L, Hollies, N. Factors involved in the study of clothing. In: Clothing: comfort and function. Marcel Dekker Inc., New York, 1970, p. 1–30.
[3] Vu D, Krejčí J. Evaluating of temperature difference between target and background using measurement and simulation. In: 2017 International Conference on Military Technologies (ICMT), 2017, p. 16–21.
[4] Havenith G. Clothing and thermoregulation. In: Textiles and the skin. Karger, Switzerland, 2003 p. 35–49.
[5] Rubežienė V, Padleckienė I, Varnaitė-Žuravliova S, Baltušnikaitė J. Reduction of thermal signature using fabrics with conductive additives. In: Materials Science (Medžiagotyra), 2013, 19(4), p. 409–414.
[6] Kumar R, Agarwal A, Ramakrishna S. Development of a metamaterial structure for large-area surfaces with specified infrared emissivity. In: Optical Engineering, 2018, 57(08), p. 087109.
[7] Pimenta C., Morais C., Fangueiro R. The thermal colour and the emissivity of printed pigments on knitted fabrics for application in diurnal thermal camouflage garment. In: Key Engineering Materials, 2019, 812, p.127–133.
[8] Pimenta C, Fangueiro R, Morais C. The behavior of textile materials in thermal camouflage. In: Textiles, Identity and Innovation: In Touch, 2020, p. 281-287.

A NOVEL METHOD FOR COMPRESSIVE LOAD-DISPLACEMENT MEASUREMENTS AT VERY HIGH STRAIN RATES OF PARA-ARAMID FABRICS

Afonso Gregório[1(*)], Tiago dos Santos[2], Rodrigo Rossi[2], Abílio Jesus[3], Raul Fangueiro[4], Pedro Rosa[1]

[1] IDMEC, Instituto Superior Técnico, Universidade de Lisboa, Lisboa, Portugal

[2] DEM, Universidade Federal do Rio Grande do Sul, Porto Alegre, Brazil

[3] INEGI, Faculty of Engineering, University of Porto, Porto, Portugal

[4] Centre for Textile Science and Technology, University of Minho, Guimarães, Portugal

[(*)] E-mail: afonsogregorio@tecnico.ulisboa.pt

ABSTRACT

This paper proposes an innovative method to improve the accuracy of strain determination on the split-Hopkinson pressure bar experiments. This is essential for assessing the energy absorption capability of para-aramid fabrics and composite panels used in ballistic protections. The presentation is focused on a specially designed inductive coil extensometer and experimental technique to accurately measure strain. Results from force–displacement characterization of para-aramid fabrics under impact loading are presented to demonstrate the validity of the proposed concept.

INTRODUCTION

Recent innovations in materials and manufacturing technologies led to the development ofnew advanced materials in order to improve energy absorption capability. The use of thesematerials in ballistic protection against armour piercing projectiles can be adequatelyreplicated by the split-Hopkinson pressure bar experiments (SHPB). However, due tocomplex phenomena, the traditionally used reflected pulse technique may be unreliable whendetermining the specimens' strain (Bazle, 2004). Non-contact measuring methods, such as high-speed imaging techniques, are often an alternative to the reflected pulse technique.

However, for thin specimens such as fabrics, with undefined shape and ragged loose fibres, the visual data becomes low-quality definition with an unclear-cut "specimen-tool" contour. A novel measuring technique called inductive coil extensometer is then proposed for measuring the distance between the incident and transmission bar ends, thus improving the accuracy of strain determination.

The plan of experiments consisted of uniaxial compressive tests on plain-woven para-aramid (area weight of 300 g/m2 and square geometry of 100mm), designed in order to characterize its energy absorption capacity for a wide range of loading rates at room temperature, and were carried out in a universal testing machine (quasi-static) and in a custom made equipment (high velocity) based on the work of Silva (2009). Load–displacement curves were obtained using conventional load cell and the proposed inductive coil extensometer, respectively. This innovative inductive displacement sensor for the compressive SHPB makes use of an alternating magnetic field (flux) generated by a transmitting coil to induce an electrical current in a receiving coil. The closer the coils are, the more flux reaches the receiver and the better the coils are electromagnetically coupled. Therefore, this technique is particularly useful for impact tests on thin textile fabrics and composites where the thickness depends on the number of overlying layers, orientation between layers and applied preload before testing.

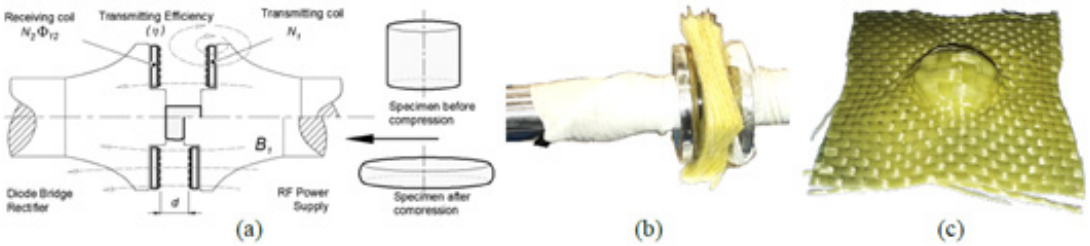

Fig.1 (a) Schematic representation of the inductive coil extensometer; (b) Compression of multi-layered stack and; (c) plain-woven para-aramid after impact test.

RESULTS AND CONCLUSIONS

Figure 2 shows that the absorption capability increases with the impact velocity and number of stacked layers. The force can be taken as the direct load on the human body and the distance between platens as the gap between the bullet and the skin. Results indicate that mechanical behaviour of para-aramid fabrics presents not only significant layered structure sensitivity but also some material rate dependence.

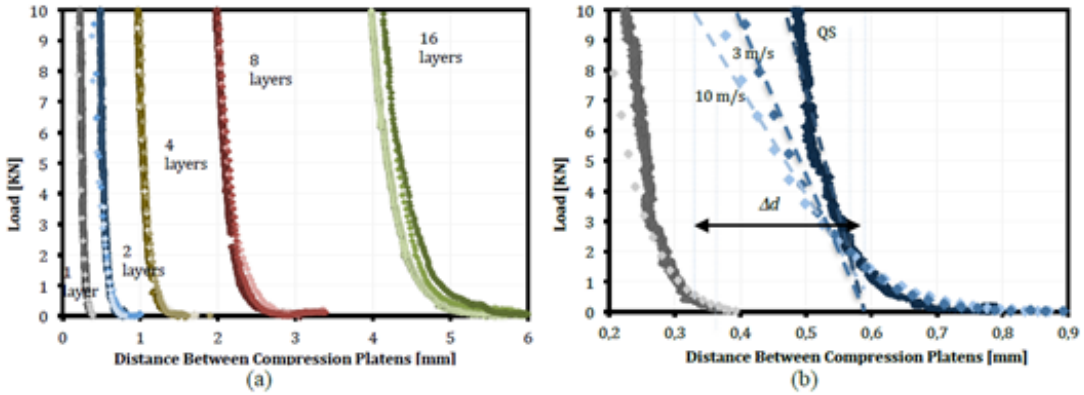

Fig.2 (a) Load-Distance curves (1,2, 4, 8 and 16 layers); (b) Slope of load curves (2 layers) for QS, 3 and 10 m/s.

The inductive coil extensometer is a complementary displacement monitoring method for the cases where the often-used techniques are limited. Moreover, the authors believe that this method is capable of surpassing existing techniques in most impact testing due to its fast response, high accuracy, low cost and high operation reliability under severe solicitations.

ACKNOWLEDGMENTS

This work was supported by FCT, through IDMEC, under LAETA, project UIDB/50022/2020. The authors would also like to thank Fibrenamics for providing the paraaramid fabrics required for the experimental tests.

REFERENCES

Bazle, AG, Gillespie JW. Numerical Hopkinson bar analysis: uni-axial stress and planar bar-specimen interface conditions by design. Report MD 21005-5069, ARL-CR-553, Army Research Laboratory, Aberdeen Proving Ground, 2004.
Silva CMA, Rosa PAR, Martins PAF. An Innovative Electromagnetic Compressive Split Hopkinson Bar. Int. J. Mechanics and Materials in Design, 2009, 5, p.281-288.

FABRICATING DUAL-LAYER NANOFIBROUS MEMBRANE SYSTEMS FOR ENHANCING WEARER COMFORT

Seojin Lee and Seungsin Lee(*)
Department of Clothing and Textiles, Yonsei University, Seoul, Korea
(*) E-mail: SL158@yonsei.ac.kr

ABSTRACT

The objectives of this study are to fabricate dual-layer porous nanofibrous membrane systems to enhance the push-pull effect and capillary forces and to compare the moisture transport properties of porous nanofibrous membrane systems with their counterpart, solid nanofibrous membrane systems. This study also examines the effect of base fabric (on which nanofibrous membranes are laminated) on the water transport properties of the membrane systems. The results demonstrate that porous nanofibrous membrane systems tend to absorb water quicker and in larger areas than solid nanofibrous membrane systems due to the quantity of water transport passages created by their intrafiber pores.

INTRODUCTION

In protective and military clothing, the water transport properties of textiles are important because they are associated with maintaining the comfort of the human body. Water transmission and quick-drying properties can be imparted to textiles by maximizing their capillary action through porosity enhancement of the fibers (Fangueiro et al., 2010).
Electrospinning is an effective and promising technique for the production of fibers with small diameters. The technique provides an ultrathin membrane-like web of extremely fine fibers with very small pore sizes, which is attractive for various applications from filtration to tissue scaffolds, sensors, and protective clothing (Lee, 2009). The large surface area of electrospun nanofibrous membrane and its ease of functionalizing make it an ideal material for use in defense technology (Teo, 2015). Moreover, electrospun nanofibrous membranes are light-weight and mechanically flexible; thus, nanofiber technology has been investigated for its application in the development of lightweight protective clothing for agricultural and military personnel (Lee and Obendorf, 2007). For military use, nanofibers were functionalized with a detoxification property and have been mainly investigated for their protective ability against chemical/biological warfare. However, the high porosity and small interfiber pore size of nanofibrous membranes can be used to enhance the comfort of the wearer. In particular, porous nanofibers with extremely large surface areas tend to have a higher porosity than their solid nanofiber counterparts because of the presence of intrafiber pores. Porous nanofibers have minuscule passages leading from the surface to the inside of the fiber that increase the capillary motion through the textile. In addition, dual-layer textiles composed of a hydrophilic outer layer and a hydrophobic inner layer (near the skin) have great potential to achieve better water transport properties than single-layer textiles (Dong et al., 2014).
This study aims to fabricate porous polyacrylonitrile (PAN) nanofibrous membrane systems to enhance the push-pull effect and capillary forces and to evaluate whether porous nanofibrous membranes possess better moisture transport properties than solid nanofibrous membranes. All the nanofibrous membranes were laminated on a base fabric to fabricate dual-layer membrane systems to induce the push-pull effect. Then, the water absorption and transport properties of each nanofibrous membrane system were assessed.

RESULTS AND CONCLUSIONS

Porous PAN nanofibers were successfully fabricated by electrospinning; the processing and environmental conditions that were suitable for fabricating porous nanofibers were identified. The scanning electron microscopy (SEM)

images showed that porous PAN nanofibers had an extremely porous structure at the cross section as well as on the surface of the fiber. The transmission electron microscopy (TEM) images confirmed that each porous PAN nanofiber had open-structure interiors that would create many water transport passages and improve capillary forces.

By evaluating the water transport properties of the PAN nanofibrous membrane systems, it was found that applying nanofibrous membranes to a single-layer base fabric improved the water transport properties of the nanofibrous membrane systems. In all the experiments, the absorbency of the porous nanofibrous membrane systems with web area densities of 1.0 g/m2 was better than that of the solid nanofibrous membrane systems; they tended to absorb water faster and in larger areas. This is possibly due to the presence of many water transport passages in the porous nanofibrous membranes because they have both interfiber and intrafiber pores.

This study shows that dual-layer porous nanofibrous membrane systems have considerable potential to achieve better water transport properties. The combination of a hydrophobic PAN nanofibrous membrane and a hydrophilic base fabric exhibited a strong push-pull effect to transport water from the PAN to the base fabric layer. Water absorbency and water transport properties were significantly enhanced in dual-layer nanofibrous membrane systems.

ACKNOWLEDGMENTS

This research was funded by Basic Science Research Program through the National Research Foundation of Korea (NRF) funded by the Ministry of Education, project NRF-2019R1A2C1006171.

REFERENCES

[1] Dong Y, Kong J, Phua SL, Zhao C, Thomas NL, Lu X. Tailoring surface hydrophilicity of porous electrospun nanofibers to enhance capillary and push-pull effects for moisture wicking. ACS Applied Materials & Interfaces, 2014, 6, p. 14087-14095.

[2] Fangueiro R, Filgueiras A, Soutinho F, Meidi X. Wicking behavior and drying capability of functional knitted fabrics. Textile Research Journal, 2010, 80, p. 1522-1530.

[3] Lee S. Developing UV-protective textiles based on electrospun zinc oxide nanocomposite fibers. Fibers and Polymers, 2009, 10, p. 295-301.

[4] Lee S, Obendorf SK. Use of electrospun nanofiber web for protective textile materials as barriers to liquid penetration. Textile Research Journal, 2007, 77, p. 696-702.

[5] Teo WE. (2015, November 13). Introduction to electrospun fibers for defence technology. Retrieved from http://electrospintech.com/defenceintro.html#.XkgW99h7I9A

THE EFFECT OF ANNEALING ON THE CHANGE OF THE PROPERTIES OF COMPOSITES ZnO:Ag

Pavels Sarajevs[1(*)], Vjaceslavs Gerbreders[1], Edmunds Tamanis[1], Eriks Sledevskis[1]

[1] G. Liberts' Innovative Microscopy Centre, Institute of Life Sciences and Technology, Daugavpils University, Daugavpils, Latvia

[(*)] E-mail: pavelsar@inbox.lv

ABSTRACT

This work describes the study of the effect of thermal annealing on the properties ZnO:Ag of thin-film composites, which are the basis of sensors of heavy metal ions, as well as sensors of poisonous and explosive substrates. Changes of the optical properties and morphology of the surfaces of composites with five different component ratios were analysed. The studies performed have revealed significant changes in the properties of nanocomposites ZnO:Ag. This study may become the basis for further works on improving the sensitivity of sensors of poisonous weapons and explosive substances.

INTRODUCTION

Today, due to the growing threat of terrorism, the problems of timely detection of traces of explosive and poisonous substances are becoming more and more topical, and increasingly important. Many poisonous substances form stable organic compounds that dissolve well in water and result in the migration of poisonous agents in aquatic and terrestrial systems, thereby resulting in high levels of contamination. That is why the creation of a sensor that could detect the presence of poisonous or explosive substances, even in small quantities, is an important and topical task. Zink Oxide is promising candidate for use in such sensors. The sensors based on ZnO (especially on ZnO nanostructures) are sensitive to various types of contamination, including almost all toxic and organic pollutants, and show very good adsorption results for the most hazardous ions. Generally, ZnO is chemically inactive, so it will not become a secondary source of contamination. Furthermore, ZnO nanostructures can have various types of morphologies, thus making it possible to diversify the electrical and optical properties of the nanostructured layer for the particular application without changing the actual substance.

Electrochemical methods such as cyclic voltammetry (CV), impedance spectroscopy (IS) and differential pulse voltammetry (DPV) are highly efficient in both qualitative and quantitative analysis of solutions. These methods allow for the detection of hazardous chemicals even at very low concentrations. Furthermore, combined with a sensor platform based on nanomaterials and nanostructures, as well as introduction of dopant elements into the sensor's main material, these electrochemical methods contribute to the improvement of sensor performance in terms of sensitivity and specificity, primarily as a result of the large working electrode surface area, and consequently, large number of active links that raises the overall sorption capability.

The purpose of our research was to follow the processes which are going during the annealing of ZnO and Ag composite to further improve sensor sensitivity based on ZnO.

The initial composite films were obtained by were obtained by the method of simultaneous magnetron sputtering from two neighbor magnetrons respectively. The sputtering performed using ZnO and Ag targets respectively. The difference in concentration of components achieved by changing the deposition rate of the corresponding components. The deposition rates adjusted by changing the operating settings of the magnetrons.

RESULTS AND CONCLUSIONS

The results from the study are shown in Fig. 1. The optical properties undergo changes in the process of samples annealing. The optical transmission curves are different before annealing. After the annealing the transmission spectra

of each sample (Fig.1.2) are the same as a spectra of the pure ZnO both cases, before (Fig.1.1a) and after (Fig.1.2a') annealing.

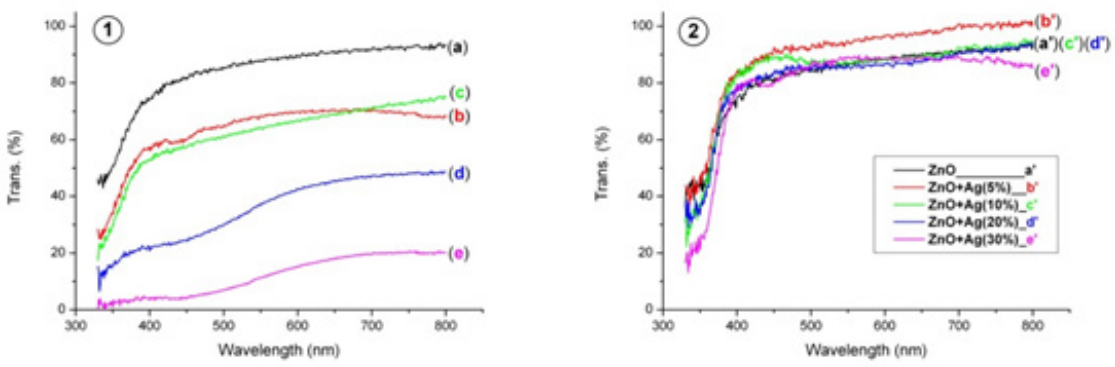

Fig.1 Optical spectra of Ag:ZnO composite before(1) and after(2) annealing

In the process of annealing cluster formations of monocrystal cubic form appear on the film surface (Fig.2), what may indicate the presence of monocrystals of silver oxide. Moreover, its amount and size are depend on the ratio of Ag:Zn atoms in the film.

According to X-ray diffraction analysis in the case when the ratio of components Ag:Zn is 1:2, along with zinc oxide, both silver oxide and pure form of silver are present in the film. At the same time, as seen in electron microscopy images (Fig.2), a large number of silver atoms prevent the growth of ordered structures of silver oxide. The size of crystals in that case is much smaller (~0.1μ) in comparison with crystals of silver oxide in cases when the ratio of Ag:Zn atoms was 1:9 or 1:4.

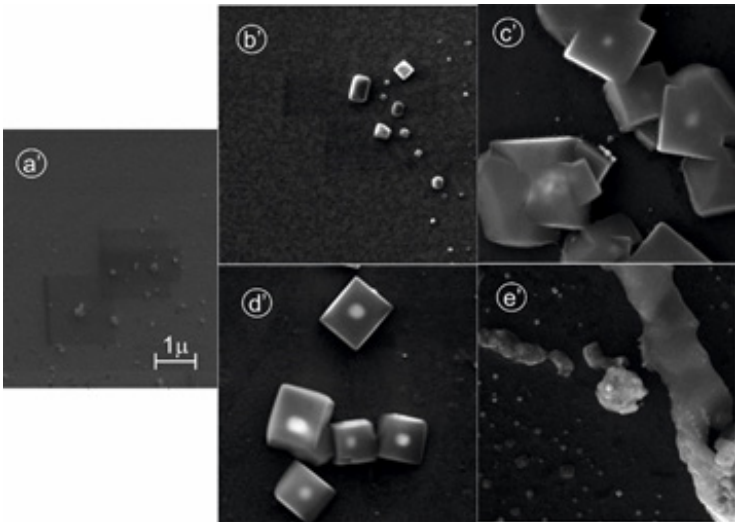

Рис.8. SEM images of composite Ag:ZnO after annealing (0, 5, 10, 20 and 30% of Ag)

This study shows that in the process of annealing silver atoms are displaced to the surface of the film and assembled into separate clusters. Doping atoms are not embedded into the crystal lattice of the base material (ZnO) and do not have a significant effect on it. Sizes or formed clusters depend on the amount of the doping material.

IMPROVEMENT OF MECHANICAL BEHAVIOR AND MICROSTRUCTURE OF MICROCRYSTALLINE CELLULOSE (MCC)-SISAL FIBRE REINFORCED MULTISCALE CEMENTITIOUS COMPOSITES

Aloysio Gomes de Souza Filho[1(*)], Shama Parveen[2], Sohel Rana[2,] Romel Vanderlei[3], Raul Fangueiro[4,5]

[1] Department of Civil Engineering, Federal University of Technology - Paraná - UTFPR, Apucarana Campus, Apucarana, Brazil

[2] School of Applied Sciences, University of Huddersfield, Queensgate, Huddersfield, UK

[3] Post Graduate Program in Civil Engineering (PCV), State University of Maringá - UEM, Maringá, Brazil

[4,5] Department of Mechanical Engineering, University of Minho, Azurém Campus, Guimarães, Portugal Centre for Textile Science and Technology, University of Minho, Azurém Campus, Guimarães, Portugal.

(*)Email: asouza@utfpr.edu.br

ABSTRACT

This work reports the development of multiscale cementitious composites containing sisal fibres and microcrystalline cellulose (MCC), previously dispersed by ultrasonication and cetyltrimethylammonium bromide (CTAB), as the novel dispersing agent. The mechanical tests performed allowed to identify significant improvement in the mechanical properties, hydration degree, and microstructure.

INTRODUCTION

Cementitious materials are extensively used in construction applications, with good compressive strength. However, one inherent problem of cementitious materials is their brittleness and proneness towards crack formation (Parveen et al., 2017). Nano/micro cracks are formed within cementitious composites during manufacturing or service and propagate with time, eventually leading to failure (Alshaghel et al., 2018).

Multiscale cementitious composites could be used to improve mechanical properties due to the excellent properties of MCC and sisal fibres. The MCC could prevents the formation of microcracks and sisal fibre prevent the propagation of macrocracks.

RESULTS AND CONCLUSIONS

The results from the Crack Mouth Opening Displacement (CMOD) tests, with plain mortar and multiscale composite reinforced with 0.1% MCC + 0.5% sisal, at 56 days, are shown in Fig. 1. Fig. 2 shows the results from the crack propagation analysis by Digital Image Correlation (DIC), for these composites.

This study shows that there are substantial differences on the mechanical properties and crack propagation in the multiscale cementitious composites containing sisal fibres and microcrystalline cellulose (MCC) due to the improvement of the microstructure and hydration of the cement.

The developed multiscale cement composites with better strength and prevention of crack propagation could be further optimized and used in high performance and lighter construction for defense applications.

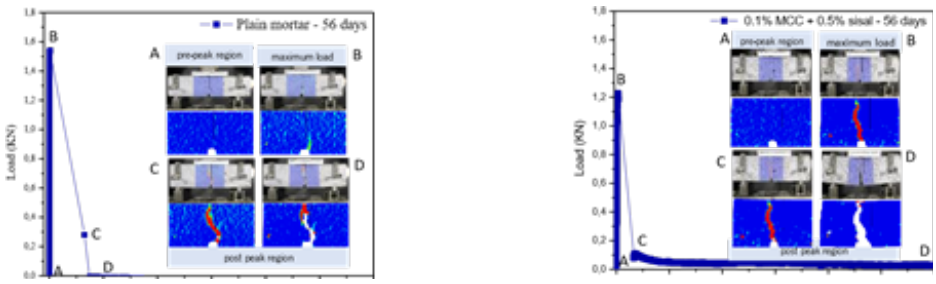

Fig.1 Crack Mouth Opening Displacement – CMOD (mm) at 56 days: plain mortar (a), 0.1% MCC + 0.5% sisal (b).

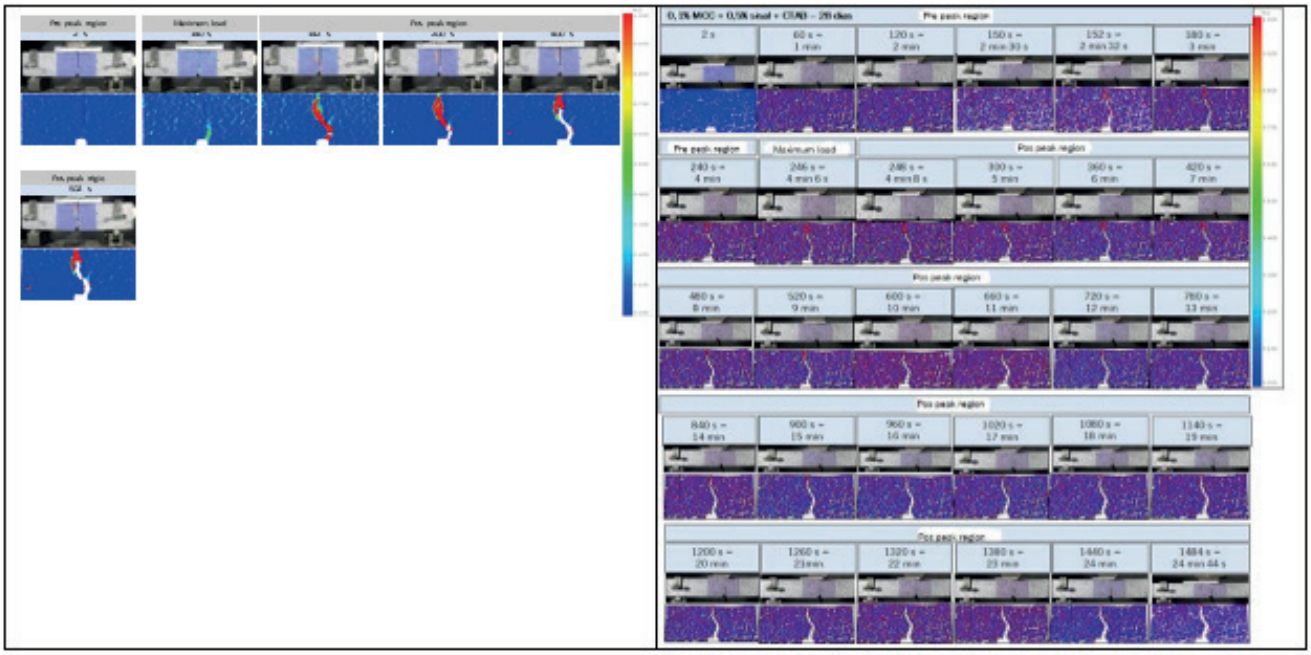

Fig.2 Crack propagation analysis by Digital Image Correlation (DIC): plain mortar (a); multiscale composite reinforced with 0.1% MCC + 0.5% sisal.

ACKNOWLEDGMENTS

The authors gratefully acknowledge the funding by Araucária Foundation to Support Scientific and Technological Development of the State of Paraná, Federal University of Technology – Paraná – UTFPR - Apucarana Campus - Brazil, Fibrenamics and University of Minho – Guimarães, Portugal, Project UID/CTM/00264/2019 of 2C2T – Centre for Textile Science and Technology, funded by National Founds through FCT/MCTES".

REFERENCES

[1] Alshaghel, A. et al. (2018) 'Effect of multiscale reinforcement on the mechanical properties and microstructure of microcrystalline cellulose-carbon nanotube reinforced cementitious composites', Composites Part B: Engineering, 149 (February), pp. 122–134. doi: 10.1016/j.compositesb.2018.05.024.

[2] Parveen, S. et al. (2017) 'A novel approach of developing micro crystalline cellulose reinforced cementitious composites with enhanced microstructure and mechanical performance', Cement and Concrete Composites. Elsevier Ltd, 78, pp. 146–161. doi: 10.1016/j.cemconcomp.2017.01.004.

NEW IMPACT PROTECTION POLYMER - IPP - TO REDUCE THE TRAUMA EFFECT OF BULLET VESTS WHEN UNDER FIRE

Klaus Richter[1(*)], Dirk Huschke[1], Prof. Dr. Klaus Heinemann[2], Dr. Lars Blankenburg[2], Prof. Dr. Dieter Klemm[3], Dr. Katrin Petzold-Welcke[3], Vanessa Raddatz[3]

[1] ITP GmbH Society for Intelligent Textile Products, Weimar, Germany

[2] Thuringian Institute of Textile and Plastics Research Rudolstadt e.V. Rudolstadt, Germany

[3] KKF Unternehmergesellschaft UG (limited liability) Jena, Germany

[(*)] E-mail: richter@itp-gmbh.de

ABSTRACT

The reduction of trauma when using bulletproof vests under active fire is an important task to improve the protective effect and readiness of the wearer of the vest.

It is shown how such a positive, pressure-absorbing effect can be achieved with the help of a newly developed polymer material, the IPP polymer. In a further step it was examined how the developed material can be kept in shape without losing its characteristic properties. Bio-cellulose has been identified as very suitable.

INTRODUCTION

The so-called "bulletproof vests" offer protection against most penetrating injuries; in case of a hit, the energy is distributed; behind the vest, haematomas or contusions can form. In extreme cases, this blunt impact on the body can lead to serious injuries and even death even though the projectile has not penetrated the vest at all. Therefore, special, mostly hard, trauma plates have been developed, which are placed in inserts in the bulletproof vest or are not used for reasons of comfort or weight.

With a newly developed polymer, the function of the trauma plate with lower weight and extremely flexible haptics as the last layer to the body should now solve this problem with greater comfort.Therefore, the synthesis of a dilatant fluid was carried out.

The synthesis of the dilatant fluids included the testing of differently functionalized starting materials, fillers and additional additives in combination with crosslinking agents. After numerous experiments with varying the ratios and viscosities of the educts, these so-called dilatant materials, i.e. non-Newtonian or shear-thickening fluids, could be prepared, which have the desired properties such as homogeneity of the samples, good flow behavior, low stickiness and, above all, dilatant behavior. In the condensation reaction of the basic components, a building block is covalently integrated into the polymer structure, which induces the dilatant properties. The first preparations were carried out on a 30-100 g laboratory scale, later the reaction in the kneader could be scaled up to 5 kg batch sizes. The material is thermally stable. In thermogravimetric analyses, less than 0.5 % mass loss was found up to 200 °C, and only about 1 % up to 300 °C. The viscosities of the dilatant fluids can also be specifically adjusted over a wide range, which enables the application to be adapted.

The application-related requirement is to fix the polymer in a carrier in such a way that the mobility is lost, and the energy consumption is retained with shock absorption. The natural product bionanocellulose (BNC) was used as the base material. It is characterized by high mechanical stability and an open and interconnected microporous system. It could be shown that the project-relevant polymer can be integrated from solution as well as by mechanical incorporation in the required amount and in the application-relevant dimensions. Insertion under hot pressing did not lead to success. Other nanocellulose materials that do not have the BNC-typical pore structure also proved unsuitable.

RESULTS AND CONCLUSIONS

Tests were carried out on the reaction of the material to an incoming impulse with objects in free fall and a first test as a dream plate. As can be seen from the following diagrams, the damping of the impact in the time axis (Figure 1) is much faster than with other materials, here foam. There is also only a slight overshoot. (Figure 2).
These tests were used to reduce the results of an impact from a heavy object.

In the next steps, tests are carried out with a bullet prove vest. For this purpose, the IPP is fixed in BNC and integrated as the last protective layer of the vest.

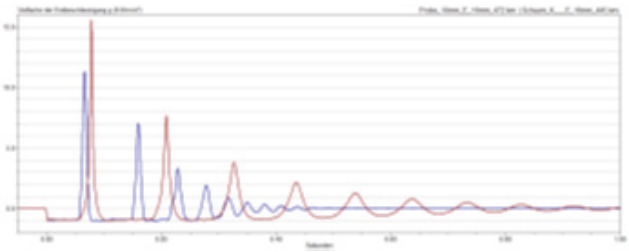

Fig.1 shows the course of an impact on the IPP material with the blue curve and on the reference material foam in the red curve. It can be clearly seen that the damping curve of the IPP material decays faster. The amplitudes are also significantly lower. IPP and foam have 10 mm thickness

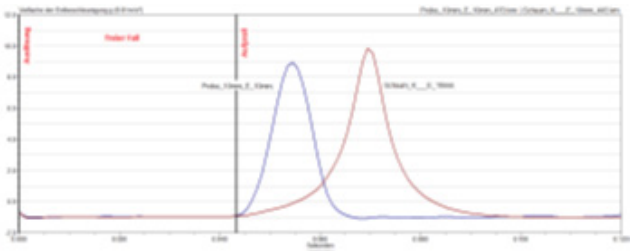

Fig.2 the damping reaction of the blue curve, the IPP material, is significantly shorter than that of the reference material in RED. This means that the impulse is broken down more quickly.

ACKNOWLEDGMENTS

The authors would like to thank the Federal Ministry of Economics and Energy BMWi of the Federal Republic of Germany for funding in the programme BMWi/IGF.

REFERENCES

[1] D. Plant, “Active amour for the sporting good market”, Kpt. in “Sports Innovation, Technology and Research”, Ed.: D.F.L Southgate, P.R.N Childs, A.M.J. Bull, World Scientific, Singapur (2016) 75-96
[2] P. Venkatraman, D. Tyler, “Impact-resitant materials and their an der potentials” Kpt. in “Materials and Technology for Sportswear and Performance Apparel”, Ed. S.G. Hayes und P. Venkatraman, CRC Press, Boca Taton (2016) 205-229
[3] H.M Rao, M.V Hosur, S. Jeelani, “Stab characterization of STF and thermoplastic-impregnated ballistic fabric composites” Kpt. in “Advanced Fibrous Composite Materials for Ballistic Protection”, Ed.: X. Chen, Elsevier, Kidlington, (2016) 363-386Y.S. Lee, E.D. Wetzel, N.J. Wagne, „The ballistic impact characteristics of Kevlar woven fabrics impregnated with a colloidal shear thickening fluid”, J. Mater. Sci. 38 (2004) 2825-2833

IMPROVEMENT OF BIOCOMPOSITE PERFORMANCE UNDER LOW VELOCITY IMPACT TEST- A REVIEW

Usha Kiran Sanivada[1(*)], Aka G.Mármol[2], F. P. Brito[3], Raul Fangueiro[4]

[1,3] Mechanical Engineering and Resource Sustainability Centre (MEtRICS), University of Minho, Guimarães

[2,4] Centre for Textile Science and Technology (2C2T), University of Minho, Guimarães

[3, 4] Department of Mechanical Engineering, University of Minho, Guimarães, Portugal

[(*)] E-mail: ushakiran.sanivada@gmail.com

ABSTRACT

The study of the impact energy and the composite behavior plays a vital role in the efficient design of the composite structures. Among the various categories of impact tests, it is essential to study low velocity impact tests as the damage generated due to these loads is often not visible to the naked eye. The internal damages can reduce the strength of the composites and hence the impact behavior must be addressed clearly specifically for improving its applications in transport industry. The main aim of this paper is to provide a comprehensive review of the work focusing on the assessment of biocomposites performance under low velocity impact, the different deformations and damage mechanisms, as well the ways found to improve the impact resistance.

INTRODUCTION

The composites which are prepared by reinforcing biopolymers with natural fibers are referred to as green composites. Coir, flax, sisal and hemp are examples of natural fibers, while starch, poly-lactic acid (PLA) and PHA are examples of biopolymers used for the preparation of Green Composites. The development of the first green composites date back to the late 1980s. They are not only eco-friendly but also renewable, displaying low weight and good strength. For all these reasons these composites are gathering attention by aerospace and automobile industries. Nevertheless, their limitations such as the moisture absorption, propensity improper interfacial adhesion between matrix and fibre, poor wettability and poor compatibility of natural fibres with hydroscopic matrices hinders its widespread application. However, these limitations are reduced to an extent with the usage of physical and chemical treatments.

Impact strength can be defined as the resistance of the material to with stand maximum impact load with out fracturing or rupturing. The impact properties of the polymeric composites depend upon the toughness of the material. Toughness of the material is the ability to absorb the dynamic impact energy (Ahmad, 2018). The overall toughness of the composites is highly dependent on the matrix and fibre interface, geometry and construction of the composites, testing conditions and the nature of constituent materials. The interfacial properties depend on the type of polymer matrix, functionalization of fibres and methods of fabrication. The natural fibre reinforced composites with good interfacial properties are able to dissipate a large portion of the impact energy through failure modes such as fibre breakage and fibre pull-out. The materials with good toughness can be used in applications such as automotive industry, construction, renewable equipment's (eg windmill blades) and so on (Ahmad, 2018).

RESULTS AND CONCLUSIONS

Table 1 shows the tensile and impact properties that were obtained from the experimental results of various researchers during the last 5 years. It was observed that the few chemical treatments such as alkaline, silane, borax treatments and hybridization techniques are used for the improvement of the tensile and impact properties of the green composites.

Table 1 Tensile and Impact properties of PLA reinforced with different natural fibres

Volume Fraction wt (%)	Fibres	Process	Tensile Strength (MPa)	Impact Energy (J/m)	Additional Informaiton	Ref
5	Sisal	IM	55.35	30.65	UT-CMF	Johari, 2016
5	Sisal	IM	67.22	28.92	NCMF	
5	Sisal	IM	65.46	34.39	GCMF	
5	Sisal	IM	62.33	32.85	CMF with 5 wt % MAH	
55-5	OPEFBF-KCF	CM	35.59	12.29	No treatments	Birinin-Yauri, 2014
55-5	OPEFBF-KCF	CM	30.92	16.12	PLA with MA	
55-5	BR(OPEFBF-KCF)	CM	37.44	16.75	Borax treated	
55-5	BR(OPEFBF-KCF)	CM	47.54	32.53	Borax treated and PLA with MAH	

CM- Compression Molding; CMF- Cellulose Microfibrils; GCMF- Saline treated CMF; IM- Injection Molding; KCF- Kenaf Core Fiber; MA- Maleic Anhydride; PC- Polymer Coated; NCMF- Alkali treated CMF; OPEFBF- Oil Palm Empty Fruit Bunch Fiber; ST-Silane Treated; UT- Untreated; WCF- Waste Cellulose Fibres.

Researchers have used low velocity impact tests such as Izod impact test, Charpy impact test and drop weight test for studying the behavior of the green composites when subjected to impact loading. It is observed that there are different modes of failure such as matrix cracking, debonding, delamination, fibre breakage and fibre pull-out depending on the impact loading. The kinetic energy is absorbed by the plastic deformation and formation of indentation on the surface of the impact. Low velocity impacts occur in the range of 1-10 m/s. It is of importance to study this impact range as it is prone to occur during production or service activities and considered as dangerous for the composite laminates (Safri, 2014).

Clearly there is a need for improving the impact energy of green composites and understanding their behavior when subjected to low velocity impact in automotive and aerospace applications.

REFERENCES

[1] A.-M. Ahmad Y and S. Polat, “Review of the Main Factors Controlling the Fracture Toughness and Impact Strength Properties of Natural Composites,” Mater. Res. Express, vol. 6, no. 2, 2018

[2] A. P. Johari, S. Mohanty, S. K. Kurmvanshi, and S. K. Nayak, “Influence of Different Treated Cellulose Fibers on the Mechanical and Thermal Properties of Poly(lactic acid),” ACS Sustain. Chem. Eng., vol. 4, no. 3, pp. 1619–1629, 2016.

[3] A. U. Birnin-yauri, N. A. Ibrahim, N. Zainuddin, K. Abdan, Y. Y. Then, and B. W. Chieng,
“Effect of maleic anhydride-modified poly(lactic acid) on the properties of its hybrid fiber biocomposites,” Polymers (Basel)., vol. 9, no. 5, pp. 1–16, 2017

[4] S. Safri, M. Sultan, N. Yidris, and F. Mustapha, “Low Velocity and High Velocity Impact Test on Composite Materials–A review,” Int. J. Eng. Sci, pp. 50–60, 2014

INFLUENCE OF FLAME RETARDANT FIBRES ON THE MECHANICAL BEHAVIOUR OF HIGH PERFORMANCE TEXTILE STRUCTURES

Francisca Guedes[1(*)], Cristina Silva[2], Elisabete Silva[3], Dionísio Silveira[3], Raul Fangueiro[1,2]

[1] Department of Mechanical Engineering, University of Minho, Braga, Portugal

[2] Center for Textile Science and Technology (2C2T), University of Minho, Braga, Portugal

[3] Mehler, R. Nova de Segures, Vila Nova de Famalicão, Braga, Portugal

[(*)] E-mail: franciscaguedes@fibrenamics.com

ABSTRACT

The present work intends to compare the mechanical properties of eleven different highperformance textile structures, which are composed of fibrous flame-retardant materials, varying only the materials and percentages of the entrance to the weft. For the correlation analysis between structures were evaluated the tear strength, flexural rigidity and air permeability, with a view to being integrated into fire protection devices. The performed experimental procedures allowed to better understand the performance aspects for the intended application, and to identify significant differences in the mechanical behaviour of the studied flame-retardant fabrics. Thus, regarding the obtained results it was concluded that the samples with the most promising performance are samples FG and B in their composition.

INTRODUCTION

The ignitability has always been considered a major restrain regarding the application of textiles. Indeed, most fibres and fabrics are becoming the subject of several research studies, in order to increase the flame retardancy properties for garment assemblies [1]. Nowadays, the use of flame retardant materials is especially important, since the large volume of electronic equipment, coupled with a higher volume of combustible materials, can increase the potential for fire hazards [2]. In this sense, to promote safety and prevent threats, it is necessary to develop fire-resistant devices able to be implemented in different environments, combining high performance with low weight solutions. In this regard, different innovative strategies, are currently being applied, to enhance fabrics properties to attain fire and smoke barriers [3]. Among several approaches, the combination of synthetic and inorganic fibres proves to be an interesting solution, regarding their mechanical and thermal characteristics [4]. Therefore, in this study, 11 woven samples were designed encompassing flame retardant fibres such as fibreglass (FG), Basalt (B), Trevira® (T), Meta-aramid (MA) and Modacrylic (M), in the weft entrance, maintaining the same weave structure and with the same warp composition (100% FG), in order to assess the feasibility in fire-protection devices, such as fire-retardant curtains.

RESULTS AND CONCLUSIONS

For the characterization of the behaviour of the studied woven fibrous structures, the tests corresponding to the standards ASTM D2261 and ISO 9237:1997 standards were performed. For the analysis of flexural rigidity, it was followed the procedure developed by BS 3356:1961 .The results are then presented in table 1. Air permeability tests allowed to comprise the barrier effect of the structure with respect to the passage of gaseous substances. According to the literature, flame-retardant devices require their matrix composition to have lower air permeability, since it prevents the promotion of the combustion phenomenon. It is possible to observe that the incorporation of M and/or MA increase the air permeability, due to the yarn structure and porosity. In contrast, the entrance of B, have lower air flux through the fabric, mainly due to the tightening of the structure which leads to a decrease of porosity, making it more interesting for the intended purpose. Considering the flexural rigidity tests, it can be verified that the introduction of B to the weft direction (sample 2) increases the rigidity of the fabrics and does not significantly influence the results in the warp direction. Also, the introduction of 50% B combined with other materials to the weft (samples 5, 7

and 8) isn't enough to achieve similar stiffness values, as recorded for sample 2. On the other hand, the introduction of MA in fabrics promotes the flexibility of the substrate, being verified the decrease of flexural rigidity in the weft direction. Flexibility is an important feature, since these materials when used in mobile protection equipment, need to be flexible enough to allow a quick and effective unfold process. Analyzing the tear strength results, it's observed that the variation of the weft material as an impact on the tear behaviour of the structures. Thus, fibrous structures that don't have FG in the weft composition tend to present greater resistance in the warp direction. Corroborating with this claim, Sample 10, reaching approximately 1,2 N(g/m2), showed the best performance in this experiment.

The overall comparative study showed that besides the chosen woven structure, the selection of fibrous materials has a substantial impact on the achieved mechanical and structural properties. Although the high-performance fibres

Table 1 Results of the mechanical and structural characterization essays

Fabrics	Thickness (mm)	Areal weight (g/m^2)	Composition		Air permeability $l/m^2/s$	Flexural rigidity G/mm		Tear strenght N(g/m^2)	
			warp	weft		warp	weft	warp	wef
Sample nº1	0.38	434.96	FV	FV(100%)	42.44±3.6	8725	8724	0.4	0.5
Sample nº2	0.45	504.85	FV	B(100%)	23.32±1.2	8371	41180	0.6	0.4
Sample nº3	0.8	438.84	FV	MA(100%)	79.48±3.2	11565	299	1.0	0.5
Sample nº4	0.51	416.89	FV	T(100%)	55.1±3.1	6499	1953	1.1	0.6
Sample nº5	0.42	467.96	FV	B/ FV(50/50%)	22.36±0.8	7456	4264	0.6	0.5
Sample nº6	0.42	432.06	FV	T/FV(50/50%)	75.98±2.7	6884	3937	0.7	0.5
Sample nº7	0.45	468.44	FV	B/T(50/50%)	44.84±1.5	4091	5358	0.9	0.6
Sample nº8	0.58	472.33	FV	B/MA(50/50%)	137.4±3.0	5490	6889	0.9	0.7
Sample nº9	0.56	439.53	FV	MA/FV(50/50%)	174.2±3.4	7057	2183	1.0	0.7
Samplenº10	0.69	436.78	FV	MA/T(50/50%)	79.8±2.0	5578	80	1.2	0.4
Sample nº11	0.81	426.84	FV	M(100%)	235.8±5.3	12138	203	0.4	0.2

used in this work are commercially available for flame-retardance application, their behaviour varies widely within the same structure, even with the same warp composition. The performed tests showed that samples 2 and 5, are the most promising fibrous structures composition, for the development of fire protective devices.

ACKNOWLEDGEMENTS

The authors would like to express appreciation for the support of Portugal2020 for funding the project POCI-01-0247-FEDER033637," ThermFire4Woven", granted by Fundo Europeu do Desenvolvimento Regional (FEDER), through Programa Operacional Regional do Norte (NORTE 2020).

REFERENCES

[1] R. Kozlowski, B. Mieleniak, and M. Muzyczek, "Fire resistant composites for upholstery," Polym. Degrad. Stab., vol. 64, no. 3, pp. 511–515, Jun. 1999.

[2] S. Gaan, V. Salimova, P. Rupper, A. Ritter, and H. Schmid, Flame retardant functional textiles. Woodhead Publishing Limited, 2011.

[3] G. Song and Y. Lu, "Flame resistant textiles for structural and proximity fire fighting," Handb. Fire Resist. Text., pp. 520–548, 2013.

[4] M. Owais and R. Siddiqui, "Geometrical Modelling and Numerical Analysis of Thermal Behaviour of Textile Structures," 2015.

SIMULATION OF VACUUM ASSISTED RESIN INFUSION (VARI) PROCESS FOR THE PRODUCTION OF A COMPOSITE MATERIAL HULL OF A VESSEL PREPARED TO WORK IN EXPLOSIVE ATMOSPHERES

Joana Malheiro[1(*)], Miguel Vasconcelos[2], Rafael Alves[3], Filipe Duarte[4], Bárbara Marques[5], Carlos Aroeira[6]

[1, 2, 3] Innovation in Polymer Engineering (PIEP), University of Minho, Guimarães, Portugal

[4] SWB – Seismic Workboats, Lda, Peniche, Portugal

[5] AMY – Antartic Module Yard, S.A., Peniche, Portugal

[6] dBwave – Group ISQ, Portugal

[(*)] E-mail: joana.malheiro@piep.pt

ABSTRACT

The aim of the APEX (Combating Pollution in Explosive Atmospheres) project is to create the first worldwide vessel totally prepared to operate efficiently and completely safe in different scenarios of sea pollution combat. To meet all the specifications required, the hull of the vessel is produced with advanced composite materials using an infusion process (VARI), in order to obtain a lighter structure with high resistance, less % of voids and higher % of fibre volume. In this work, the production process of the hull is numerically analysed, using a finite element based software. The numerical simulation of the VARI process implies the modelling of two main phenomena: the resin flow through the laminate (flow in a porous medium) and the chemical reaction of the resin (variation of viscosity and temperature during the cure of the resin). Therefore, both laminate and resin were, first, experimentally characterized, and different resin entry and exit points were defined. Various simulations of the production process were then performed to find the best infusion strategy (ensuring complete impregnation of the laminate in the least time possible). To validate the simulation results, the selected infusion strategy was implemented in the production of a small-scale prototype of the hull. The simulation work revealed that the numerical results are a good reference for the production of the full size hull of the vessel. However, the simulation also shown that the accuracy of the numerical results is highly dependent on the precision of materials experimental characterization.

INTRODUCTION

The significance of numerically simulate the manufacturing process of composite material is increasing, especially in the production of and/or high mechanical performance parts by out-of-autoclave (OOA) processing techniques, such as wind turbine blades, structural components, wings of aircrafts, etc. And this is particularly important in success of the Vacuum Assisted Resin Infusion (VARI) manufacturing process, which is highly dependent upon operator skill and experience (Dereims, 2012). Also, the resin infusion process of continuous fiber reinforced materials is particularly complex to model, but two main phenomena are accounted for: the physical draping of the fabric and the subsequent resin flow through the material (Pierce, 2017).

In this paper, the accuracy of the results obtained by the simulation of Vacuum Assisted Resin Infusion (VARI) manufacturing process of the hull of the APEX vessel is assessed through the production of a small scale prototype. First, the simulation of the infusion of the composite part is described step by step, where the main limitations of the numerical model are pointed out, as well as the considerations and premises necessary to obtain more accurate numerical results. Then, the numerical analysis is used to find the optimized infusion strategy, which will be used to produce the hull prototype. Finally, numerical and experimental results are compared and the accuracy of the

simulation is assed.

RESULTS AND CONCLUSIONS

This study shows that the simulations were in very good agreement with the experimental results. The assumptions and simplifications considered helped to simplify the simulation and decrease the simulation time while ensuring the accuracy of the results in the production of the hull of the boat.

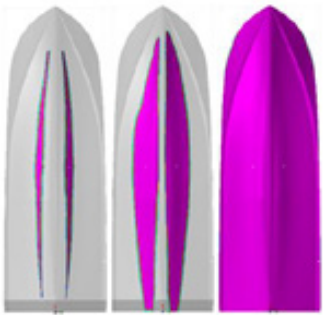

Fig.1 Optimized infusion strategy: resin front advance.

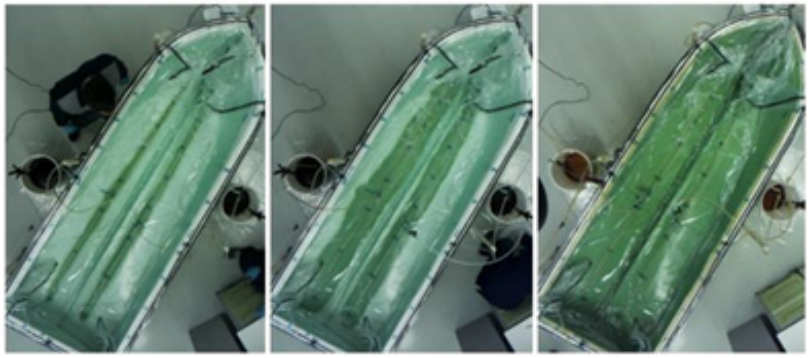

Fig.2 Production of the hull using the optimized infusion strategy.

ACKNOWLEDGMENTS

The authors gratefully acknowledge the funding: Project 18005 – APEX, co-financed by Portugal 2020 and European Union, through the European Regional Development Fund.

REFERENCES

[1] Dereims, A., Troian, R., Drapier, S., Bergheau, J-M, de Luca, P. Simulation of liquid resin infusion process by finite element method. ECCM15-15th, 24-28 June 2012, Venice, Italy (2012).

[2] Pierce, R.S., Falzon, B.G. Simulating Resin Infusion through textile reinforcement materials for the manufacture of complex composite structures. Engineering 3, 596-607 (2017).

NATURAL FIBRES AND MgO NANOPARTICLES: THE ROLE IN ADSORPTION AND DECONTAMINATION OF DMMP

Joana C. Araújo[1(*)], Diana P. Ferreira[1], Raul Fangueiro[1,2]

[1] Centre for Textile Science and Technology (2C2T), University of Minho, 4800 Guimarães, Portugal

[2] Department of Mechanical Engineering, University of Minho, Guimarães, Portugal

[(*)] E-mail: joanaaraujo@det.uminho.pt

ABSTRACT

This work aims to develop a fibrous material, capable of adsorb and degrade dimethyl methylphosphonate (DMMP), based on magnesium oxide (MgO) nanoparticles (NPs) and natural fibres (NF). NF were functionalized with the MgO NPs by a simple and sustainable in-situ method. In order to do this, different reducing agents, reaction and calcination temperatures and reaction times were tested. All the developed systems were characterized by Field Emission Scanning Electron Microscopy (FESEM), Attenuated Total Reflectance-Fourier-Transform Infrared Spectroscopy (ATR-FTIR) and Ground-State Diffuse Reflectance (GSDR). The adsorption and decontamination of DMMP was also evaluated.

INTRODUCTION

In the last years, the development of technologies to protect the human being has grown substantially, due to the increased exposure to several threats, harmful to the public health. Inside this group of hazards, Chemical Warfare Agents (CWAs) have attracted a considerable amount of attention, since they are chemical substances whose toxic properties are used to injure, incapacitate and even to kill not only soldiers, but also civilians. Thus, the protection and decontamination of these agents is one of the most important challenges to governments worldwide (Vu, Ho, & Lee, 2016). Sarin is considered a G-series nerve agent and is an organophosphorus compound that can be lethal, even at very low concentrations. This CWA can kill in few minutes after inhalation. In most cases, the adsorption and degradation of CWA's are tested in compounds that act as simulants of these agents. DMMP is the most used simulant for phosphorous compounds like sarin, due to its similar structure and lower toxicity, when compared with the real agent (Lee et al., 2017). There's one type of NPs that has been gaining attention as an effective material for the adsorption and decomposition of toxic chemicals, the metal oxide NPs. This great capacity is related to their high surface area, large number of reactive edges, high surface-to-volume ratio and reusability. MgO NPs have been one of the most studied metal oxides for the decontamination of toxic chemicals, due to their high absorption capacity and decomposition ability (Vu et al., 2016).Nowadays, there has been an increasing interest in the use of natural fibres (NF), because of their biodegradability, biocompatibility, low-weight, high abundance and low-cost (Costa, Ferreira, Ferreira, Vaz, & Fangueiro, 2018). The functionalization of NF with MgO NPs, due their higher surface area and great properties, can be a great and sustainable alternative for the development of self- decontamination fibrous systems. The main goal of this work is the development of a fibrous material, based on NF and MgO NPs for the adsorption and decontamination of DMMP.

RESULTS AND CONCLUSIONS

The in-situ synthesis of MgO NPs onto jute fabrics surface was performed by the immersion of the pre-treated fabrics in an aqueous solution of Mg(NO2)3 and the posterior addition of the reducing agent. This reaction was made under mechanical stirring, at 50˚C. Several concentrations of the precursor and the reducing agent and different reducing

agents (Sodium hydroxide (NaOH), polyethylene glycol (PEG) and citric acid) were tested in order to optimize the process. At the end, the functionalized fabrics were calcinated at 150 ˚C for 6 hours. In order to compare the behaviour of these NPs with the commercial ones, jute fabrics were impregnated with commercial MgO NPs. The FESEM images of these jute fabrics are shown in Fig.1 It's possible to clearly see the presence of MgO NPs onto the fabrics and it's also possible to observe that the NPs are homogenously distributed. These results were also corroborated ATR-FTIR and GSDR (data not shown in this abstract).

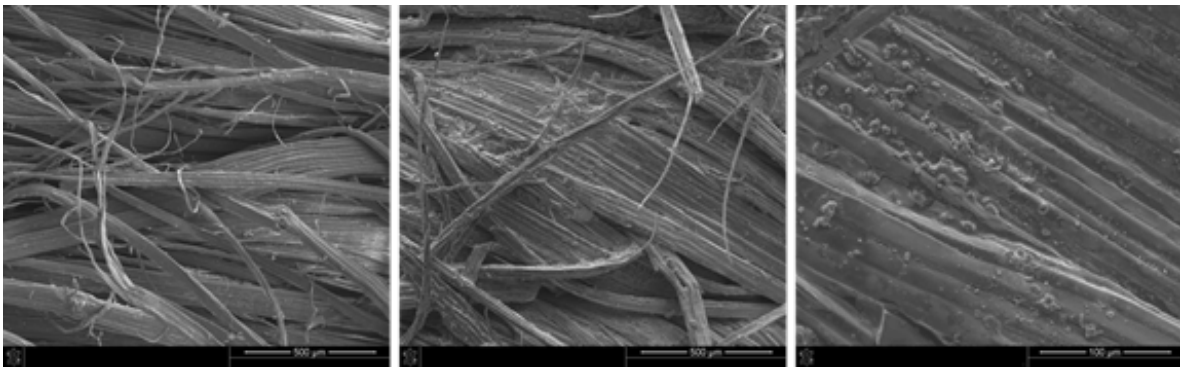

Fig.1 FESEM images of jute fabrics a) without NPs and b), c) impregnated with MgO NPs by in-situ synthesis.

After the successful synthesis, the ability of adsorb and degrade DMMP was evaluated. Several concentrations of DMMP were tested, and the monitorization of the fabrics was made by ATR-FTIR. These preliminary tests indicate promising results in the DMMP adsorption and degradation hability of jute/MgO systems. Thus, this work demonstrates the potential of fibrous systems, based on NF and MgO NPs as self-decontamination materials for noxious chemical compounds.

ACKNOWLEDGMENTS

The authors are thankful to project UID/CTM/00264/2019 of 2C2T – Centro de Ciência e Tecnologia Têxtil, funded by National Founds through FCT/MCTES" and FCT PhD Scholarship (SFRH/BD/147812/2019). Diana Ferreira is also thankful to CEECIND/02803/2017.

REFERENCES

[1] Costa, S. M., Ferreira, D. P., Ferreira, A., Vaz, F., & Fangueiro, R. (2018). Multifunctional Flax Fibres Based on the Combined Effect of Silver and Zinc Oxide (Ag / ZnO) Nanostructures, 1–21.

[2] Lee, J., Member, S., Jeong, S., Kim, D., Park, C., & Jin, B. (2017). Improving DMMP (Salin simulant) Sensing Characteristics of TFQ Functionalized Graphene Chemiresistive Sensors. In IEEE International Conference on Nanotechnology (pp. 675–677).

[3] Vu, A., Ho, K., & Lee, C. (2016). Removal of gaseous sulfur and phosphorus compounds by carbon-coated porous magnesium oxide composites. Chemical Engineering Journal, 283, 1234–1243.

ELECTROSPUN SMART MATERIAL BASED ON BIODEGRADABLE POLYMER AND GRAPHENE NANOPLATELETS FOR MILITARY APPLICATIONS

Paola Francavilla[1], Diana P. Ferreira[1(*)] and Raúl Fangueiro[1,2]

[1] Centre for Textile Science and Technology (2C2T), University of Minho, 4800 Guimarães, Portugal

[2] Department of Mechanical Engineering, University of Minho, Guimarães, Portugal

[(*)] E-mail: diana.ferreira@det.uminho.pt

ABSTRACT

Micro and nanofibres produced by electrospinning are becoming one of the most interesting and advantageous structures for the development of protective textiles, including military protection (Bhardwaj & Kundu, 2010). In this work, poly-e-caprolactone (PCL) electrospun microfibres were functionalized with graphene nanoplatelets (GNPs) in order to produce green textile materials with enhanced conductive properties. GNPs were incorporated in the PCL microfibres. FESEM images demonstrated that the GNPs were successfully incorporated. The electrical conductivity behaviour was excellent, showing a semiconductor performance.

INTRODUCTION

In terms of security, not only for direct users but also for the whole community, today there are countless chemical agents classified as dangerous that can be dispersed in the environment, due to terrorist attacks, industrial accidents, chemical incidents, mishandling of materials, among other issues (Calder, 2018).

Taking into account the imminent global need to develop new devices that ensure human health, and considering their remarkable characteristics, such as high surface area, flexibility, lightweight, optimized breathability and capability to adapt in diverse shapes (Ferreira, 2018), micro and nanofibers produced by electrospinning, turn one of the most interesting and advantageous structures for the development of protective textiles, including personal protective equipment (PPE) for military protection (Bhardwaj & Kundu, 2010). Also in alignment with the technology trends, the addition of carbon-based nanomaterials, graphene nanoplatelets (GNPs), for instance, in electrospun membranes make it possible to obtain enhanced micro/nanofibres with high conductive properties and piezo-resistive behaviour. Incorporating these membranes into PPE can allow the development of military application systems, with innovative functionalities as improved monitoring and sensitivity to contaminants, better filtering capabilities, enhanced response to electromagnetic stimuli, between others (Bellucci, 2018)(Vaseashta, 2018).

In this work, several formulations of PCL with GNPs were produced by electrospinning. Also, the technique parameters, such as flow rate, collector speed, supplied electric voltage, the distance between nozzle and collector, between others, were studied, in order to obtain the most homogeneous fibres, in terms of morphology, diameter and alignment. Field Emission Scanning Electron Microscopy (FESEM) technique was used to observe the correct GNPs incorporation into the microfibres. The two-points probe method was performed for the electrical conductivity measurement. The developed systems presented high electrical conductivity, giving the membranes semiconductor characteristics.

RESULTS AND CONCLUSIONS

PCL-GNPs microfibers were successfully produced using different GNPs percentages. The FESEM images presented in Figure 1 a) to d) show the influence of different GNPs % under use on the size and uniformity of the microfiber membranes. Without GNPs, more homogeneous micrometer dimensions of the fibers were obtained. However, the

presence of the nanoplatelets inside the fibers lead to fibers with more heterogeneous diameters as can be observed in Figure 1 from e) to h) FESEM images exhibited the different fibers morphology obtained using different amounts of GNPs. In all cases the graphene nanoplatelets were completely inside the PCL fibers showing the successful optimization of the electrospinning parameters for graphene microfibers production. Electrical conductivity of the obtained membranes was analyzed, and the results are very promising: 7 S/m for unwashed samples and 0.1 S/m for samples after washing cycles.

Further studies will be performed in order to characterize and determine the better system for military protection, especially for chemical and biological degradation.

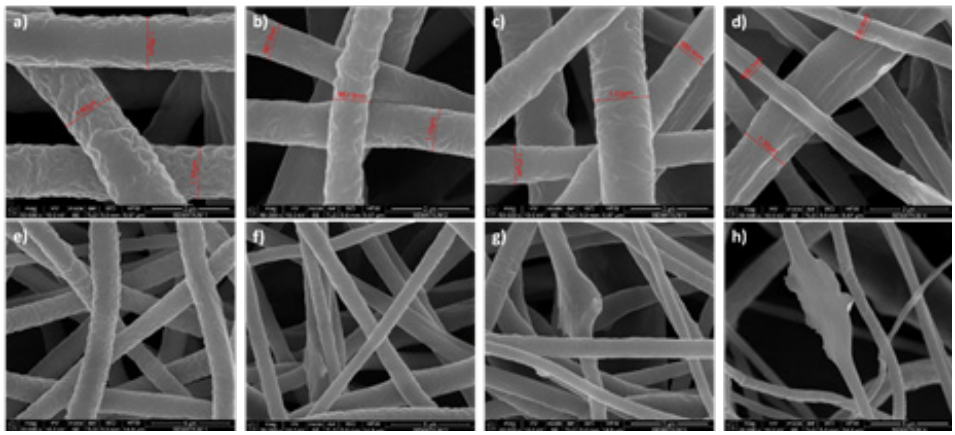

Fig.1. a), e) PCL; b), f) 0.2% GNPs microfibres; c), g) 1% GNPs microfibres; d), h) 5% GNPs microfibres with different magnifications: a) to d) 5 mm and e) to h) 2 mm.

ACKNOWLEDGEMENTS

The authors are thankful to TSSiPRO project, UID/CTM/00264/2019 of 2C2T – Centro de Ciência e Tecnologia Têxtil, funded by National Funds through FCT/MCTES and CEECIND/02803/2017.

REFERENCES

[1] Bellucci, S. (2018). Development of biosensors using carbon nanotubes and few layered graphene. NATO Science for Peace and Security Series A: Chemistry and Biology, 19–29.

[2] Bhardwaj, N., & Kundu, S. C. (2010). Electrospinning: A fascinating fibre fabrication technique. Biotechnology Advances, 28(3), 325–347.

[3] Calder, A., & Bland, S. (2018). CBRN considerations in a major incident. Surgery (Oxford), 36(8), 417–423.

Ferreira, D. P., Ferreira, A., & Fangueiro, R. (2018). Searching for Natural Conductive Fibrous Structures via a Green Sustainable Approach Based on Jute Fibers and Silver Nanoparticles. Polymers, 10(1).

[4] Vaseashta, A. (2018). Loaded electrospun nanofibers: Chemical and biological defense. NATO Science for Peace and Security Series A: Chemistry and Biology, 31–45.

UV PROTECTION PERFORMANCE OF ELECTROSPUN FIBERS FUNCTIONALIZED WITH TiO2 AND ZnO NANOPARTICLES

Vânia Pais[1,2(*)], Miguel Navarro[1,2], Pedro Silva[1,2], Catarina Guise[3], Rui Martins[3], Raul Fangueiro[1,2,4]

[1] Fibrenamics, University of Minho, Guimarães, Portugal

[2] Centre for Textile Science and Technology (2C2T), University of Minho, Guimarães, Portugal

[3] Inovafil Fiação S.A, S. Cosme do Vale, Portugal

[4] Department of Mechanical Engineering, University of Minho, Guimarães, Portugal

[(*)] E-mail: vaniapais@fibrenamics.com

ABSTRACT

In the current work, fibrous structures based on biodegradable polymer ε-caprolactone (PCL) functionalized with zinc oxide (ZnO) and titanium dioxide (TiO2) nanoparticles (NPs) were produced by electrospinning, to achieve materials with ultraviolet (UV) protection properties. These nanofiber-based webs were produced either with ZnO or TiO2 NPs in different concentrations, as well with different densities, in order to study their influence in the UV protection properties. The webs were evaluated in terms of UV protection through the measurement of transmittance values with a spectrophotometer UV/Vis, followed by the calculation of the UVA transmission and ultraviolet protection factor (UPF) values. A set of nanofiber webs has shown UV protection capability, namely those with nanofibers functionalized with TiO2, that presented lower UVA transmission and higher UPF values. In opposition, the nanofibers produced without NPs, didn't reveal UV protection properties, highlighting the potential of ZnO and TiO2 NPs in this field.

INTRODUCTION

UV radiation is responsible for several impairs in human health, ranging from simple skin burns to aggressive skin cancers. The use of UV protective equipment is crucial for outdoor workers, so they can be exposed to UV radiation for an extended period of time without the risk of skin cancer development [1]. In terms of UV protection, according to EN 13758, a material has excellent UV protection properties, if the average UVA transmission is lower than 5% and the UPF value is higher than 40 [2], [3].

To enhance the protective behaviour against UV radiation, UV protective materials should be addressed to the equipment. ZnO and TiO2 NPs are two suitable solutions to be considered for UV protection considering their performance as UV blockers. ZnO and TiO2 NPs have a large band gap between their low-energy valence band and high-energy conduction band. Therefore, when exposed to light, the energy of the photons is absorbed by electrons and they cross the band gap causing the production of holes and pair of electrons. This behavior allows TiO2 and ZnO NPs to have two unique abilities: UV protection and to act as a catalyzer [4] Furthermore, the performance of NPs is enhanced when compared to their related materials in bigger scales, due to their large surface area/volume ratio and high reactivity. Other studies have been studied for the same purpose like the one conducted by Dadvar et al. to develop a mat by sol-gel process with 0,8%TiO2 which, in terms of UV protection, was categorized as excellent [5].

Nowadays, the electrospinning technique is being widely explored in order to produce nanofiber webs, that can be easily functionalized with NPs. It's a simple technique that by the manipulation of several parameters – applied voltage, type of collector, flow rate and type of polymer – allows the production of ultrafine fibers [1]. Additionally, as observed earlier, the presence of NPs provides specific functionality to the electrospun fibers.

In this research, a set of nanofiber webs was produced by electrospinning technique with an applied voltage of 25 kV, 20 w/v% PCL and tip-to-collector distance equal to 240 mm. The influence of different parameters were studied

(type of NPs - ZnO or TiO2; nanoparticle's concentration - 0,1%; 0,5%; 1% and 2% w/v; flow rate - 2; 3,5 and 5 mL/h; deposition time - 5, 10 or 15 minutes) for their influence on the UV protection effect. including UPF value and the average UVA and UVB.

RESULTS AND CONCLUSIONS

From the results obtained, it was verified that 8 samples match the requirements established in EN 13758-2, allowing to establish the optimum experimental conditions required to have UV protective characteristics. Figure 1 shows the samples presenting the best UV protection capability and the ones obtained without NPs. Also, it's important to underline that, when the same conditions were tested in samples without NPs, the UPF and UVA values obtained weren't categorized as excellent to the UV protection.

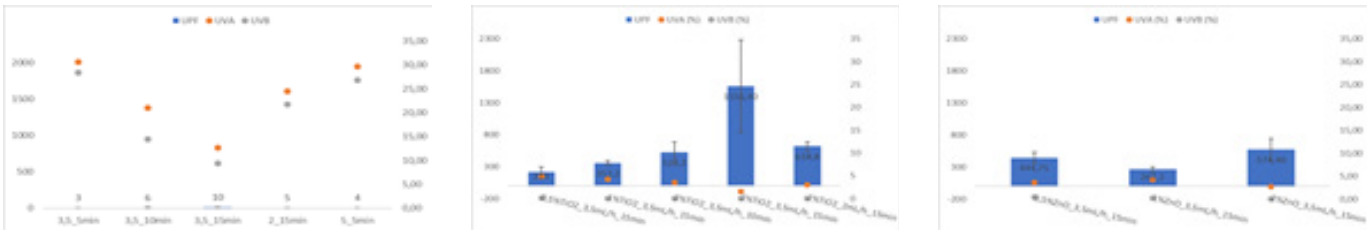

Fig.1- UPF, UVA% and UVB% values corresponding to the nanofiber web which values are in accordance with the ones defined on the standard EN 13758 and to the nanofibers produced without NPs.

From these results, it is possible to conclude that a higher number of samples functionalized with TiO2 NPs exhibit values in accordance with the standard as excellent when compared with the samples functionalized with ZnO NPs. This is probably because TiO2 NPs present higher refractive index than ZnO NPs [4]. In addition, the highest UPF value and lower average UVA was obtained with a specimen functionalized with TiO2 NPs (2%TiO2_3,5mL/h_15min). Furthermore, for both NPs tested, the best results were always obtained for the samples produced on electrospinning with higher web area densities. Lastly, it was observed that with the presence and increase of NPs concentration, an improvement in UPF values have been noticed.

With this study, electrospun fibers with excellent UV protection properties were obtained, mainly those functionalized with TiO2 NPs, observed either by the bigger number of samples in accordance with EN 13758, either for the UPF and UVA values obtained.

ACKNOWLEDGEMENTS

The authors are thankful to Portugal2020 for funding the project 23958," TECHNICAL STAPLE CELLULOSIC YARN", granted by Fundo Europeu do Desenvolvimento Regional, through Compete 2020.

REFERENCES

[1] S. Lee, "Developing UV-protective textiles based on electrospun zinc oxide nanocomposite fibers," Fibers Polym., vol. 10, no. 3, pp. 295–301, 2009.

[2] E. Standard, "Textiles - Solar UV protective properties - Part 1: Method of test for apparel fabrics, EN 13758," 2001.

[3] E. Standard, "Textiles - Solar UV protective properties - Part 2: Classification and marking of apparel Textiles, EN 13758-2," 2006.

[4] H. Yang, S. Zhu, and N. Pan, "Studying the mechanisms of titanium dioxide as ultraviolet-blocking additive for films and fabrics by an improved scheme," J. Appl. Polym. Sci., vol. 92, no. 5, pp. 3201–3210, 2004.

[5] S. Dadvar, H. Tavanai, H. Dadvar, M. Morshed, and F. E. Ghodsi, "UV-protection and photocatalytic properties of electrospun polyacrylonitrile nanofibrous mats coated with TiO2 nanofilm via sol-gel," J. Sol-Gel Sci. Technol., vol. 59, no. 2, pp. 269–275, 2011.

NANOSTRUCTURED ELECTRODES-BASED KILOHERTZ ELECTROCHEMICAL CAPACITORS FOR AC FILTERING AND PULSE ENERGY STORAGE

Sakibul Azam, Wenyue Li, Nazifah Islam, Zhaoyang Fan(*)
Department of Electrical & Computer Engineering, Nano Tech Center, Texas Tech University, Lubbock, Texas
(*) E-mail: Zhaoyang.Fan@ttu.edu

ABSTRACT

Kilohertz frequency electrochemical capacitors (KF-ECs), with a compact size, are being pursued for ripple current filtering, pulse power storage and other applications. We report crosslinked carbon nanofiber aerogel (CCNA), derived from bacterial cellulose (BC), and edge oriented vertical graphene network (EOG), deposited on carbonized metal organic framework (MOF), as electrodes for KF-EC studies. The fabricated ECs exhibit very low equivalent series resistance and very attractive cell performance such as capacitance of 1.02 mF cm-2 and phase angle of -85.9o or 2.34 mF cm-2 and -80.6o at 120 Hz, which are the best reported overall performances thus far. We further demonstrate their applications in ripple current filtering for AC/DC conversion and rapid pulse energy storage for vibrational energy harvesting. The promising results suggest KF-ECs have great potential in substitution of the bulky aluminum electrolytic capacitors (AECs) for several crucial applications.

INTRODUCTION

The key to develop high-performance KF-ECs lies at a tailored electrode structure that has a trivial resistivity, and a straightforward porous structure that offers a reasonable large surface area while allowing rapid electrical double layer formation. In our studies, two carbon nanostructures, CCNA-based and EOG-based were investigated. Crosslinked BC aerogel, derived from freeze-dried as-grown BC hydrogel, was rapidly pyrolyzed in a high-temperature (~ 1200oC) plasma for only 15 minutes to obtain the freestanding CCNA mat. Prussian blue (PB) MOF cubes as a precursor was pyrolyzed into a 3D conductive porous network as the substrate for EOG deposition. In a rapid (< 7 minutes) plasma-enhanced chemical vapor deposition process, the PB cube layer coated on a current collector was converted into Fe3C-nanoparticle/carbon-based core/shell cubes that were further covered by EOG nanosheets. A seamless interface between the current collector and these active materials was simultaneously formed.

Symmetrical cells using the above electrodes were assembled with 6 M KOH as the electrolyte. Their electrochemical performance was characterized. For ripple current filtering demonstration, KF-ECs was applied as the filtering capacitor in a full-wave AC/DC converter with different ac signals as the input. For environmental pulse energy harvest testing, a piezoelectric element was used to generate a pulsed signal from external mechanical noises. Here we used hand finger tapping to simulate the environmental pulse energy.

RESULTS AND CONCLUSIONS

For CCNA electrode, it was found that the rapid plasma pyrolysis is the crucial process to ensure that a high conductivity is achieved while micropores, which are generated in a conventional thermal pyrolysis process but detrimental to the frequency response, are avoided.

As plotted in Fig. 1(a), CCNA-based ECs from three different electrode thickness, all exhibited excellent performances in terms of the characteristic frequency (f0) when the phase reaches − 45o, the cell areal capacitance density at 120 Hz (CA120), and the absolute phase angle at 120 Hz (− Φ). 3D EOG grown around PB derived conducting scaffold have straightforward pore structure, offering a high specific surface area but easily accessed pores by electrolyte

ions. The well-connected components in the electrode warrantee a low electrode resistance. The fabricated ECs based on EOG electrodes delivered outstanding performance, as plotted in Fig. 1(a).

The ripple filtering capability of our KF-ECs was demonstrated. Fig. 1(b) shows the output voltages on a load of 470 Ω to 1 MΩ after rectification by a full-wave bridge and ripple filtering by our KF-ECs, where a 60 Hz sine signal was applied as the input. Fig. 1(c) is the result when a simulated electro-cardio wave was used as the input. The circuit in Fig 1(d) was used for environmental noise energy harvesting, where the irregular pulse voltage generated by the piezoelectric element under hand finger tapping (Vi) was rectified and stored in the KF-EC (Vo) to power a micropower load continuously or a LED in a pulse mode.

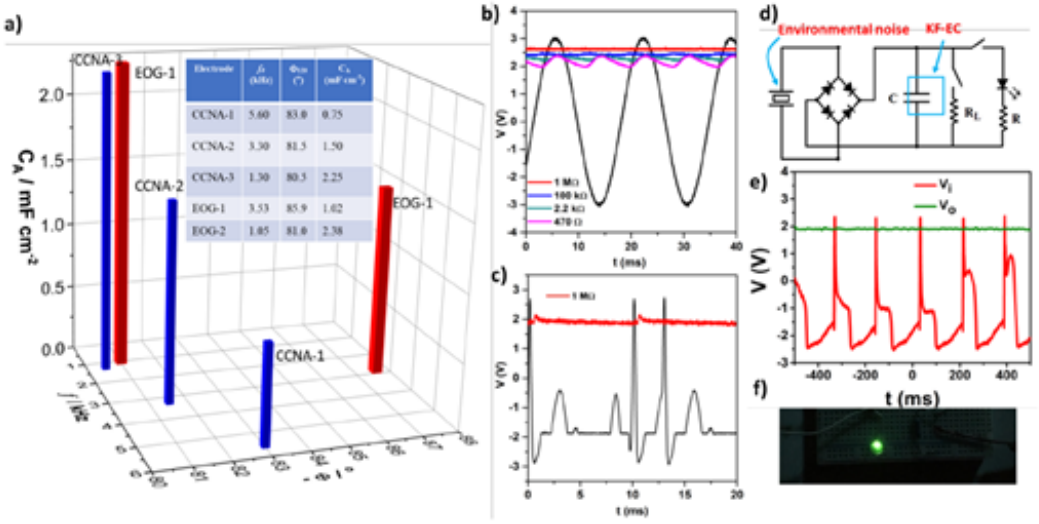

Fig.1 (a) The demonstrated performance of KF-ECs. (b) The output voltage from the AC/DC converter for 60 Hz input sine wave. (c) The output voltage for a simulated electro-cardio wave as the input. (d) the circuit diagram for noise energy harvesting. (e) The input and output when powering a micropower load. (f) the photo showing the harvested energy to power a LED in the pulse mode.

ACKNOWLEDGMENTS

The authors gratefully acknowledge the funding by National Science Foundation (1611060).

REFERENCES

[1] Fan Z, Islam N, Bayne S. Towards kilohertz electrochemical capacitors for filtering and pulse energy harvesting. Nano Energy, 2017, 39, p. 306-320.

[2] Islam N, Li S, Ren G, Zu Y, Warzywoda J, Wang S, Fan Z. High-frequency electrochemical capacitors based on plasma pyrolyzed bacterial cellulose aerogel for current ripple filtering and pulse energy storage. Nano energy, 2017, 40, p. 107-114.

[3] Li W, Azam S, Dai G, Fan Z. Prussian Blue Based Vertical Graphene 3D Structures for High Frequency Electrochemical Capacitors. Submitted.

HARD CHROME REPLACEMENT WITH CIRRUS DOPED ELECTROLESS NICKEL COATINGS

See Leng Tay[1(*)], Pratik Jadhav[2], Annie Wang[3], and Chris Gooode[4]

[1, 2, 4] Cirrus Materials Science, Auckland, New Zealand

[3] Department of Chemicals and Materials Engineering, University of Auckland, Auckland, New Zealand

[(*)] E-mail: seeleng.tay@cirrusmaterials.com

ABSTRACT

The intrinsic hardness, high abrasive wear resistance, and corrosion properties of hard chrome coatings have resulted in their wide industry application. However, chrome plating involves hazards associated with chrome 6+ which affects human health and is driving the need to identify viable alternatives. In this research, alumina Cirrus doped electroless Ni-P was studied to investigate the performance of coatings as a potential candidate to replacement for hard chrome. Characterization was performed to investigate the effect of incorporation of alumina Cirrus Dopant™. Results showed that Al-doped electroless nickel possessed a hardness minimum of 850HV0.1, high corrosion resistance, and excellent abrasive wear resistance, with a Taber Wear Index of 2.25mg/1000 cycles. These attributes may make Cirrus Dopant™ for electroless nickel an outstanding candidate to replace hard chrome coatings in many applications.

INTRODUCTION

Hard chrome coatings have been specified for the protection of high strength steel substrates for a variety of applications such as aircraft landing gear, hydraulic rams, gas turbine engines, propeller hubs, etc. However, due to both environmental and health concerns, Registration, Evaluation, Authorization and Restriction of Chemicals (REACh) in the Europe and the Environmental Protection Agency (EPA) and Occupational Safety and Health Administration (OSHA) in the USA has banned to use hexavalent chrome. A suitable replacement for hard chrome has not so far been identified for many applications. Nickel and Cobalt alloy coatings have been long identified as possible substitute materials, but each suffers shortcomings especially in abrasive wear performance.

Incorporation of a variety of hard particles into plating baths, including Cr3C2, SiC, Al2O3 and nano-diamond to create composite coatings has enabled nano-composite coatings to achieve the desired hardness, and abrasive wear resistance. Unfortunately, to achieve the required results very high particle densities have been required, creating sediment in the bath and limiting the practicality of these composites as an industrial process. This problem could be overcome by using a stable aqueous suspension of appropriate nano-particles. Cirrus Dopant is such an aqueous dopant comprising a nano-structured precursor material that creates in-situ nanoparticles during the plating process. In contrast to hard particle methods, incorporation of Cirrus Dopant™ does not create any sedimentation in the bath solution, and nanoparticles will codeposit uniformly into the nickel or cobalt surface.

In this research, an alumina dopant was introduced into low phosphorous electroless nickel (LPEN) coating to study the performance of composite coating prepared using Cirrus DopantTM. Electroless plating is an autocatalytic coating process, which is based on chemical reaction between the plating solution and the substrate.

RESULTS AND CONCLUSIONS

Fig. 1 compares the microhardness and Taber wear index measurements for both undoped and doped electroless nickel coatings. The incorporation an Al-dopant in the LPEN bath increased coating hardness from 597 to 862 HV. This hardness is much greater than that of common hard chrome, about 600HV [1], and increased with heat treatment unlike hard chrome.

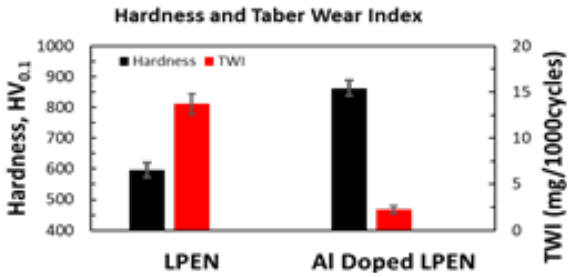

Fig. 1: Comparison of hardness of LPEN and Al Doped LPEN.

The Taber Wear Index (TWI) of doped LPEN was 2.25 mg/1000 cycles, which is lower than the reference hard-chrome coating where the TWI is about 3-4 mg/1000 cycles [2]. The measured TWI of doped LPEN directly results from the reported hardness improvements and is in line with sliding wear test results where the coefficient of friction of doped LPEN about 0.3. According to Archard's law, TWI generally decreases with increasing hardness [3].
Fig. 2 shows the comparative Tafel plots of three coatings. Data derived from these curves was used to calculate, the corrosion potential, the corrosion current density and the corrosion rate. Incorporating dopant improved the corrosion rate to 0.0243 mm/year, a 16% improvement.

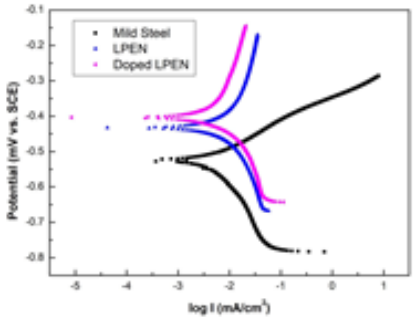

Fig. 2: Polarization curves of LPEN, LPEN doped Al coating and mild steel substrate.

The Cirrus research demonstrated that Al doped low phosphorous electroless nickel coatings can achieve hardness and Taber wear resistance equivalent to hard chrome. Furthermore, the electroless deposition process limited hydrogen evolution from the plating surface making high strength steel coated parts much less susceptible to hydrogen embrittlement. Finally, doped LPEN created a compact coating with low porosity which provide excellent corrosion resistance.

ACKNOWLEDGMENTS

The authors gratefully acknowledge the Ijya Srivastava and Jon McCrea for helping us to carry out Taber wear testing.

REFERENCES

[1] Lausmann G A, Electrolytically deposited hard chrome. Surface and Coatings Technology, 1996,86-87, p.814-820.
[2] Klingenberg M L, Brooman E W and Naguy T A, Nano-particle composite plating as an alternative to hard chromium and nickel coatings. Plating & Surface Finishing, 2005, p.42-48.
[3] McCrea J L, Palumbo G, Hibbard G D and Erb U, Properties and applications for electrodeposited nanocrystalline Fe-Ni alloys. Reviews on Advanced Materials Science, 2003,5, p.252-258.

INFLUENCE OF CHEMICAL AND MECHANICAL PROPERTIES OF POLYUREAS IN THE BLAST PROTECTION

C. Mota(*), [1], F. Leite1, J. Bessa[1] , F. Cunha[1] , G.J. Gomes[3,4,5] , J.L. Mingote[3], R. Fangueiro[1,2]

[1] Centre for Textile Science and Technology (2C2T), University of Minho, Guimarães, Portugal

[2] Department of Mechanical Engineering, University of Minho, Guimarães, Portugal

[3] NATO Counter IED Centre of Excellence (Hoyo de Manzanares-Madrid).C-IED COE.

[4] Centro de Investigação e Desenvolvimento do Instituto Universitário Militar. Lisboa (Portugal)

[5] PhD Student at Faculdade de Ciências e Tecnologia da Universidade Nova de Lisboa, Portugal.

(*) E-mail:cmota@tecminho.uminho.pt

ABSTRACT

This work compares two polyureas used in blast mitigation through a chemical and mechanical characterization, by FTIR and tensile tests, respectively. The FTIR test performed allowed to identify some differences regarding the content of hard domains of the polyureas. The tensile tests carried out allowed to analyse the influence of the content of hard domains of the polyureas on its mechanical properties. In this sense, it was verified an increase of 29% in the Young's Modulus of the polyurea with higher content comparatively to the other polyurea. In spite of the different mechanical properties presented both polyureas are very suitable for use on blast mitigation structures.

INTRODUCTION

Elastomeric coatings are being often referred as excellent materials for strategic applications, particularly for blast mitigation, in order to minimize the damage caused by the blast in the underlying structure of buildings, as well as in the ballistic protection [1]. Polyurea, an elastomer formed by the reaction of isocyanate and amine, possesses hard domains dispersed randomly within the soft domains. The hard domains are formed by hydrogen bonded to urea polar linkages (–NH–CO–NH–) and possibly -stacking of aromatic fractions, if the polyurea is prepared using aromatic diisocyanates. The soft domains consist of well-mixed hard and soft long chain aliphatic chains. The blast mitigation and ballistic protection ability of a polyurea is decided by the hard and soft domains fractions of the elastomer. The polymer needs to be tuned for a particular application through meticulous choice of the raw materials [2]. The content of the hard segment of a polyurea in combination with the degree of phase separation (hard and soft phases) determines the mechanical properties of a polyurea system [3]. In this study, two polyureas coatings commercially available on the market, that are used to blast protection, have been studied in order to understand what are the characteristics that give them this capacity. For this purpose, chemical and mechanical tests were carried out, by FTIR and tensile tests, respectively. The FTIR tests for the polyurea samples were carried out performing 60 scans with 16 cm-1 resolution to obtain IR spectra (4000 - 400 cm-1). The tensile tests were conducted on a universal testing machine, according to the ISO 527 standard, in which 5 specimens of each polyureas samples were tested with a crosshead speed of 5 mm/min and with a gauge length of 110 mm.

RESULTS AND CONCLUSIONS

The results from the FTIR tests presented in Fig. 1 show that the polyurea PX (B) presents a higher reflectance (0.138) than the polyurea PW (A) (0.120) in the absorption band at around 1680 cm-1. This absorption band indicates the hydrogen bonding formed by one C=O with two nearby N-H in urea group, typically called as "ordered" bonding, which forms the hard phase (–NH–CO–NH–) of the polyureas. Table 1 shows the results for the tensile test made on the polyureas.

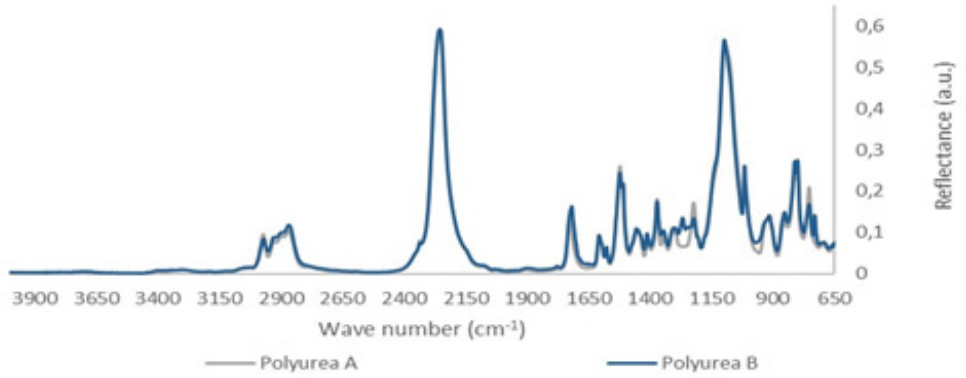

Fig.1 FTIR test results.

Table 1 Tensile test results.

Polyurea	Maximum Stress (MPa)	Maximum Strain (%)	Young Modulus (GPa)
PW (A)	14,51 ± 0,62	258 ± 0,10	0,14 ± 0,01
PX (B)	14,68 ± 0,58	228 ± 0,25	0,18 ± 0,01

This study shows that the presence of higher content of hard domains in the polyurea PX led to an increase of the mechanical properties of this polyurea comparatively to the polyurea PW, namely around 29% on the Young's Modulus. While we can see that exists some differences regarding the mechanical properties of both polyureas, it can be concluded that both products are very suitable for use on blast mitigation structures.

ACKNOWLEDGMENTS

The authors gratefully acknowledge the funding under the NATO Defense Against Terrorism Program of Work and NATO Counter IED COE.

REFERENCES

[1] Szafran J, Matusiak A. Polyurea coating systems: definition, research, applications. XXII LIGHTWEIGHT STRUCTURES in CIVIL ENGINEERING (LSCE), Olsztyn, 2016.

[2] Iqbal N, Tripathi M, Parthasarathy S, Kumar D, Roy PK. Polyurea coatings for enhanced blastmitigation: a review. RSC Adv., 2016, 6, p. 109706–109717.

[3] Zhou Q, Cao L, Li Q, Yao Y, Ouyang Z, Su Z, Chen X. Investigation of the Curing Process of Spray Polyurea Elastomer by FTIR, DSC, and DMA. Journal of Applied Polymer Science, 2012, 125, p. 3695-3701.

TEXTILE CAMOUFLAGE PROPERTIES IMPROVEMENT BY IMPREGNATION WITH SYSTEM PVB/IF-WS2

Aleksandra Samolov[1], Danica Simić[1(*)], Bojana Fidanovski[1]
[1] Military Technical Institute, Ratka Resanovica 1, 11000 Belgrade, SERBIA
[(*)] E-mail: simic_danica@yahoo.com, aleksandrasamolov@yahoo.com

ABSTRACT
Textile material with camouflage print was impregnated with system PVB/IF-WS2 in order to enhance its resistance to wetting, abrasion, and mechanical resistance. Besides the reinforcing effect and wear protection, fullerene-like nanoparticles of tungsten disulfide, IF-WS2, have a positive effect on spectrophotometric characteristics. FTIR excluded any possible chemical interaction of IF-WS2, PVB, and the fabric. Spectrophotometric properties were observed to evaluate the camouflage behavior, as well as specular gloss. Diffuse reflection was measured on UV VIS NIR spectrophotometer and color coordinates were determined on black, brown, and dark green shades on the examined fabric samples.

INTRODUCTION
Textile materials are being colored in different camouflage prints for the needs of armed forces and other security units. Besides the camouflage function, it is often important to enhance fabrics resistance to wetting, abrasion and its mechanical resistance generally. Different polymers are used as impregnation of fabrics for this reason, and nowadays, nanotechnologies play important role in enhancing the textile materials for various purposes. Within this research a new method of camouflage textile impregnation has been examined, with a polymer and nanostructures that was earlier proven to be beneficial in aspects of decreasing erosive wear, increasing mechanical resistance and enhancing camouflage properties [1-3]. Poly(vinyl butyral), PVB was chosen as a tough, ductile polymer which does not dissolve in water, i.e. resistant to wetting. Fullerene-like nanoparticles of tungsten disulfide,IF-WS2, were used as a nanoreinforcement due to their mechanical resistance and solid lubricating behavior [3, 4]. Also, in earlier research, a positive effect on spectrophotometric characteristics of military camouflage paints was shown[5, 6]. As a base material, cotton fabric was used, intended for protective clothing and other items that need to be camouflaged.
Cotton fabric with camouflage print was impregnated with solution of PVB with and without nanoparticles of IF-WS2. Automatic applicator was used to apply the impregnation evenly onto the fabric surface. Concentration of IF-WS2 was 2 wt.% regarding the mass of PVB. After solvent evaporation the fabric samples were analyzed regarding the effect of the added nanostructures on impregnated material properties. FTIR analysis was performed in order to examine any possible chemical interaction of IF-WS2, PVB and the fabric. Spectrophotometric properties were observed to evaluate the camouflage behavior. Specular gloss at angle 85°, which is important for fabric materials in field of military camouflage, was measured. Diffuse reflection was measured on UV VIS NIR spectrophotometer and color coordinates were determined as well on black, brown and dark green shades.

RESULTS AND CONCLUSIONS
FTIR analysis confirmed the chemical inertness of IF-WS2/PVB in contact with the fabric. The results show that impregnation did not affect camouflage behaviour of the fabric. However the significant drop in value of the diffuse reflection of the dark green shade was observed. The most distinctive difference in colour shade to the observer's eye was observed for the same shade when the colour coordinates were determined and compared. Specular gloss, on the other hand, did not change. This means that PVB/IF-WS2 could be used for the improvement of fabrics resistance to wetting and mechanical resistance, not disturbing the camouflage protection.

ACKNOWLEDGMENTS

The authors acknowledge the support of Ministry of Education, Science and Technological Development of the Republic of Serbia, research grant No. 451-03-68/2020-14/200325, as well as COST Action CERTBOND (CA18120) and COST Action CONTEXT (CA17107).

REFERENCES

[1] D.Simić, D.B. Stojanović, A.Kojović, M.Dimić, Lj.Totovski, P.S. Uskoković, R.Aleksić, Inorganic fullerene-like IF-WS2/PVB nanocomposites of improved thermo-mechanical and tribological properties, Materials Chemistry and Physics 184 (2016) 335-344, doi: 10.1016/j.matchemphys.2016.09.060

[2] D. S. Lazić, D. M. Simić, A. D. Samolov, D. Jovanović, Properties of standard polymeric and water-based coatings for military camouflage protection with addition of inorganic fulerene-like tungsten disulphide (IF-WS2) nanoparticles, Scientific Technical Review, 2017, Vol. 67, No.1,pp.38-44.

[3] N. Rezgui, D. Simić, C. Boulahbal, D. Micković. Fullerene-like nanoparticles of WS2 as a promising protection from ero-sive wear of gun bore nozzles. Nanoscience, 16, 2020, 1-9.DOI : 10.2174/1573413715666181217115448 Current

[4] D. M. Simić, D. B. Stojanović, V. Obradović, M. Zrilić, P. S. Uskoković, R. Aleksić. Stab resistance of p-aramid fabric protective composites reinforced with nanostructures of tungsten disulfide, AUTEX2019 – 19th World Textile Conference on Textiles at the Crossroads, 11-15 June 2019, Ghent, Belgium, 0378, ISBN 9789079892068

[5] A. Samolov, D. Simić, Lj. Totovski, Spectrophotometric properties of PVB/WS2 thin films, 8th International Scientific Conference on Defensive Technologies OTEH 2018, Belgrade, 11-12 October 2018. Proceedings, ISBN 978-8681123-88-1, pp. 416-420.

[6] D. Lazić, D. Simić, A. Samolov, Effect of nano-IF-WS2 and INT-WS2 on physical-mechanical and camouflage proper-ties of military coatings, Book of Abstracts / COST MP1402 Scientific Workshop "ALD and related ultra-thin film processes for advanced devices", 29-30 August, 2017, Belgrade, p. 30, ISBN 978-86-81405-22-2.

PRE-CORROSION EFFECTS ON THE ULTRASONIC FATIGUE ENDURANCE OF INCONEL 718 AND CRACK PROPAGATION

Gonzalo Mariano Domínguez Almaraz [1(*)], Alexiane Dominguez [2], Manuel Guzmán Tapia [1]

[1] Posgrado en Ciencias en Ingeniería Mecánica U. M. S. N. H. Av. Francisco J. Múgica S/N C. P. 58140, Morelia, Michoacán, México

[2] Université Paris-Sud 11, URF Sciences et Techniques, BCST: Biologie Chimie Sciences de la Terre, 15 Rue Georges Clemenceau, 91400 Orsay, France.

(*) E-mail: dalmaraz@umich.mx

ABSTRACT

Ultrasonic fatigue endurance of Inconel 718 (I-718) has been investigated for the base material and specimens with pre-corrosion. Specimens of base material and with pre-corrosion were tested under ultrasonic loading at room temperature and R = -1, revealing a factor of 10 on fatigue endurance advantaged for the first ones. The principal trends of pitting at the specimen neck section were reproduced by numerical models in order to investigate the stress concentration factors and its impact in fatigue endurance. Finally, the stress intensity factor in mode I was evaluated numerically at the specimen neck section from crack initiation to fracture and the stress intensity factor range threshold KTH was determined for the two type of specimens: base material and pre-corroded.

INTRODUCTION

The nomination I-718 is a nickel-based superalloy, also known as Ni-Fe alloy, which was developed as a high-strength material for the aircraft industry; specifically, for the hot sections of jet engines as: parts of the compressor, blades and discs, due to its excellent mechanical properties at high temperatures and corrosive resistance. Blades and discs are subjected to extreme operating conditions during flight, such as: 1) operating environment: high temperatures, air or fuel contamination, solid particles, etc., 2) high levels of stress, such as: vibrations, aerodynamic and centrifugal forces, and 3) large thermal stresses due to thermal gradients (Ma, 2010; Chen, 2005; Mazur, 2005).

Round bars of I-718 were received with dimensions of 0.5 inch in diameter and 3 inches in length; the chemical composition (wt %) of the material is: 0.62Al, 0.94Ti, 2.89Mo, 5.13Nb, 18.46Cr, 18.7Fe and balance Ni. Other elements present in I-718 alloy are: Bi, Pb, Se, S, Ca, B, P, Ta, Mg, C, Cu, Si, Mn and Co; nevertheless, these elements are in chemical composition lower than 1% wt.

Figure 1 shows a considerable increase of stress induced by the pre-corrosion pits, which leads to a high stress concentration factor: 2752/667= 4.12 approximately. This stress increase is related to the proximity of pitting holes presenting perpendicular direction in regard the applied load, as observed in the same figure. In addition, in the same picture is noticed the decrease of stress between contiguous pitting in longitudinal direction in regard the applied load, as it has been reported in previous numerical investigations (Zuñiga, 2019).

RESULTS AND CONCLUSIONS

The pre-corrosion pits induce stress concentration which is associated with the drastic decrease on fatigue life on metallic alloys. In Figure 2 are plotted the ultrasonic fatigue results obtained in the Inconel 718 subjected to pre-corrosion attack, confronted with ultrasonic fatigue results on specimens without pre-corrosion. It is observed that the difference between these two specimens increases with increasing the applied load, as consequence of stress concentration associated with pitting corrosion: for the high load stress (746 MPa or the 90% of its elastic limit), the difference is with a factor of 10. For the low applied load (510 MPa, the 60% of the elastic limit of this material), the fatigue endurance of both type of specimens are similar, but most of pre-corroded specimens present a lower fatigue endurance.

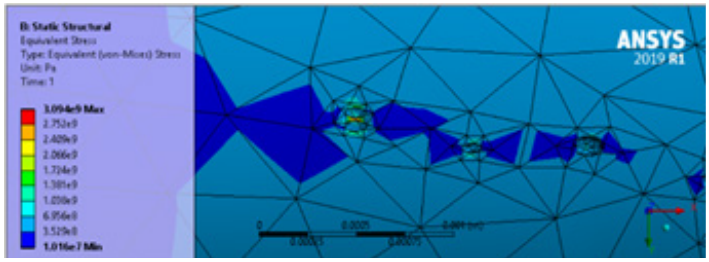

Fig.1 Figure 10. Pre-corroded specimen, loaded with 47 μm of displacement at the specimen ends

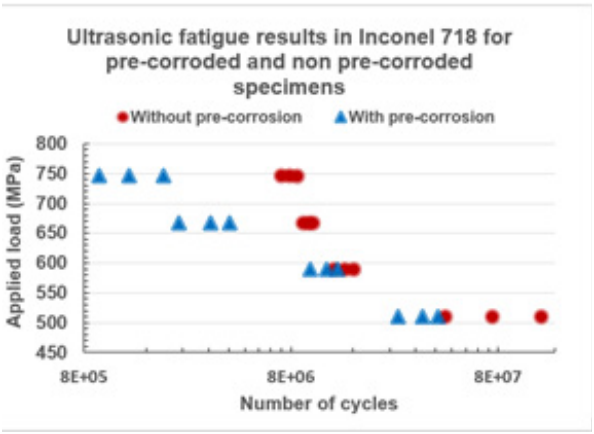

ACKNOWLEDGMENTS

The authors express their special mention of gratitude to CONACYT (The National Council for Science and Technology, Mexico), for the financial support destined to this study through the program grant: CB-241117-2014. An additional mention of gratitude to the University of Michoacán in Mexico for the received support in the development of this work.

REFERENCES

[1] X. Ma, Z..Duan, H. Shi, R. Murai, E. Yanagisawa, Fatigue and fracture behavior of nickel-based superalloy Inconel 718 up to very high cycle regime, Journal of Zhejiang University- SCIENCE A App. Phys. & Eng. 2010, 11(10), p. 727-737.

[2] Q. Chen, N. Kawagoishi, Q.Y. Wang, N. Yan, T. Ono, G. Hashigushi, Small crack behavior and fracture of nickel-based superalloy under ultrasonic fatigue, Int. J. of Fatigue, 2005, 27, p. 1227-1232.

[3] Z. Mazur, A. Luna-Ramírez, , J.A. Islas, , A. Campos-Amezcua, Failure analysis of a gas turbine blade made of Inconel 738LC. Eng. Fail. Anal. 2005,12, p. 474-486.

[4] I.F. Zuñiga Tello, G.M. Domínguez Almaraz, V. López Garza, M. Guzmán Tapia, Numerical investigation of the stress concentration on 7075-T651 aluminum alloy with one or two hemispherical pits under uniaxial or biaxial loading, Adv. In Eng. Sofware, 2019, 131, 23-35.

PROBLEMS OF NONDESTRUCTIVE INSPECTION OF ARMOR GLASS QUALITY

Yuri Merkulov(*), Boris Dobriakov, Sergey Solk, Sergey Shevtsov.
JSC “Scientific Research Institute for Optoelectronic Instrument Engineering”
Ministry of Industry and Trade, Sosnovy Bor, Russian Federation.
(*) E-mail: melas33@yandex.ru

ABSTRACT
The aim of the work is to develop a method of nondestructive inspection of armor glass quality. Transmission and resolution ability of armor glasses of different protection classes and manufactured by different technologies have been compared in the work. The study of spectral transmission of the armor glasses with different service lives has shown that the more the difference in spectral transmission of the protective glasses (with different service lives) the worse their ballistic properties.

INTRODUCTION
At the present time interest to the protective (armor) glasses or transparent armor has increased significantly. The transparent armor is used in military aircraft and ship building, manufacturing of military and civil armored automobile equipment to protect the crew. Viewing ports for armored shields and visor assemblies for armored helmets are made of the transparent armor (Kobylkin, 2014). There is a big problem in protection of optics at the orbital stations against the ballistic impact of "space debris" (Merkulov, 2017).
Inorganic glasses and transparent polymers (organic glasses) are widely used for transparent armor manufacturing. Transparent ceramic materials Leucosapphire (monocrystalline aluminium oxide Al2O3), polycrystalline aluminium oxynitride Al23O27N5 (ALON), and magnesium-aluminium spinel MgAl2O4 possess higher protective properties. At that these materials are transparent in a wide spectral range, including the IR. But their high cost presents a considerable disadvantage. The most promising material is the strong glass-ceramics (armored sitall) developed in Russia with the exclusively efficient ratio between cost and properties (Merkulov, 2001).
Usually the transparent armor consists of three components:
1) a surface layer, which takes an impact directly and keeps the striking element from penetration;
2) a power block, which buffs the most part of the impact energy;
3) a back surface layer, which buffs the impact energy and keeps the secondary glass shards from flying-off.
The polymer compositions and films inserted between the glasses during manufacturing are the subject to natural aging (Tcherezova, 2012). Aging rate of the polymer materials depends on inner factors conditioned by the structure and composition of the polymer material and external factors, namely, environment and load.
The results show that from the sixth year of the shelf time (or service time) of the protective glasses the percentage ratio of the damaged samples to the total number of samples under the test starts to grow. At the sixth year of the service time the ratio makes up more 20%, at the seventh it is more than 35%, and at the tenth it is more than 85%.

RESULTS AND CONCLUSIONS
An example of the measurement results is given in Fig.1.

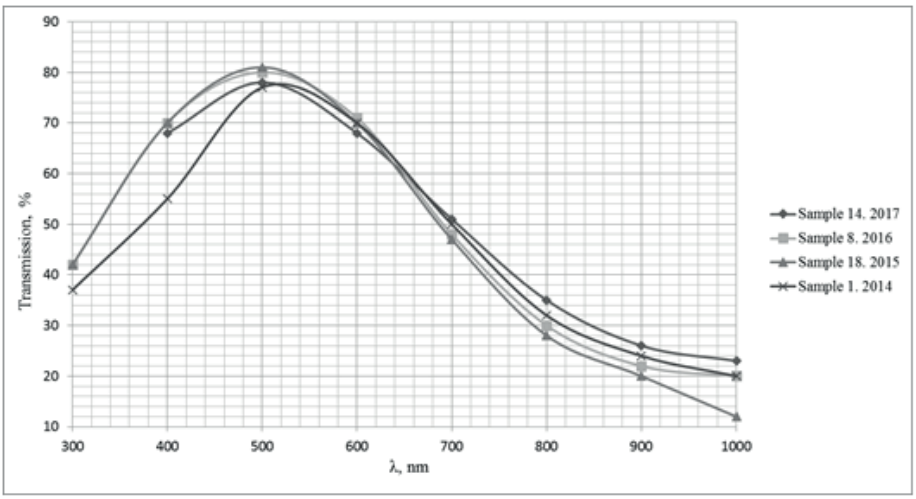

Fig.1 Diagram of spectral transmission of the 3rd protection class samples. The sample thickness is 38.5 mm.

1. Both of the parameters – spectral transmission and resolving ability vary with the service life for all protective glasses under the test;
2. The more the difference in spectral transmission of the protective glasses (with different service lives) the worse their ballistic characteristics;
3. The measurement of spectral transmission of the protective glasses using the method of qualitative evaluation of the protective glasses properties seems more easy and illustrative than the measurement of their resolving ability;
4. There are most priority ranges of wavelengths, at which the effect of degradation of the ballistic properties of the protective glasses is most noticeable;
5. Spectral transmission of the protective glasses should be measured in a wider range (0.2 to 12.5 μm);
6. Both methods (the spectral transmission measurement and the resolving ability measurement) are applicable to evaluate the ballistic characteristics quality of the protective glasses in relation to their service life.

REFERENCES

[1] Kobylkin I.F., Selivanov V.V. The materials and structures of the light-weight armor protection. – Textbook for universities/ - M.: Publishing House of the N.E.Bauman Moscow State Technical University, 2014. - p.161.
[2] Merkulov Yu. Yu., Solk S.V., Lebedev O.A. Protection of orbital station optics against high – speed damaging elements // Acta Astronautica. 2017. V. 135. p.21-25.
[3] Merkulov Yu. Yu. Glass ceramics, a method for obtaining it and a protective construction based on it - Pat. Russian Federation No. 2176624, 2001, BI No. 34.
[4] Tcherezova E.N., Mukameneva N.A., Arkhirejev V.P. Polymers ageing and stabilization.- Tutorial, part 1/ Kazan: Publishing House of the Kazan National Research Technical University, 2012 - p.140.

In partnership with

REPÚBLICA PORTUGUESA
DEFESA NACIONAL

Organizers

Universidade

Fibrenamics

SCIENCENTRIS

ISBN 978-989-54808-4-5